PHYSIOLOGICAL REGULATION AND HOMEOSTASIS AMONG CORAL HOLOBIONT PARTNERS

EDITED BY: Zhi Zhou, Senjie Lin and Kefu Yu
PUBLISHED IN: Frontiers in Physiology and Frontiers in Marine Science

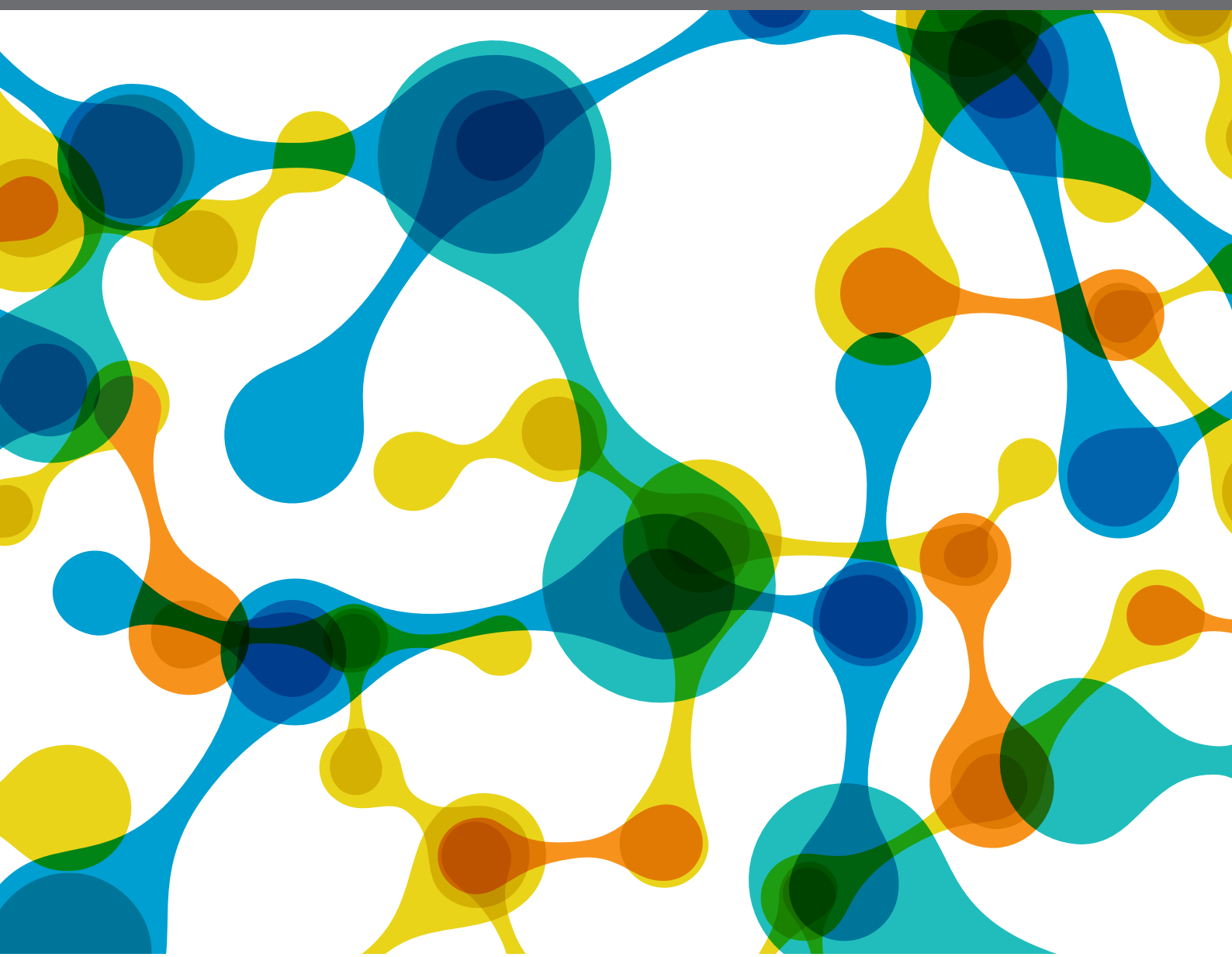

frontiers Research Topics

frontiers

ISSN 1664-8714
ISBN 978-2-88976-286-6
DOI 10.3389/978-2-88976-286-6

About Frontiers

Frontiers is more than just an open-access publisher of scholarly articles: it is a pioneering approach to the world of academia, radically improving the way scholarly research is managed. The grand vision of Frontiers is a world where all people have an equal opportunity to seek, share and generate knowledge. Frontiers provides immediate and permanent online open access to all its publications, but this alone is not enough to realize our grand goals.

Frontiers Journal Series

The Frontiers Journal Series is a multi-tier and interdisciplinary set of open-access, online journals, promising a paradigm shift from the current review, selection and dissemination processes in academic publishing. All Frontiers journals are driven by researchers for researchers; therefore, they constitute a service to the scholarly community. At the same time, the Frontiers Journal Series operates on a revolutionary invention, the tiered publishing system, initially addressing specific communities of scholars, and gradually climbing up to broader public understanding, thus serving the interests of the lay society, too.

Dedication to Quality

Each Frontiers article is a landmark of the highest quality, thanks to genuinely collaborative interactions between authors and review editors, who include some of the world's best academicians. Research must be certified by peers before entering a stream of knowledge that may eventually reach the public - and shape society; therefore, Frontiers only applies the most rigorous and unbiased reviews.
Frontiers revolutionizes research publishing by freely delivering the most outstanding research, evaluated with no bias from both the academic and social point of view. By applying the most advanced information technologies, Frontiers is catapulting scholarly publishing into a new generation.

What are Frontiers Research Topics?

Frontiers Research Topics are very popular trademarks of the Frontiers Journals Series: they are collections of at least ten articles, all centered on a particular subject. With their unique mix of varied contributions from Original Research to Review Articles, Frontiers Research Topics unify the most influential researchers, the latest key findings and historical advances in a hot research area! Find out more on how to host your own Frontiers Research Topic or contribute to one as an author by contacting the Frontiers Editorial Office: frontiersin.org/about/contact

PHYSIOLOGICAL REGULATION AND HOMEOSTASIS AMONG CORAL HOLOBIONT PARTNERS

Topic Editors:
Zhi Zhou, Hainan University, China
Senjie Lin, University of Connecticut, United States
Kefu Yu, Guangxi University, China

Citation: Zhou, Z., Lin, S., Yu, K., eds. (2022). Physiological Regulation and Homeostasis Among Coral Holobiont Partners. Lausanne: Frontiers Media SA. doi: 10.3389/978-2-88976-286-6

Table of Contents

frontiers | Frontiers in Physiology

EDITORIAL
published: 10 May 2022
doi: 10.3389/fphys.2022.921401

Editorial: Physiological Regulation and Homeostasis Among Coral Holobiont Partners

Senjie Lin[1]*, *Kefu Yu*[2]* and *Zhi Zhou*[3]*

[1]Department of Marine Sciences, University of Connecticut, Groton, CT, United States, [2]School of Marine Sciences, Guangxi University, Nanning, China, [3]Department of Marine Sciences, College of Marine Sciences, Hainan University, Haikou, China

Keywords: coral holobiont, physiological regulation, homeostasis, heat stress, nutrient, microbiome, Symbiodiniaceae, bleaching

Editorial on the Research Topic

Physiological Regulation and Homeostasis Among Coral Holobiont Partners

Scleractinian corals form the biological and physical framework for the most productive marine ecosystem in the oligotrophic oceans and play an important role in oceanographic processes (Costanza et al., 1997). The ecological success of coral reefs hinges on the symbiosis between the stony corals and the photosynthetic symbiodiniacean dinoflagellate (zooxanthellae), in which stony coral provides inorganic nutrients and carbon dioxide for the photosynthetic symbiont, whereas the symbionts supply the coral host with indispensable organic nutrients and oxygen (Shinzato et al., 2011). However, coral reefs, the home of the highest biodiversity in the ocean, are degrading rapidly in response to climate change and environmental pollution in the Anthropocene (Renegar and Riegl, 2005; Hughes et al., 2017; Serrano et al., 2018). Revealing how the symbiotic system adaptively responds to the variability of temperature and nutrients and maintain their homeostasis is necessary for efforts to rescue, restore, and protect the disappearing reefs in the face of climate change and environmental deterioration.

Coral lives in a complex holobiont composed of not only the cnidarian and zooxanthellae, but also the internal and external microbes (Rosenberg et al., 2007). For a long time, research on coral health and problems has laser focused on the mutualistic relationship between the cnidarian and the endosymbiotic symbiodiniacean dinoflagellates (zooxanthellae). With the advances of multi-omic technologies and physiological methodologies, a great deal has been learned about how the symbiotic relationship is started and maintained (Davy et al., 2012). A recent study indicated that the differential binding efficiency and specificity of coral lectins to the mannose moieties on the cell surface of different symbiodiniacean species might have significant effects on the success to initiate the symbiosis and maintain it during heat stress (Wang X et al., 2021). Nutrient compound exchanges are essential for the maintenance of a healthy and productive mutualism, and for the exchange, the compatibility of nutrient transport, assimilation, and storage machinery is vital (e. g., for translocation of glucose or glycerol, Lin et al., 2015), which might determine the symbiont preference (Lin et al., 2019). Environmental nutrients may also be important for the symbiodiniacean dinoflagellates to withstand heat stress (Zhou et al., 2021; Kirk et al. Nat Comm), but on the contrary nutrient overloading (eutrophication), particularly in combination with heat stress, can adversely impact the symbiosis and cause bleaching (D'Angelo and Wiedenmann, 2014; Lam et al., 2015; Humanes et al., 2016; Decarlo et al., 2020; Donovan et al., 2020). In addition, symbiont cell

OPEN ACCESS

Edited and reviewed by:
Pung Pung Hwang,
Academia Sinica, Taiwan

***Correspondence:**
Senjie Lin
senjie.lin@uconn.edu
Kefu Yu
kefuyu@scsio.ac.cn
Zhi Zhou
zhouzhi@hainanu.edu.cn

Specialty section:
This article was submitted to Aquatic Physiology, a section of the journal Frontiers in Physiology

Received: *15 April 2022*
Accepted: *20 April 2022*
Published: *10 May 2022*

Citation:
Lin S, Yu K and Zhou Z (2022) Editorial: Physiological Regulation and Homeostasis Among Coral Holobiont Partners. Front. Physiol. 13:921401. doi: 10.3389/fphys.2022.921401

cycle modulation and host immunity are also critical for the maintenance of the symbiosis (Rivera and Davies, 2021).

In parallel to the continued effort to understand the coral-zooxanthella mutualism, there is a growing appreciation for the importance of bacteria in shaping the physiology and acclimatization of coral holobionts under novel and changing environments (Voolstra et al., 2021). In the last decade or so, an increasing number of studies examined the community structure and function of bacteria inside or on the surface of (mucus-associated) the host coral (e.g., Shnit-Orland and Kushmaro, 2009; Glasl et al., 2016). The need to study coral systems as holobionts is clear. Such effort has revealed that coral hosts, Symbiodiniaceae, and bacteria participate in the environmental adaptation of scleractinian coral (Yu et al., 2020a). For example, studies on scleractinian coral of the South China Sea have found that the trophic status (Xu et al., 2021), colony tissue thickness (Qin et al., 2020), Symbiodiniaceae density, Chl*a* content and tissue biomass (Qin et al., 2019), Symbiodiniaceae and bacteria diversity and community structure (Chen et al., 2019; Chen et al., 2021) of scleractinian corals are primarily driven by SST with latitudinal gradient shifts. These factors have important effects on coral holobionts tolerance; however, there are some differences between regions, coral species and even coral individuals (Yu et al., 2021a; Yu et al., 2021b; Yu et al., 2020b).

This Research Topic on *Physiological regulation and homeostasis among coral holobiont partners* aims to bring novel research findings together to bear on the molecular and physiological mechanisms in the partners of coral holobionts that underlie the establishment, maintenance and stability of symbiosis and adaptation to environmental changes. Nine exciting articles have been published.

One of the papers surveys the literature and draws perspectives about the importance of studying corals as holobionts using a holistic approach. Goulet et al. discussed the ramifications of how different genotypic combinations of the consortium constituents affected the coral holobiont entity. It was noted, using the zooxanthellae as the example, that the holobiont attributes might not necessarily be the sum of the constituents. The holobiont properties are consequential to holobiont fitness, which are in turn contributed by the myriad constituent organisms. The authors clearly articulated that a holistic approach requires evaluating the entire consortium instead of focusing on one species or component of the holobiont, investigating holobiont characteristics and performance, assessing parameters of as many of the holobiont participants as possible. The literature survey also revealed the paucity of data on the microbiome.

Four papers of the papers investigate the role of symbiotic microbiome in environmental adaptation of coral holobionts. Three papers focus on symbiotic Symbiodiniaceae. Wang et al. established monoclonal culture techniques and documented the physiological and ecological characteristics of Symbiodiniaceae C1 strain from the scleractinian coral *Galaxea fascicularis,* and this will be instrumental to further unraveling the roles of Symbiodiniaceae in the adaptive evolution of coral holobionts in future studies Wang et al. The work reported in Kirk et al. deals with transcriptional responses to trophic shifts in Symbiodiniaceae. The results showed that *Breviolum minutumstrain* SSB01 grew at a much faster rate and maintained stable photosynthetic efficiency when supplemented with organic nutrients compared to when only inorganic nutrients or no nutrient were provided. The authors concluded that these physiological changes were driven by massive transcriptomic changes involving DNA topoisomerases, histones, chromosome structural components, translation, ion transport, generation of second messengers, and phosphorylation. There was a high genetic diversity in Symbiodiniaceae with broad physiological plasticity within and between species, conferring great thermal tolerance.

Russnak et al. performed a comprehensive comparative experiment to explore the photosynthetic performance and tolerance as function of light and temperature of different genetic types of Symbiodiniaceae. The results clearly demonstrated that there were significant eco-physiological differences in light affinity and temperature tolerance among the tested species as well as strains within a species. The authors concluded that genetically different Symbiodiniaceae all had a broad photophysiological tolerance and substantial thermal plasticity. The effect of coral-associated bacterial communities on holobiont heat tolerance were examined by Connelly et al. The researchers investigated the microbial interactions in four *Pocillopora* coral colonies under heat stress and antibiotic treatment. The results showed that combined antibiotics and heat stress treatment significantly altered coral-associated bacterial communities and caused major changes in gene expression in both the coral and the symbiont *Cladocopium*. This study indicates the potential that the alteration of the bacterial community may contribute to or even exacerbate the stress imposed by heat. This paper provides further evidence that corals and their associated Symbiodiniaceae and bacteria communities engage in highly coordinated metabolic interactions that are crucial for coral holobiont health, homeostasis, and heat tolerance.

Three papers deal with nutrients and energy. One of these investigated the diversity of N_2-fixing bacteria in the coral holobionts in the South China Sea (Liang et al.). Sixty-eight coral colonies were collected from six coral reef areas encompassing different environments ranging from 9°20′06″N to 22°34′55″N. PCR amplification and sequencing of *nifH* gene from the samples revealed a diverse diazotrophic flora dominated by Proteobacteria, Chlorobi, Cyanobacteria, and two unclassified phyla. Data further showed that coral-associated diazotrophs were common among coral demonstrate the potential importance of N_2-fixing bacteria as the source of N-nutrient for corals, which live in the oligotrophic environment.

Lipids and fatty acids (FAs) are important constituents of cell and organelle membranes and have become a hot topic of research to understand the effects of eutrophication on corals. Liu et al. investigated the effects of nitrate (NO_3^-) enrichment on the respiration, photosynthesis, and FA compositions of *Pocillopora damicornis* larvae. Their survey showed that saturated FAs (SFAs) were the most abundant in *P. damicornis* larvae followed by polyunsaturated FAs (PUFAs) and monounsaturated FAs (MUFAs). Nitrate enrichment

significantly changed the FA composition of *P. damicornis* larvae. The lipids of *P. damicornis* larvae became progressively saturated when the nitrate concentration was below 10 mM, due to the decreases of PUFAs and concomitant increases in SFAs. Such changes enabled the *P. damicornis* larvae to adapt to low-level nitrate enrichment (<10 mM). Moreover, with high nitrate levels, biomembrane restructuring in larvae may become ineffective, increasing respiration and rapidly consuming lipids, which could adversely affect the successful settlement and development of the larvae.

To understand how nutrient assimilation by the coral-Symbiodiniaceae entity is affected by heat stress, Tang et al. (2020) exposed *Pocillopora damicornis* to 32°C and measured the activity of ammonium assimilation enzymes among other physiological parameters. They found that the glutamine synthetase and glutamine oxoglutarate aminotransferase activities in the coral increased under heat stress, whereas that in the symbionts showed no significant changes. When the activities of glutamine synthetase were inhibited through glufosinate treatment, the heat stress response of the entity was intensified as indicated by the decline of symbiont density and chlorophyll content as well as the induction of coral antioxidant capacity and apoptosis. Therefore, ammonium assimilation contributes to the acclimatization of the coral-Symbiodiniaceae symbiotic association to high temperature.

While treatment experiments are powerful for controlling experimental conditions to test effects of one or few variables at a time, *in situ* studies provide understanding on the physiologies and behavior of the organisms in the natural complex environment. Xu et al. conducted a comparative study on corals in two distinct environments, the northern and southern sides of Weizhou Island in the South China Sea. They measured *in situ* electron transport rate (rETR), zooxanthella density and Chl*a* concentration, genetic diversity of the symbionts, stable isotopic signals of carbon, coral biomass, energy storage (in terms of carbohydrates), and superoxide dismutase (SOD) activity. ITS2 genotyping showed that *Galaxea fascicularis* contained either type C21 or D1a as the dominant symbiodiniacean symbiont depending on the regional environmental stress. Furthermore, the response of photosynthetic performance (the light use efficiency) and energy metabolism to the north-south environmental differences varied between species, and in the case of *P. verrucose* and *Montipora truncate*, the symbiont density (C1) in the north was higher, compensating for their lower photosynthetic efficiencies there, in comparison to the southern population.

The papers published in this special topic provide novel insights into how the coral holobionts respond to the environmental conditions, how the host, zooxanthellae, and bacteria may differentially contribute to the holobiont performance in the face of environmental stress. These findings demonstrate the value of *in situ* studies and treat the holobiont holistically in experiments. The *in situ* and holistic approach, coupled with omics and isotopic technologies, dealing with heat stress combined with different nutrient conditions, should be pursued much more in the future. Insights from such studies about how the coral holobionts respond and adapt to projected future climate and environment will be helpful for screening or breeding resilient genotypes in the urgently needed effort to rescue and restore the disappearing coral reefs, the treasure of the ocean. Finally, the Topic Editors would like to sincerely thank all the authors for their valuable contributions and all the reviewers for their efforts.

AUTHOR CONTRIBUTIONS

SL conceived the concept and wrote the manuscript. KY wrote the manuscript. ZZ wrote the manuscript.

REFERENCES

Chen, B., Yu, K., Liang, J., Huang, W., Wang, G., Su, H., et al. (2019). Latitudinal Variation in the Molecular Diversity and Community Composition of Symbiodiniaceae in Coral from the South China Sea. *Front. Microbiol.* 10, 1278. doi:10.3389/fmicb.2019.01278

Chen, B., Yu, K., Liao, Z., Yu, X., Qin, Z., Liang, J., et al. (2021). Microbiome Community and Complexity Indicate Environmental Gradient Acclimatisation and Potential Microbial Interaction of Endemic Coral Holobionts in the South China Sea. *Sci. Total Environ.* 765, 142690. doi:10.1016/j.scitotenv.2020.142690

Costanza, R., d'Arge, R., de Groot, R., Farber, S., Grasso, M., Hannon, B., et al. (1997). The Value of the World's Ecosystem Services and Natural Capital. *Nature* 387, 253–260. doi:10.1038/387253a0

D'Angelo, C., and Wiedenmann, J. (2014). Impacts of Nutrient Enrichment on Coral Reefs: New Perspectives and Implications for Coastal Management and Reef Survival. *Curr. Opin. Environ. Sustain* 7, 82–93.

Davy, S. K., Allemand, D., and Weis, V. M. (2012). Cell Biology of Cnidarian-Dinoflagellate Symbiosis. *Microbiol. Mol. Biol. Rev.* 76 (2), 229–261. doi:10.1128/mmbr.05014-11

Decarlo, T. M., Gajdzik, L., Ellis, J., Coker, D. J., Roberts, M. B., Hammerman, N. M., et al. (2020). Nutrient-Supplying Ocean Currents Modulate Coral Bleaching Susceptibility. *Sci. Adv.* 6 (34), eabc5493.

Donovan, M. K., Adam, T. C., Shantz, A. A., and Burkepile, D. (2020). Nitrogen Pollution Interacts With Heat Stress to Increase Coral Bleaching Across the Seascape. *Proc. Natl. Acad. Sci. USA* 117 (10), 5351–5357.

Glasl, B., Herndl, G. J., and Frade, P. R. (2016). The Microbiome of Coral Surface Mucus Has a Key Role in Mediating Holobiont Health and Survival upon Disturbance. *ISME J.* 10, 2280–2292. doi:10.1038/ismej.2016.9

Hughes, T. P., Barnes, M. L., Bellwood, D. R., Cinner, J. E., Cumming, G. S., Jackson, J. B. C., et al. (2017). Coral Reefs in the Anthropocene. *Nature* 546, 82–90. doi:10.1038/nature22901

Humanes, A., Noonan, S. H. C., Willis, B. L., Fabricius, K. E., and Negri, A. P. (2016). Cumulative Effects of Nutrient Enrichment and Elevated Temperature Compromise the Early Life History Stages of the Coral *Acropora Tenuis*. *PLoS One* 11, e0161616. doi:10.1371/journal.pone.0161616

Lam, E. K. Y., Chui, A. P. Y., Kwok, C. K., Ip, A. H. P., Chan, S. W., Leung, H. N., et al. (2015). High Levels of Inorganic Nutrients Affect Fertilization Kinetics, Early Development and Settlement of the Scleractinian Coral *Platygyra Acuta*. *Coral Reefs* 34, 837–848. doi:10.1007/s00338-015-1317-8

Lin, M. F., Takahashi, S., Forêt, S., Davy, S. K., and Miller, D. J. (2019). Transcriptomic Analyses Highlight the Likely Metabolic Consequences of Colonization of a Cnidarian Host by Native or Non-native Symbiodinium Species. *Biol. Open* 8 (3), bio038281. doi:10.1242/bio.038281

Lin, S., Cheng, S., Song, B., Zhong, X., Lin, X., Li, W., et al. (2015). The *Symbiodinium kawagutii* Genome Illuminates Dinoflagellate Gene Expression and Coral Symbiosis. *Science* 350, 691–694. doi:10.1126/science.aad0408

Qin, Z., Yu, K., Liang, Y., Chen, B., and Huang, X. (2020). Latitudinal Variation in Reef Coral Tissue Thickness in the South China Sea: Potential Linkage with Coral Tolerance to Environmental Stress. *Sci. Total Environ.* 711, 134610. doi:10.1016/j.scitotenv.2019.134610

Qin, Z., Yu, K., Wang, Y., Xu, L., Huang, X., Chen, B., et al. (2019). Spatial and Intergeneric Variation in Physiological Indicators of Corals in the South China Sea: Insights into Their Current State and Their Adaptability to Environmental Stress. *J. Geophys. Res. Oceans* 124, 3317–3332. doi:10.1029/2018jc014648

Renegar, D., and Riegl, B. (2005). Effect of Nutrient Enrichment and Elevated CO2 Partial Pressure on Growth Rate of Atlantic Scleractinian Coral *Acropora cervicornis*. *Mar. Ecol. Prog. Ser.* 293, 69–76. doi:10.3354/meps293069

Rivera, H. E., and Davies, S. W. (2021). Symbiosis Maintenance in the Facultative Coral, *Oculina Arbuscula*, Relies on Nitrogen Cycling, Cell Cycle Modulation, and Immunity. *Sci. Rep.* 11, 21226. doi:10.1038/s41598-021-00697-6

Rosenberg, E., Koren, O., Reshef, L., Efrony, R., and Zilber-Rosenberg, I. (2007). The Role of Microorganisms in Coral Health, Disease and Evolution. *Nat. Rev. Microbiol.* 5, 355–362. doi:10.1038/nrmicro1635

Serrano, X. M., Miller, M. W., Hendee, J. C., Jensen, B. A., Gapayao, J. Z., Pasparakis, C., et al. (2018). Effects of Thermal Stress and Nitrate Enrichment on the Larval Performance of Two Caribbean Reef Corals. *Coral Reefs* 37, 173–182. doi:10.1007/s00338-017-1645-y

Shinzato, C., Shoguchi, E., Kawashima, T., Hamada, M., Hisata, K., Tanaka, M., et al. (2011). Using the *Acropora digitifera* Genome to Understand Coral Responses to Environmental Change. *Nature* 476, 320–323. doi:10.1038/nature10249

Shnit-Orland, M., and Kushmaro, A. (2009). Coral Mucus-Associated Bacteria: a Possible First Line of Defense. *FEMS Microbiol. Ecol.* 67, 371–380. doi:10.1111/j.1574-6941.2008.00644.x

Tang, J., Wu, Z., Wan, L., Cai, W., Chen, S., Wang, X., et al. (2020). Differential Enrichment and Physiological Impacts of Ingested Microplastics in Scleractinian Corals *In Situ*. *J. Hazard. Mat.* 404, 124205. doi:10.1016/j.jhazmat.2020.124205

Voolstra, C. R., Suggett, D. J., Peixoto, R. S., Parkinson, J. E., Quigley, K. M., Silveira, C. B., et al. (2021). Extending the Natural Adaptive Capacity of Coral Holobionts. *Nat. Rev. Earth Environ.* 2, 747–762. doi:10.1038/s43017-021-00214-3

Wang X, X., Wu, Z., Wu, Y., An, M., Zhou, Z., and Lin, S. (2021). Differential Affinities of a Pocillopora Damicornis Galectin to Five Genera of Symbiodiniaceae at Different Temperatures. *Front. Mar. Sci.* 8, 754808. doi:10.3389/fmars.2021.754808

Xu, S., Zhang, Z., Yu, K., Huang, X., Chen, H., Qin, Z., et al. (2021). Spatial Variations in the Trophic Status of Favia Palauensis Corals in the South China Sea: Insights into Their Different Adaptabilities under Contrasting Environmental Conditions. *Sci. China Earth Sci.* 64, 839–852. doi:10.1007/s11430-020-9774-0

Yu, X., Yu, K., Chen, B., Liao, Z., Liang, J., Yao, Q., et al. (2021a). Different Responses of Scleractinian Coral *Acropora pruinosa* from Weizhou Island during Extreme High Temperature Events. *Coral Reefs* 40, 1697–1711. doi:10.1007/s00338-021-02182-y

Yu, X., Yu, K., Chen, B., Liao, Z., Qin, Z., Yao, Q., et al. (2021b). Nanopore Long-Read RNAseq Reveals Regulatory Mechanisms of Thermally Variable Reef Environments Promoting Heat Tolerance of Scleractinian Coral *Pocillopora Damicornis*. *Environ. Res.* 195, 110782. doi:10.1016/j.envres.2021.110782

Yu, X., Yu, K., Huang, W., Liang, J., Qin, Z., Chen, B., et al. (2020a). Thermal Acclimation Increases Heat Tolerance of the Scleractinian Coral *Acropora Pruinosa*. *Sci. Total Environ.* 733, 139319. doi:10.1016/j.scitotenv.2020.139319

Yu, X., Yu, K., Liao, Z., Liang, J., Deng, C., Huang, W., et al. (2020b). Potential Molecular Traits Underlying Environmental Tolerance of *Pavona decussata* and *Acropora pruinosa* in Weizhou Island, Northern South China Sea. *Mar. Pollut. Bull.* 156, 111199. doi:10.1016/j.marpolbul.2020.111199

Zhou, Z., Zhang, K., Wang, L., Su, Y., Wang, J., Song, T., et al. (2021). Nitrogen Availability Improves the Physiological Resilience of Coral Endosymbiont *Cladocopium goreaui* to High Temperature. *J. Phycol.* 57 (4), 1187–1198. doi:10.1111/jpy.13156

Conflict of Interest: The authors declare that the research was conducted in the absence of any commercial or financial relationships that could be construed as a potential conflict of interest.

Publisher's Note: All claims expressed in this article are solely those of the authors and do not necessarily represent those of their affiliated organizations, or those of the publisher, the editors and the reviewers. Any product that may be evaluated in this article, or claim that may be made by its manufacturer, is not guaranteed or endorsed by the publisher.

frontiers in Physiology

ORIGINAL RESEARCH
published: 29 April 2020
doi: 10.3389/fphys.2020.00390

Physiological Characteristics and Environment Adaptability of Reef-Building Corals at the Wuzhizhou Island of South China Sea

*Huili Xu[1,2], Boxuan Feng[2], Minrui Xie[2], Yuxiao Ren[2], Jingquan Xia[2], Yu Zhang[2], Aimin Wang[1,2] and Xiubao Li[1,2]**

[1] State Key Laboratory of Marine Resource Utilization in South China Sea, Hainan University, Haikou, China, [2] College of Marine Science, Hainan University, Haikou, China

The health of coral reef has declined significantly around the world due to the impact of human activities and natural environment changes, and corals have to develop effective resistance mechanisms to survive. In this study, we examined the physiological characteristics and *Symbiodiniaceae* types of four dominant scleractinian corals in the reefs at the Wuzhizhou Island (WZZ) in South China Sea. The water environmental conditions are complex on the north side of WZZ due to regional geography and tourism development, and all corals had their unique physiological conditions and *Symbiodiniaceae* types. For all corals of this study, the $rETR_{max}$ and protein content were significantly lower and the SOD enzyme activity was significantly higher in the north than in the south. Interestingly, ITS2 genotyping showed that *Galaxea fascicularis* contained dominant *Symbiodiniaceae* either genotype C21 or D1a depending on the regional environmental stress, and had stronger heterotrophy than the other three coral species. In addition, the light use efficiency of the dominant *Symbiodiniaceae* type C1 for *Pocillopora verrucosa* was significantly lower in the north and the half saturating irradiance was stable. Besides, *Montipora truncata* and *P. verrucosa* increased their density of the symbiotic zooxanthella C1 in the north to offset the decline of photosynthetic efficiency and thus supply energy. For *Porites lutea* and *G. fascicularis*, their half saturating irradiance declined sharply in the north, where *P. lutea* resorted to heterotrophic feeding to balance the energy budget when the number of zooxanthellas fell short and *G. fascicularis* reduced its energy reserve significantly when the energy source was limited. We thus demonstrated the differences in the physiological responses and energy metabolism strategies between the zooxanthella and the host coral of the four reef-building coral species under the stress of complex water environment on the north side of WZZ. The corals were found to cope with natural and anthropogenic stressors by adjusting the nutrient input sources and the energy structure metabolism of coral hosts or adapting to more sustainable relationship with *Symbiodiniaceae* clades. The corals exhibited their capacity against long-term disturbances by developing their own successful resistance mechanisms at symbiotic relationship and energy metabolism level.

Keywords: scleractinian coral, environmental stress, zooxanthella, trade-off, Wuzhizhou Island

OPEN ACCESS

Edited by:
Senjie Lin,
University of Connecticut,
United States

Reviewed by:
Filippo Garofalo,
University of Calabria, Italy
Guowei Zhou,
South China Sea Institute of Oceanology (CAS), China

***Correspondence:**
Xiubao Li
xiubaoli@hainanu.edu.cn

Specialty section:
This article was submitted to Aquatic Physiology, a section of the journal Frontiers in Physiology

Received: *25 November 2019*
Accepted: *01 April 2020*
Published: *29 April 2020*

Citation:
Xu H, Feng B, Xie M, Ren Y, Xia J, Zhang Y, Wang A and Li X (2020) Physiological Characteristics and Environment Adaptability of Reef-Building Corals at the Wuzhizhou Island of South China Sea. Front. Physiol. 11:390. doi: 10.3389/fphys.2020.00390

INTRODUCTION

In recent decades, coral reef ecosystems have seriously degraded worldwide due to anthropogenic impact and natural stress (Guest et al., 2016). Degradations may be triggered by a series of incidents, including coral bleaching, sewage discharge from coastal development, eutrophication, disease outbreak, widespread failure of larva supplements, etc. (Hughes et al., 2010). Coral bleaching results from the physical and symbiotic changes in the algae and the stress related to the host, and involves the symbiotic relationship between corals and zooxanthellae (Fitt et al., 2000). After bleaching events, different species of corals may recover or adapt differently. During the 1998 Maldivian bleaching event, the dominant species (e.g.: Acroporidae and Pocilloporidae) were practically disappeared and Poritidae survived partly, while in the subsequent recovery, Agariciidae (esp. Pavona) became a new dominant community and regenerations of Porites increased obviously (Loch et al., 2002). In the coral reefs of Panama, there was a significant increase in the number of corals symbiotic with clade D zooxanthellae, which increased from 43% in 1995 to 63% in 2001 (Baker et al., 2004). Thus, corals may continue to survive if they can withstand the impacts of environment changes.

Environmental stress (e.g., typhoon, high temperature, strong ultraviolet radiation, increased turbidity, and higher nutrient concentration) can cause coral bleaching (Fabricius et al., 2007; Humphrey et al., 2008; Lirman and Manzello, 2009). Corals respond to stress events by changing their growth rate, losing zooxanthellae, varying their fecundity, reducing planula larval survival, and altering their metabolism (Brown and Howard, 1985). For example, studies have reported that high levels of dissolved inorganic nitrogen and phosphorus could significantly change the physiology of stony corals, including reduced calcification, increased zooxanthellae concentration, and potentially higher rate of coral diseases (Marubini and Davies, 1996; Bruno et al., 2003). Investigations of the coral reefs in the northeast of Brazil (Costa et al., 2000) and in Kenya (Lambo and Ormond, 2006) indicate that the rising turbidity from land-derived input is the main factor culpable for the high bleaching rate and the low recovery degree of coral. Xing et al. (2012) showed that corals with higher density of zooxanthella exhibit stronger tolerance and anti-albinism in turbid water. In the three worldwide coral thermal bleaching events, i.e., in 1997–1998, 2010, and 2015–2016 (Hughes et al., 2018), Acropora and Pocillopora spp. (branching coral) appeared susceptible, while *Porites* and *Goniopora* spp. appeared resistant to environmental stress. Other studies also suggested that different types of reef-building corals had varying tolerance to water turbidity (Xing et al., 2012; Li et al., 2015), and massive corals (e.g., *Galaxea fascicularis* and *Porites lutea*) appeared relatively more tolerant than branched corals (e.g., *Acropora millepora*, *A. nasuta*, and *Pocillopora damicornis*). Furthermore, each coral species responded differently to stress depending on their own shape, scope of the stress tolerance, resistance to pressure, ability to regenerate after disturbance, as well as the associated *Symbiodiniaceae* (Buddemeier and Fautin, 1993; Fabricius, 2005).

Generally, key factors for corals on their resilience against and recovery from bleaching include the level of energy reserve, the shift in endosymbiont type, and the heterotrophic plasticity (Schoepf et al., 2015; Castrillón-Cifuentes et al., 2017). Grottoli et al. (2014) reported that *Porites astreoides* is more sensitive to bleaching than *Orbicella faveolata* and *Porites divaricata* because it has a relatively inflexible assemble of *Symbiodiniaceae* with different genetic types and also a much lower energy reserve baseline than the others. *G. fascicularis* was found to have a complex symbiotic system (Blackall et al., 2015), like flexible symbiotic systems with both clades C and D at regional scales (Huang et al., 2011) and local scales (Zhou et al., 2012) in the South China Sea. Besides, the heat tolerant *Symbiodiniaceae* clade D1a was observed in corals after bleaching events in the Pacific and the Caribbean (Baker et al., 2004; Lajeunesse et al., 2009; Keshavmurthy et al., 2012). Heterotrophy can be crucial in maintaining the physiological functions of corals when autotrophy is depressed. For example, Rodrigues and Grottoli (2006, 2007) studied the change of physiological indicators in the recovery of bleached corals and found dynamic change in trophic status of *Montipora capitata,* and found that photoautotrophy was predominant before bleaching and after recovery but heterotrophy was the major energy source in early recovery. Both heterotrophic ability and energy reserve were found to have a significant impact on the resilience of bleached corals from the studies of *Porites compressa, P. lobata*, and *M. capitata* (branching form) in Kaneohe Bay, Hawaii (Grottoli et al., 2006). Nevertheless, Schoepf et al. (2015) demonstrated that for *P. divaricata*, *P. astreoides*, and *O. faveolata* suffering from annual bleaching, rapid recovery relies less on heterotrophic source but more on the level of energy reserve. These findings indicate that coral species with high carbon retention capability have an advantage in recovering from bleaching.

Corals in the South China Sea have experienced bleaching due to environment perturbation, e.g., global warming, typhoon, flood, coastal pollution, *etc.* (Yu, 2012). Mild to moderate bleaching events have been documented in the South China Sea, including Dongsha (Tkachenko and Soong, 2017), the southern Hainan Island (Li et al., 2012), Taiwan (Kuo et al., 2012), Hong Kong (Xie et al., 2017), *etc.* When effective mechanisms for stress resistance are lacking, regional mortality of corals may rise severely (Ladner et al., 2012). Research interest is increasing on understanding how stress decreases the resistance of corals to perturbation and how acclimatization enhances the resilience of corals against future stress (Castrillón-Cifuentes et al., 2017). Nevertheless, for corals about the Hainan Island of the South China Sea, little has been studied on the effects of chronic negative environment on their physiology, adaptive strategies, and acclimatization. More research is needed to reveal the physiological and biochemical characteristics of corals and their physiological responses and coping strategies to environmental changes, to thus help understand which coral species will become dominant as a result of natural selection and then provide theoretical guidelines for the conservation and restoration efforts in managing the coral reef ecosystems (Hughes et al., 2013; Li et al., 2015).

In 2018, we collected the data of the water environment and the coral reef communities about the Wuzhizhou Island (WZZ) in South China Sea. In this work, we studied the physiological changes of four dominant reef-building corals determined in the prior work, including *Galaxea fascicularis*, *Pocillopora verrucosa*, *Montipora truncata*, and *Porites lutea*. We used both physiological and biochemical methods to assess the long-term acclimatization of these four corals species at WZZ under chronic environmental disturbance. From these reef-building corals we evaluated (i) how do the coral holobiont adapt to perennial environment stress, (ii) which traits are associated with long-term acclimatization, and (iii) what are the intrinsic metabolic strategies of different corals under external environmental stress.

MATERIALS AND METHODS

Study Site and Sample Collection

The WZZ Island (109°45′ E, 18°18′ N) is located off the southeastern coast of the Hainan Island in South China Sea. It is affected by northeast wind and waves in the winter and southerly wind and waves in the summer (Zhang et al., 2006). The 13 study sites are divided by cluster analysis into the south zone (1–7) and the north zone (8–13) based on the benthic composition of the coral reefs (Li et al., 2019). The northern zone has a sandy coastline while the southern zone has a rocky coastline, and the coastline pattern may have a strong impact on the reef development at WZZ (Li et al., 2019). In July 2018, coral samples were collected at the depth of 4–6 m from the northern zone (site 9 in **Figure 1**) and southern zone (sites 3 and 4 in **Figure 1**) of WZZ. Coral samples were collected with a chisel from four to six healthy coral colonies that were separated by at least 5 m. Small branches of corals were collected for branching coral communities, and massive corals were chipped into pieces of about 20 cm^2 in size. All samples were placed in individual plastic bags filled with seawater. The partial coral pieces were immediately washed with filtered seawater, preserved in 95% ethanol on board, transported to the lab without delay, and stored at −20°C in a refrigerator until use.

Environmental Data

All parameters were measured three times. Steady readings of temperature were measured at the sampling area with HOBO loggers (Tempcon Inc., United States). The seawater salinity and pH were recorded *in situ* with a portable pH/conductivity meter (420C-01A Orion Star, Thermo Fisher Scientific, United States). Turbidity was assessed using an AQUAlogger 210 (Aquatec, United Kingdom). Effective underwater light intensity was determined with a LI-COR (LI-192SA, United States) underwater photo quantum measurement recorder. Samples of bottom level water were collected (100 mL) and filtered (Whatman GF/F, Φ47 mm, United Kingdom) to analyze the composition of inorganic nutrients on a Skalar SAN^{plus} auto-analyzer (Skalar, Netherlands). The dissolved nutrients (DIN) is the sum of ammonium salt, nitrite and nitrate.

In situ Photobiological Variables

A mini-PAM fluorometer (Walz, Germany) was used to determine the photosynthetic variables of corals. This instrument can measure the rapid light curves (RLCs) and the relative electron transport rate (ETR, μmol electron $m^{-2}s^{-1}$) for photosystem II with previously described settings (Schreiber et al., 1986; Hennige et al., 2008). Data were fitted to the Jassby and Platt (1976) model, which describes the dependency of ETR on the incident light intensity (E), by least squares non-linear regression to determine the light use efficiency (i.e., light-limited) α (mol electron per mol photon), the maximum relative electron transport rate (i.e., light-saturated) $rETR_{max}$ (μmol electron $m^{-2}s^{-1}$), and the minimum saturating irradiance (E_k), respectively (Suggett et al., 2012). After the photosynthetic variables of corals were measured, coral samples were pretreated and cryogenically transported to the laboratory for subsequent physiological and biochemical determinations.

Physiological Parameters

All parameters were measured for three times. Coral samples were collected in a plastic bag after photobiological measurements. Tissues were removed from the skeleton with a Waterpik flosser (WP-70EC, Water pik, Inc.) containing filtered seawater (0.45 μm, Whatman, United Kingdom), and tissue biomass was then measured (Fitt et al., 2000). The surface area of corals was determined by the aluminum foil method (Li et al., 2006), and the ratio between the ash-free dry weight and the surface area was calculated to give the tissue biomass. Chlorophyll a (Chl a) from coral samples was extracted with 100% acetone in darkness and determined with a spectrophotometer (Lei et al., 2008). The density of symbiotic algae was assessed according to the method of Li et al. (2006).

Carbohydrates were measured as previously described (Dubois et al., 1956). Total lipid was determined according to the method of Grottoli et al. (2004) with modification. The coral samples (wet weight about 2 g) were extracted with 36 ml of CM solution ($V_{methanol}$:$V_{chloroform}$ = 1:2), add 1/5 of solution volume (7 ml) of 0.88% KCl, followed by dark treatment for extraction about 24 h, then the extract was placed in the 39°C N_2 gas vacuum environment to evaporate and dry. Total protein was measured by the bicinchoninic acid method (Smith et al., 1985) with a Modified BCA Protein Assay Kit (Sangon Biotech, China). Total energy reserves were calculated as the sum of total lipids, carbohydrates, and proteins. The SOD (superoxide dismutase) enzyme was measured with an Activity Kit (Nanjing Jiancheng Bio-Engineering Institute Co., Ltd.).

DNA Extraction and Amplicon Sequencing

Total DNA was extracted according to the method given in Zhou and Huang (2011). The DNA Extraction Kit for Marine Animal Genome (TIANGEN, Beijing, China) was used. The extracted DNA samples were used as PCR templates after quality check and purity filter. The primers of ITSintfor2 and ITS2clamp (F: 5′-GAATTGCAGAACTCCGTG-3′; R: 5′-CGCCCGCCGCGCCCCGCGCCCGTCCCGCCGCCCCCGCC

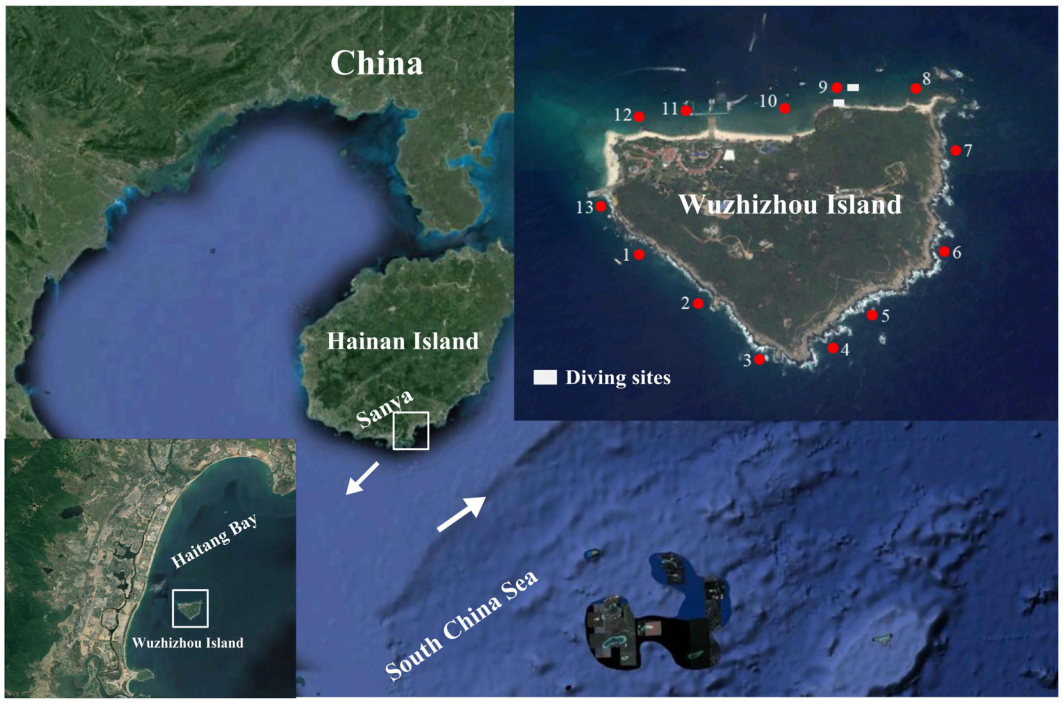

FIGURE 1 | Three sampling sites (3, 4, and 9) in coral reefs of the Wuzhizhou Island. **Figure 1** is modified with permission from Li et al. (2019). The 13 study sites are divided by cluster analysis into the south zone (1–7) and the north zone (8–13) based on the benthic composition of the coral reefs (Li et al., 2019).

CGGGATCCATATGCTTAAGTTCAGCGGGT-3′) (LaJeunesse, 2002) were used to produce PCR amplification of the *Symbiodiniaceae* ITS2 region of the rDNA. The 330–360 bp ITS2 fragments were purified using the SanPrep Column DNA Gel Extraction Kit (Sangon Biotech, China). All amplified PCR products were then sequenced with a paired-end (PE) 300 bp × 2 strategy on a ABI3730 sequencer operated by Sangon Biotech (Shanghai, China). DNA sequences were identified in GenBank by BLAST and by phylogenetic analysis (Zhou and Huang, 2011). Data were submitted to the GenBank under accession number MN630169-MN630173. The ITS2 sequences generated in this study and previous studies (LaJeunesse et al., 2005; Granados-Cifuentes and Rodriguez-Lanetty, 2011; Zhou et al., 2012; Kavousi et al., 2015; Ng and Ang, 2016; Wong et al., 2016) were aligned using CLUSTAL W version 1.8. A phylogenetic tree of ITS2 was constructed using the neighbor-joining algorithms within the MEGA version 7.0 (Kumar et al., 2016). A bootstrap resampling was carried out for 1,000 replicates to assess relative branch support.

Stable Isotopic Analysis

Samples for carbon isotope analysis were prepared according to the method given in Rodrigues and Grottoli (2006). The zooxanthellae and coral tissue were separated and washed by repeated centrifugation at different speeds before collection. The $\delta^{13}C$ values were finally measured on a Delta Plus XP Isotope Ratio Mass Spectrometer at the Guangzhou Institute of Geochemistry, Chinese Academy of Sciences (Guangzhou, China). The relative contribution of autotrophy versus heterotrophy for corals was determined by calculating $\Delta = \delta^{13}C_h - \delta^{13}C_z$, that is, subtracting the carbon isotopic value of the host tissue ($\delta^{13}C_h$) by that of the zooxanthellae ($\delta^{13}C_z$) (Muscatine et al., 1989). Compared with photosynthesis, heterotrophy contributes little to the fixed carbon pool when $\delta^{13}C_h$ is greater than $\delta^{13}Cz$, but contributes more when $\delta^{13}C_h$ is less than $\delta^{13}Cz$. Therefore, the relative contribution of heterotrophy to the fixed carbon of the coral increases when Δ is lower (Rodrigues and Grottoli, 2006; Schoepf et al., 2015).

Data Analysis

All experiments were repeated at least three times. Statistical analysis was carried out using the statistical package SPSS 17.0 for Windows (SPSS Inc., Chicago, IL, United States). Independent-Samples T Test was adopted to compare data at a significance level of $P < 0.05$. Descriptive statistics were expressed as mean ± standard deviation.

RESULTS

Molecular Analysis of Zooxanthellae Clades and Types

PCR amplification of ITS2 from zooxanthella of four host species produced a single amplicon of approximate 330-360 base pair (**Supplementary Figure S1**). All sequences of zooxanthella in this study were identified based on phylogenetic analysis,

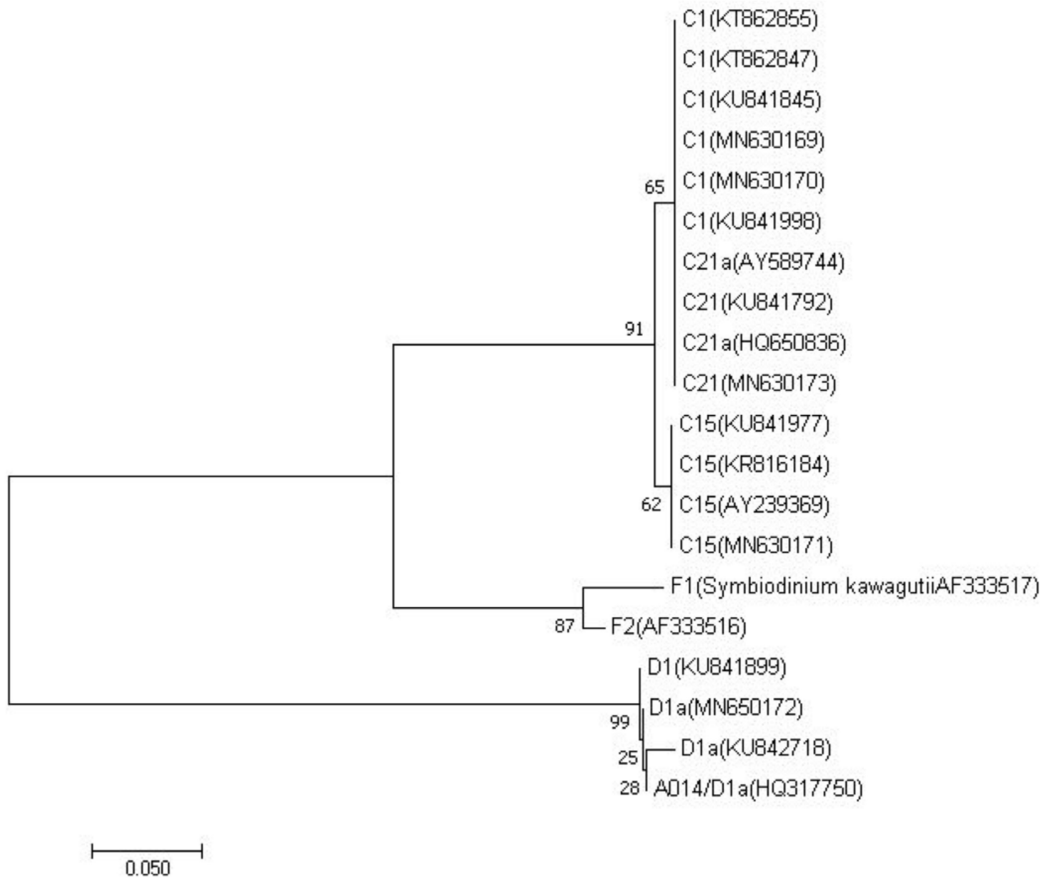

FIGURE 2 | Phylogenetic reconstruction of internal transcribed spacer 2 genes from different symbionts within clade C and D detected in the reef building corals from this study and previous studies (LaJeunesse et al., 2005; Granados-Cifuentes and Rodriguez-Lanetty, 2011; Seyfabadi et al., 2011; Zhou et al., 2012; Arif et al., 2014; Kavousi et al., 2015; Ng and Ang, 2016; Wong et al., 2016) using neighbor joining algorithms. Sister lineages to clade C represented by F1 (Symbiodinium kawagutii AF333517) and F2 (AF333516) in clade F were used as outgroups. Corresponding GenBank accession numbers are provided next to each symbiont type.

covering clades C and D (**Figure 2**). Four subfamilies were identified, namely C1, C15, C21, and D1a (**Supplementary Table S1**, Supporting Information). Among them, *M. truncata* and *P. verrucosa* were mainly associated with the zooxanthella type C1, while *P. lutea* was mainly associated with the zooxanthella type C15. Interestingly, *G. fascicularis* was mainly symbiotic with the zooxanthella type C21 in the north (site 9) but with zooxanthella type D1a in the south (site 4).

The Variation of Environmental Parameters

Supplementary Table S3 lists the variation of the environmental parameters during the survey time. Turbidity, NO_3^-, and seawater temperature were notably higher at site 9 than at sites 3 and 4 ($P < 0.05$). For instance, the average turbidity at site 9 in the north was 3.20 FTU, whereas the average turbidity at sites 3 and 4 in the south was 1.22 FTU, approximately only half as much compared with that of the north. In addition, the seawater temperature was on average 1°C higher in the north than in the south (**Supplementary Table S3**). No significant difference was noted for the variation of pH across the studied sites. The DIN and salinity were significantly higher at site 9 than at sites 3 and 4 at the depth of 3 m, but not so significant difference at 8 m. On the whole, the DIN value ranged from 4.04 to 8.02 μM.

Changes in the Photosynthesis of Corals

The average maximum relative electron transport rate ($rETR_{max}$) was 55.22 and 75.86 μmol electrons m^{-2} s^{-1} for corals in the north and south side, respectively (**Figure 3A**). For all coral species, $rETR_{max}$ was significantly lower ($P < 0.05$) in the north than in the south. The light use efficiency (α) of *P. verrucosa* was significantly lower in the north than in the south (**Figure 3B**), but the light use efficiency of the other three coral species were not distinguishable between the north and the south. The minimum saturating irradiance (E_k) of *P. lutea* and *G. fascicularis* was significantly lower in the north than in the south (**Figure 3C**).

Zooxanthellae Density and Chl a of Corals

The average density of zooxanthella was 1.35×10^6 and 1.81×10^6 cells cm^{-2} for the corals in the north and in the south, respectively (**Figure 4A**). The density of zooxanthella ranged in

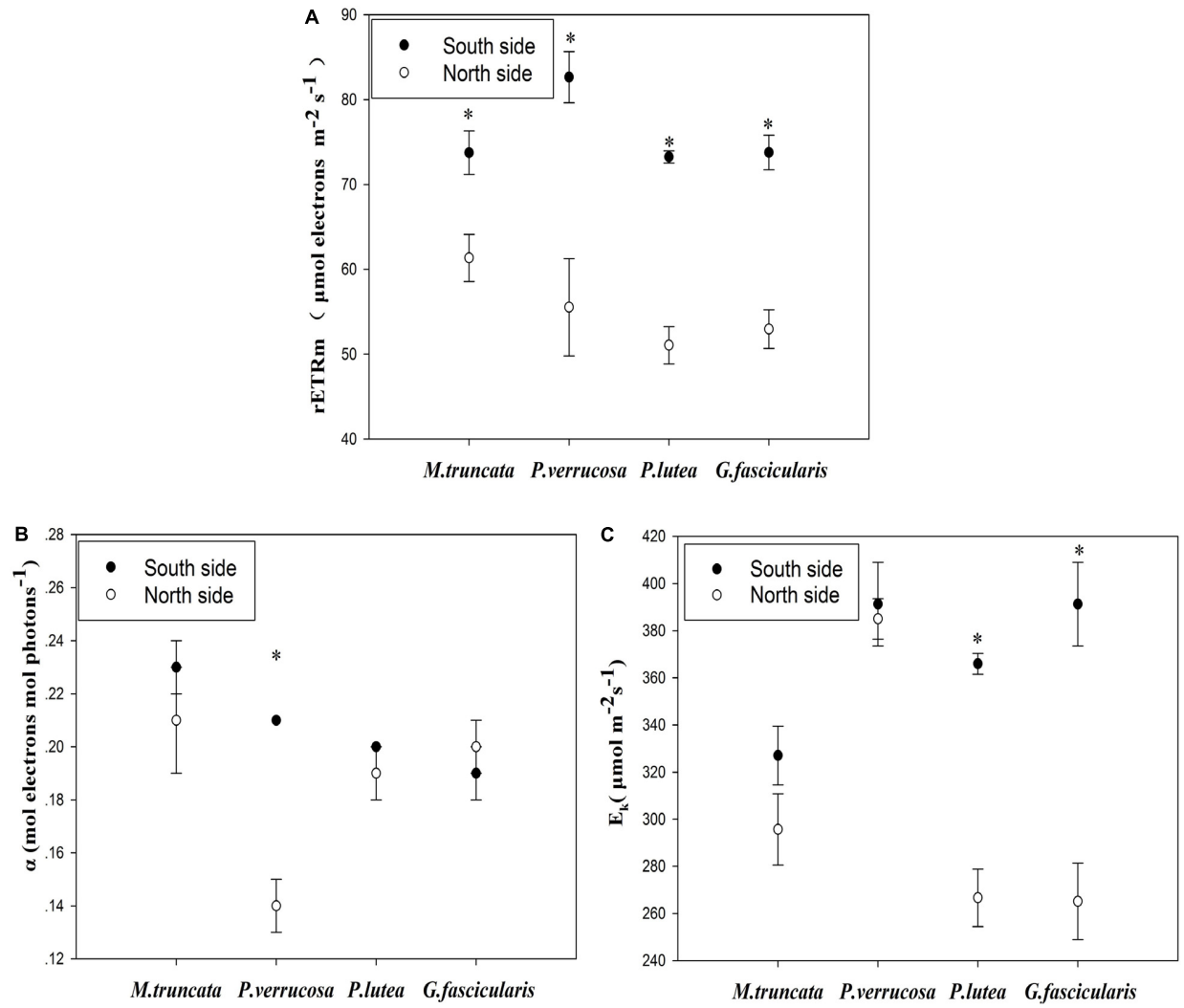

FIGURE 3 | Photosynthesis of corals. **(A)** The maximum relative electron transport rate (rETRmax). **(B)** The light use efficiency (α). **(C)** The minimum saturating irradiance (Ek).

0.36–3.08 × 10^6 cells cm^{-2}. For *P. verrucosa* and *M. truncata*, the density of zooxanthella was significantly higher in the north than in the south, but the reverse was noted for *P. lutea*. No significant difference was found in the density of zooxanthella of *G. fascicularis* between the north and the south.

The Chl a content of corals varied essentially in the same way as the density of zooxanthella. The Chl a content of *G. fascicularis* was significantly lower in the north than in the south (**Figure 4B**). Besides, the Chl a content of each zooxanthellae cell in *P. lutea* was significantly lower ($P < 0.05$) than that in all three other coral species (**Figure 4C**).

Biomass of Corals

The average biomass of corals reached 9.01 and 11.31 mg cm^{-2} in the north and in the south, respectively (**Figure 5**). The values of coral biomass ranged in 4.44–15.09 mg cm^{-2}, and the average biomass of *P. verrucosa* was 14.53 mg cm^{-2}. The biomass of *G. fascicularis* and *M. truncate* was significantly lower in the north than in the south ($P < 0.05$), but no such difference was found for *P. verrucosa* and *P. lutea*.

Stable Isotopic C of Corals

For all coral species, the average Δ ranged in 0.58–3.86 mg cm^{-2} (**Supplementary Table S2**). Specifically, the average Δ was 2.85 and 0.65 mg cm^{-2} for *P. verrucosa* and *G. fascicularis*, respectively. For *P. lutea*, Δ was significantly lower in the north than that in the south ($P < 0.05$), but the reverse was true for *M. truncata*.

Energy Reserve of Corals

As shown in **Figure 6A**, *P. verrucosa* had notably higher carbohydrate content in the north than in the south, but no such difference could be found for the other three species ($P < 0.05$). The average protein content of the corals was 0.49 and 0.94 mg

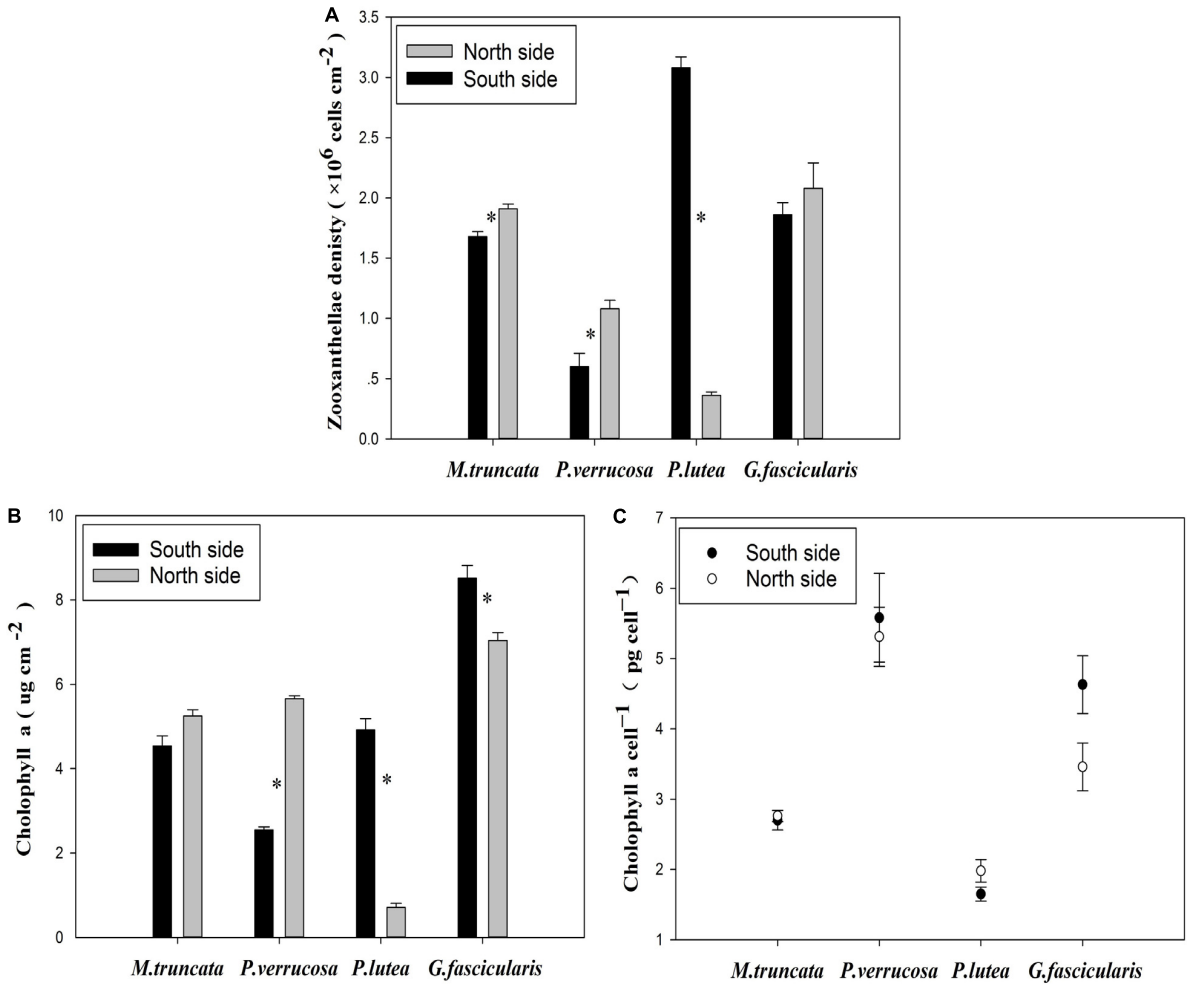

FIGURE 4 | The zooxanthellae density of corals. **(A)** Zooxanthellae density. **(B)** The content of Chl a. **(C)** The Chl a content of each zooxanthellae cell.

cm^{-2} in the north and in the south, respectively (**Figure 6B**), and all four coral species had lower protein content in the north than in the south. In addition, **Figure 6C** shows that the lipid content of *P. lutea* was significantly higher in the north than in the south ($P < 0.05$), but the reverse was true for *G. fascicularis*.

The average energy reserve of the corals was 4.40 and 4.99 mg cm^{-2} in the north and in the south, respectively (**Figure 6D**). The average energy reserve fell in the range of 2.55–8.05 mg cm^{-2}. Specifically, the average energy reserve was 7.70 and 3.07 mg cm^{-2} for *P. lutea* and *P. verrucosa*, respectively. The average energy reserve was significantly lower in the north than in the south for *G. fascicularis* ($P < 0.05$), but the reverse was true for *P. lutea* ($P < 0.05$). No significant difference was found in the average energy reserve between the north and the south for *M. truncata* and *P. verrucosa*.

SOD Enzyme Activity of Coral

The average SOD enzyme activity of the corals was 183.67 and 95.72 U mg^{-1} in the north and in the south, respectively (**Figure 7**). The SOD enzyme activity of all four corals species fell in the range of 79.82–250.45 U mg^{-1}, and was always significantly higher in the north than in the south ($P < 0.05$). In particular, the SOD enzyme activity was more than twice as much in the north than in the south for both *M. truncata* and *P. verrucosa*.

DISCUSSION

Physiological Traits and Environment Status

Significant differences were found between the north and the south for the four coral species in their photosynthetic and biochemical traits, including the $rETR_{max}$, biomass, protein content, and the SOD enzyme. The $rETR_{max}$ reflects the maximum potential photosynthetic capacity of an organism in its natural environment, and is an important indicator of the growth state of symbiotic algae (Schreiber et al., 1997; Gao and Zheng, 2010). The results clearly showed that the $rETR_{max}$ of the four coral species was significantly lower in the north than

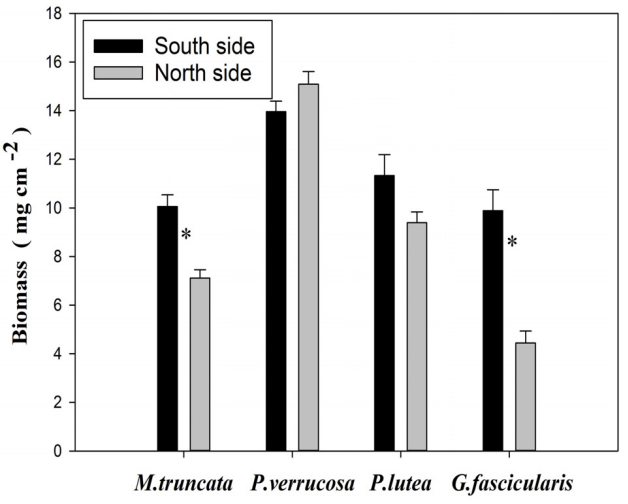

FIGURE 5 | Biomass changes of corals. *$P < 0.05$.

in the south. Down-regulation of photosynthesis or damage to the photosystem has been previously reported for the northern coral at the Florida Key Largo National Marine Sanctuary (Warner et al., 1999). In fact, impaired photosynthetic function of symbionts is one of the first consequences of thermal stress (Warner et al., 1999; Fitt et al., 2009).

Previous studies also found that exogenous antioxidant enzymes (e.g., SOD) may play an important role in suppressing reoxygenation injury (Mccord, 1985; Bhagooli and Hidaka, 2004a) for photosynthetic organisms suffering from hyperoxia, high temperature, or UV radiation (Valenzeno and Pooler, 1987; Lesser et al., 1990). The current results found that the SOD enzyme activity of the four coral species were significantly higher in the north than in the south. Bhagooli and Hidaka (2004a) demonstrated the defensive mechanism of corals that induces the synthesis of antioxidant enzymes upon oxidative stress. Thus, the higher SOD of the stony corals in the north indicates stronger stress response. The change in SOD activity has been taken as an early warning for the variation in the concentration of nutrients in the seawater hosting the coral reef (Main et al., 2010). Detrimental variation of environmental parameters such as light intensity, turbidity, and temperature will generate reactive oxygen that are harmful to biological organisms and trigger stress response in corals (Aguilera et al., 2010; Lesser, 2011). Presumably, the corals suffer from higher environmental stress in the north side of WZZ than in the south, such as high nutrient concentration, temperature perturbation, and turbidity (changes in sedimentation and suspending particles). Indeed, turbidity, nitrate concentration (NO_3^-), and seawater temperature were significantly higher in summer of 2018 at site 9 (**Supplementary Table S3**), all of which contributed to greater disturbances to the corals. The results were consistent with previous reports that showed heavier environmental stress in the north side of WZZ because of tourism development and human activities (yearly mean values of four seasons, temperature: 27.10 and 26.54°C, turbidity: 0.41 and 0.28 FTU, DIN: 3.37 and 2.87 μM for north and south side of WZZ, Li et al., 2019).

Environmental Impact on Symbiotic Relationship

The healthy growth of corals relies on the relationship between reef-building corals and the symbiotic dinoflagellates (zooxanthellae). Clade C zooxanthella is widely distributed in low-latitude tropical corals (Rodriguez-Lanetty et al., 2001; Lajeunesse et al., 2008). The current results clearly showed a dominating presence of clade C (**Supplementary Table S1**) zooxanthella at all sampled sites. However, *G. fascicularis* was mainly symbiotic with either zooxanthella C21 or D1a because *G. fascicularis* can be flexibly symbiotic with either clade C or D according to local conditions. It has been found in the waters of Singapore that symbiosis between coral and clade D decreases with rising turbidity (Cooper et al., 2011). Studies have shown that many clade C zooxanthella members are more beneficial to promoting coral growth and calcification than other zooxanthella (Mieog et al., 2009; Jones and Berkelmans, 2010). In the Indo-Pacific region, clades C and D have been reported as the dominant types of zooxanthella for corals (Baker, 2003; LaJeunesse, 2005). Besides, it has been hypothesized that corals can adapt to environmental perturbations by shifting from existing symbionts and switching to novel symbionts (Buddemeier and Fautin, 1993; Baker, 2003; Baker et al., 2004). Our results suggested that *G. fascicularis* shifted its primary zooxanthella because of local environmental stress at site 9 of WZZ, *i.e.*, from both chronic high turbidity and rising temperature.

The four coral species adopted significantly different photosynthetic physiology of symobiotic zooxanthella in response to the environmental stress in the north region of WZZ. In particular, the density of C1 zooxanthellae from *M. truncata* and *P. verrucosa* was significantly higher in the north than in the south, and the C1 zooxanthellae from *P. verrucosa* in the north had significantly lower light use efficiency. It has been proposed that elevated temperatures and UV radiation can cause photosynthesis suppression when symbiotic dinoflagellates suffer from chronic or dynamic photoinhibition (Lesser, 1996; Bhagooli and Hidaka, 2004a,b). Moreover, higher turbidity also reduces the amount of light available for photosynthesis (Pollock et al., 2014). Xing et al. (2012) showed that corals with higher density of zooxanthella exhibit stronger tolerance and anti-albinism in turbid water. Since the minimum saturating irradiance for *M. truncata* and *P. verrucosa* were the same in the north compared with in the south, the photosynthetic tolerance of *M. truncata* and *P. verrucosa* must be strong. It is possible that the zooxanthella of *M. truncata* and *P. verrucosa* in the north reversibly regulate photosynthesis between periods of high radiation and high turbidity. The decreased efficiency, as was observed, is the trade-off between protection and damage, by which extra energy can dissipate in the form of heat or through the conversion of key proteins (especially D1) of the photosystem II (PSII) (Chow, 1994; Osmond, 1994). In the case of high turbidity, sediment deposition covers corals and requires energy to be removed through energy budget allocation

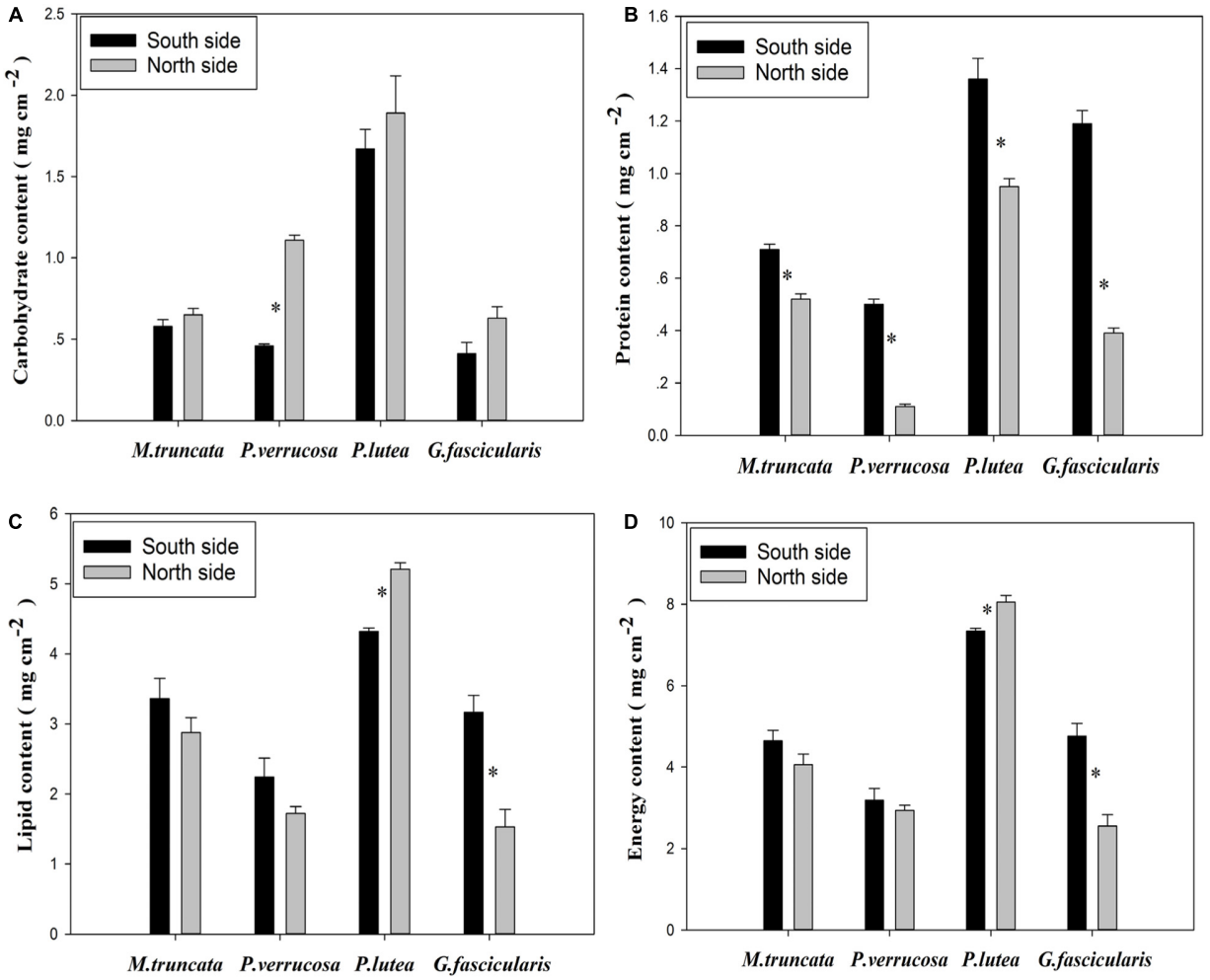

FIGURE 6 | The energy reserve of corals.

(Pollock et al., 2014), and *M. truncata* and *P. verrucosa* in the north might have increased their density of zooxanthella as a coping mechanism (Warner et al., 1999; Salih et al., 2000). The density of zooxanthellae and the Chl a content of *M. truncata* and *P. verrucosa* were indeed higher in the north than in the south. Thus, *M. truncata* and *P. verrucosa* can maintain adequate autotrophic nutrient input for growth and energy supply under the negative environment.

However, no difference was found between the north and the south in the density of zooxanthella for *G. fascicularis*, and the density of zooxanthella was significantly lower in the north than in the south for *P. lutea*. Higher sea surface temperature and photosynthetic radiation have been suggested to reduce symbiont density for some shallow-water corals (Warner et al., 1996, 1999; Brown et al., 2000). Since the minimum saturating irradiance of *P. lutea* and *G. fascicularis* was significantly reduced in the north of WZZ, the photosynthetic tolerance of *P. lutea* and *G. fascicularis* must be poor under such unfavorable environment. Some visible or UV radiations can generate oxygen radicals via photodynamic production to damage the photosystem II at the D1 protein (Valenzeno and Pooler, 1987; Richter et al., 1990; Tschiersch and Ohmann, 1993). Thus, the zooxanthella of *P. lutea* and *G. fascicularis* in the north of WZZ might have suffered from irreversible photosystem damage during periods of high radiation. Besides, *P. lutea* showed lower Chl a content of single zooxanthella cell than the other three coral species. Although the *Porites* sp. with thick tissues have shown resistance in several bleaching events (Bruno et al., 2001; Aeby et al., 2003; De'ath et al., 2012), *P. lutea* in the north side of WZZ largely released the weak C15 zooxanthellae to reduce load consumption, possibly because the symbiotic decomposition depends on the degree of stress and involves both the zooxanthella and the host (Bhagooli and Hidaka, 2004b). The collaboration between a robust host equipped with good photo-protection capacity and a robust zooxanthella with photo-physiological tolerance will constitute the best resistance to stress. That is, enhanced resistance of the zooxanthellae and/or the host can surely improve the robustness of corals against environmental disturbance (Keshavmurthy et al., 2012, 2014). Therefore, the robust host of *P. lutea* might release the weak

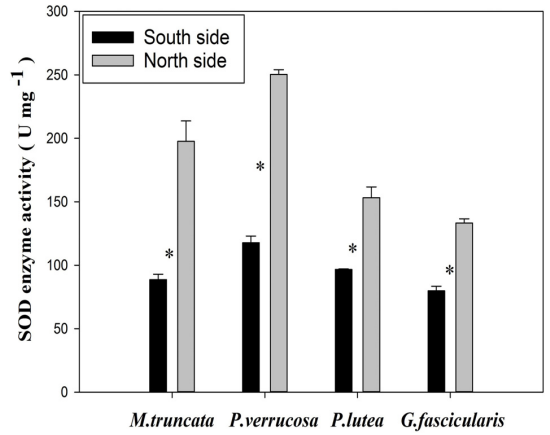

FIGURE 7 | The SOD enzyme activity of corals. *$P < 0.05$.

zooxanthellae and/or combine with other robust zooxanthellae to adapt to the unfavorable environment in the north of WZZ. As a result, both the Chl a content and the density of zooxanthella for *P. lutea* were significantly lower in the north than in the south.

Heterotrophic Energy Contribution

The host in corals may change its trophic mode to enhance resistance and sustain a positive energy balance in an environment with long-term disturbance (Anthony and Larcombe, 2000; Schoepf et al., 2015). When corals suffer from environmental stress and lose their zooxanthellae, phototrophic input attenuates and heterotrophy sometimes becomes the primary source of nutrients (Sebens et al., 1996; Houlbrèque and Ferrierpagès, 2010). The interaction between light intensity and other environmental factors (e.g., temperature, Franklin, 1994; turbidity, Anthony and Fabricius, 2000) may cause a shift in the balance between protection and damage. We measured $\Delta = \delta^{13}C_h - \delta^{13}C_z$ to evaluate the heterotrophy of the studied corals. It was found that Δ was significantly higher for *P. lutea* in the north than in the south, which corresponded to a higher contribution of heterotrophic intake in the north where the environment was adverse. In the case of *G. fascicularis*, the Δ value did not change significantly from the south to the north, indicating that the host in the north still keeps high autotrophic ability. Leal et al. (2016) found that the autotrophic intake is firstly used for the respiration consumption of the symbiont when the autotrophy of corals is limited, and the energy needed for coral growth depends mainly on heterotrophy. Therefore, by increasing the ingesting rate of heterotrophic food (e.g., suspended particulate matter, SPM), *P. lutea* can compensate for lower phototrophic input at higher turbidity to thus alleviate stress and sustain energy input.

Energy Balance and Budget

Lipids, proteins, and carbohydrates are the main energy substances of reef building corals, and they readily reflect changes in coral health (Yellowlees et al., 2008; Lesser, 2013). The synthesized carbon surplus from biological functions is the main energy source for calcification and reproduction (Castrillón-Cifuentes et al., 2017). According to our energy survey, the four identified coral species all had significantly lower protein content in the north compared with in the south, showing an adjusted energy structure. Thanks to sufficient autotrophic input after a dramatic increase in the number of zooxanthella, *M. truncata* and *P. verrucosa* had similar energy reserve in the north and in the south, but they had different energy structure. For instance, the carbohydrate content of *P. verrucosa* significantly increased in the north than that in the south. Besides, *P. lutea* seems to maintain a higher energy reserve than other coral species even though its autotrophic input is limited, probably because *P. lutea* has higher baseline energy reserve and/or the energy budget is balanced by subtraction. Grottoli et al. (2014) and Schoepf et al. (2015) showed that *Porites astreoides* keeps a high level of energy reserve in response to long-term bleaching stress, which is essential for a rapid recovery. Besides, during stressful periods, trade-off is made to maintain crucial functions by compromising obvious scope to growth (Zamer and Shick, 1987; Grottoli et al., 2014) or aberrant fecundity (Patton et al., 1977; Castrillón-Cifuentes et al., 2017), and energy budget is balanced by subtraction (Edmunds and Davies, 1989). For *G. fascicularis*, although it maintains high heterotrophic ability, its energy reserve was notably lower in the north compared with in the south side of WZZ. Therefore, its survival in the north of WZZ might be threatened in the future. The current results demonstrated different adaptive strategies of the coral species under environmental stress.

Coral Community Change

The coral coverage and the juvenile coral density in the north of WZZ were significantly lower than in the south, and at a water depth of 8 m, the diversity of coral species was significantly lower in the north than in the south (Li et al., 2019). The predominant coral communities were *Proties*, *Montipora*, *Acropora* and *Pocillopora* in the north, and *Montipora*, *Galaxea*, *Acropora,* and *Pocillopora* in the south (Li et al., 2019), probably because these species differ in their environmental tolerance and resistance to bleaching. For example, in 2003, coral bleaching mainly occurred in *Montipora* and *Pocillopora* corals, whereas the *Porties* corals that suffered from massive bleaching in the Hawaii islands were few (Aeby, 2002). In general, branching *Acropora* and *Pocillopora* are more susceptible to thermal stress than other massive growth forms of corals. Interestingly, the turbid shallow reef communities at Pulau Satumu of Singapore exhibited an unorthodox pattern of bleaching susceptibility in July 2010 (Guest et al., 2016). The unusual pattern may be ascribed to several factors, including symbiotic relationship, turbidity, and heterotrophy, prior acclimatization, all of which contributed to the high overall resistance of corals to acute thermal stress at the observed site. Some corals that have been classified as losers under climate change may be more resilient and/or adaptive than previously expected (Grottoli et al., 2014). If environmental disturbance is too stressful for the corals to adapt, changes may occur in the coral community such that species with phenotypic plasticity or genetic adaptation will gradually dominate (Bell, 2013).

However, the dominant coral species is selected by a variety of natural factors according to local conditions and is therefore not immutable.

CONCLUSION

Corals at the waters about the WZZ suffer from greater environmental stress in the north than in the south, including stronger radiation, higher turbidity, and more suspended particles. As a result, significant differences were found for the four dominant coral species in their physiological and biochemical characteristics, including $rETR_{max}$, SOD, and protein content, between the north and the south. The physiological states were healthier in the south than in the north, and matched the spatial variation of the coral communities.

The four dominant reef-building corals in the north responded to complex environmental stress and showed different adaptation strategies. *M. truncata* and *P. verrucosa* increase the density of symbiotic zooxanthella to balance the decline of photosynthetic efficiency and supply energy. *P. lutea* releases a number of zooxanthellaes to improve heterotrophic feeding, and/or change the energy budget mode to maintain high energy reserve. *G. fascicularis* alters its primary symbiotic zooxanthella type and hosts to maintain high heterotrophy. These corals maintain their presence by adopting their own successful resistance mechanisms at symbiotic relationship and energy metabolism level over time against long-term disturbances such as elevated turbidity or temperature.

DATA AVAILABILITY STATEMENT

These DNA data were submitted to the GenBank under accession number MN630169–MN630173.

ETHICS STATEMENT

All animal-involving experiments of this study were approved by the Ethics Committee of Hainan University and local government.

AUTHOR CONTRIBUTIONS

HX and XL wrote the manuscript. HX, BF, MX, YR, JX, and YZ performed the research. HX analyzed the data. HX, XL, and AW designed the research. All authors reviewed the manuscript.

FUNDING

This work was financially supported by National Key R&D Program of China (2019YFD0901304), the National Natural Science Foundation of China (41476134) and the Foundation of Hainan University [KYQD(ZR)1805].

ACKNOWLEDGMENTS

The authors were grateful for constructivs suggestions and technical support from all the members of the laboratory and support from Sanya Wuzhizhou Island Tourism Zone, Hainan Wuzhizhou Tourism Development Co., Ltd.

SUPPLEMENTARY MATERIAL

The Supplementary Material for this article can be found online at: https://www.frontiersin.org/articles/10.3389/fphys.2020.00390/full#supplementary-material

REFERENCES

Aeby, G. (2002). Trade-offs for the butterflyfish, chaetodon multicinctus, when feeding on coral prey infected with trematode metacercariae. *Behav. Ecol. Sociobiol.* 52, 158–165. doi: 10.1007/s00265-002-0490-2

Aeby, G. S., Kenyon, J. C., and Maragos, J. E. (2003). First record of mass coral bleaching in the Northwestern Hawaiian Islands. *Coral Reefs* 22, 256–256. doi: 10.1007/s00338-003-0309-2

Aguilera, A., Elena González-Toril, L., Souza-Egipsy, V., Amaral-Zettler, L., Zettler, E., and Amils, R. (2010). "Phototrophic biofilms from río tinto, an extreme acidic environment, the prokaryotic component," in *Microbial Mats. Cellular Origin, Life in Extreme Habitats and Astrobiology*, Vol. 14, eds J. Seckbach and A. Oren (Dordrecht: Springer).

Anthony, K. R., and Fabricius, K. E. (2000). Shifting roles of heterotrophy and autotrophy in coral energetics under varying turbidity. *J. Exp. Mar. Biol. Ecol.* 252, 221–253. doi: 10.1016/s0022-0981(00)00237-9

Anthony, K. R., and Larcombe, P. (2000). "Coral reefs in turbid waters: sediment-induced stresses in corals and likely mechanisms of adaptation," in *Proceedings of the International Coral Reef Symposium Ninth International Coral Reef Symposium* (Bali: ICRS).

Arif, C., Daniels, C., Bayer, T., Banguera-Hinestroza, E., Barbrook, A., and Howe, C. J. (2014). Assessing Symbiodinium diversity in scleractinian corals via next-generation sequencing-based genotyping of the its2 rdna region. *Mol. Ecol.* 23, 4418–4433. doi: 10.1111/mec.12869

Baker, A. C. (2003). Flexibility and specificity in coral-algal symbiosis: diversity, ecology, and biogeography of *Symbiodinium*. *Ann. Rev. Ecol. Evol. Syst.* 34, 661–689. doi: 10.1146/annurev.ecolsys.34.011802.132417

Baker, A. C., Starger, C. J., Mcclanahan, T. R., and Glynn, P. W. (2004). Coral reefs: corals' adaptive response to climate change. *Nature* 430:741.

Bell, G. (2013). Evolutionary rescue and the limits of adaptation. *Philos. Trans. R. Soc. Lond.* 368:20120080. doi: 10.1098/rstb.2012.0080

Bhagooli, R., and Hidaka, M. (2004a). Photoinhibition, bleaching susceptibility and mortality in two scleractinian corals, *Platygyra ryukyuensis* and *Stylophora pistillata*, in response to thermal and light stresses. *Comp. Biochem. Physiol. A. Mol. Integr. Physiol.* 137, 547–555. doi: 10.1016/j.cbpb.2003.11.008

Bhagooli, R., and Hidaka, M. (2004b). Release of zooxanthellae with intact photosynthetic activity by the coral *Galaxea fascicularis* in response to high temperature stress. *Mar. Biol.* 145, 329–337.

Blackall, L. L., Wilson, B., and Van Oppen, A. J. H. (2015). Coral-the world's most diverse symbiotic ecosystem. *Mol. Ecol.* 24, 5330–5347. doi: 10.1111/mec.13400

Brown, B. E., Dunne, R. P., and Warner, M. E. (2000). Damage and recovery of *Photosystem* II during a manipulative field experiment on solar bleaching in the coral *Goniastrea aspera*. *Mar. Ecol. Progress Series* 195, 117–124. doi: 10.3354/meps195117

Brown, B. E., and Howard, L. S. (1985). Assessing the effects of "stress" on reef corals. *Adv. Mar. Biol.* 22, 1–63. doi: 10.1016/s0065-2881(08)60049-8

Bruno, J., Siddon, C., and Witman, J. (2001). El Nino related coral bleaching in Palau, western Caroline Islands. *Coral Reefs* 20, 127–136. doi: 10.1007/s003380100151

Bruno, J. F., Petes, L. E., Harvell, C. D., and Hettinger, A. (2003). Nutrient enrichment can increase the severity of coral diseases. *Ecol. Lett.* 6, 1056–1061. doi: 10.1046/j.1461-0248.2003.00544.x

Buddemeier, R. W., and Fautin, D. G. (1993). Coral bleaching as an adaptive mechanism: a testable hypothesis. *Bioscience* 43, 320–326. doi: 10.2307/1312064

Castrillón-Cifuentes, A. L., Lozano-Cortés, D. F., and Zapata, F. A. (2017). Effect of short-term subaerial exposure on the cauliflower coral, Pocillopora damicornis, during a simulated extreme low-tide event. *Coral Reefs* 36, 1–14.

Chow, W. S. (1994). Photoprotetion and photoinhibitory damage. *Adv. Mol. Cell Biol.* 10, 151–196. doi: 10.1016/s1569-2558(08)60397-5

Cooper, T. F., Berkelmans, R., Ulstrup, K. E., Weeks, S., Radford, B., and Jones, A. M. (2011). Environmental factors controlling the distribution of symbiodinium harboured by the coral acropora millepora on the Great Barrier Reef. *PLoS One* 6:e25536. doi: 10.1371/journal.pone.0025536

Costa, O. S., Leão, Z. M. A. N., Nimmo, M., and Attrill, M. J. (2000). Nutrification impacts on coral reefs from northern bahia, brazil. *Hydrobiologia* 440, 307–315. doi: 10.1007/978-94-017-1982-7_28

De'ath, G., Fabricius, K. E., and Sweatman, H. (2012). The 27-year decline of coral cover on the Great Barrier Reef and its causes. *Proc. Natl. Acad. Sci. U.S.A.* 109, 17995–17999. doi: 10.1073/pnas.1208909109

Dubois, M., Gilles, K. A., Hamilton, J. K., Rebers, P. A., and Smith, F. (1956). Colorimetric method for determination of sugars and related substances. *Anal. Chem.* 28, 350–356. doi: 10.1021/ac60111a017

Edmunds, P. J., and Davies, P. S. (1989). An energy budget for *Porites porites* (scleractinia), growing in a stressed environment. *Coral Reefs* 8, 37–43. doi: 10.1007/bf00304690

Fabricius, K. E. (2005). Effects of terrestrial runoff on the ecology of corals and coral reefs: review and synthesis. *Mar. Pollut. Bull.* 50, 125–146. doi: 10.1016/j.marpolbul.2004.11.028

Fabricius, K. E., Hoegh-Guldberg, O., and Johnson, J. E. (2007). *Vulnerability of Coral Reefs Of The Great Barrier Reef To Climate Change*. Available online at: http://hdl.handle.net/11017/549 (accessed October, 2019).

Fitt, W. K., Gates, R. D., Hoegh-Guldberg, O., Bythell, J. C., Jatkar, A., and Grottoli, A. G. (2009). Response of two species of indo-pacific corals, *Porites cylindrica* and *Stylophora pistillata*, to short-term thermal stress: the host does matter in determining the tolerance of corals to bleaching. *J. Exp. Mar. Biol. Ecol.* 373, 102–110. doi: 10.1016/j.jembe.2009.03.011

Fitt, W. K., McFarland, F. K., Warner, M. E., and Chilcoat, G. C. (2000). Seasonal patterns of tissue biomass and densities of symbiotic dinoflagellates in reef corals and relation to coral bleaching. *Limnol. Oceanogr.* 45, 677–685. doi: 10.4319/lo.2000.45.3.0677

Franklin, L. A. (1994). The effects of temperature acclimation on the photoinhibitory responses of ulva rotundata blid. *Planta* 192, 324–331.

Gao, K. S., and Zheng, Y. Q. (2010). Combined effects of ocean acidification and solar UV radiation on photosynthesis, growth, pigmentation and calcification of the coralline alga *Corallina sessilis* (Rhodophyta). *Glob. Chang. Biol.* 16, 2388–2398. doi: 10.1111/j.1365-2486.2009.02113.x

Granados-Cifuentes, C., and Rodriguez-Lanetty, M. (2011). The use of high-resolution melting analysis for genotyping *Symbiodinium* strains: a sensitive and fast approach. *Mol. Ecol. Resour.* 11, 394–399. doi: 10.1111/j.1755-0998.2010.02933.x

Grottoli, A. G., Rodrigues, L. J., and Juarez, C. (2004). Lipids and stable carbon isotopes in two species of Hawaiian corals, *Porites compressa* and *Montipora verrucosa*, following a bleaching event. *Mar. Biol.* 145, 621–631.

Grottoli, A. G., Rodrigues, L. J., and Palardy, J. E. (2006). Heterotrophic plasticity and resilience in bleached corals. *Nature* 440:1186. doi: 10.1038/nature04565

Grottoli, A. G., Warner, M. E., Levas, S. J., Aschaffenburg, M. D., Schoepf, V., Mcginley, M., et al. (2014). The cumulative impact of annual coral bleaching can turn some coral species winners into losers. *Glob. Chang. Biol.* 20, 3823–3833. doi: 10.1111/gcb.12658

Guest, J. R., Tun, K., and Low, J. (2016). 27 years of benthic and coral community dynamics on turbid, highly urbanised reefs off singapore. *Sci. Rep.* 6: 36260.

Hennige, S., Smith, D., Perkins, R., Consalvey, M., Paterson, D., and Suggett, D. (2008). Photoacclimation, growth and distribution of massive coral species in clear and turbid waters. *Mar. Ecol. Prog.* 369, 77–88. doi: 10.3354/meps07612

Houlbrèque, F., and Ferrierpagès, C. (2010). Heterotrophy in tropical scleractinian corals. *Biol. Rev. Camb. Philos. Soc.* 84, 1–17. doi: 10.1111/j.1469-185x.2008.00058.x

Huang, H., Dong, Z., Huang, L., Yang, J., Di, B., and Li, Y. (2011). Latitudinal variation in algal symbionts within the scleractinian coral *Galaxea fascicularis* in the South China Sea. *Mar. Biol. Res.* 7, 208–211. doi: 10.1080/17451000.2010.489616

Hughes, T. P., Anderson, K. D., Connolly, S. R., Heron, S. F., Kerry, J. T., and Lough, J. M. (2018). Spatial and temporal patterns of mass bleaching of corals in the anthropocene. *Science* 359, 80–83. doi: 10.1126/science.aan8048

Hughes, T. P., Graham, N. A., Jackson, J. B., Mumby, P. J., and Steneck, R. S. (2010). Rising to the challenge of sustaining coral reef resilience. *Trends Ecol. Evol.* 25, 633–642. doi: 10.1016/j.tree.2010.07.011

Hughes, T. P., Huang, H., and Young, M. A. L. (2013). The Wicked problem of China's disappearing coral reefs. *Conserv. Biol.* 27, 261–269. doi: 10.1111/j.1523-1739.2012.01957.x

Humphrey, C., Weber, M., Lott, C., Cooper, T., and Fabricius, K. (2008). Effects of suspended sediments, dissolved inorganic nutrients and salinity on fertilisation and embryo development in the coral *Acropora millepora* (ehrenberg, 1834). *Coral Reefs* 27, 837–850. doi: 10.1007/s00338-008-0408-1

Jassby, A. D., and Platt, T. (1976). Mathematical formulation of the relationship between photosynthesis and light for phytoplankton. *Limnol. Oceanogr.* 21, 540–547. doi: 10.4319/lo.1976.21.4.0540

Jones, A., and Berkelmans, R. (2010). Potential costs of acclimatization to a warmer climate: growth of a reef coral with heat tolerant vs. sensitive symbiont types. *PLoS One* 5:e10437. doi: 10.1371/journal.pone.0010437

Kavousi, J., Reimer, J. D., Tanaka, Y., and Nakamura, T. (2015). Colony-specific investigations reveal highly variable responses among individual corals to ocean acidification and warming. *Mar. Environ. Res.* 109, 9–20. doi: 10.1016/j.marenvres.2015.05.004

Keshavmurthy, S., Hsu, C. M., Kuo, C. Y., Meng, P. J., Wang, J. T., and Chen, C. A. (2012). Symbiont communities and host genetic structure of the brain coral *Platygyra verweyi*, at the outlet of a nuclear power plant and adjacent areas. *Mol. Ecol.* 21, 4393–4407. doi: 10.1111/j.1365-294x.2012.05704.x

Keshavmurthy, S., Meng, P. J., Wang, J. T., Kuo, C. Y., Yang, S. Y., Hsu, C. M., et al. (2014). Can resistant coral-Symbiodinium associations enable coral communities to survive climate change? A study of a site exposed to long-term hot water input. *PeerJ* 2:e327. doi: 10.7717/peerj.327

Kumar, S., Stecher, G., and Tamura, K. (2016). MEGA7: molecular evolutionary genetics analysis version 7.0 for bigger datasets. *Mol. Biol. Evol.* 33, 1870–1874. doi: 10.1093/molbev/msw054

Kuo, C. Y., Yuen, Y. S., Meng, P. J., Ho, P. H., Wang, J. T., and Liu, P. J. (2012). Recurrent disturbances and the degradation of hard coral communities in Taiwan. *PLoS One* 7:e44364. doi: 10.1371/journal.pone.0044364

Ladner, J. T., Barshis, D. J., and Palumbi, S. R. (2012). Protein evolution in two co-occurring types of symbiodinium: an exploration into the genetic basis of thermal tolerance in symbiodinium clade D. *BMC Evol. Biol.* 12:217. doi: 10.1186/1471-2148-12-217

LaJeunesse, T. (2002). Diversity and community structure of symbiotic dinoflagellates from Caribbean coral reefs. *Mar. Biol.* 141, 387–400. doi: 10.1007/s00227-002-0829-2

LaJeunesse, T. C. (2005). "Species" radiations of symbiotic dinoflagellates in the Atlantic and Indo-Pacific since the Miocene-Pliocene transition. *Mol. Biol. Evol.* 22, 570–581. doi: 10.1093/molbev/msi042

Lajeunesse, T. C., Bonilla, H. R., Warner, M. E., Wills, M., Schmidt, G. W., and Fitt, W. K. (2008). Specificity and stability in high latitude eastern pacific coral-algal symbioses. *Limnol. Oceanogr.* 53, 719–727. doi: 10.4319/lo.2008.53.2.0719

LaJeunesse, T. C., Lee, S., Bush, S., and Bruno, J. F. (2005). Persistence of non-Caribbean algal symbionts in Indo-Pacific mushroom corals released to Jamaica 35 years ago. *Coral Reefs* 24, 157–159. doi: 10.1007/s00338-004-0436-4

Lajeunesse, T. C., Smith, R. T., Finney, J., and Oxenford, H. (2009). Outbreak and persistence of opportunistic symbiotic dinoflagellates during the 2005 Caribbean mass coral \"bleaching\" event. *Proc. R. Soc. B Biol. Sci.* 276, 4139–4148. doi: 10.1098/rspb.2009.1405

Lambo, A. L., and Ormond, R. F. (2006). Continued post-bleaching decline and changed benthic community of a Kenyan coral reef. *Mar. Pollut. Bull.* 52, 1617–1624. doi: 10.1016/j.marpolbul.2006.05.028

Leal, M. C., Ferrier-Pagès, C., and Petersen, D. (2016). Coral aquaculture: applying scientific knowledge to ex situ production. *Rev. Aquacult.* 8, 136–153. doi: 10.1111/raq.12087

Lei, X. M., Huang, H., Wang, H. J., Xiu-Bao, L. I., and Lian, J. S. (2008). A preliminary study of effect of elevated temperature stress on three reef corals and their zooxanthellae. *J. Trop. Oceanogr. Chin.* 27, 55–59.

Lesser, M. P. (1996). Elevated temperatures and ultraviolet radiation cause oxidative stress and inhibit photosynthesis in symbiotic dinoflagellates. *Limnol. Oceanogr.* 41, 271–283. doi: 10.4319/lo.1996.41.2.0271

Lesser, M. P. (2011). "Coral bleaching: causes and mechanisms," in *Coral Reefs: An Ecosystem In Transition*, eds Z. Dubinsky and N. Stambler (Dordrecht: Springer), 405–419. doi: 10.1007/978-94-007-0114-4_23

Lesser, M. P. (2013). Using energetic budgets to assess the effects of environmental stress on corals: are we measuring the right things? *Coral Reefs* 32, 25–33. doi: 10.1007/s00338-012-0993-x

Lesser, M. P., Stochaj, W. R., Tapley, D. W., and Shick, J. M. (1990). Bleaching in coral reef anthozoans: effects of irradiance, ultraviolet radiation, and temperature on the activities of protective enzymes against active oxygen. *Coral Reefs* 8, 225–232. doi: 10.1007/bf00265015

Li, X. B., Huang, H., Qu, F. U., Dong, Z. J., and Huang, L. M. (2006). Effects of temperature on bleaching of *Acropora nasuta*. *J. Trop. Oceanogr. Chin.* 25, 58–62.

Li, X. B., Li, Y. C., and Xu, Q. (2019). *Current Situation, Ecological Restoration And Protection Measures Of Coral Reefs in Wuzhizhou Island, Sanya*. Beijing: Chinese Science press.

Li, X. B., Liu, S., Huang, H., Huang, L. M., Jing, Z. Y., and Zhang, C. L. (2012). Coral bleaching caused by an abnormal water temperature rise at Luhuitou fringing reef, Sanya Bay, China. *Aquat. Ecosyst. Health Manag.* 15, 227–233. doi: 10.1080/14634988.2012.687651

Li, X. B., Wang, D. R., Hui, H., Zhang, J., Lian, J. S., Yuan, X. C., et al. (2015). Linking benthic community structure to terrestrial runoff and upwelling in the coral reefs of northeastern hainan island. *Estuar. Coast. Shelf Sci.* 156, 92–102. doi: 10.1016/j.ecss.2014.09.021

Lirman, D., and Manzello, D. (2009). Patterns of resistance and resilience of the stress-tolerant coral Siderastrea radians (pallas) to sub-optimal salinity and sediment burial. *J. Exp. Mar. Biol. Ecol.* 369, 72–77. doi: 10.1016/j.jembe.2008.10.024

Loch, K., Loch, W., Schuhmacher, H., and See, W. R. (2002). Coral recruitment and regeneration on a maldivian reef 21 months after the coral bleaching event of 1998. *Mar. Ecol.* 23, 219–236. doi: 10.1046/j.1439-0485.2002.02773.x

Main, W. P. L., Ross, C., and Bielmyer, G. K. (2010). Copper accumulation and oxidative stress in the sea anemone, *Aiptasia pallida*, after waterborne copper exposure. *Comparat. Biochem. Physiol. Toxicol. Pharmacol. CBP* 151, 216–221. doi: 10.1016/j.cbpc.2009.10.008

Marubini, F., and Davies, P. S. (1996). Nitrate increases zooxanthellae population density and reduces skeletogenesis in corals. *Mar. Biol.* 127, 319–328. doi: 10.1007/bf00942117

Mccord, J. M. (1985). Oxygen-derived free radicals in postischemic tissue injury. *N. Engl. J. Med.* 312, 159–163. doi: 10.1056/nejm198501173120305

Mieog, J. C., Olsen, J. L., Berkelmans, R., Bleulermartinez, S. A., Willis, B. L., and Oppen, M. J. H. V. (2009). The roles and interactions of symbiont, host and environment in defining coral fitness. *PLoS One* 4:e6364. doi: 10.1371/journal.pone.0006364

Muscatine, L., Porter, J. W., and Kaplan, I. R. (1989). Resource partitioning by reef corals as determined from stable isotope composition. *Mar. Biol.* 100, 185–193. doi: 10.1007/bf00391957

Ng, T. Y., and Ang, P. (2016). Low symbiont diversity as a potential adaptive strategy in a marginal non-reefal environment: a case study of corals in Hong Kong. *Coral Reefs* 35, 941–957. doi: 10.1007/s00338-016-1458-4

Osmond, C. B. (1994). "What is photoinhibition: some insights from comparisons of sun and shade plants?," in *Photoinhibition of Photosynthesis: From Molecular Mechanisms to the Field*, eds N. K. Baker and J. R. Bowyer (Oxford: BIOS Scientific Publishers), 95–110.

Patton, J. S., Abraham, S., and Benson, A. A. (1977). Lipogenesis in the intact coral Pocillopora capitata and its isolated zooxanthellae: evidence for a light-driven carbon cycle between symbiont and host. *Mar. Biol.* 44, 235–247. doi: 10.1007/bf00387705

Pollock, F. J., Lamb, J. B., Field, S. N., Heron, S. F., Schaffelke, B., Shedrawi, G., et al. (2014). Sediment and turbidity associated with offshore dredging increase coral disease prevalence on nearby reefs. *PLoS One* 9:e102498. doi: 10.1371/journal.pone.0102498

Richter, M., Rühle, W., and Wild, A. (1990). Studies on the mechanism of photosystem ? photoinhibition ?. a two-step degradation of D1-protein. *Photosynth. Res.* 24, 229–235.

Rodrigues, L. J., and Grottoli, A. G. (2006). Calcification rate and the stable carbon, oxygen, and nitrogen isotopes in the skeleton, host tissue, and zooxanthellae of bleached and recovering Hawaiian corals. *Geochim. Cosmochim. Acta* 70, 2781–2789. doi: 10.1016/j.gca.2006.02.014

Rodrigues, L. J., and Grottoli, A. G. (2007). Energy reserves and metabolism as indicators of coral recovery from bleaching. *Limnol. Oceanogr.* 52, 1874–1882. doi: 10.4319/lo.2007.52.5.1874

Rodriguez-Lanetty, M., Loh, W., Carter, D., and Hoegh-Guldberg, O. (2001). Latitudinal variability in symbiont specificity within the widespread scleractinian coral *Plesiastrea versipora*. *Mar. Biol.* 138:1175. doi: 10.1007/s002270100536

Salih, A., Larkum, A., Cox, G., Kühl, M., and Hoeghguldberg, O. (2000). Fluorescent pigments in corals are photoprotective. *Nature* 408, 850–853. doi: 10.1038/35048564

Schoepf, V., Grottoli, A. G., Levas, S. J., Aschaffenburg, M. D., Baumann, J. H., and Matsui, Y. (2015). Annual coral bleaching and the long-term recovery capacity of coral. *Proc. Biol. Sci.* 282:1819.

Schreiber, U., Gademann, R., Ralph, P. J., and Larkum, A. W. D. (1997). Assessment of photosynthetic performance of prochloron in *Lissoclinum patella* in hospite by chlorophyll fluorescence measurements. *Plant Cell Physiol.* 38, 945–951. doi: 10.1093/oxfordjournals.pcp.a029256

Schreiber, U., Schliwa, U., and Bilger, W. (1986). Continuous recording of photochemical and non-photochemical chlorophyll fluorescence quenching with a new type of modulation fluorometer. *Photosynth. Res.* 10, 51–62. doi: 10.1007/bf00024185

Sebens, K. P., Vandersall, K. S., and Savina, L. A. (1996). Zooplankton capture by two scleractinian corals, *Madracis mirabilis* and *Montastrea cavernosa*, in a field enclosure. *Mar. Biol.* 127, 303–317. doi: 10.1007/bf00942116

Seyfabadi, J., Shokri, N., and Fatemi, M. R. (2011). Spatial variation of symbiotic Dinoflagellates on coral reefs of the northern Persian Gulf. *Iran. J. Fisher. Sci.* 10, 475–486.

Smith, P. K., Krohn, R. I., Hermanson, G. T., Mallia, A. K., Gartner, F. H., and Provenzano, M. D. (1985). Measurement of protein using bicinchoninic acid. *Anal. Biochem.* 150, 76–85. doi: 10.1016/0003-2697(85)90442-7

Suggett, D. J., Kikuchi, R. K. P., Oliveira, M. D. M., Spanó, S., Carvalho, R., and Smith, D. J. (2012). Photobiology of corals from brazil's near-shore marginal reefs of abrolhos. *Mar. Biol.* 159, 1461–1473. doi: 10.1007/s00227-012-1925-6

Tkachenko, K. S., and Soong, K. (2017). Dongsha atoll: a potential thermal refuge for reef-building corals in the South China Sea. *Mar. Environ. Res.* 127, 112–125.

Tschiersch, H., and Ohmann, E. (1993). Photoinhibition in *Euglena gracilis*: involvement of reactive oxygen species. *Planta* 191, 316–323.

Valenzeno, D. P., and Pooler, J. P. (1987). Photodynamic action. *Bioscience* 37, 270–276.

Warner, M. E., Fitt, W. K., and Schmidt, G. W. (1996). The effects of elevated temperature on the photosynthetic efficiency of zooxanthellae in hospite from four different species of reef coral: a novel approach. *Plant Cell Environ.* 19, 291–299. doi: 10.1111/j.1365-3040.1996.tb00251.x

Warner, M. E., Fitt, W. K., and Schmidt, G. W. (1999). Damage to photosystem ? in symbiotic dinoflagellates: a determinant of coral bleaching. *Proc. Natl. Acad. Sci. U.S.A.* 96, 8007–8012. doi: 10.1073/pnas.96.14.8007

Wong, J. C., Thompson, P., Xie, J. Y., Qiu, J. W., and Baker, D. M. (2016). Symbiodinium clade C generality among common scleractinian corals in subtropical Hong Kong. *Reg. Stud. Mar. Sci.* 8, 439–444. doi: 10.1016/j.rsma.2016.02.005

Xie, J. Y., Lau, D. C. C., Kei, K., Yu, V. P. F., Chow, W. K., and Qiu, J. W. (2017). The 2014 summer coral bleaching event in subtropical Hong Kong. *Mar. Pollut. Bull.* 124, 653–659. doi: 10.1016/j.marpolbul.2017.03.061

Xing, S., Tan, Y. H., Zhou, L. B., Lian, X. P., and Huang, L. M. (2012). Effects of water turbidity on the symbiotic zooxanthella of hermatypic corals. *Chin. Sci. Bull.* 57:348.

Yellowlees, D., Rees, T. A. V., and Leggat, W. (2008). Metabolic interactions between algal symbionts and invertebrate hosts. *Plant Cell Environ.* 31, 679–694.

Yu, K. F. (2012). Coral reefs in the South China Sea: their response to and records on past environmental changes. *Sci. China Earth Sci.* 55, 1217–1229.

Zamer, W. E., and Shick, J. M. (1987). Physiological energetics of the intertidal sea anemone *Anthopleura elegantissima*. *Mar. Biol.* 93, 481–491.

Zhang, Q. M., Shi, Q., Chen, G., Fong, T. C. W., Wong, D. C. C., Huang, H., et al. (2006). Status monitoring and health assessment of *Luhuitou fringing* reef of Sanya, Hainan, China. *Chin. Sci. Bull.* 3, 81–88.

Zhou, G. W., and Huang, H. (2011). Low genetic diversity of symbiotic dinoflagellates (Symbiodinium) in scleractinian corals from tropical reefs in southern Hainan Island, China. *J. Syst. Evol.* 49, 598–605.

Zhou, G. W., Huang, H., Lian, J. S., Zhang, C. L., and Li, X. B. (2012). Habitat correlation of *Symbiodinium* diversity in two reef-building coral species in an upwelling region, eastern Hainan Island, China. *J. Mar. Biol. Assoc. U.K.* 92, 1309–1316.

Conflict of Interest: The authors declare that the research was conducted in the absence of any commercial or financial relationships that could be construed as a potential conflict of interest.

frontiers in Physiology

ORIGINAL RESEARCH
published: 17 June 2020
doi: 10.3389/fphys.2020.00615

Diazotroph Diversity Associated With Scleractinian Corals and Its Relationships With Environmental Variables in the South China Sea

Jiayuan Liang[1,2,3], Kefu Yu[1,2,3†], Yinghui Wang[1,2,3], Xueyong Huang[1,2,3], Wen Huang[1,2,3], Zhenjun Qin[1,2,3], Guanghua Wang[1,2,3], Hongfei Su[1,2,3], Biao Chen[1,2,3] and Zhengchao Wu[4]*

[1] Coral Reef Research Center of China, Guangxi University, Nanning, China, [2] Guangxi Laboratory on the Study of Coral Reefs in the South China Sea, Nanning, China, [3] School of Marine Sciences, Guangxi University, Nanning, China, [4] State Key Laboratory of Tropical Oceanography (LTO), South China Sea Institute of Oceanology, Chinese Academy of Sciences, Guangzhou, China

Coral reef ecosystems cannot operate normally without an effective nitrogen cycle. For oligotrophic coral reef areas, coral-associated diazotrophs are indispensable participants in the nitrogen cycle. However, the distribution of these diazotrophs and the correlation with the physical and chemical variables of the surrounding seawater remain unclear. To this end, 68 scleractinian coral colonies were sampled from 6 coral reef areas with different environmental variables in the South China Sea to investigate the composition of associated diazotrophs based on *nifH* gene amplification using high-throughput sequencing. The six coral reefs can be clearly divided into two types (fringing reefs and island reefs), are affected by varying degrees of human activities and are located at different latitudes from 9°20'06"N to 22°34'55"N with different seawater temperatures. Alpha- and beta-diversity analyses showed that the distribution of diazotrophs among coral reefs exhibited significant geographical fluctuations ($p \leq 0.05$) and non-significant interspecific fluctuations ($p > 0.05$). The predominant bacterial phyla included Proteobacteria, Chlorobi, Cyanobacteria, and two unclassified phyla. Chlorobi exhibited a relative abundance of 47–96% in coral samples from the high-latitude Daya Bay fringing reef affected by eutrophication. Unclassified bacteria II, with a relative abundance of 28–87%, was found in all coral samples from the midlatitude Luhuitou fringing reef affected by eutrophication. However, unclassified bacteria I and Proteobacteria dominated (>80% relative abundance) in most of the coral samples from the Weizhou Island fringing reef, which is far from land, and three island reefs (Huangyan Island, Xinyi Reef, and Sanjiao Reef) at relatively low latitudes. At the genus level, some core diazotrophs were found in different coral sample groups. In addition, correlation analysis with various environmental variables revealed that the variables were positively or negatively correlated with different diazotrophic genera. Coral-associated diazotrophs were common among coral individuals. However, their composition was closely related to the different environmental variables. These results provide insights into the geographical distribution characteristics of coral-associated diazotrophs and their evolutionary trends in response to environmental change in the South China Sea.

Keywords: coral reef ecosystem, nitrogen fixation, *nifH* gene, geographical differences, different latitudes

OPEN ACCESS

Edited by:
Silvia Franzellitti,
University of Bologna, Italy

Reviewed by:
Tali Mass,
University of Haifa, Israel
Madeleine J. H. Van Oppen,
University of Melbourne, Australia

****Correspondence:***
Kefu Yu
kefuyu@scsio.ac.cn

†ORCID:
Kefu Yu
orcid.org/0000-0003-3409-9945

Specialty section:
This article was submitted to Aquatic Physiology, a section of the journal Frontiers in Physiology

Received: *09 December 2019*
Accepted: *15 May 2020*
Published: *17 June 2020*

Citation:
Liang J, Yu K, Wang Y, Huang X, Huang W, Qin Z, Wang G, Su H, Chen B and Wu Z (2020) Diazotroph Diversity Associated With Scleractinian Corals and Its Relationships With Environmental Variables in the South China Sea. Front. Physiol. 11:615. doi: 10.3389/fphys.2020.00615

INTRODUCTION

Although coral reef ecosystems are located in oligotrophic seas, their biodiversity and primary productivity are extremely high (Connell, 1978). This phenomenon is mainly due to the efficient biogeochemical cycles of carbon, nitrogen, phosphorus, and other basic elements in which coral symbiotic microbes participate (Nakajima et al., 2013). In an ocean environment with very low concentrations of nutrients, the primary productivity of coral reefs is often limited by available nitrogen, which is one of the primary nutrients essential for the survival of all living organisms (Muscatine et al., 1989; Rädecker et al., 2015). The nitrogen fixation system of coral-associated diazotrophs (reduction of N_2 to ammonia) is considered the major source of available nitrogen in coral reef waters (Piniak et al., 2003; Olson et al., 2009). Previous studies have shown that corals have their own internal nitrogen circulation system and protection mechanism (Crossland and Barnes, 1976; Davey et al., 2008). In addition, abundant nitrogen-fixing bacteria associated with corals have been detected in different coral compartments, including mucus (Wegley et al., 2007; Chimetto et al., 2008), tissue (Lesser et al., 2004; Lema et al., 2012), and skeleton (Crossland and Barnes, 1976; Yang et al., 2016). In addition, some studies predicted that diazotrophs associated with corals not only provided sufficient nitrogen sources for coral holobionts, including coral hosts and all microbial organisms that live with them, but also supplied ˜6% of the organic nitrogen for the whole coral reef ecosystem when the available nitrogen was low (Wilkinson et al., 1984; Williams et al., 1987). Recent studies found that coral-associated diazotrophs could significantly respond to human-induced environmental changes, thermal stress, and coral bleaching. For example, the key physiological traits (severe loss of zooxanthellae, net photosynthesis, and N_2 fixation rates) of coral hosts, zooxanthellae, and diazotrophs associated with *Stylophora pistillata* were found to show less resilience to thermal stress than those associated with *Acropora hemprichii*. In addition, it was found that the N_2 fixation rate drastically increased in daylight due to high temperature stress, but increased only in the dark after the temperature was reduced again to *in situ* levels. Concurrently, coral hosts, particularly bleached individuals, were found to exhibit reduced organic matter release and heterotrophic feeding on picoplankton. These results indicated that coral-associated diazotrophs play an important role in the responses of the coral holobiont to ocean warming (Cardini et al., 2016). The relationship between the bleaching mortality and nitrogen fixation rates of diazotrophs in the coral *Acropora aspera* showed that the N_2 fixation rates on coral skeletons following bleaching mortality (caused by thermal or cold bleaching) were up to 30 times greater than those measured in live colonies (Davey et al., 2008).

Currently, the following three main routes are involved in the provision of nitrogen to coral reef ecosystems: (1) terrestrial input, (2) input from ocean currents with rich nutrients, and (3) nitrogen fixation by diazotrophs in coral reef ecosystems (Crossland and Barnes, 1976; Rougerie and Wauthy, 1993; Yamamuro et al., 1995; Sammarco et al., 1999; Sarhan et al., 2000). However, isotope (δ13C and δ15N) tracer experiments have shown that the sources of nitrogen for the primary producers in coral reefs (in Palau and Ishigaki) were mainly derived from biological nitrogen fixation (Yamamuro et al., 1995). Furthermore, the photosynthetic fixation of CO_2 was found to occur simultaneously with the absorption and fixation of new nitrogen. This finding suggests that biological nitrogen fixation plays an important role in the assimilation of carbon and nitrogen by the whole coral reef ecosystem.

Recently, the diversity of the diazotrophic communities associated with different coral species, including *S. pistillata* and *A. hemprichii* (Cardini et al., 2016), *Cladopsammia gracilis* and *Porites* sp. (Grover et al., 2014), *Montipora capitata* and *Montipora flabellata* (Olson et al., 2009), and others (Lema et al., 2012, 2016; Grover et al., 2014), were investigated. These coral species were investigated in different geographical locations, including the Great Barrier Reef (Kelso Reef, Knife Reef, and Davies Reef), the Luhuitou fringing reef of Sanya Bay (South China Sea), the Marine Science Station in Aqaba (Jordan), the Gulf of Aqaba (Red Sea), Leleiwi Reef (Hawaii Island), and Green Island (southeastern Taiwan). However, the geographical distribution and host specificity of coral-associated diazotrophs as well as the correlation with the physical and chemical variables of the surrounding seawater remain unclear.

In the South China Sea, there is a large area of coral reefs at a latitudinal range of 4–21°N (Yu K. -F. et al., 2004). These coral reefs have long been affected by extreme marine events (El Niño, strong storms, high-frequency winter cooling, etc.), human activities, and varying geographical climates (Yu K. -F. et al., 2004; Yu K. et al., 2004; Yu et al., 2009; Yu, 2012; Zhang et al., 2019). Coral skeletons, as carriers of high-resolution environmental records, clearly recorded the climate mutation events during the Holocene, the intensity of El Niño activity at the millennium scale, sea level fluctuations at the millennium-hundred-year scale, periodic strong wind storm activities, East Asian monsoon records, and information on seawater acidity, pollution status, etc. That is, the existing living corals (including members of the internal symbiotic microorganisms) in the South China Sea have evolved slowly through different environmental stresses. Therefore, coral reefs in the South China Sea are natural laboratories that can be used to study the ecological characteristics of coral-associated diazotrophs. To this end, 68 colonies representing 11 species were collected from 6 geographical locations at different latitudes and with different eutrophication levels in the South China Sea to investigate the composition of the coral-associated diazotroph community. This work is meaningful for understanding the ecological characteristics of coral-associated diazotrophs and the possible changes in the face of climate change and human activities.

MATERIALS AND METHODS

Study Sites, Coral Sample Collection, and Species Identification

In this study, six locations in the South China Sea, abbreviated as DyB (Daya Bay), HyI (Huangyan Island), Lht (Luhuitou), SjR (Sanjiao Reef), XyR (Xinyi Reef), and WzI (Weizhou

Island), were selected (**Figure 1**). Coral samples were collected using a hammer and chisel by way of scuba diving at a depth of 5–8 m from a specific site in each selected location (**Table 1**). Three replicate samples (∼6 × 6 cm) were collected from the sides of each colony. The distance between two colonies on the same reef was greater than 10 m. Coral species are represented by the abbreviations Gf (*Galaxea fascicularis*), Gr (*Goniastrea retiformis*), Pd (*Pavona decussate*), Hm (*Hydnophora microconos*), Pl (*Porites lutea*), Pv (*Plesiastrea versipora*), Fp (*Favia palauensis*), Pc (*Plesiastrea curta*), Me (*Montipora efflorescens*), Pe (*Pocillopora eydouxi*), and Ar (*Acropora rosaria*). Not all coral species could be collected from each sampling location. The collected samples were washed with sterile seawater three times and then placed in sterile plastic bags. All samples were briefly stored at low temperatures (0–4°C) and then immediately transported back to the laboratory for DNA extraction.

After genomic DNA was extracted, three replicate samples of each colony were merged equally. A total of 68 coral colonies, which included 6 families, 9 genera, and 11 species (**Table 1**), were identified and selected as the study subjects according to their ecological and morphological characteristics.

Seawater Collection, Nutrition, and Environmental Factor Detection

Three to five liters of seawater was collected at a depth of 5–8 m using a water sampler around each site. The distance between two sampling sites was not less than 100 m. The temperature (Tem), salinity (Sal), turbidity (Tur), dissolved oxygen (DO), and pH values were immediately measured on site using a thermometer, salinometer, turbidimeter, dissolved oxygen meter, and acidometer, respectively. Pore water was extracted from sediments by centrifugation (3,500 rpm, 40 min), filtered through 0.45 μm-pore-size cellulose acetate filters, and then collected in acid-precleaned vials. Finally, all samples were stored in an icebox for transport to the laboratory and stored in deep freezers (–20°C) until analyses (Guo et al., 2017). All nutrient statuses, including the concentrations of dissolved inorganic nitrogen (DIN; DIN = $NH_4^+ + NO_2^- + NO_3^-$), soluble reactive phosphorus (SRP; PO_4^{3-}, and SiO_3^{2-}, were measured according to "Specifications for oceanographic survey" (General Administration of Quality Supervision, Inspection and Quarantine of the People's Republic of China, 1991) (Guo et al., 2017). The average physical and chemical parameters from at least three samples from each coral reef were tested. Longitudes (Lng) and latitudes (Lat) were detected by a global positioning system (GPS). All the data were measured three times and then averaged.

DNA Extraction, PCR Amplification, and Illumina MiSeq Sequencing

Small pieces of coral samples, including tissue, mucus and skeleton (˜50 mg), were cut with a pair of scissors and used for genomic DNA extraction with the TIANamp Marine Animals DNA Kit [Tiangen Biotech (Beijing) Co., Ltd., Beijing, China] according to the manufacturer's instructions. The nitrogen-fixing gene (*nifH*) of diazotrophs was amplified using the specific forward primer nifH-F (5′-AAAGGYGGWATCGGYAARTCCACCAC-3′) and reverse primer nifH-R (5′-TTGTTSGCSGCRTACATSGCCATCAT-3′), where the barcode was an eight-base sequence unique to each sample (Rösch et al., 2002; Hamady et al., 2008; Mori et al., 2014; Xu et al., 2016). The reaction system and procedure for PCR using an ABI GeneAmp® 9700 thermal cycler and TransGen AP221-02 PCR kit (TransStart FastPfu DNA Polymerase, 20 μL reaction system) were the same as those described in a previous report (Sun et al., 2014). The following steps were employed in the PCR: a 3-min hot start at 95°C after the reaction system was configured according to the manufacturer's instructions; 35 cycles of denaturation at 95°C for 30 s, annealing at 57°C for 30 s, and elongation at 72°C for 45 s; an extension at 72°C for 10 min; and preservation at 10°C until halted by the user. Triplicate PCR products were pooled for each sample, and fragments with size ranges of 421–440 bp were then purified and quantified using an AxyPrep DNA gel extraction kit (Axygen Biosciences, Union City, CA, United States) and QuantiFluor™-ST fluorometer (Promega, United States). Purified amplicons were pooled in equimolar amounts and paired-end sequenced (2 × 250 bp) on the Illumina MiSeq platform according to standard protocols (Majorbio Bio-Pharm Technology Co., Ltd., Shanghai, China). The datasets analyzed during the current study are available at the NCBI Sequence Read Archive repository under accession number SRP145254[1].

Data Analysis

Raw sequences were demultiplexed, quality-filtered by Trimmomatic, and merged by FLASH with the following criteria (Magoč and Salzberg, 2011): (i) The reads were truncated at any site receiving an average quality score <20 over a 50 bp sliding window (Bolger et al., 2014). (ii) Primers were exactly matched allowing two nucleotide mismatching, and reads containing ambiguous bases were removed. (iii) Sequences whose overlap longer than 10 bp were merged according to their overlap sequence. The merged sequences were clustered into operational taxonomic units (OTUs) with a 97% similarity cutoff (Dang et al., 2018) using UPARSE software (version 7.1)[2] and chimeric sequences were then identified and removed using UCHIME software (Edgar, 2010). The taxonomy of representative sequences was analyzed by the RDP Classifier algorithm[3] against the fgr/nifH database (release 7.3)[4] using confidence threshold of 70% (Edgar, 2010). The OTUs were then analyzed: alpha diversity index were estimated using mothur (version v.1.30.1) (Schloss et al., 2011), and beta diversity analyze and other analyses were calculated using QIIME and R packages.

In the present study, the rarefaction curve basing on sobs index was used to assessment whether the sequencing depth is enough for each sample. ACE was used to estimate community richness and the larger value indicates the higher richness.

[1]https://www.ncbi.nlm.nih.gov/search/all/?term=SRP145254
[2]http://drive5.com/uparse/
[3]http://rdp.cme.msu.edu/
[4]http://fungene.cme.msu.edu/nifH

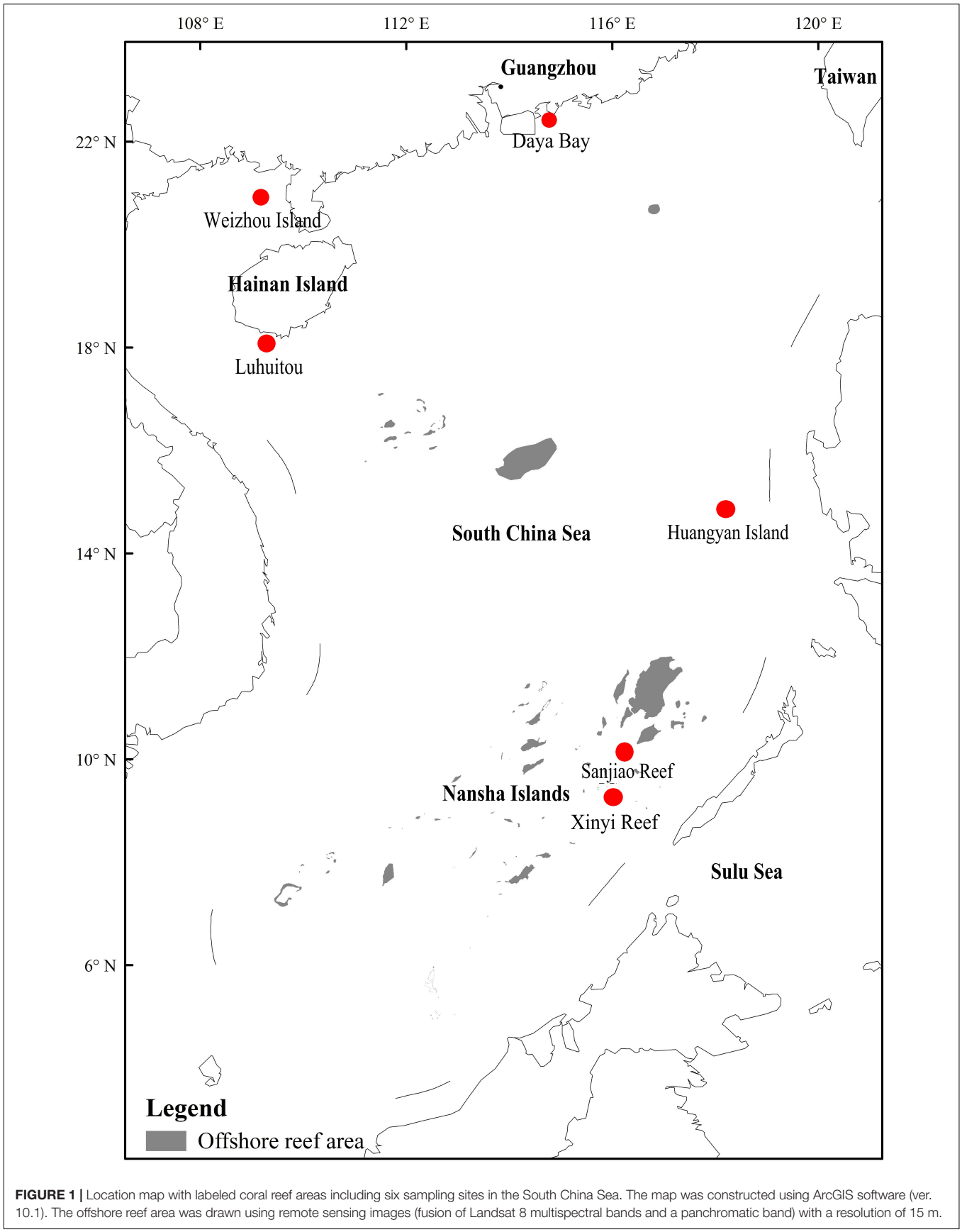

FIGURE 1 | Location map with labeled coral reef areas including six sampling sites in the South China Sea. The map was constructed using ArcGIS software (ver. 10.1). The offshore reef area was drawn using remote sensing images (fusion of Landsat 8 multispectral bands and a panchromatic band) with a resolution of 15 m.

TABLE 1 | The locations, coral species, and numbers of sampled corals.

Site location (longitude, latitude)	Sampling date	Coral species	Coral code[#]	Colony number
Daya Bay (114°38′40″E, 22°34′57″N)	01 September 2015	*Galaxea fascicularis*	Gf1_DyB, Gf2_DyB	2
		Goniastrea retiformis	Gr1_DyB, Gr2_DyB, Gr3_DyB, Gr4_DyB	4
		Pavona decussata	Pd1_DyB, Pd2_DyB	2
		Hydnophora microconos	Hm1_DyB	1
Weizhou Island (109°06′40″E, 21°04′30″N)	23 October 2015	*Porites lutea*	Pl1_WzI, Pl2_WzI, Pl3_WzI, Pl4_WzI	4
		Favia palauensis	Fp1_WzI, Fp2_WzI, Fp3_WzI	3
		Plesiastrea versipora	Pv1_WzI, Pv2_WzI, Pv3_WzI	3
Luhuitou (109°29′16″E, 18°13′18″N)	15 October 2016	*Porites lutea*	Pl1_Lht, Pl2_Lht, Pl3_Lht, Pl4_Lht	4
		Plesiastrea versipora	Pv1_Lht, Pv2_Lht, Pv3_Lht	3
		Favia palauensis	Fp1_Lht	1
Huangyan Island (117°44′49″E, 15°13′08″N)	15 July 2015	*Porites lutea*	Pl1_HyI, Pl2_HyI, Pl3_HyI, Pl4_HyI, Pl5_HyI	5
		Goniastrea retiformis	Gr1_HyI, Gr2_HyI, Gr3_HyI	3
		Plesiastrea versipora	Pv1_HyI, Pv2_HyI, Pv3_HyI	3
		Plesiastrea curta	Pc1_HyI, Pc2_HyI	2
Sanjiao Reef (115°12′41″E, 10°13′24″N)	19 May 2015	*Porites lutea*	Pl1_SjR, Pl2_SjR, Pl3_SjR, Pl4_SjR	4
		Montipora efflorescens	Me1_SjR, Me2_SjR	2
		Pavona decussata	Pd1_SjR, Pd2_SjR	2
		Hydnophora microconos	Hm1_SjR, Hm2_SjR	2
		Pocillopora eydouxi	Pe1_SjR	1
		Favia palauensis	Fp1_SjR	1
		Plesiastrea curta	Pc1_SjR, Pc2_SjR, Pc3_SjR	3
Xinyi Reef (115°55′49″E, 9°20′06″N)	21 May 2016	*Porites lutea*	Pl1_XyR, Pl2_XyR, Pl3_XyR, Pl4_XyR	4
		Goniastrea retiformis	Gr1_XyR, Gr2_XyR, Gr3_XyR, Gr4_XyR, Gr5_XyR	5
		Acropora rosaria	Ar1_XyR, Ar2_XyR, Ar3_XyR	3
		Favia palauensis	Fp1_XyR	1

[#] *The letters before the underscore are the initials of the coral genus and species, which represent the species of corals. The numbers indicate the order of coral individuals. The letters after the underscore represent the abbreviations for the coral reef locations.*

Shannon was used to estimate community diversity and the larger value indicates the higher diversity. The calculation formulas for ACE and Shannon could be viewed on this website[5].

The differences in the indices between each group of samples were tested using Student's *t*-test. Significance was declared at $P \leq 0.05$. The taxonomy was assigned and compared with that in the fgr/nifH database (Quast et al., 2013) using the QIIME platform[6]. Moreover, similarities or differences in the composition of bacterial communities were reflected by principle coordinate analysis (PCoA) using Bray-Curtis distances at the OTU level (Lozupone and Knight, 2005). A heatmap of the correlations between environmental variables and nitrogen-fixing bacteria associated with corals was constructed by Spearman's correlation test and GraphPad Prism version 6.00 (GraphPad Software, San Diego, CA, United States). Significance was assigned at $P \leq 0.05$.

RESULTS

Nutrient Parameters of Sampling Sites

Six sampling locations were distributed across different areas in the South China Sea. The results of the analysis in **Table 2** indicate that concentrations of DIN and other nutrients were very high (3.17 μmol/L ≥ DIN ≥ 2.31 μmol/L, 29.75 μmol/L ≥ SiO_3^{2-} ≥ 17.25 μmol/L, and 0.51 μmol/L ≥ SRP ≥ 0.38 μmol/L) in some coastal sampling locations (e.g., the high-latitude DyB, WzI, and Lht sites). In contrast, the concentrations of these nutrients were relatively low in the low-latitude island reefs at HyI, XyR, and SjR, which were far from land (1.42 μmol/L ≥ DIN ≥ 1.27 μmol/L, 2.40 μmol/L ≥ SiO_3^{2-} ≥ 1.62 μmol/L, and 0.07 μmol/L ≥ SRP ≥ 0.03 μmol/L). The turbidity was also significantly higher at the fringing reefs than at the island reefs (3.25 NTU ≥ Tur ≥ 1.16 NTU and 0.4 NTU ≥ Tur ≥ 0.2 NTU, respectively). The high-latitude DyB, WzI, and Lht sites were constantly disturbed by human activity, while the low-latitude HyI, XyR, and SjR sites were less disturbed. This difference was the cause of the difference in nutrient distribution.

Diversity of Coral-Associated Diazotrophs

A total of 1,223,398 reads recovered from 68 coral samples, with lengths ranging from 421 to 440 bp, were obtained from the sequencing database. Good's coverage of each sequencing database was greater than 99% (**Supplementary Table S1** and **Supplementary Figure S1**). Thus, these sequencing results accurately represented the diazotrophs in the coral samples. Other indices, including the abundance-based coverage estimator (ACE) and Shannon index, are shown more intuitively in

[5]http://www.mothur.org/wiki/Calculators

[6]http://qiime.org/scripts/assign_taxonomy.html

TABLE 2 | Nutrient parameters from different sampling sites in the South China Sea.

Index	DyB	WzI	Lht	HyI	XyR	SjR
DO (mg/L)	7.18	6.67	7.22	6.88	7.29	7.24
Tem (°C)	28.00	27.40	29.00	30.90	31.1	30.81
pH	8.20	8.38	8.29	8.42	8.28	8.10
Sal (%)	3.35	3.26	3.31	3.38	3.34	3.33
DIN (μmol/L)	3.17	2.67	2.31	1.27	1.27	1.42
SRP (μmol/L)	0.38	0.51	0.45	0.07	0.03	0.04
SiO_3^{2-} (μmol/L)	20.21	29.75	17.25	2.57	1.62	2.40
Lng (°)	114.60	109.10	109.90	117.70	115.90	115.20
Lat (°)	22.60	21.07	20.20	15.20	9.30	10.20
Tur (NTU)	1.16	1.30	3.25	0.20	0.40	0.30

Figure 2. The detailed data showed that the ACE, which reflects community richness, varied greatly among coral samples (**Supplementary Table S1**). The lowest values were 21.35, 30.79, and 31.54 from Pv3_Lht, Pl1_SjR, and Pl2_SjR, respectively, while the highest values were 300.4, 293.57, and 286.85 from Gr3_XyR, Fp3_WzI, and Ar3_XyR, respectively. The Shannon index (**Supplementary Table S1**), which reflects community diversity, also differed significantly among coral samples (ranging from 0.58 to 4.48). When coral individuals were grouped according to different species and sampling regions, these indices showed non-significant differences between most species at $P > 0.05$ but significant differences between most sampling regions at $P \leq 0.05$ (**Figure 2**). The average ACE values for WzI, HyI, XyR, and SjR (146.99, 139.83, 145.23, and 102.12, respectively) were obviously higher than those for Lht and DyB (71.07 and 75.54, respectively). Meanwhile, the average Shannon values for WzI, HyI, and XyR (3.34, 2.76, and 2.70, respectively) were also higher than those for DyB, SjR, and Lht (1.98, 1.82, and 1.70, respectively). However, the ACE and Shannon index averages for different coral species ranged from 101.73 to 150.28 and 2.12 to 2.73, respectively, with small ranges of fluctuations between them (**Figures 2B,D**). These findings suggest that geographical factors have a strong effect on the community richness and diversity of coral-associated diazotrophs.

The number of OTUs and the diversity at various taxonomic levels are listed in **Supplementary Table S2**. The results showed great differences in the number of communities of diazotrophs between coral individuals, even for the same coral species in the same sampled location. For example, 6 phyla, 21 genera, and 280 OTUs were detected in Gr3_XyR, but the numbers were 5, 11, and 50 in Gr1_XyR, respectively.

Clustering of Coral-Associated Diazotrophs Based on Similarity

The similarity among the diazotrophic communities associated with the 68 coral samples from 6 locations was evaluated using PCoA at the OTU level. The diazotrophic composition of coral individuals differed between some coral reefs, regardless of whether the coral individuals were of the same species (**Figure 3A**). Coral individuals from Lht and DyB were clustered together differently from the other four reef areas (WzI, HyI, XyR, and SjR). This difference may be related to the surrounding seawater environment. Lht and DyB are high-latitude fringing reefs, and the other sites are low-latitude island reefs (except WzI, which is a high-latitude fringing reef). In comparison with the grouping of regions, coral individuals from the same species did not cluster together (**Figure 3B**). This results indicated that the diazotrophic composition associated with corals was somewhat species specific. Overall, the key factor affecting diazotrophic composition was geographical position, rather than interspecific differences.

Composition of Diazotrophs Associated With Corals

Eleven bacterial phyla capable of nitrogen fixation, including three unclassified bacteria (I, II, and III), were identified from the sequencing database of 68 coral samples (**Figure 4**). Among these phyla, unclassified bacteria I, which had a very high relative abundance, was present in almost all the coral samples. In addition, the dominant bacterial phyla were Proteobacteria, Chlorobi, and Cyanobacteria. The relative abundance of these coral-associated bacterial phyla exhibited significant differences between sites. For example, unclassified bacteria I and Proteobacteria were the dominant bacterial phyla (>80% relative abundance) in most of the coral samples from WzI, HyI, XyR, and SjR. In contrast, the relative abundance of these two bacterial phyla was low (<35%) in most of the coral samples from Lht and DyB. In particular, the relative abundance of Proteobacteria was generally very low (<10%) in most of the coral samples from these two locations; the dominant diazotrophs in these locations were unclassified bacteria II (Lht) and Chlorobi (DyB). Of course, there were special cases. For example, the relative abundance of Chlorobi, which was the dominant group, was 84% in Pl3_SjR from SjR. Unclassified group II was the dominant group, with a relative abundance of 89%, in Hm1_SjR from SjR. Cyanobacteria, members of which are capable of nitrogen fixation, was also a common bacterial phylum in these coral samples. The relative abundance of Cyanobacteria ranged from 0.21% (Pl2_SjR, Pl3_Lht, Pv3_Lht, etc.) to 51% (Pl5_HyI). The other nitrogen-fixing groups, including Euryarchaeota, Firmicutes, and Verrucomicrobia, were detected in a small number of coral samples and had very low relative abundance (except marine stromatolite eubacteria in Pd2_SjR). At the class level (**Supplementary Figure S2**), the

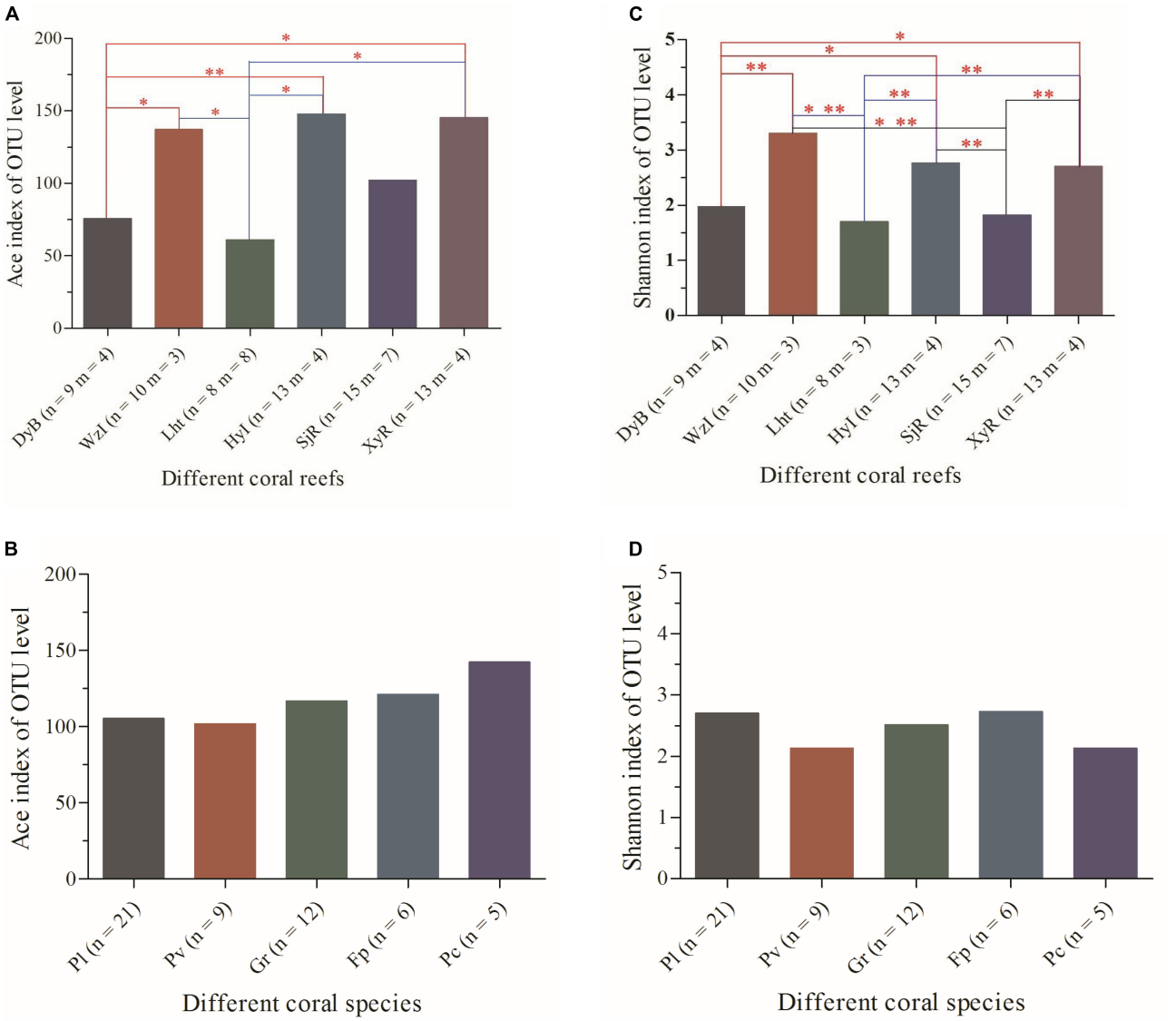

FIGURE 2 | Analysis of the differences in alpha-diversity indices of coral-associated diazotrophs between sample groups at the OTU level. **(A)** ACE between coral reefs, **(B)** ACE between coral species, **(C)** Shannon index between coral reefs, and **(D)** Shannon index between coral species. The analysis used was Student's *t*-test. Significant differences are indicated by different numbers of asterisks ($0.01 < p \leq 0.05$ *, $0.001 < p \leq 0.01$ **). Non-significant correlations do not have an asterisk. *n*, number of coral individuals; *m*, number of coral species.

dominant taxa were unclassified_p_unclassified bacteria I and unclassified Proteobacteria in most coral samples from WzI, HyI, XyR, and SjR. Chlorobi was the dominant class in all coral samples from DyB (ranging from 47 to 96%) and Pl3_SjR (84%) from SjR. In addition, unclassified_p_unclassified bacteria II was the dominant group in most coral samples from Lht (ranging from 28 to 87%) and Hm1_SjR from SjR (89%). The relative abundance of most other classes, including Alphaproteobacteria, Betaproteobacteria, and Deltaproteobacteria, was very low. At other taxonomic levels (order, family, genus, and species), the unclassified diazotrophs were the dominant groups. These results indicated that the coral holobionts contained many diazotrophs that have not been isolated and recognized.

At the genus level, Venn diagrams showed that most diazotrophic genera were common (14 and 20 among coral species and sampling regions, respectively) in multiple sample groups, which were core members (**Figure 5**). Among these genera, *Vibrio* and *Chlorobium* overlapped exactly among coral reefs and coral species (**Table 3**). In addition to the overlapping genera, there were some unique diazotrophic genera for each sample group, whether in coral species or sampling regions (**Table 4**). For example, *Desulfobacter* was restricted to coral individuals from DyB. *Chroococcidiopsis* appeared only in the coral species *Goniastrea retiformis*. Overall, 15 diazotrophic genera were restricted to different groups of sampling regions, and 14 genera were specific to different groups of coral species.

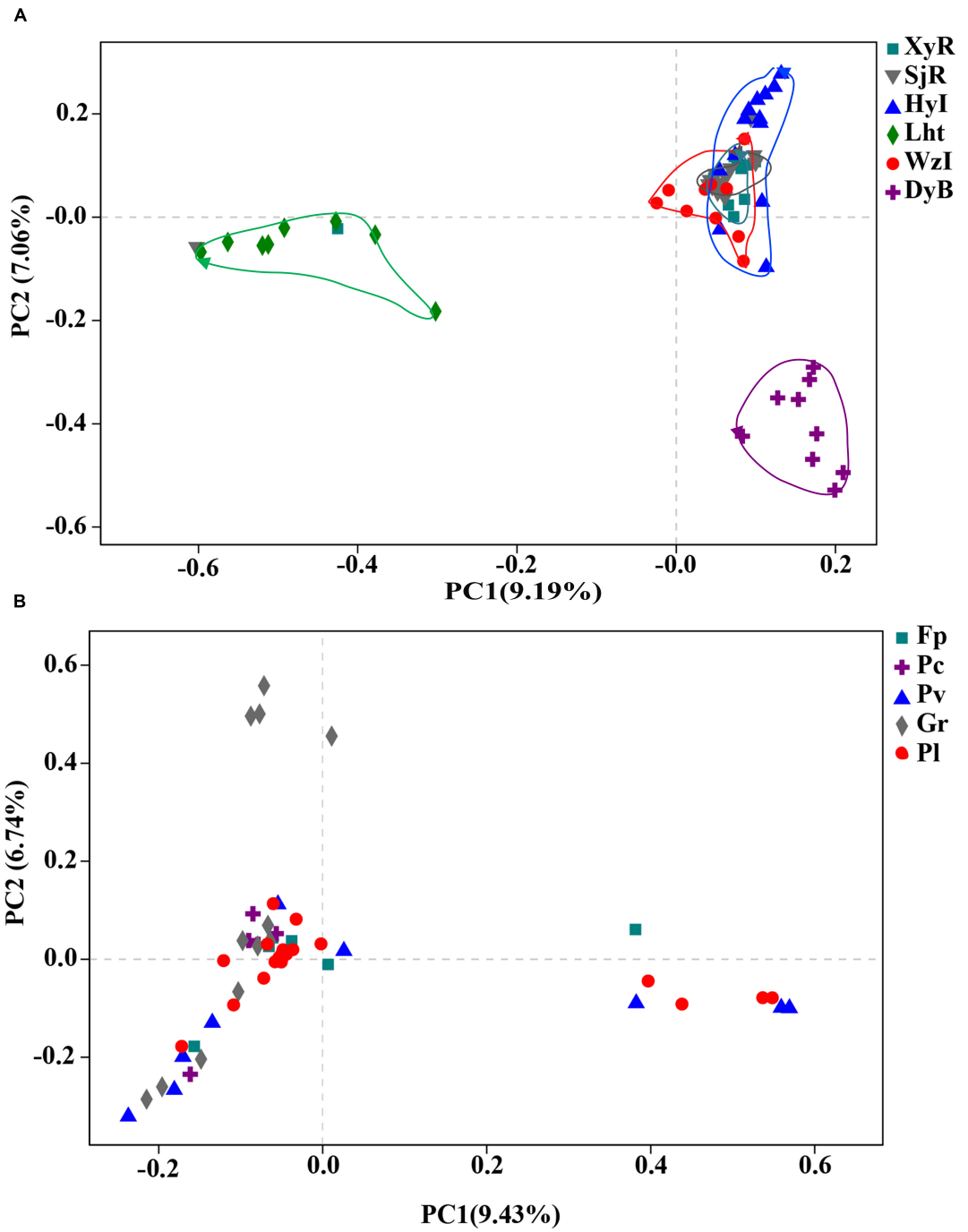

FIGURE 3 | PCoA plot at the OTU level for all coral samples collected from six different coral reefs. Coral samples were grouped according to **(A)** collection site and/or **(B)** species with ≥5 colonies from the same coral reef. Scatter plot showing principal coordinate 1 (PC1) vs. principal coordinate 2 (PC2). PC1 and PC2 represent the principal factors affecting the composition of coral-associated diazotrophs.

Environmental Variables Affecting the Distribution of Diazotrophic Species

The six sampling locations were distributed in different areas of the South China Sea. These coral reefs were affected by different environmental factors due to their geographical locations (**Table 2**). The concentrations of DIN and other nutrients were lower in HyI, XyR, and SjR, which were far from land, than in the other locations. In contrast, these nutrient concentrations were 2–10 times higher in some coastal sampling locations (e.g., DyB, WzI, and Lht) than in those far from

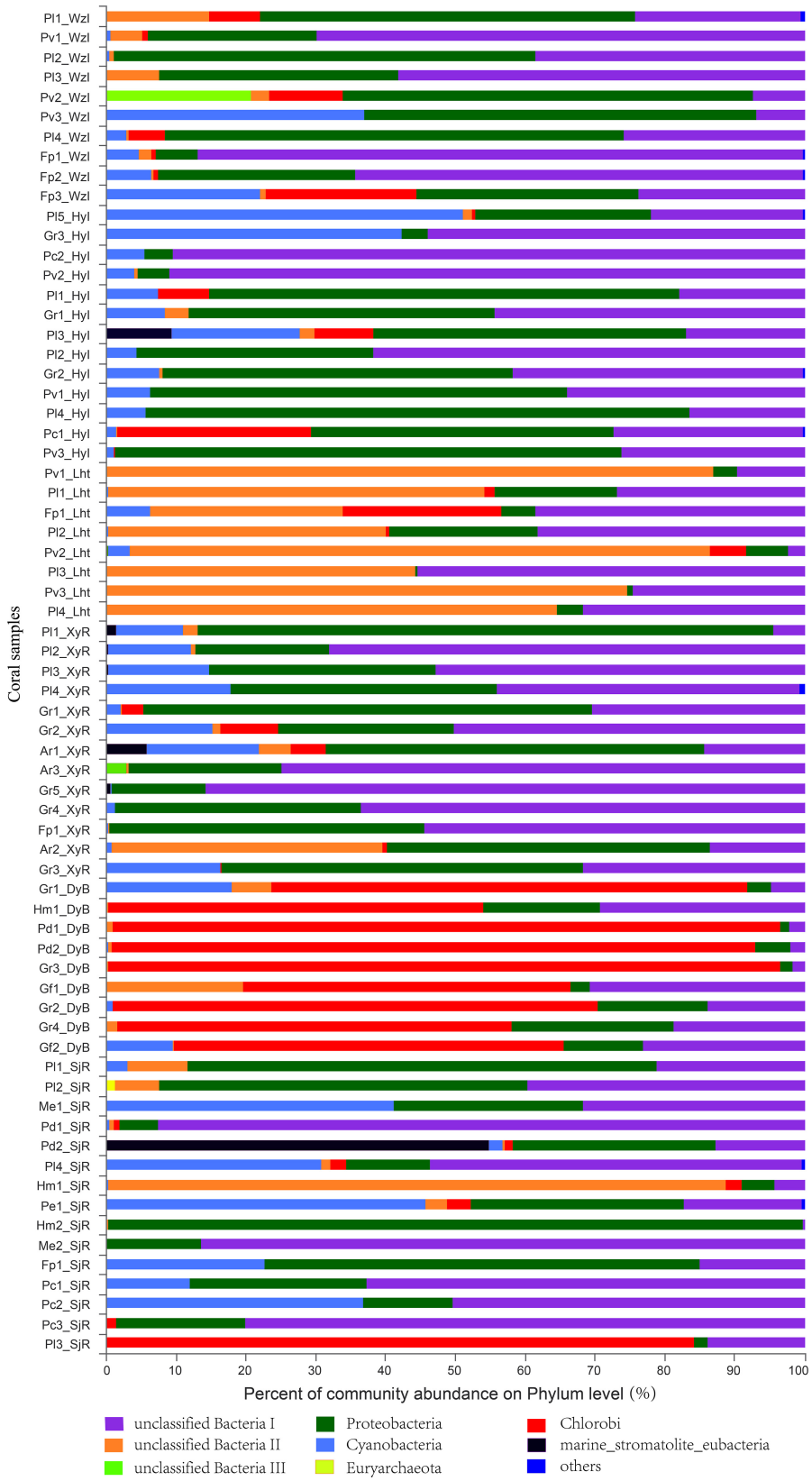

FIGURE 4 | Composition profiles of diazotrophs. Taxonomic classification of bacterial reads retrieved from all coral samples at the phylum level using RDP Classifier.

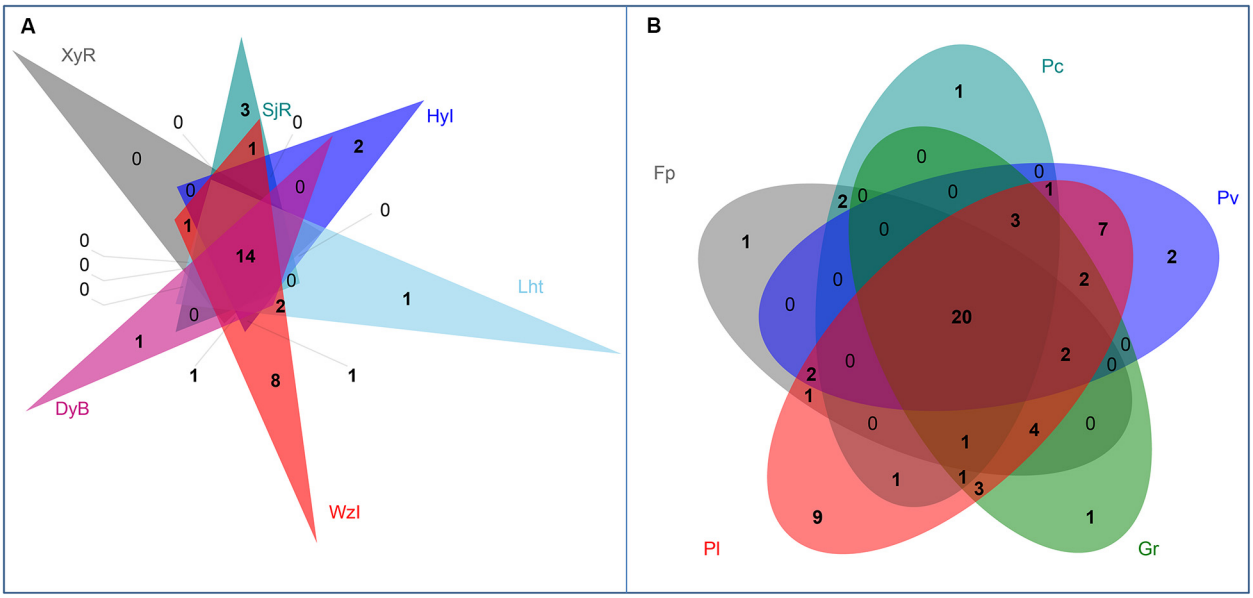

FIGURE 5 | Venn diagrams showing the number of diazotrophs at the genus level from different coral reefs **(A)** and coral species **(B)**.

TABLE 3 | Overlapping diazotrophic genera in different sample groups.

Bacterial genera in different coral reefs	Bacterial genera in different coral species
[DyB (n = 9, m = 4), WzI (n = 10, m = 3), Lht (n = 8, m = 8), HyI (n = 13, m = 4), SjR (n = 15, m = 7), and XyR (n = 13, m = 4)]	[Pl (n = 21), Pv (n = 9), Gr (n = 12), Fp (n = 6), and Pc (n = 5)]
g_unclassified_f_Chlorobiaceae	g_unclassified_o_Rhizobiales
g_*Teredinibacter*	g_*Vibrio*
g_*Vibrio*	g_unclassified_o_Desulfuromonadales
g_norank_c_unclassified_Cyanobacteria	g_norank_c_unclassified_Cyanobacteria
g_unclassified_c_Alphaproteobacteria	g_unclassified_c_Alphaproteobacteria
g_unclassified_c_norank_p_Cyanobacteria	g_unclassified_c_norank_p_Cyanobacteria
g_unclassified_k_norank_d_Bacteria	g_unclassified_k_norank_d_Bacteria
g_unclassified_p_Cyanobacteria	g_unclassified_ o_Chroococcales
g_unclassified_o_Rhizobiales	g_*Desulfuromonas*
g_unclassified_p_Proteobacteria	g_*Mastigocoleus*
g_unclassified_c_Gammaproteobacteria	g_unclassified_f_Chromatiaceae
g_unclassified_p_unclassified Bacteria II	g_unclassified_p_Cyanobacteria
g_*Chlorobium*	g__unclassified_f__Chlorobiaceae
g_unclassified_c_Deltaproteobacteria	g__unclassified_o__Chromatiales
	g_unclassified_p_Proteobacteria
	g_unclassified_c_Gammaproteobacteria
	g_unclassified_p_unclassified Bacteria II
	g_*Bradyrhizobium*
	g_*Chlorobium*
	g_unclassified_c_Deltaproteobacteria

n, number of coral individuals; m, number of coral species. The red-labeled bacteria are the species with exact overlap between coral reefs and coral species.

land. Tur was also significantly higher in the coastal reefs than in the offshore reefs. The correlations between various environmental parameters and communities of coral-associated diazotrophs (the top 20 taxa based on total abundance at the genus level) were then evaluated (**Figure 6**). The results showed that the effects of different environmental factors on bacterial communities were significantly different. According to similar effects, environmental factors were clustered into two groups: group I, including DIN, Tur, Lat, SRP, and SiO_3^{2-}, and group II, including pH, DO, Lng, Tem, and Sal. Group I was positively correlated with unclassified_f_Chlorobiaceae ($0.26 \leq R \leq 0.49$), *Chlorobium* ($0.29 \leq R \leq 0.37$), unclassified_p_unclassified Bacteria II ($0.30 \leq R \leq 0.43$) and unclassified_o_Desulfuromonadales ($0.25 \leq R \leq 0.44$) and negatively correlated with four other bacterial genera, namely, unclassified_c_norank_p_Cyanobacteria ($-0.42 \leq R \leq -0.24$), norank_p_unclassified Bacteria I ($-0.37 \leq R \leq -0.25$), unclassified_c_Alphaproteobacteria ($-0.44 \leq R \leq -0.30$),

TABLE 4 | Specific diazotrophic genera in different sample groups.

Coral reefs	Bacterial genera	Coral species	Bacterial genera
DyB (*n* = 9, *m* = 4)	g_*Desulfobacter*	PI (*n* = 21)	g_*Stenotrophomonas* g_*Zoogloea* g_norank_p_unclassified bacteria g_norank_f_ Deltaproteobacteria g_unclassified_c_Clostridia g_*Rhodospirillum* g_*Tolumonas* g_unclassified_p_Euryarchaeota g_unclassified_f_Desulfobacteraceae
WzI (*n* = 10, *m* = 3)	g_*Calothrix* g_*Stenotrophomonas* g_unclassified_f_Desulfobacteraceae g_norank_p_unclassified bacteria g_norank_f_ Deltaproteobacteria g_*Klebsiella* g_unclassified_f_Rhodocyclaceae g_*Rhodospirillum*		
Lht (*n* = 8, *m* = 3)	g_*Azotobacter*	Pv (*n* = 9)	g_*Klebsiella* g_unclassified_f_Rhodocyclaceae
HyI (*n* = 13, *m* = 4)	g_*Desulfarculus* g_unclassified_o_Clostridiales	Gr (*n* = 12)	g_*Chroococcidiopsis*
		Fp (*n* = 6)	g_*Skermanella*
SjR (*n* = 15, *m* = 7)	g_*Rhizobium* g_unclassified_c_Clostridia g_unclassified_p_Euryarchaeota	Pc (*n* = 5)	g_unclassified_o_Clostridiales
XyR (*n* = 13, *m* = 4)	None		

The indications for "n" and "m" are consistent with those in ***Table 3****.*

and unclassified_p_Cyanobacteria ($-0.44 \leq R \leq -0.30$). The correlations of other environmental factors with a series of bacterial genera in group II were generally opposite to those in group I (**Figure 6**).

DISCUSSION

Microbial nitrogen fixation requires a nitrogenase gene, *nifH*, which has been confirmed to be consistent with the phylogenesis of the 16S rRNA gene (Zehr et al., 2003). Our annotation results revealed that microorganisms capable of nitrogen fixation were ubiquitously present in coral holobionts. Their presence was not related to the external environment. The six sampling locations were distributed in different areas of the South China Sea. The concentrations of DIN and other nutrients were very high at some fringing reef sampling locations (e.g., DyB, WzI, and Lht). In contrast, the concentrations of these nutrients were low in some island reefs (HyI, XyR, and SjR) that were far from land. It is possible that the nutrients in coastal coral reefs could completely meet the nitrogen demands of coral holobionts, even without biological nitrogen fixation. There was evidence that the coral had established symbiotic relationships with some bacteria (including diazotrophs) in their early life history stages, and the bacterial communities then transitioned into a state of long-term dynamic change (Lema et al., 2014). This finding is a reflection of the response of coral holobionts to environmental changes. It can also be speculated that coral-associated diazotrophs have many other biological functions in addition to nitrogen fixation, such as the coordination of carbon fixation. For example, Cyanobacteria is a phylum of prokaryotic microorganisms that can carry out photosynthesis with oxygen production (Hamilton et al., 2016). They can also fix atmospheric nitrogen and convert it into ammonia (NH_3), nitrite (NO_2^-), or nitrate (NO_3^-), which can provide available nitrogen to other organisms (Lesser et al., 2004; Charpy et al., 2010).

In this study, the most striking finding was that the community composition of coral-associated diazotrophs, which was identified via the analysis of alpha- and beta-diversity and species differences, was highly significantly different between sampling regions (**Figure 2**). Notably, community richness, which was reflected by the ACE, was lower for the coral-associated diazotrophs from DyB and Lht than for those from WzI, HyI, SjR, and XyR (**Figure 2A**). This difference may be attributed to the reef types of DyB and Lht, which are typical fringing reefs that are frequently affected by human activities and contain high concentrations of nutrients and DO. The sites with low community diversity, which was reflected by the Shannon index, exhibited the same trend as the ACE for the coral-associated diazotrophs from DyB and Lht (**Figure 2C**). This finding may be related to the fact that high concentrations of nutrients (especially DIN) can meet some of the nitrogen requirements of corals. However, this finding was contrary to the results of the analysis of the coral-associated bacterial diversity obtained by high-throughput sequencing based on 16S rRNA gene amplification. Li et al. (2013) studied the bacterial diversity associated with *P. lutea*, *G. fascicularis*, and *Acropora millepora* sampled from Lht. The results showed that the ACE and Shannon index were 855.53–8970.90 and 4.16–7.04, respectively. Additionally, our previous study found that the ACE and Shannon index values of 25 scleractinian coral samples from XyR were 332.22–1500.66 and 1.91–5.88, respectively (Liang et al., 2017). McKew et al. (2012) also showed that the bacterial communities from Caribbean corals were significantly more diverse than those from Indonesian corals.

In fact, the relationships between coral-associated bacteria were structured by multiple factors at different scales. For

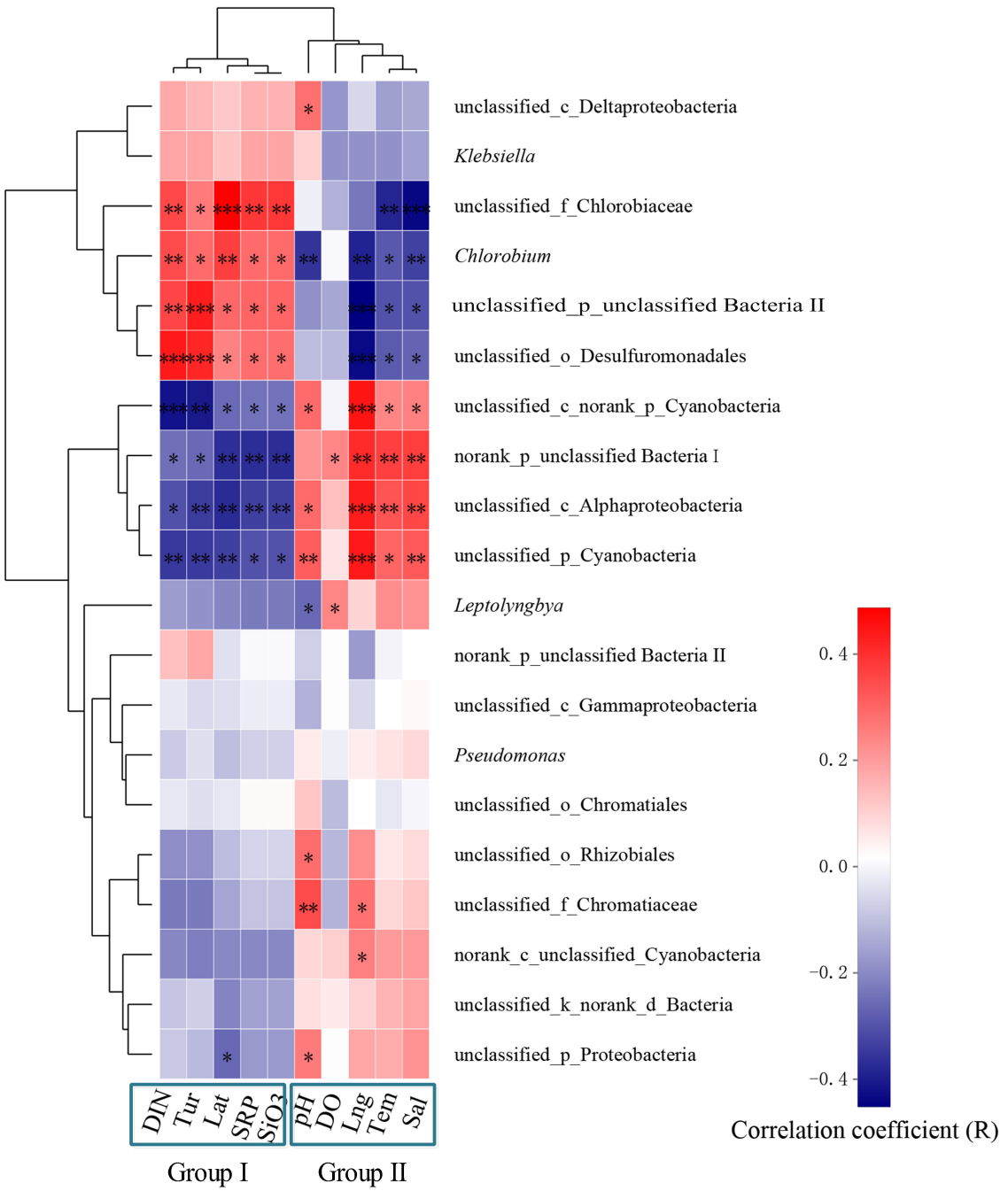

FIGURE 6 | Correlation analyses between environmental parameters and populations of diazotrophs at the genus level. The diazotrophs analyzed were the top 20 genera in terms of total abundance. Hierarchical clustering of environmental variables was performed based on the raw data, while diazotrophic species were clustered based on averages. Significant differences are indicated by different numbers of asterisks ($0.01 < p \leq 0.05$ *, $0.001 < p \leq 0.01$ **, $p \leq 0.001$ ***). Non-significant correlations do not have an asterisk. The R value represents the correlation coefficient, and the closer it is to 1, the more significant the correlation is.

example, the diversity and composition of the bacterial communities associated with corals are significantly affected by various factors, including coral species (Hong et al., 2009), geography (McKew et al., 2012), skeletal morphology (Liang et al., 2017), and others (Bourne et al., 2008; Ceh et al., 2012). However, the relationship between coral-associated nitrogen-fixing bacteria and other bacteria is not yet clear. In this study, the characteristics of the dominant coral-associated diazotrophs, which exhibited significant geographical differences, were clearly recognized. At the same time, some core diazotrophs were found in different coral reefs or coral species. In addition, there were some unique diazotrophs

in different coral reefs or coral species. The PCoA also showed that coral samples from different locations were clearly separated based on their diazotrophic composition (**Figure 3**). We speculate that the selection of coral-associated diazotrophs is directly related to the environmental factors of the surrounding seawater. Because the environmental variables significantly differed between these coral reefs, correlation analysis revealed that various environmental factors were positively or negatively correlated with different bacterial genera (**Figure 6**). For example, the effects of group I (Lat, SRP, SiO_3^{2-}, DIN, and Tur) and group II (pH, DO, Tem, Sal, and Lng) on most of the diazotrophic communities were similar. The correlations between the distribution of nitrogen-fixing bacteria associated with corals and environmental factors were reported for the first time in this study. The findings of this study shed light on the communities and dominant groups of diazotrophs in characteristic coral reefs and their relationships with key environmental variables.

In summary, our results fully reflected the diversity of diazotrophs associated with different coral species sampled from several coral reefs that exhibited differences in environmental variables in the South China Sea. Although many diazotrophic species were unclassified, it was shown that the predominant taxa of diazotrophs among six different coral reefs exhibited more significant geographical differences than interspecific differences. In addition, the correlation analysis revealed that various environmental factors were positively or negatively correlated with different bacterial genera. We believe that corals tend to be associated with unclassified_f_Chlorobiaceae, *Chlorobium*, unclassified_p_unclassified Bacteria II, and unclassified_o_Desulfuromonadales as symbiotic nitrogen-fixing bacteria under changing nutrient enrichment conditions. In addition, corals from high-latitude reefs may tend to be associated with unclassified_c_norank_p_Cyanobacteria, norank_p_unclassified Bacteria I, unclassified_c_Alphaproteobacteria, and unclassified_p_Cyanobacteria under the effects of global warming. This finding occurs because with the influence of global warming and human activities, the environmental stress on global coral reefs is becoming increasingly serious. In the South China Sea, coral reefs at low latitudes are also often subjected to unusually high temperatures. Statistics show that the Nansha Islands (where XyR and SjR are located) had annual maximum temperatures between 30 and 31°C from 1985 to 2015 (Qin et al., 2019). The coral reefs located in high-latitude regions (e.g., Lht and DyB) are affected by human activities all year, resulting in serious eutrophication of the surrounding seawater. The live coral cover rapidly decreased from greater than 60% to less than 20% from 1984 to 2015 (Zhao et al., 2012; Qin et al., 2019). Diazotrophs are essential components of coral holobionts, which are involved in the nitrogen cycle (Piniak et al., 2003; Olson et al., 2009) and are important for energy supply (Hamilton et al., 2016). There was a significant positive correlation between four diazotrophic bacterial genera (unclassified_c_norank_p_Cyanobacteria, norank_p_unclassified Bacteria I, unclassified_c_Alphaproteobacteria, and unclassified_p_Cyanobacteria) and seawater temperature ($0.001 < p \leq 0.05$). Therefore, we believe that with global warming, functional nitrogen-fixing bacteria in corals will gradually evolve to be dominated by genera such as Cyanobacteria and Alphaproteobacteria to adapt to increasing sea surface temperatures, especially in low-latitude coral reefs such as SjR and XyR. In addition, although the number of living corals is decreasing under high nutrient stress, some individuals with environmental tolerance can survive. This phenomenon is closely related to the adaptability of symbiotic microorganisms in coral. Our results showed that four diazotrophic bacterial genera (unclassified_f_Chlorobiaceae, *Chlorobium*, unclassified_p_unclassified Bacteria II, and unclassified_o_Desulfuromonadales) were positively correlated with the concentrations of nutrients such as DIN, SRP, and SiO_3^{2-} ($p \leq 0.05$). It is possible that genera such as Chlorobiaceae, *Chlorobium*, and Desulfuromonadales will become the dominant diazotroph groups in coral if the surrounding eutrophication continues to deteriorate at high-latitude fringing reefs (e.g., Lht and DyB). In fact, the results of the diazotroph composition also verified this conjecture (**Figure 4**). In particular, the relative abundance of Chlorobi was very high at the high-latitude DyB site where the annual average temperature was low. This finding may be related to the photosynthetic energy demand of coral holobionts. The effective photochemical efficiency provided by *Symbiodinium* is relatively weak under low temperature conditions (Xu et al., 2017). Chlorobi may not only perform the function of nitrogen fixation but also supplement photosynthetic energy. An understanding of the diazotrophic communities associated with scleractinian corals from different reef areas will help us to understand that the evolution of microbial populations with specific functions, which represent a strategy for coral hosts to adapt to environmental changes.

DATA AVAILABILITY STATEMENT

The datasets analyzed during the current study are available from the [NCBI Sequence Read Archive] repository under accession number SRP145254 [https://www.ncbi.nlm.nih.gov/search/all/?term=SRP145254].

ETHICS STATEMENT

Permits for coral sampling were provided by the State Oceanic Administration, People's Republic of China, and the local Department of Ocean and Fisheries.

AUTHOR CONTRIBUTIONS

KY and JL conceived the research and wrote the manuscript. YW, XH, WH, and ZW contributed to the materials. JL performed all the experiments. ZQ and GW constructed all the figures.

BC and HS identified coral species. All authors edited and approved the manuscript.

FUNDING

This work was funded by the National Natural Science Foundation of China (Nos. 91428203 and 41666005), Science and Technology Project of Guangxi (Nos. AD17129063 and AA17204074), BaGui Scholars Program Foundation (No. 2014BGXZGX03), and the Basic Ability Promotion Project for Young and Middle-aged Teachers in Universities of Guangxi (No. 2017KY0021).

SUPPLEMENTARY MATERIAL

The Supplementary Material for this article can be found online at: https://www.frontiersin.org/articles/10.3389/fphys.2020.00615/full#supplementary-material

REFERENCES

Bolger, A. M., Lohse, M., and Usadel, B. (2014). Trimmomatic: a flexible trimmer for Illumina sequence data. *Bioinformatics* 30, 2114–2120. doi: 10.1093/bioinformatics/btu170

Bourne, D., Iida, Y., Uthicke, S., and Smith-Keune, C. (2008). Changes in coral-associated microbial communities during a bleaching event. *ISME J.* 2, 350–363. doi: 10.1038/ismej.2007.112

Cardini, U., Hoytema, N. V., Bednarz, V. N., Rix, L., Foster, R. A., Al-Rshaidat, M. M. D., et al. (2016). Microbial dinitrogen fixation in coral holobionts exposed to thermal stress and bleaching. *Environ. Microbiol.* 18, 2620–2633. doi: 10.1111/1462-2920.13385

Ceh, J., Raina, J. B., Soo, R. M., Van, K. M., and Bourne, D. G. (2012). Coral-bacterial communities before and after a coral mass spawning event on Ningaloo Reef. *PLoS One* 7:e36920. doi: 10.1371/journal.pone.0036920 doi: 10.1371/journal.pone.0036920

Charpy, L., Palinska, K. A., Casareto, B., Langlade, M. J., Suzuki, Y., Abed, R. M., et al. (2010). Dinitrogen-fixing cyanobacteria in microbial mats of two shallow coral reef ecosystems. *Microb. Ecol.* 59, 174–186. doi: 10.1007/s00248-009-9576-y

Chimetto, L. A., Brocchi, M., Thompson, C. C., Martins, R. C., Ramos, H. R., and Thompson, F. L. (2008). Vibrios dominate as culturable nitrogen-fixing bacteria of the Brazilian coral *Mussismilia hispida*. *Syst. Appl. Microbiol.* 31, 312–319. doi: 10.1016/j.syapm.2008.06.001

Connell, J. H. (1978). Diversity in tropical rain forests and coral reef. *Science* 199, 1302–1310. doi: 10.1126/science.199.4335.1302

Crossland, C. J., and Barnes, D. J. (1976). Acetylene reduction by coral skeletons. *Limnol. Oceanogr.* 21, 153–156. doi: 10.4319/lo.1976.21.1.0153

Dang, C., Liu, W., Lin, Y., Zheng, M., Jiang, H., Chen, Q., et al. (2018). Dominant role of ammonia-oxidizing bacteria in nitrification due to ammonia accumulation in sediments of Danjiangkou reservoir, China. *Appl. Microbiol. Biot.* 102, 3399–3410. doi: 10.1007/s00253-018-8865-0

Davey, M., Holmes, G., and Johnstone, R. (2008). High rates of nitrogen fixation (acetylene reduction) on coral skeletons following bleaching mortality. *Coral Reefs* 27, 227–236. doi: 10.1007/s00338-007-0316-9

Edgar, R. C. (2010). Search and clustering orders of magnitude faster than BLAST. *Bioinformatics* 26, 2460–2461. doi: 10.1093/bioinformatics/btq461

Grover, R., Ferrier-Pagès, C., Maguer, J.-F., Ezzat, L., and Fine, M. (2014). Nitrogen fixation in the mucus of Red Sea corals. *J. Exp. Biol.* 217, 3962–3963. doi: 10.1242/jeb.111591

Guo, J., Yu, K., Wang, Y., Xu, D., Huang, X., Zhao, M., et al. (2017). Nutrient distribution in coral reef degraded areas within Sanya Bay, South China Sea. *J. Coast. Res.* 33, 1148–1160.

Hamady, M., Walker, J. J., Harris, J. K., Gold, N. J., and Knight, R. (2008). Error-correcting barcoded primers for pyrosequencing hundreds of samples in multiplex. *Nat. Methods* 5, 235–237. doi: 10.1038/nmeth.1184

Hamilton, T. L., Bryant, D. A., and Macalady, J. L. (2016). The role of biology in planetary evolution: cyanobacterial primary production in low-oxygen Proterozoic oceans. *Environ. Microbiol.* 18, 325–340. doi: 10.1111/1462-2920.13118

Hong, M.-J., Yu, Y.-T., Chen, C. A., Chiang, P.-W., and Tang, S.-L. (2009). Influence of species specificity and other factors on bacteria associated with the coral *Stylophora pistillata* in Taiwan. *Appl. Environ. Microbiol.* 75, 7797–7806. doi: 10.1128/aem.01418-09

Lema, K. A., Bourne, D. G., and Willis, B. L. (2014). Onset and establishment of diazotrophs and other bacterial associates in the early life history stages of the coral *Acropora millepora*. *Mol. Ecol.* 23, 4682–4695. doi: 10.1111/mec.12899

Lema, K. A., Clode, P. L., Kilburn, M. R., Thornton, R., Willis, B. L., and Bourne, D. G. (2016). Imaging the uptake of nitrogen-fixing bacteria into larvae of the coral *Acropora millepora*. *ISME J.* 10, 1804–1808. doi: 10.1038/ismej.2015.229

Lema, K. A., Willis, B. L., and Bourne, D. G. (2012). Corals form characteristic associations with symbiotic nitrogen-fixing bacteria. *Appl. Environ. Microbiol.* 78, 3136–3144. doi: 10.1128/aem.07800-11

Lesser, M. P., Mazel, C. H., Gorbunov, M. Y., and Falkowski, P. G. (2004). Discovery of symbiotic nitrogen-fixing *Cyanobacteria* in corals. *Science* 305, 997–1000.

Li, J., Chen, Q., Zhang, S., Huang, H., Yang, J., Tian, X.-P., et al. (2013). Highly heterogeneous bacterial communities associated with the South China Sea reef corals *Porites lutea*, *Galaxea fascicularis* and *Acropora millepora*. *PLoS One* 8:e71301. doi: 10.1371/journal.pone.0071301

Liang, J., Yu, K., Wang, Y., Huang, X., Huang, W., Qin, Z., et al. (2017). Distinct bacterial communities associated with massive and branching scleractinian corals and potential linkages to coral susceptibility to thermal or cold stress. *Front. Microbiol.* 8:979. doi: 10.3389/fmicb.2017.00979

Lozupone, C., and Knight, R. (2005). UniFrac: a new phylogenetic method for comparing microbial communities. *Appl. Environ. Microbiol.* 71, 8228–8235. doi: 10.1128/aem.71.12.8228-8235.2005

Magoč, T., and Salzberg, S. L. (2011). FLASH: fast length adjustment of short reads to improve genome assemblies. *Bioinformatics* 27, 2957–2963. doi: 10.1093/bioinformatics/btr507

McKew, B. A., Dumbrell, A. J., Daud, S. D., Hepburn, L., Thorpe, E., Mogensen, L., et al. (2012). Characterization of geographically distinct bacterial communities associated with coral mucus produced by *Acropora* spp. and *Porites spp*. *Appl. Environ. Microbiol.* 78, 5229–5237. doi: 10.1128/aem.07764-11

Mori, H., Maruyama, F., Kato, H., Toyoda, A., Dozono, A., Ohtsubo, Y., et al. (2014). Design and experimental application of a novel non-degenerate universal primer set that amplifies prokaryotic 16S rRNA genes with a low possibility to amplify eukaryotic rRNA genes. *DNA Res.* 21, 217–227. doi: 10.1093/dnares/dst052

Muscatine, L., Falkowski, P. G., Dubinsky, Z., Cook, P. A., and Mccloskey, L. R. (1989). The effect of external nutrient resources on the population dynamics of Zooxanthellae in a reef coral. *Proc. R. Soc. Lond. B Biol. Sci.* 236, 311–324. doi: 10.1098/rspb.1989.0025

Nakajima, R., Tsuchiya, K., Nakatomi, N., Yoshida, T., Tada, Y., Konno, F., et al. (2013). Enrichment of microbial abundance in the sea-surface microlayer over a coral reef: Implications for biogeochemical cycles in reef ecosystems. *Mar. Ecol. Prog. Ser.* 490, 11–22. doi: 10.3354/meps10481

Olson, N. D., Ainsworth, T. D., Gates, R. D., and Takabayashi, M. (2009). Diazotrophic bacteria associated with Hawaiian *Montipora* corals: Diversity and abundance in correlation with symbiotic dinoflagellates. *J. Exp. Mar. Biol. Ecol.* 371, 140–146. doi: 10.1016/j.jembe.2009.01.012

Piniak, G. A., Lipschultz, F., and Mcclelland, J. (2003). Assimilation and partitioning of prey nitrogn within two anthozoans and their endosymbiotic zooxanthellae. *Mar. Ecol. Prog. Ser.* 262, 125–136. doi: 10.3354/meps262125

Qin, Z., Yu, K., Wang, Y., Xu, L., Huang, X., Chen, B., et al. (2019). Spatial and intergeneric variation in physiological indicators of corals in the South China Sea: insights Iinto their current state and their adaptability to environmental stress. *J. Geophys. Res. Oceans* 124, 3317–3332. doi: 10.1029/2018jc014648

Quast, C., Pruesse, E., Yilmaz, P., Gerken, J., Schweer, T., Yarza, P., et al. (2013). The SILVA ribosomal RNA gene database project: improved data processing and web-based tools. *Nucl. Acids Res.* 41, D590–D596.

Rädecker, N., Pogoreutz, C., Voolstra, C. R., Wiedenmann, J., and Wild, C. (2015). Nitrogen cycling in corals: The key to understanding holobiont functioning? *Trends Microbiol.* 23, 490–497. doi: 10.1016/j.tim.2015.03.008

Rösch, C., Mergel, A., and Bothe, H. (2002). Biodiversity of denitrifying and dinitrogen-fixing bacteria in an acid forest soil. *Appl. Environ. Microbiol.* 68, 3818–3829. doi: 10.1128/aem.68.8.3818-3829.2002

Rougerie, F., and Wauthy, B. (1993). The endo-upwelling concept: from geothermal convection to reef construction. *Coral Reefs* 12, 19–30. doi: 10.1007/bf00303781

Sammarco, P. W., Risk, M. J., Schwarcz, H. P., and Heikoop, J. M. (1999). Cross-continental shelf trends in δ15N in coral on the great barrier reef: further consideration of the reef nutrient paradox. *Mar. Ecol. Prog. Ser.* 180, 131–138. doi: 10.3354/meps180131

Sarhan, T., Vargas, M., Vargas, J. M., and Plaza, F. (2000). Upwelling mechanisms in the northwestern Alboran Sea. *J. Mar. Syst.* 23, 317–331. doi: 10.1016/s0924-7963(99)00068-8

Schloss, P. D., Gevers, D., and Westcott, S. L. (2011). Reducing the effects of PCR amplification and sequencing artifacts on 16S rRNA-based studies. *PLoS One* 6:e27310. doi: 10.1371/journal.pone.0027310 doi: 10.1371/journal.pone.0027310

Sun, Z., Li, G., Wang, C., Jing, Y., Zhu, Y., Zhang, S., et al. (2014). Community dynamics of prokaryotic and eukaryotic microbes in an estuary reservoir. *Sci. Rep.* 4:6966.

Wegley, L., Edwards, R., Rodriguez-Brito, B., Liu, H., and Rohwer, F. (2007). Metagenomic analysis of the microbial community associated with the coral *Porites astreoides*. *Environ. Microbiol.* 9, 2707–2719. doi: 10.1111/j.1462-2920.2007.01383.x

Wilkinson, C. R., Williams, D. M., Sammarco, P. W., Hogg, R. W., and Trott, L. A. (1984). Rates of nitrogen fixation on coral reefs across the continental shelf of the central great barrier reef. *Mar. Biol.* 80, 255–262. doi: 10.1007/bf00392820

Williams, W. M., Viner, A. B., and Broughton, W. J. (1987). Nitrogen fixation (acetylene reduction) associated with the living coral *Acropora variabilis*. *Mar. Biol.* 94, 531–535. doi: 10.1007/bf00431399

Xu, L., Yu, K., Li, S., Liu, G., Tao, S., Shi, Q., et al. (2017). Interseasonal and interspecies diversities of *Symbiodinium* density and effective photochemical efficiency in five dominant reef coral species from Luhuitou fringing reef, northern South China Sea. *Coral Reefs* 36, 477–487. doi: 10.1007/s00338-016-1532-y

Xu, N., Tan, G., Wang, H., and Gai, X. (2016). Effect of biochar additions to soil on nitrogen leaching, microbial biomass and bacterial community structure. *Eur. J. Soil Biol.* 74, 1–8. doi: 10.1016/j.ejsobi.2016.02.004

Yamamuro, M., Kayanne, H., and Minagawao, M. (1995). Carbon and nitrogen stable isotopes of primary producers in coral reef ecosystems. *Limnol. Oceanogr.* 40, 617–621. doi: 10.4319/lo.1995.40.3.0617

Yang, S.-H., Lee, S. T. M., Huang, C.-R., Tseng, C.-H., Chiang, P.-W., Chen, C.-P., et al. (2016). Prevalence of potential nitrogen-fixing, green sulfur bacteria in the skeleton of reef-building coral *Isopora palifera*. *Limnol. Oceanogr.* 61, 1078–1086. doi: 10.1002/lno.10277

Yu, K. (2012). Coral reefs in the South China Sea: their response to and records on past environmental changes. *Sci. Chin. Ear. Sci.* 55, 1217–1229. doi: 10.1007/s11430-012-4449-5

Yu, K., Zhao, J., Shi, Q., and Meng, Q. (2009). Reconstruction of storm/tsunami records over the last 4000 years using transported coral blocks and lagoon sediments in the southern South China Sea. *Quat. Int.* 195, 128–137. doi: 10.1016/j.quaint.2008.05.004

Yu, K. -F., Zhao, J.-X., Liu, T.-S., Wei, G.-J., Wang, P.-X., and Collerson, K. D. (2004). High-frequency winter cooling and reef coral mortality during the holocene climatic optimum. *Earth Planet. Sc. Lett.* 224, 143–155. doi: 10.1016/j.epsl.2004.04.036

Yu, K., Zhao, J., Collerson, K. D., Shi, Q., Chen, T., Wang, P., et al. (2004). Storm cycles in the last millennium recorded in Yongshu Reef, southern South China Sea. *Palaeogeogr. Palaeoclimat. Palaeoecol.* 210, 89–100. doi: 10.1016/j.palaeo.2004.04.002

Zehr, J. P., Jenkins, B. D., Short, S. M., and Steward, G. F. (2003). Nitrogenase gene diversity and microbial community structure: a cross-system comparison. *Environ. Microbiol.* 5, 539–554. doi: 10.1046/j.1462-2920.2003.00451.x

Zhang, R., Yu, K., Li, A., Wang, Y., and Huang, X. (2019). Antibiotics in corals of the South China Sea: occurrence, distribution, bioaccumulation, and considerable role of coral mucus. *Environ. Pollut.* 250, 503–510. doi: 10.1016/j.envpol.2019.04.036

Zhao, M., Yu, K., Zhang, Q., Shi, Q., and Price, G. J. (2012). Long-term decline of a fringing coral reef in the northern South China Sea. *J. Coast. Res.* 28, 1088–1099.

Conflict of Interest: The authors declare that the research was conducted in the absence of any commercial or financial relationships that could be construed as a potential conflict of interest.

frontiers in Marine Science

ORIGINAL RESEARCH
published: 07 July 2020
doi: 10.3389/fmars.2020.00531

Effects of Nitrate Enrichment on Respiration, Photosynthesis, and Fatty Acid Composition of Reef Coral *Pocillopora damicornis* Larvae

Cheng-Yue Liu[1,2,3,4,5], *Fang Zhang*[1,4,5,6], *You-Fang Sun*[1,6], *Xiao-Lei Yu*[1,6] *and Hui Huang*[1,2,3,4,5]*

[1] *Key Laboratory of Tropical Marine Bio-resources and Ecology, South China Sea Institute of Oceanology, Chinese Academy of Sciences, Guangzhou, China,* [2] *Guangdong Provincial Key Laboratory of Applied Marine Biology, South China Sea Institute of Oceanology, Chinese Academy of Sciences, Guangzhou, China,* [3] *Innovation Academy of South China Sea Ecology and Environmental Engineering, South China Sea Institute of Oceanology, Chinese Academy of Sciences, Guangzhou, China,* [4] *Hainan Tropical Marine Biological Research Station, South China Sea Institute of Oceanology, Chinese Academy of Sciences, Sanya, China,* [5] *Hainan Key Laboratory of Tropical Marine Biotechnology, Sanya, China,* [6] *University of Chinese Academy of Sciences, Beijing, China*

In the foreseeable future, coastal coral reef ecosystems are likely to face further increases in eutrophication. Lipids and fatty acids (FAs), as important components of corals, are becoming a hot topic to study the effects of eutrophication on corals. This study investigated the effects of nitrate (NO^{3-}) enrichment (0, 5, 10, 20, and 40 μM) on the respiration, photosynthesis, and FA compositions of *Pocillopora damicornis* larvae. Our results showed that saturated FAs (SFAs) were the most abundant in *P. damicornis* larvae over all treatment groups, followed by polyunsaturated FAs (PUFAs). The unsaturated-to-SFA ratio (U/S) and unsaturation index (UI) reduced at low nitrate concentrations (<10 μM), since the level of SFAs (mainly 16:0 and 18:0) increased whereas PUFAs (mainly 18:3n3, 20:3n6, and 22:6n3) decreased. Consequently, the biomembranes of the larvae may have become more rigid and viscous, which slowed excessive nitrate entry. Moreover, significantly enhanced photosynthetic functions of zooxanthellae in larvae were found in the N5 group (5 μM). However, the opposite FA patterns were observed in *P. damicornis* larvae at higher nitrate concentrations (>20 μM). The UI and U/S levels were elevated due to the increased PUFAs levels and decreased SFA levels at higher nitrate concentrations. Compared with the N5 and N10 groups, the fluidity of the biomembrane of the larvae did not continue to decrease but instead increased at higher nitrate concentrations, indicating that the biomembrane restructuring in the larvae may have become ineffective. Moreover, respiration increased and the consumption of numerous lipids led to a significant decrease in TFAs. These could adversely affect the dispersal, settlement, and development of larvae. Overall, *P. damicornis* larvae can adapt to low levels of nitrate (<10 μM) due to biomembrane restructuring through changes in FA composition. However, negative effects occur in larvae when nitrate exceeds 20 μM.

Keywords: *Pocillopora damicornis* larvae, fatty acid composition, nitrate enrichment, biomembrane restructuring, respiration, photosynthesis

OPEN ACCESS

Edited by:
Zhi Zhou,
Hainan University, China

Reviewed by:
Tingting Xiang,
University of North Carolina at Charlotte, United States
Zhaoqun Liu,
Dalian Ocean University, China

***Correspondence:**
Hui Huang
huanghui@scsio.ac.cn

Specialty section:
This article was submitted to Coral Reef Research, a section of the journal Frontiers in Marine Science

Received: *09 April 2020*
Accepted: *11 June 2020*
Published: *07 July 2020*

Citation:
Liu C-Y, Zhang F, Sun Y-F, Yu X-L and Huang H (2020) Effects of Nitrate Enrichment on Respiration, Photosynthesis, and Fatty Acid Composition of Reef Coral Pocillopora damicornis Larvae. Front. Mar. Sci. 7:531. doi: 10.3389/fmars.2020.00531

INTRODUCTION

Reef ecosystems are among the world's most productive and biodiverse marine ecosystems (Hughes et al., 2018; Kubicek et al., 2019). Scleractinian corals serve as the framework for these ecosystems (Zaneveld et al., 2016). Coral reef waters usually contain low levels of inorganic nutrients (Renegar and Riegl, 2005). However, increased human population densities, the use of chemical fertilizers in agriculture, and domestic sewage discharge could significantly increase the input of nutrients into coastal zones (D'Angelo and Wiedenmann, 2014; Serrano et al., 2018). For the foreseeable future, coastal coral reef ecosystems are likely to face further increases in eutrophication (Humanes et al., 2016). The effect of nutrients on corals and their algal symbionts is still subject to debate. Some researchers have suggested that elevated nutrient levels can significantly decrease the growth and calcification of coral (Ferrierpagès et al., 2000; Renegar and Riegl, 2005). However, positive responses in coral to increased nutrient availability have also been found, including reduced thermal stress, zooxanthellae supplementation, and moderate bleaching (Atkinson et al., 1995; Bender-Champ et al., 2017).

Lipids and fatty acids (FAs) are the primary constituents of the cells and subcellular organelle membranes in marine organisms. They are vital structural components of biomembranes that adapt to variations in environmental conditions by changing their FA composition (Sinensky, 1974; Hazel, 1979; Wijekoon, 2011; Bennett et al., 2018). This process, called homeoviscous adaptation, can affect membrane-associated physical attributes and biological functions such as fluidity, phase behavior, thickness, permeability, and related enzymes (Yeagle, 1989; Ernst et al., 2016; Bennett et al., 2018). Lipids represent a major component of the coral composition (10–40% of dry biomass in adult corals and 34–85% of dry biomass in larvae) (Bhojoo et al., 2017; Conlan et al., 2017). Although most endogenous lipids and FAs in coral are provided by CO_2 fixation of zooxanthellae, corals also modify these lipids and FAs according to their own needs for development, reproduction, and adaptation to environmental change. Lipids and FAs are becoming a hot topic to study the effects of environmental changes on corals.

Successful dispersal, settlement, and development of larvae are critical for the maintenance of coral populations (Figueiredo et al., 2012; Jiang et al., 2019). Many physiological characteristics of coral larvae (e.g., immature cellular defenses and smaller biomass) may render them more susceptible than adult corals when exposed to the same stressors (Jiang et al., 2017; Serrano et al., 2018). However, there are few studies on the effects of nutrient enrichment on the early life stages of coral. The limited data available suggest that nitrate enrichment significantly affects performance (such as survival, growth, and settlement) (Ward and Harrison, 2000; Harrison and Ward, 2001; Lam et al., 2015; Humanes et al., 2016) and metabolism (Serrano et al., 2018). To our knowledge, no studies have yet investigated the effects of nitrate enrichment on lipids and FA composition of coral larvae.

Sanya (Hainan Province, China) is a typical tourist city, and the coastal region around it suffers from eutrophication, especially in terms of nitrates. Indeed, the nutrient levels have become significantly elevated with the rapid development of tourism and increasing population (Jing et al., 2017). Moreover, *Pocillopora damicornis* is widely distributed in this region and functions as a major hermatypic coral on reef flats. The present study assessed the respiration, photosynthesis, and FA composition of *P. damicornis* larvae with different nitrate concentrations and explored the tolerance and acclimation mechanism of *P. damicornis* larvae to nitrate enrichment from the perspective of biomembrane restructuring. These findings could provide a theoretical basis to evaluate and predict the recruitment and community reassembly of *P. damicornis* in coastal regions, especially in eutrophic areas.

MATERIALS AND METHODS

Coral Sampling and Larvae Collection

On 18 August 2018, 10 adult colonies of *P. damicornis* were collected from Luhuitou Fringing Reef (N18°12.7', E109°28.5') at depths of 2–3 m. The colonies were transported to the Tropical Marine Biological Research Station and acclimated for 24 h in fiberglass cylindrical tanks, then placed individually into 18 L flow-through tanks at ambient temperature (28.7 ± 0.5°C) under partially shaded conditions (noon irradiance, ∼300 μmol photonsm^{-2}s^{-1}). The outflow of each tank was passed through a cup fitted with a 180-μm net on the bottom to trap larvae. Larvae released from these colonies were collected at 07:00 on 19 August 2018 and then pooled.

Experimental Design

Laboratory experiments were performed to study the effects of nitrate enrichment on *P. damicornis* larvae. Five different treatments were established: a control group (N0) and the N5, N10, N20, and N40 groups (nitrate concentrations for each treatment are shown in **Table 1**). The *P. damicornis* larvae were stocked at a density of 300 per plastic tank (500 mL; 10.0 cm height × 10.0 cm diameter). The experiment was run for 5 days, and each treatment had three replicates. The larvae in the control group were treated with 0.5-μm-filtered seawater, and the other four nitrate-enrichment treatments involved seawater with different KNO_3 levels. The temperature was maintained at 29 ± 0.5°C, and a series of full-spectrum fluorescent bulbs (Giesemann, Nettetal, Germany) was used for irradiance (∼300 μmol photonsm^{-2}s^{-1}, photoperiod 12:12).

TABLE 1 | Nitrate concentration of each treatment.

Treatment	The concentration of NO_3^-/μM)
Control	2.5 ± 0.53
N5	6.8 ± 0.79
N10	11.1 ± 1.1
N20	18.5 ± 1.84
N40	36.4 ± 1.9

Values are mean ± SD.

Respiration and Photosynthesis

Dark respiration (R_D) and net photosynthesis (P_{Net}) of the larvae were measured after the fifth day of the experiment. A miniature stir bar (3 × 5 mm) and 20 larvae randomly sampled from each tank were transferred into a 2-mL glass vial with an oxygen optical sensing patch on the inside wall. The filtered seawater in the vial was from the corresponding experimental tank. After turning on the magnetic stirrer (300 r/min) and dissolved oxygen meter (OXY-4 mini; Presens, Regensburg, Germany), we continuously recorded the oxygen concentration at 10-s intervals over 10 min under the same illumination as the experiment. Then, P_{Net} was calculated using the least squares linear regression of the oxygen concentration plotted against time and expressed as nanomoles of oxygen per min per larvae. R_D was measured after 2 h dark adaptation. Except that the measurement of R_D was taken with no light, the details and methods were the same as those for the P_{Net} measurements. Two additional vials containing only filtered seawater were run as the blank control for each treatment, and the results showed that the background respiration was negligible. The ratios of P_{Net} to R_D (P_{Net}/R_D) were calculated to assess autotrophic capacity (Muscatine et al., 1981). A P_{Net}/R_D ratio > 1 indicated that the net organic carbon fixed by photosynthesis of symbiotic zooxanthellae was enough to sustain the consumption of respiration. Otherwise, it implied that the endogenous reserves of the larvae were consumed.

Lipid Extraction and FA Analysis

Approximately 500 larvae (0.1 g) were collected from each group and analyzed (n = 3). The samples was homogenized, and each lipid fraction was extracted using chloroform/methanol (2:1, v/v) containing 0.01% butylated hydroxytoluene as an antioxidant, as previously described by Liu et al. (2019). The chloroform layer was separated from the methanol layer and dried to a constant weight under a stream of nitrogen to obtain lipids. FA methyl esters (FAMEs) were obtained by esterification with 2 mL methyl esterification reagent (hydrochloric acid/methanol, 1:5, v/v) at 90°C for 3 h, as described by Liu et al. (2018). The upper phase was dried under nitrogen and resuspended in hexane.

Fatty acid methyl esters were quantified by injecting 1 μL of sample into a gas chromatograph (GC-2010 Plus; Shimadzu,

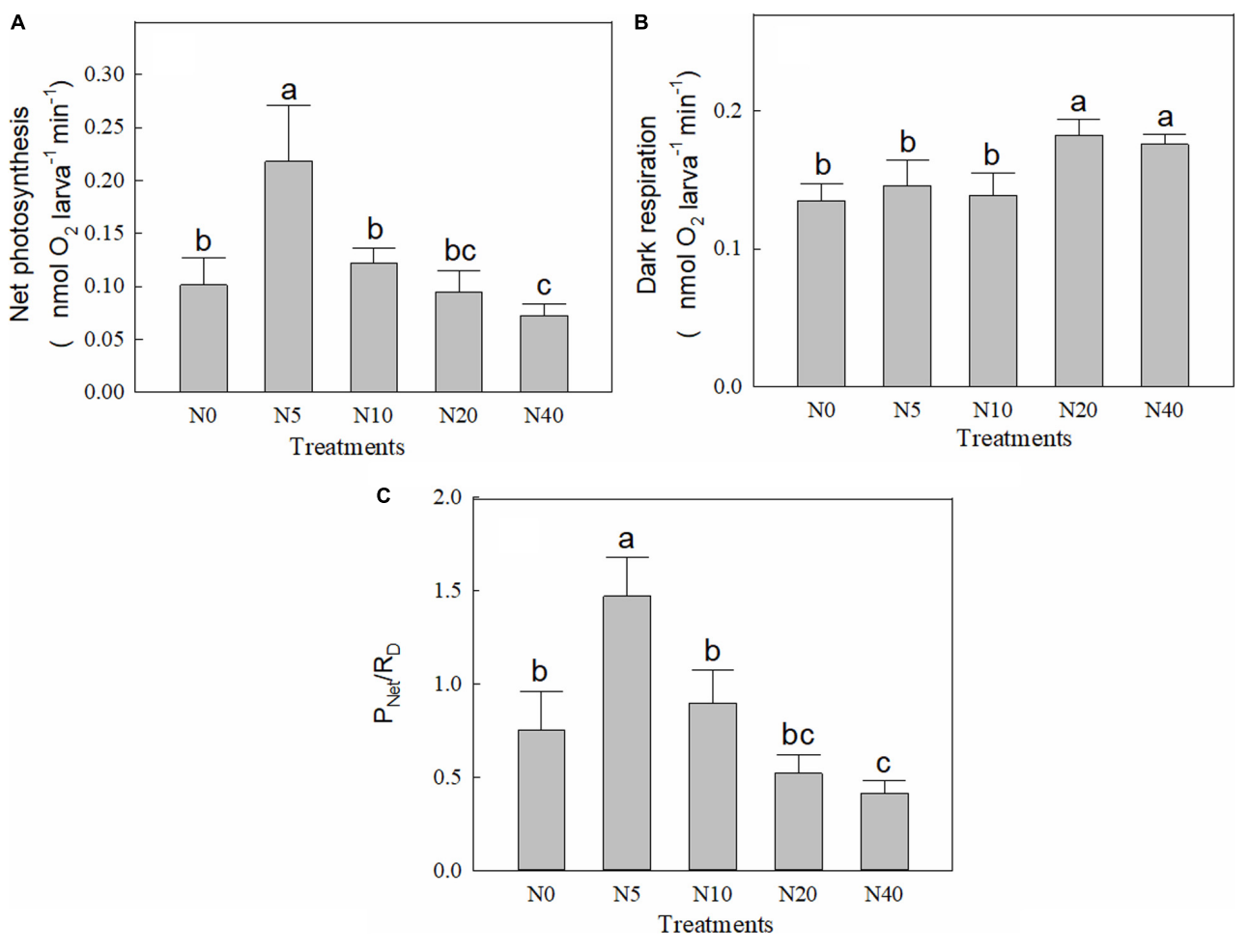

FIGURE 1 | Net photosynthesis **(A)**, dark respiration **(B)**, ratio of photosynthesis to respiration **(C)** of *P. damicornis* larvae in each treatment.

Kyoto, Japan) equipped with a flame-ionization detector (GC-2010; Shimadzu) and an RTX-WAX fused-silica capillary column (length, 30 m; internal diameter, 0.25 mm; thickness, 0.25 μm; Phenomenex, Torrance, CA, United States). The gradient temperature program was set as follows: (i) initial temperature of 60°C for 1.0 min; (ii) increase at a rate of 10°Cmin^{-1} to 190°C, (iii) increase at 2.0°Cmin^{-1} to 260°C; (iv) hold at 260°C for 0.6 min. FAME identification and quantification were performed by comparing the retention times (identification) and peak areas (quantification) with 37-FAME Mix calibration solution (Supelco, Bellefonte, PA, United States).

Statistical Analyses

SAS statistical software version 9.4 (SAS Institute, Cary, NC, United States) was used for statistical analyses. The distribution of data was evaluated for normality with the Kolmogorov–Smirnov test ($P > 0.05$). The Levene's test ($P > 0.05$) was used to assess the homogeneity of variance. All data were then evaluated by one-way analysis of variance, followed by the Student–Newman–Keuls multiple-comparisons test to identify significant differences ($P < 0.05$) between the means of the different treatment groups. Moreover, principal component analysis (PCA) was used to display significant differences in FA profiles among the five treatment groups.

To facilitate comparison of the FA compositions, we calculated the unsaturation index (UI) and the unsaturated-to-saturated FA ratio (U/S) as reported by Wallaert and Babin (1994) and Snyder and Hennessey (2003). The UI and U/S algorithms were as follows:

$$UI = \Sigma(\%\text{monoenes} + 2 \times \%\text{dienes} + 3 \times \%\text{trienes}\ldots)/100 \quad (1)$$

$$U/S = \Sigma(\%UFA)/\Sigma(\%SFA) \quad (2)$$

where monoenes, dienes, trienes... are FAs containing 1, 2, 3... double bonds, respectively; %: weight percentage; UFA: unsaturated FAs; SFA: saturated FAs.

RESULTS

Respiration and Photosynthesis of *P. damicornis* Larvae With Nitrate Enrichment

The P_{Net} of *P. damicornis* larvae showed an initial increase and then a decrease with increasing nitrate concentration (**Figure 1A**). The highest P_{Net} (0.2180 nmol O_2 $larvae^{-1}$ min^{-1}) was observed in the N5 group, which was more than double that of the control group (N0, 0.1012 nmol O_2 $larvae^{-1}$ min^{-1}). Subsequently, P_{Net} decreased with increasing nitrate concentration, and the lowest P_{Net} was observed in N40 (0.0726 nmol O_2 $larvae^{-1}$ min^{-1}). Although the R_D showed no change ($p > 0.05$) at nitrate concentrations ≤ 10 μM (N0, N5, and N10 groups), it significantly increased ($p < 0.05$) in the N20 and N40 groups (**Figure 1B**). The ratio of P_{Net}/R_D ranged from 0.4151 to 1.4724 (**Figure 1C**). The P_{Net}/R_D showed similar changes to those of P_{Net} and, except for N5, P_{Net}/R_D of the treatment groups were less than 1. The lowest P_{Net}/R_D was in the N40 group (0.4151).

Total Fatty Acids (TFAs) of *P. damicornis* Larvae

The TFA levels present in the *P. damicornis* larvae after each treatment are shown in **Table 2**. When the nitrate concentration was less than 10 μM (N0, N5, and N10 groups), the TFA levels in *P. damicornis* larvae were not significantly different ($p > 0.05$). When the nitrate concentration was further elevated, the TFAs significantly decreased ($p < 0.05$). The lowest TFA levels (45.87 μg/g) were observed when the nitrate concentration was 40 μM (N40 group), and were less than half those in the control group.

FA Compositions of *P. damicornis* Larvae

Twenty-three FA species were identified among the *P. damicornis* larvae, including nine SFAs, eight monounsaturated FAs (MUFAs), and nine polyunsaturated FAs (PUFAs). Seven major FAs were recurrently found in *P. damicornis* larvae, including palmitic acid (16:0), stearic acid (18:0), heneicosanoic acid (21:0), oleic acid (18:1n9), palmitoleic acid (16:1n7), EPA (20:5n3), and DHA (22:6n3).

The *P. damicornis* larvae had the highest abundance of SFAs (more than 60%), followed by PUFAs (approximately 30%), and the lowest abundance of MUFAs (only 10%). The predominant SFA, MUFA, and PUFA were 16:0, 16:1n7, and 22:6n3, respectively. Moreover, the UI ranged between 1.35 and 1.07, and the U/S ratio ranged between 0.65 and 0.51. The maximum and minimum UI and U/S levels occurred in the N5 and N0 groups, respectively.

FA Composition Change in *P. damicornis* Larvae With Nitrate Enrichment

The FA profiles of the *P. damicornis* larvae with different nitrate enrichments are shown in **Table 3** and **Figure 2**. To better visualize the FA changes in the *P. damicornis* larvae with different nitrate concentrations, six line charts for UI, U/S, SFA, MUFA, and PUFA are presented in **Figure 3**. When the nitrate concentration was less than 10 μM, the SFA levels in the *P. damicornis* larvae were significantly elevated, primarily due to increased 16:0 and 18:0 levels and decreased PUFA concentrations (18:2n6, 18:3n3, 20:3n6, and 22:6n3), with corresponding reductions in UI and U/S.

In contrast, the SFA levels of larvae decreased and the UFAs increased in the N20 group, leading to elevated UI and U/S. Compared with the N20 group, no significant difference ($p > 0.05$) was observed in the FA profiles of the *P. damicornis* larvae in the N40 group. Although the levels of some monoenes altered significantly throughout the

TABLE 2 | Total fatty acids of *Pocillopora damicornis* larvae with different nitrate concentrations (μg/g).

Nitrate	0	5	10	20	40	*P*-value
TFA	97.08 ± 1.09^{a}	90.77 ± 0.58^{a}	88.8 ± 0.22^{a}	57.37 ± 0.26^{b}	45.87 ± 0.45^{c}	<0.0001

Values are mean ± SD, significant differences (P < 0.05) each row are indicated by different lower-case letters. TFA, total fatty acids.

TABLE 3 | Fatty acid compositions (% total fatty acids) of *P. damicornis* larvae with different nitrate concentrations.

Nitrate	0	5	10	20	40	*P*-value
Saturated fatty acids						
14:0	4.18 ± 0.15^{a}	3.96 ± 0.04^{ab}	3.86 ± 0.02^{b}	3.91 ± 0.02^{b}	4.02 ± 0.15^{ab}	0.0204
15:0	0.06 ± 0.01	0.07 ± 0.01	0.07 ± 0.00	0.09 ± 0.01	0.08 ± 0.02	0.0622
16:0	32.69 ± 0.33^{b}	33.99 ± 0.36^{a}	34.26 ± 0.31^{a}	32.66 ± 0.12^{b}	32.63 ± 0.1^{b}	< 0.0001
17:0	0.10 ± 0.01^{b}	0.11 ± 0.01^{b}	0.16 ± 0.02^{a}	0.12 ± 0.01^{b}	0.11 ± 0.01^{b}	0.0016
18:0	14.23 ± 0.71^{c}	17.63 ± 0.57^{a}	20.3 ± 0.09^{a}	17.16 ± 0.22^{b}	16.94 ± 0.14^{b}	< 0.0001
20:0	0.86 ± 0.02^{a}	0.74 ± 0.02^{b}	0.83 ± 0.07^{a}	0.80 ± 0.01^{ab}	0.79 ± 0.01^{ab}	0.0116
21:0	6.95 ± 0.43^{a}	5.77 ± 0.17^{c}	5.51 ± 0.22^{c}	6.43 ± 0.03^{b}	6.44 ± 0.06^{b}	0.0001
22:0	0.16 ± 0.01	0.14 ± 0.01	0.16 ± 0.02	0.15 ± 0.00	0.15 ± 0.00	0.2055
23:0	1.45 ± 0.21	1.51 ± 0.24	1.28 ± 0.06	1.38 ± 0.08	1.39 ± 0.02	0.4752
ΣSFA	60.69 ± 0.9^{d}	63.92 ± 0.18^{b}	66.43 ± 0.37^{a}	62.68 ± 0.1^{c}	62.54 ± 0.11^{c}	< 0.0001
Monounsaturated fatty acids						
14:1n5	0.06 ± 0.01	0.06 ± 0.01	0.04 ± 0.01	0.06 ± 0.01	0.05 ± 0.00	0.2237
15:1n5	0.77 ± 0.03	0.88 ± 0.06	0.80 ± 0.11	0.72 ± 0.01	0.77 ± 0.01	0.0008
16:1n7	4.29 ± 0.16	4.33 ± 0.22	4.03 ± 0.00	4.09 ± 0.01	4.13 ± 0.05	0.0049
17:1n7	0.06 ± 0.01^{b}	0.27 ± 0.37^{ab}	0.64 ± 0.00^{a}	0.56 ± 0.00^{a}	0.46 ± 0.07^{a}	0.0115
18:1n9	4.40 ± 0.40^{a}	3.50 ± 0.13^{b}	3.59 ± 0.11^{b}	3.78 ± 0.01^{b}	3.75 ± 0.02^{b}	0.0016
20:1n9	1.01 ± 0.17^{a}	0.78 ± 0.02^{b}	0.79 ± 0.04^{b}	0.82 ± 0.00^{b}	0.81 ± 0.01^{b}	0.0239
22:1n9	0.07 ± 0.01^{ab}	0.08 ± 0.02^{a}	0.05 ± 0.01^{ab}	0.06 ± 0.00^{ab}	0.05 ± 0.01^{b}	0.0335
24:1n9	0.13 ± 0.03	0.12 ± 0.01	0.12 ± 0.02	0.12 ± 0.00	0.09 ± 0.04	0.2075
ΣMUFA	10.79 ± 0.67	10.01 ± 0.64	10.07 ± 0.07	10.22 ± 0.02	10.1 ± 0.12	0.2248
Polyunsaturated fatty acids						
18:2n6	1.77 ± 0.11^{a}	1.58 ± 0.14^{b}	1.47 ± 0.00^{b}	1.58 ± 0.00^{b}	1.56 ± 0.02^{b}	0.0112
18:3n3	5.93 ± 0.38^{a}	5.43 ± 0.15^{bc}	5.2 ± 0.04^{c}	5.7 ± 0.04^{ab}	5.7 ± 0.08^{ab}	0.0063
18:3n6	1.64 ± 0.02	1.65 ± 0.08	1.52 ± 0.07	1.63 ± 0.01	1.64 ± 0.01	0.0399
20:2n6	0.92 ± 0.23	0.86 ± 0.05	0.76 ± 0.11	0.89 ± 0.01	0.91 ± 0.00	0.4375
20:3n6	3.18 ± 0.18^{a}	3.11 ± 0.04^{ab}	2.87 ± 0.03^{b}	2.95 ± 0.09^{b}	2.92 ± 0.11^{b}	0.018
20:4n6	0.51 ± 0.11	0.47 ± 0.05	0.47 ± 0.00	0.50 ± 0.00	0.50 ± 0.01	0.8297
20:5n3	2.36 ± 0.27	2.39 ± 0.13	2.12 ± 0.09	2.38 ± 0.02	2.42 ± 0.02	0.134
22.2n6	0.14 ± 0.02^{b}	0.23 ± 0.04^{b}	0.74 ± 0.19^{a}	0.61 ± 0.02^{a}	0.61 ± 0.02^{a}	< 0.0001
22:6n3	12.07 ± 0.45^{a}	10.38 ± 0.27^{c}	8.35 ± 0.36^{d}	10.87 ± 0.03^{bc}	11.09 ± 0.06^{b}	< 0.0001
ΣPUFA	28.52 ± 0.57^{a}	26.11 ± 0.53^{c}	23.5 ± 0.44^{d}	27.1 ± 0.11^{b}	27.35 ± 0.01^{b}	< 0.0001
UI	1.35 ± 0.03^{a}	1.22 ± 0.02^{c}	1.07 ± 0.03^{d}	1.26 ± 0.00^{b}	1.28 ± 0.00^{b}	< 0.0001
U/S	0.65 ± 0.02^{a}	0.57 ± 0.00^{c}	0.51 ± 0.00^{d}	0.60 ± 0.00^{b}	0.60 ± 0.00^{b}	< 0.0001

Values are mean ± SD, significant differences (P < 0.05) each row are indicated by different lower-case letters. MUFA, monounsaturated fatty acid; PUFA, polyunsaturated fatty acid; SFA, saturated fatty acid; UI, unsaturated index; U/S, the ratio of unsaturated and saturated fatty acid.

experiment (major change in 18:1n9), the total MUFA levels of the larvae did not change.

DISCUSSION

Respiration and Photosynthesis of *P. damicornis* Larvae With Nitrate Enrichment

Among all the groups, N5 had the highest P_{Net} and P_{Net}/R_D, which implied that low nitrate enrichment could promote photosynthesis in coral larval zooxanthellae. Marubini and Davies (1996) reported that low nitrate enrichment (>5 μM) enhances the photosynthesis of coral zooxanthellae by increasing zooxanthellae size and chlorophyll concentrations. Atkinson et al. (1995) also demonstrated that coral living in aquaria can thrive in relatively high-nutrient water (nitrate: about 5 μM). Nonetheless, coral species-specific responses to nitrate enrichment have been found in previous studies (Ferrier-Pagès et al., 2001; D'Angelo and Wiedenmann, 2014; Serrano et al., 2018). Contrary to our findings, Ferrier-Pagès et al. (2001) found that nitrate enrichment had no effect on *Stylophora pistillata*.

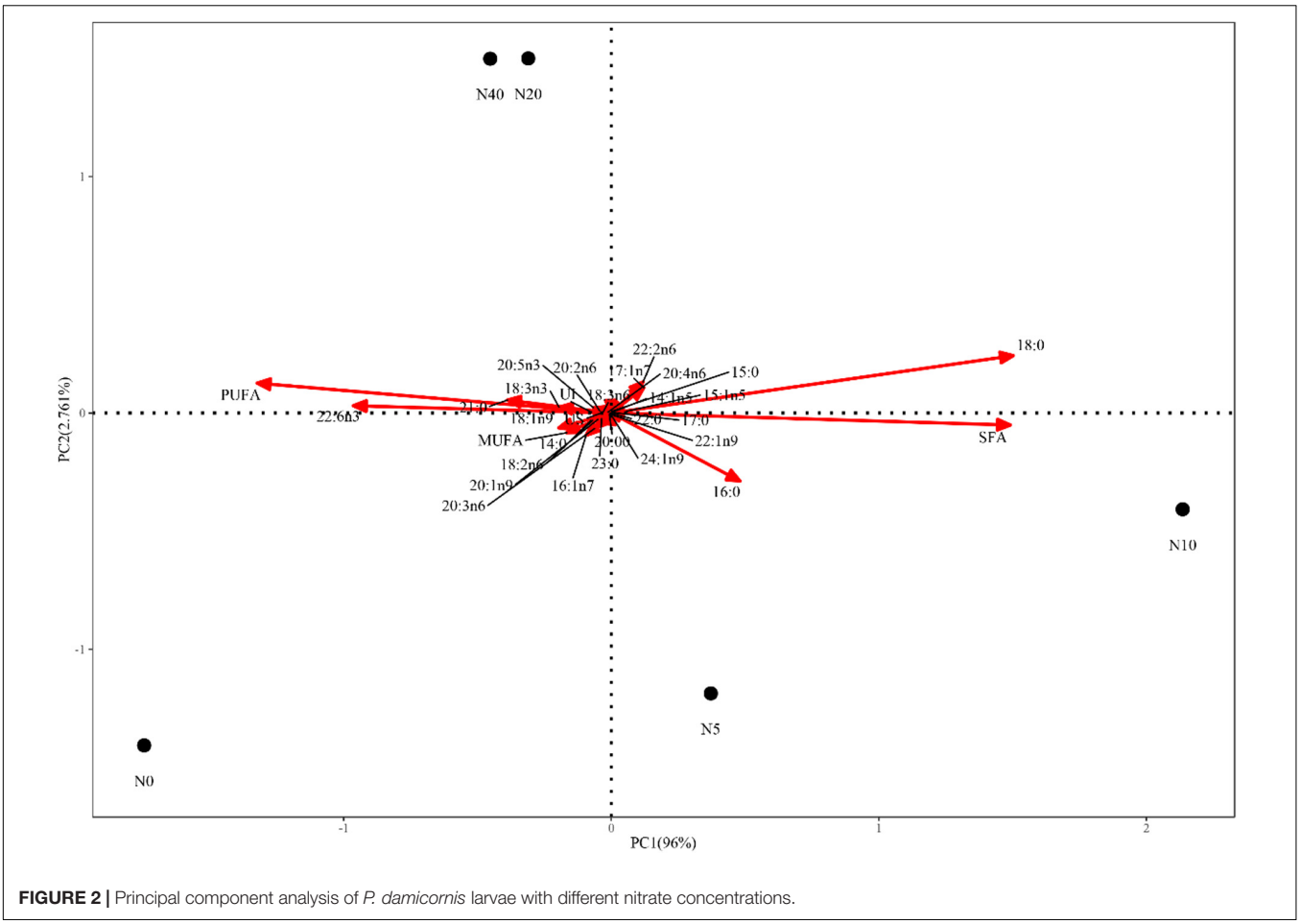

FIGURE 2 | Principal component analysis of *P. damicornis* larvae with different nitrate concentrations.

In this study, relatively higher nitrate concentrations produced P_{Net} decreases and R_D increases, resulting in decreased P_{Net}/R_D. This indicated that high levels of nitrate (>20 μM) would have a negative impact on *P. damicornis* larvae. Serrano et al. (2018) found that nitrate enrichment (12 μM) could significantly increase respiration in *Porites astreoides* larvae. Since R_D represents the metabolic rate of coral larvae, we hypothesized that *P. damicornis* larvae increase respiration in order to provide enough energy to ameliorate environmental stress. Nordemar et al. (2003) documented that the primary production of *Porites cylindrica* declined after 2 weeks of nitrate enrichment (15 μM), while zooxanthellae density and chlorophyll concentrations (photosynthesis) remained unaltered. Alternatively, increased respiration rates in nutrient-enriched *P. damicornis* larvae may affect their stress response to potential photo-physiological damage to their algal symbionts (D'Angelo and Wiedenmann, 2014).

FA Compositions of *P. damicornis* Larvae

In this study, the SFA level (mainly 16:0 and 18:0) was the highest (over 60%) for FAs in the *P. damicornis* larvae. The FA patterns of *P. damicornis* larvae were similar to those of adults of this species (previous unpublished research) and to those of *Goniastrea retiformis* (Figueiredo et al., 2012), *Acropora millepora*, *Acropora tenuis*, and *Montipora digitata* eggs (Arai et al., 1993). Both Papina et al. (2003) and Chen et al. (2015) found that palmitic acid (16:0) acted as a trophic marker of zooxanthellae and was abundant in coral larvae, especially those that inherited algal symbionts maternally from oocytes. *P. damicornis* release larvae that carry symbiotic microalgae, which may explain the higher SFAs observed in our study. Moreover, compared to PUFAs, SFAs have a more stable structure and are commonly used for bio-energy storage. Many investigators have reported that SFAs (such as 16:0 and 18:0) are the preferred sources of metabolic energy in marine organisms (Arai et al., 1993; Figueiredo et al., 2012; Wijekoon, 2012). Consequently, *P. damicornis* larvae need to store sufficient SFAs to have a capacity to delay metamorphosis until suitable settlement cues appear.

Likewise, a high abundance of several PUFAs (such as 18:3n3, 20:3n6, 20:5n3, and 22:6n3) was found. This may be due to the fact that symbiotic zooxanthellae contain high PUFA levels (Zhukova and Titlyanov, 2003) and symbionts transfer PUFAs to host tissue (Figueiredo et al., 2012), after which they are incorporated into their larvae. Although the specific functions of PUFAs for coral remain poorly studied, PUFAs, especially the n-3 and n-6 PUFAs, have been confirmed as critical to the growth, survival, and reproduction of many organisms, including corals

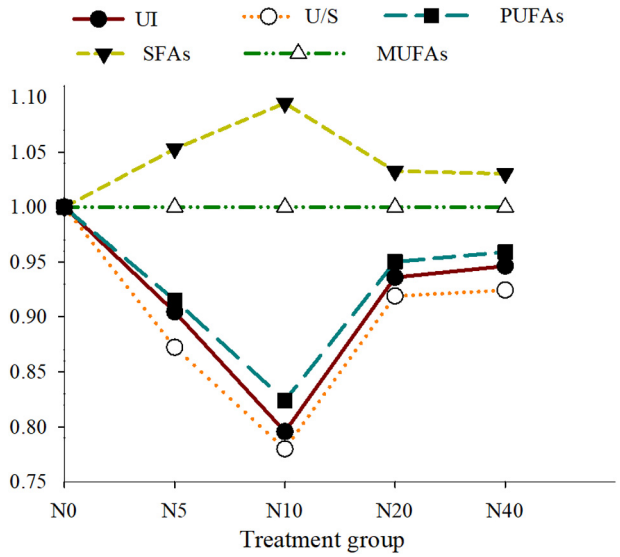

FIGURE 3 | Changes in UI, U/S, SFA, PUFA, and MUFA of *P. damicornis* larvae with different nitrate concentrations. Note: Each value is the ratio of the different treatment groups to the N0 group. MUFA, monounsaturated fatty acid; PUFA, polyunsaturated fatty acid; SFA, saturated fatty acid; UI, unsaturation index; U/S, unsaturated to saturated fatty acid ratio.

(Tchernov et al., 2004; Imbs, 2013; Chen et al., 2015; Ernst et al., 2016; Conlan et al., 2017).

Effect of Nitrate Enrichment on the FA Composition of *P. damicornis* Larvae

Significant changes in the FA compositions of *P. damicornis* larvae were observed under nitrate enrichment. Our results indicate that the lipids of *P. damicornis* larvae become progressively saturated (lower UI and U/S) when nitrate is less than 10 μM, which can be attributed to decreased PUFAs and a concomitant increase in SFAs. Moreover, no changes in TFA levels were found at the lower nitrate concentrations. Lipids and proteins are the primary constituents of biomembranes. Changes in FA composition could affect membrane-associated physical attributes and biological functions, such as membrane-phase behaviors, membrane thickness, and membrane permeability (Losa and Murata, 2004; Wijekoon, 2012; Ernst et al., 2016). Compared to UFAs, homologous SFAs have a higher melting point and occupy a smaller space within the membrane lipid bilayer, which enhances their rigidity and viscosity (Hazel, 1979; Yeagle, 1989; Liu et al., 2018). The more rigid and viscous the biomembrane, the more slowly harmful ions enter the organism. Thus, the present data indicated that *P. damicornis* larvae can adapt to low-level nitrate enrichment by biomembrane restructuring. While it is well established that FAs play an important role in stress resistance and that the ability of an organism to maintain appropriate membrane function integrity and cell homeostasis in the face of environmental change is intimately linked to tolerance, this is the first time that these responses have been demonstrated in coral larvae.

Moreover, with increases in environmental stress, organisms may produce more reactive oxygen species (ROS) (Cunning and Baker, 2013; Liu et al., 2018). Irrespective of the MUFA or PUFA contents, a higher proportion of UFAs in lipids was associated with increased ROS susceptibility, whereas SFAs did not undergo lipid peroxidation (Porter, 2013; Cengiz et al., 2017). Organisms with a higher proportion of SFAs could reduce the influence of ROS (Wada et al., 1994; Crockett, 2008; Liu et al., 2019). Thus, such adaptations with respect to lipids can minimize the influence of nitrate enrichment on *P. damicornis* larvae. Similarly, with nitrate enrichment, thermal stress can significantly affect the coral FA composition. While studying symbiotic algae in thermally bleached corals, Tchernov et al. (2004) found that higher SFAs enhanced the thermal stability of the eukaryotic thylakoid membranes of coral and simultaneously reduced the susceptibility of the membrane lipids to attacks by ROS.

One interesting result was that while UFAs were lowest in the N10 group, the P_{Net} dropped compared to the N5 group. Although higher SFA can increase biomembrane rigidity and anti-oxidation, it reduces membrane-bound enzyme activity and material exchange (Oku et al., 2002; Bachok et al., 2006; Ernst et al., 2016), which may reduce the photosynthesis of zooxanthellae. Bennett et al. (2018) reported that PUFA enrichment in the phototrophic sponge *Carteriospongia foliascens* can significantly facilitate enzyme activity. Ernst et al. (2016) showed that lipids with saturated acyl chains are packed at higher densities and tend to form non-fluid gel phases, which slow substance exchange.

Different FA patterns were observed in the *P. damicornis* larvae in the N20 and N40 groups. The UI and U/S levels were elevated due to the increased PUFA levels and decreased SFA levels at higher nitrate concentrations. Although the nitrate concentration increased, compared with the N5 and N10 groups, the fluidity of the biomembrane of the larvae did not continue to decrease but instead increased at higher nitrate concentrations, indicating that the biomembrane restructuring in the larvae may have become ineffective. In parallel, the TFAs decreased significantly. This result showed that numerous lipids were consumed rapidly. When ions exceed the threshold that the larvae can tolerate (hyperosmotic stress), the larvae need to excrete the ions via active transport in order to maintain homeostasis (Losa and Murata, 2004). Thus, a large amount of SFA, as the preferred source of metabolic energy, is oxidized to provide energy for this process. This is consistent with our findings that *P. damicornis* larval R_D increased significantly at high nitrate concentrations (N20 and N40 groups). In addition, to some extent, the increase in UFAs could promote biomembrane fluidity, enzyme activity, and internal and external exchange of substances that could enhance metabolism (Brenner, 1984; Bennett et al., 2018; Liu et al., 2018). However, a higher proportion of UFAs would reduce the antioxidant capacity of larvae. Hence, numerous lipids were consumed, and the increased risk of lipid peroxidation could adversely affect the successful settlement and development of the larvae.

CONCLUSION

The present research showed that, in all treatment groups, *P. damicornis* larvae had the highest proportion of SFAs, followed by PUFAs, and the lowest proportion of MUFAs. The FA pattern of larvae could store sufficient energy to delay metamorphosis until suitable settlement cues appeared. Nitrate enrichment significantly changed the FA composition of *P. damicornis* larvae. The lipids of *P. damicornis* larvae became progressively saturated (lower UI and U/S) when the nitrate concentration was less than 10 μM, which could be attributed to decreased PUFAs and concomitant increases in SFAs. Such changes enabled the *P. damicornis* larvae to adapt to low-level nitrate enrichment (<10 μM). Moreover, the N5 group had the highest P_{Net} and P_{Net}/D_R, which implied that low nitrate enrichment could promote photosynthesis of coral larvae zooxanthellae. However, the opposite pattern for FA compositions was found with higher nitrate concentrations (>20 μM), in which the UI and U/S levels were elevated due to increased PUFAs and decreased SFAs. With high nitrate levels, biomembrane restructuring in larvae may became ineffective, increasing respiration and rapidly consuming numerous lipids, which could adversely affect the successful settlement and development of larvae.

DATA AVAILABILITY STATEMENT

The raw data supporting the conclusions of this article will be made available by the authors, without undue reservation.

AUTHOR CONTRIBUTIONS

C-YL, FZ, and HH designed the experiments. C-YL, FZ, Y-FS, and X-LY carried out the experiments. C-YL, FZ, and HH analyzed the experimental results and wrote the manuscript.

FUNDING

This study was jointly funded by the National Natural Science Foundation of China (NSFC) (Nos. 41906097 and 41976120), Science and Technology Planning Project of Guangdong Province, China (2017B0303014052), Innovation Academy of South China Sea Ecology and Environmental Engineering, Chinese Academy of Sciences (ISEE2018PY01), and the Science and Technology Service Network Initiative of the Chinese Academy of Sciences (KFJ-STS-ZDTP-055).

ACKNOWLEDGMENTS

The authors would like to express their gratitude for the staff of the Hainan Tropical Marine Biological Research Station for providing technical assistance and facilities for conducting the work, as well as to those who critically reviewed this manuscript.

SUPPLEMENTARY MATERIAL

The Supplementary Material for this article can be found online at: https://www.frontiersin.org/articles/10.3389/fmars.2020.00531/full#supplementary-material

REFERENCES

Arai, I., Kato, M., Heyward, A., Ikeda, Y., and Maruyama, T. (1993). Lipid composition of positively buoyant eggs of reef building corals. *Coral Reefs* 12, 71–75. doi: 10.1007/bf00302104

Atkinson, M. J., Carlson, B., and Crow, G. L. (1995). Coral growth in high-nutrient, low-pH seawater: a case study of corals cultured at the Waikiki Aquarium, Honolulu, Hawaii. *Coral Reefs* 14, 215–223. doi: 10.1007/bf00334344

Bachok, Z., Mfilinge, P., and Tsuchiya, M. (2006). Characterization of fatty acid composition in healthy and bleached corals from Okinawa, Japan. *Coral Reefs* 25, 545–554. doi: 10.1007/s00338-006-0130-9

Bender-Champ, D., Diaz-Pulido, G., and Dove, S. (2017). Effects of elevated nutrients and CO2 emission scenarios on three coral reef macroalgae. *Harmful Algae* 65:40. doi: 10.1016/j.hal.2017.04.004

Bennett, H., Bell, J. J., Davy, S. K., Webster, N. S., and Francis, D. S. (2018). Elucidating the sponge stress response; lipids and fatty acids can facilitate survival under future climate scenarios. *Glob. Change Biol.* 24, 3130–3144. doi: 10.1111/gcb.14116

Bhojoo, U., Chen, M., and Zou, S. (2017). Temperature induced lipid membrane restructuring and changes in Nanomechanics. *Biochim. Biophys. Acta* 1860, 700–709. doi: 10.1016/j.bbamem.2017.12.008

Brenner, R. R. (1984). Effect of unsaturated acids on membrane structure and enzyme kinetics. *Prog. Lipid Res.* 23, 69–96. doi: 10.1016/0163-7827(84)90008-0

Cengiz, E. I., Bayar, A. S., Kızmaz, V., Başhan, M., and Satar, A. (2017). Acute toxicity of deltamethrin on the fatty acid composition of phospholipid classes in liver and gill tissues of Nile tilapia. *Int. J. Environ. Res.* 11, 1–9.

Chen, H.-K., Shin-Ni, S., Li-Hsueh, W., Mayfield, A. B., Yi-Jyun, C., Chen, W. N. U., et al. (2015). A compartmental comparison of major lipid species in a coral-*Symbiodinium* endosymbiosis: evidence that the coral host regulates lipogenesis of its cytosolic lipid bodies. *PLoS One* 10:e0132519. doi: 10.1371/journal.pone.0132519

Conlan, J. A., Rocker, M. M., and Francis, D. S. (2017). A comparison of two common sample preparation techniques for lipid and fatty acid analysis in three different coral morphotypes reveals quantitative and qualitative differences. *PeerJ* 5:e3645. doi: 10.7717/peerj.3645

Crockett, E. L. (2008). The cold but not hard fats in ectotherms: consequences of lipid restructuring on susceptibility of biological membranes to peroxidation, a review. *J. Comp. Physiol. B* 178, 795–809. doi: 10.1007/s00360-008-0275-7

Cunning, R., and Baker, A. C. (2013). Excess algal symbionts increase the susceptibility of reef corals to bleaching. *Nat. Clim. Change* 3, 259–262. doi: 10.1038/nclimate1711

D'Angelo, C., and Wiedenmann, J. (2014). Impacts of nutrient enrichment on coral reefs: new perspectives and implications for coastal management and reef survival. *Curr. Opin. Env. Sust.* 7, 82–93. doi: 10.1016/j.cosust.2013.11.029

Ernst, R., Ejsing, C. S., and Antonny, B. (2016). Homeoviscous adaptation and the regulation of membrane lipids. *J. Mol. Biol.* 428, 4776–4791. doi: 10.1016/j.jmb.2016.08.013

Ferrierpagès, C., Gattuso, J. P., Dallot, S., and Jaubert, J. (2000). Effect of nutrient enrichment on growth and photosynthesis of the zooxanthellate coral *Stylophora pistillata*. *Coral Reefs* 19, 103–113. doi: 10.1007/s003380000078

Ferrier-Pagès, C., Schoelzke, V., Jaubert, J., Muscatine, L., and Hoegh-Guldberg, O. (2001). Response of a scleractinian coral, *Stylophora pistillata*, to iron and nitrate enrichment. *J. Exp. Mar. Biol. Ecol.* 259, 249–261. doi: 10.1016/s0022-0981(01)00241-6

Figueiredo, J., Baird, A. H., Cohen, M. F., Flot, J.-F., Kamiki, T., Meziane, T., et al. (2012). Ontogenetic change in the lipid and fatty acid composition of scleractinian coral larvae. *Coral Reefs* 31, 613–619. doi: 10.1007/s00338-012-0874-3

Harrison, P., and Ward, S. (2001). Elevated levels of nitrogen and phosphorus reduce fertilisation success of gametes from scleractinian reef corals. *Mar. Biol.* 139, 1057–1068. doi: 10.1007/s002270100668

Hazel, J. R. (1979). Influence of thermal acclimation on membrane lipid composition of rainbow trout liver. *Proc. Natl. Acad. Sci. U.SA.* 236:R91.

Hughes, T. P., Kerry, J. T., Baird, A. H., Connolly, S. R., Dietzel, A., Eakin, C. M., et al. (2018). Global warming transforms coral reef assemblages. *Nature* 556:492. doi: 10.1038/s41586-018-0041-2

Humanes, A., Noonan, S. H. C., Willis, B. L., Fabricius, K. E., de Beer, D., Negri, A. P. (2016). Cumulative effects of nutrient enrichment and elevated temperature compromise the early life history stages of the coral *Acropora tenuis*. *PLoS One* 8:e0161616. doi: 10.1016/j.marpolbul.2017.08.003

Imbs, A. B. (2013). Fatty acids and other lipids of corals: composition, distribution, and biosynthesis. *Russ. J. Mar. Biol.* 39, 153–168. doi: 10.1134/s1063074013030061

Jiang, L., Guo, Y.-J., Zhang, F., Zhang, Y.-Y., McCook, L. J., Yuan, X.-C., et al. (2019). Diurnally fluctuating pCO2 modifies the physiological responses of coral recruits under ocean acidification. *Front. Physiol.* 9:1952. doi: 10.3389/fphys.2018.01952

Jiang, L., Sun, Y. F., Zhang, Y. Y., Zhou, G. W., Li, X. B., McCook, L. J., et al. (2017). Impact of diurnal temperature fluctuations on larval settlement and growth of the reef coral Pocillopora damicornis. *Biogeosciences* 14, 5741–5752. doi: 10.5194/bg-14-5741-2017

Jing, G., Yu, K., Wang, Y., Xu, D., Huang, X., Zhao, M., et al. (2017). Nutrient distribution in coral reef degraded areas within sanya bay, South China Sea. *J. Coast. Res.* 33, 1148–1160.

Kubicek, A., Breckling, B., Hoegh-Guldberg, O., and Reuter, H. (2019). Climate change drives trait-shifts in coral reef communities. *Sci. Rep.* 9:3721.

Lam, E. K. Y., Chui, A. P. Y., Kwok, C. K., Ip, A. H. P., Chan, S. W., Leung, H. N., et al. (2015). High levels of inorganic nutrients affect fertilization kinetics, early development and settlement of the scleractinian coral *Platygyra acuta*. *Coral Reefs* 34, 837–848. doi: 10.1007/s00338-015-1317-8

Liu, C., Dong, S., Zhou, Y., Shi, K., Pan, Z., Sun, D., et al. (2019). Temperature-dependent fatty acid composition change of phospholipid in steelhead trout (*Oncorhynchus mykiss*) tissues. *J. Ocean Univ. China* 18, 519–527. doi: 10.1007/s11802-019-3775-z

Liu, C., Zhou, Y., Dong, K., Sun, D., Gao, Q., and Dong, S. (2018). Differences in fatty acid composition of gill and liver phospholipids between Steelhead trout (*Oncorhynchus mykiss*) and Atlantic salmon (*Salmo salar*) under declining temperatures. *Aquaculture* 495, 815–822. doi: 10.1016/j.aquaculture.2018.06.045

Losa, D. A., and Murata, N. (2004). Membrane fluidity and the perception of environmental signals. *Biochim. Biophys. Acta* 1666, 142–157. doi: 10.1016/j.bbamem.2004.08.002

Marubini, F., and Davies, P. S. (1996). Nitrate increases zooxanthellae population density and reduces skeletogenesis in corals. *Mar. Biol.* 127, 319–328. doi: 10.1007/bf00942117

Muscatine, L., McCloskey, L. R., and Marian, R. E. (1981). Estimating the daily contribution of carbon from zooxanthellae to coral animal respiration. *Limnol. Oceanogr.* 26, 601–611. doi: 10.4319/lo.1981.26.4.0601

Nordemar, I., Nystrm, M., and Dizon, R. (2003). Effects of elevated seawater temperature and nitrate enrichment on the branching coral *Porites cylindricain* the absence of particulate food. *Mar. Biol.* 142, 669–677. doi: 10.1007/s00227-002-0989-0

Oku, H., Yamashiro, H., Onaga, K., Iwasaki, H., and Takara, K. (2002). Lipid distribution in branching coral *Montipora digitata*. *Fish. Sci.* 68, 517–522. doi: 10.1046/j.1444-2906.2002.00456.x

Papina, M., Meziane, T., and Woesik, R. V. (2003). Symbiotic zooxanthellae provide the host-coral *Montipora digitata* with polyunsaturated fatty acids. *Comp. Biochem. Physiol. B* 135, 533–537. doi: 10.1016/s1096-4959(03)00118-0

Porter, N. A. (2013). A perspective on free radical autoxidation: the physical organic chemistry of polyunsaturated fatty acid and sterol peroxidation. *J. Org. Chem.* 78, 3511–3524. doi: 10.1021/jo4001433

Renegar, D. A., and Riegl, B. M. (2005). Effect of nutrient enrichment and elevated CO2 partial pressure on growth rate of atlantic scleractinian coral *Acropora cervicornis*. *Mar. Ecol. Prog. Ser.* 293, 69–76. doi: 10.3354/meps293069

Serrano, X. M., Miller, M. W., Hendee, J. C., Jensen, B. A., Gapayao, J. Z., Pasparakis, C., et al. (2018). Effects of thermal stress and nitrate enrichment on the larval performance of two Caribbean reef corals. *Coral Reefs* 37, 173–182. doi: 10.1007/s00338-017-1645-y

Sinensky, M. (1974). Homeoviscous adaptation-a homeostatic process that regulates the viscosity of membrane lipids in *Escherichia coli*. *Proc. Natl. Acad. Sci. U.S.A.* 71, 522–525. doi: 10.1073/pnas.71.2.522

Snyder, R. J., and Hennessey, T. M. (2003). Cold tolerance and homeoviscous adaptation in freshwater alewives (*Alosa pseudoharengus*). *Fish Physiol. Biochem.* 29, 117–126. doi: 10.1023/b:fish.0000035920.60817.11

Tchernov, D., Gorbunov, M. Y., Vargas, C. D., Yadav, S. N., Milligan, A. J., Haggblom, M., et al. (2004). Membrane lipids of symbiotic algae are diagnostic of sensitivity to thermal bleaching in corals. *Proc. Natl. Acad. Sci. U.S.A.* 101, 13531–13535. doi: 10.1073/pnas.0402907101

Wada, H., Gombos, Z., and Murata, N. (1994). Contribution of membrane lipids to the ability of the photosynthetic machinery to tolerate temperature stress. *Proc. Natl. Acad. Sci. U.S.A.* 91, 4273–4277. doi: 10.1073/pnas.91.10.4273

Wallaert, C., and Babin, P. J. (1994). Thermal adaptation affects the fatty acid composition of plasma phospholipids in trout. *Lipids* 29, 373–376. doi: 10.1007/bf02537193

Ward, S., and Harrison, P. (2000). Changes in gametogenesis and fecundity of acroporid corals that were exposed to elevated nitrogen and phosphorus during the ENCORE experiment. *J. Exp. Mar. Biol. Ecol.* 246, 179–221. doi: 10.1016/s0022-0981(99)00182-3

Wijekoon, M. P. A. (2011). *Effect of Water Temperature and Diet on Cell Membrane Fluidity and Fatty Acid Composition of Muscle, Liver, Gill and Intestine Mucosa of Adult and Juvenile Steelhead Trout, Oncorhynchus Mykiss*. Ph.D. Thesis, Memorial University of Newfoundland, Newfoundland.

Wijekoon, M. P. A. (2012). *Effect of Water Temperature and Diet on Cell Membrane Fluidity and Fatty Acid Composition of Muscle, Liver, Gill and Intestine Mucosa of Adult and Juvenile Steelhead Trout, Oncorhynchus Mykiss*. Newfoundland: Memorial University of Newfoundland.

Yeagle, P. L. (1989). Lipid regulation of cell membrane structure and function. *FASEB J.* 3, 1833–1842. doi: 10.1096/fasebj.3.7.2469614

Zaneveld, J. R., Burkepile, D. E., Shantz, A. A., Pritchard, C. E., Mcminds, R., Payet, J. P., et al. (2016). Overfishing and nutrient pollution interact with temperature to disrupt coral reefs down to microbial scales. *Nat. Commun.* 7:11833.

Zhukova, N. V., and Titlyanov, E. A. (2003). Fatty acid variations in symbiotic dinoflagellates from Okinawan corals. *Phytochemistry* 62, 191–195. doi: 10.1016/s0031-9422(02)00371-0

Conflict of Interest: The authors declare that the research was conducted in the absence of any commercial or financial relationships that could be construed as a potential conflict of interest.

frontiers in Physiology

MINI REVIEW
published: 23 September 2020
doi: 10.3389/fphys.2020.566968

Conceptualization of the Holobiont Paradigm as It Pertains to Corals

Tamar L. Goulet[1], Ivan Erill[2], Marina S. Ascunce[3,4], Sheree J. Finley[5] and Gulnaz T. Javan[5]*

[1]Department of Biology, University of Mississippi, University, MS, United States, [2]Department of Biological Sciences, University of Maryland Baltimore County, Baltimore, MD, United States, [3]Emerging Pathogens Institute, University of Florida, Gainesville, FL, United States, [4]Plant Pathology Department, University of Florida, Gainesville, FL, United States, [5]Department of Physical Sciences and Forensic Science Programs, Alabama State University, Montgomery, AL, United States

Corals' obligate association with unicellular dinoflagellates, family Symbiodiniaceae form the foundation of coral reefs. For nearly a century, researchers have delved into understanding the coral-algal mutualism from multiple levels of resolution and perspectives, and the questions and scope have evolved with each iteration of new techniques. Advances in genetic technologies not only aided in distinguishing between the multitude of Symbiodiniaceae but also illuminated the existence and diversity of other organisms constituting the coral microbiome. The coral therefore is a meta-organism, often referred to as the coral holobiont. In this review, we address the importance of including a holistic perspective to understanding the coral holobiont. We also discuss the ramifications of how different genotypic combinations of the coral consortium affect the holobiont entity. We highlight the paucity of data on most of the coral microbiome. Using Symbiodiniaceae data, we present evidence that the holobiont properties are not necessarily the sum of its parts. We then discuss the consequences of the holobiont attributes to the fitness of the holobiont and the myriad of organisms that contribute to it. Considering the complexity of host-symbiont genotypic combinations will aid in our understanding of coral resilience, robustness, acclimation, and/or adaptation in the face of environmental change and increasing perturbations.

Keywords: coral reefs, symbiosis, mutualism, Symbiodiniaceae, microbiome, holobiont

OPEN ACCESS

Edited by:
Zhi Zhou,
Hainan University, China

Reviewed by:
Xiubao Li,
Hainan University, China
Davide Seveso,
University of Milano-Bicocca, Italy

****Correspondence:***
Tamar L. Goulet
tlgoulet@olemiss.edu

Specialty section:
This article was submitted to Aquatic Physiology, a section of the journal Frontiers in Physiology

Received: *29 May 2020*
Accepted: *19 August 2020*
Published: *23 September 2020*

Citation:
Goulet TL, Erill I, Ascunce MS, Finley SJ and Javan GT (2020) Conceptualization of the Holobiont Paradigm as It Pertains to Corals. Front. Physiol. 11:566968. doi: 10.3389/fphys.2020.566968

INTRODUCTION

Linnaeus hypothesized that gorgonian corals were plants which metamorphosed into animals. In 1775, John Ellis wrote to Daniel Solander (Ellis, 1776) who requested "that I (Ellis) should continue my researches into the formation and growth of … Gorgonia… known in English by the name of sea fans, sea feathers, and sea-whips… This you thought the more necessary, as the accounts already published of them by the illustrious Dr. Linnaeus and Dr. Pallas seemed to make them of a mixed nature in their growth, between animals and vegetables…" After studying gorgonian morphology, Ellis (1776) concluded: "…that though they grow in a branched form, they are no more allied to vegetables… that animal life doth not depend on bodies growing according to a certain external form."

Although Ellis debunked the hypothesis that a coral changed from a plant to an animal, a coral (either a scleractinian coral or an octocoral, herein referred to collectively as coral) is actually a coral consortium, which includes not only the coral animal but also dinoflagellates, apicomplexans, fungi, bacteria, and *Archaea* (reviewed in Knowlton and Rohwer, 2003; Olson and Kellogg, 2010; Blackall et al., 2015; Leggat et al., 2019). We posit that to understand corals, and by extension coral reefs, it is imperative to acknowledge and incorporate the role of the consortium in shaping

the coalesced characteristics. Such a holistic approach assesses the combined coral entity, the coral holobiont.

Lynn Margulis defined a biont as an "individual organism," and a holobiont as a "symbiont compound of recognizable bionts" (Margulis, 1991). Although members of a holobiont interact in a symbiosis, not every symbiotic organism is part of a holobiont. In this review, we define the coral holobiont as containing the coral and the microbiota found within the coral body, its mucus, and its skeleton, a definition in line with that of Rohwer et al. (2002). We exclude organisms that reside in the immediate vicinity of corals, such as crabs and shrimp (Glynn, 1980) or coral dwelling fish (Liberman et al., 1995), even if they engage in mutualisms with corals.

THE CORAL HOLOBIONT CONSTITUENTS

At the core of the coral reef ecosystem is the obligatory symbiosis between corals and dinoflagellate algae, family Symbiodiniaceae. This mutualism relies on "access to metabolic capabilities" and "protection from antagonists" (Douglas, 2010). The coral gains photosynthetically fixed products from the Symbiodiniaceae (Muscatine and Porter, 1977). In scleractinian corals, Symbiodiniaceae also enhance coral calcification (Goreau and Goreau, 1959; Pearse and Muscatine, 1971). Symbiodiniaceae uptake the coral's nitrogenous wastes (Muscatine and D'Elia, 1978), a valuable commodity in the oligotrophic seas, where coral reefs occur. As endosymbionts, the Symbiodiniaceae gain a degree of protection from both environmental conditions and predators (Douglas, 2010).

Knowledge about the rest of the coral holobiont microbiota lags behind information about Symbiodiniaceae. The second most studied component is the bacterial consortium. The coral enables "access to metabolic capabilities" *via* the wax ester and triglycerides in its mucus (Johannes, 1967; Benson and Muscatine, 1974). Bacteria may provide carbon, nitrogen, and sulfur (reviewed in Shashar et al., 1994; Knowlton and Rohwer, 2003; McDevitt-Irwin et al., 2017) and "protection from antagonists" by producing antibiotics and cell-to-cell communication inhibitors, inhibiting swarming, and through their own growth, outcompeting and preventing other microbes from settling on the coral (reviewed in McDevitt-Irwin et al., 2017; Peixoto et al., 2017). Data on the remainder of the holobiont consortium are sparse. The *Archaea* may be involved with nitrogen cycling, the viruses potentially with gene transfer, and the fungi may protect from environmental conditions, provide antimicrobial activity, and take part in carbon and nitrogen cycles (reviewed in Knowlton and Rohwer, 2003; Peixoto et al., 2017).

THE IDENTITY OF THE HOLOBIONT PARTNERS IS PROGRESSIVELY REVEALED IN CYCLICAL WAVES

A fundamental aspect to understanding holobionts is partner identification. For many consortium members, their small sizes, lack of morphological differences, and morphological plasticity, severely limited their identification (Wilcox, 1998). Advancements in genetic techniques, alongside cost reduction, have progressively enabled identifying the holobiont partners. Knowledge gains have occurred incrementally, as finer levels of resolution become possible, and gains grow in cyclical waves, whereby identification of one of the partner groups commands center stage, followed by the next. In coral holobionts, Symbiodiniaceae identification led the way.

Brandy in 1881 referred to the dinoflagellates as zooxanthellae (cited in Blank and Trench, 1986). Zooxanthellae were once attributed to one pandemic species, *Symbiodinium microadriaticum* (Freudenthal, 1962). Distinguishing between zooxanthellae took off in the early 1990s when utilizing differences in the nuclear genes that encode small ribosomal subunit RNA, led to placement of zooxanthellae into several groups (Rowan and Powers, 1991a, 1992), later referred to as *Symbiodinium* clades (Baker and Rowan, 1997; Baker et al., 1997; Goulet and Coffroth, 1997), a term used for the next 21 years. Other DNA regions provided within-clade, population, and individual level resolution (reviewed in Goulet et al., 2019). Only recently were these dinoflagellates placed in the family Symbiodiniaceae (LaJeunesse et al., 2018).

The feasibility of genetically distinguishing between Symbiodiniaceae led to a characterization frenzy. Numerous publications presented and/or synthesized the data available on Symbiodiniaceae genera and species identities in coral species on mesophotic reefs around the world (Goulet et al., 2019), and in different geographic locations (LaJeunesse, 2002; Savage et al., 2002; LaJeunesse et al., 2003, 2004a,b, 2008; Goulet and Coffroth, 2004; van Oppen et al., 2005; Putnam et al., 2012; Ziegler et al., 2019). With the reduction in sequencing costs, techniques involving visualization of Symbiodiniaceae DNA fragments *via* gels (Rowan and Powers, 1991a,b; Belda-Baillie et al., 1999; LaJeunesse, 2001) have given way to direct sequencing (e.g., Arif et al., 2014). The burst of Symbiodiniaceae genetic characterization is now mirrored in the bacterial component of the coral holobiont. Starting a decade later, the prevailing approaches utilize the 16S ribosomal RNA (rRNA) as a canonical biomarker. Although on a smaller scale, bacterial consortia in corals have been identified from different geographic locations (reviewed in Blackall et al., 2015; McDevitt-Irwin et al., 2017; van de Water et al., 2018) and mesophotic reefs (Olson and Kellogg, 2010; Leggat et al., 2019). The application of high-throughput amplicon and metagenomic analyses enables not only the characterization of bacteria but also of the other microbial partners such as fungi, *Archaea*, and viruses (reviewed in Wegley et al., 2007; Blackall et al., 2015; Góes-Neto et al., 2020).

THE SPECIFICITY OF THE CORAL HOLOBIONT AND THE RAMIFICATIONS OF TRANSIENT ENTITIES

A holobiont is a conglomerate of entities, representing multiple phyla. If components of this consortium leave, or new entities enter, then even the same coral colony may represent a different

holobiont at different times and/or under different environmental conditions. Coral species host specific Symbiodiniaceae genera and types, and these do not change even under stressful conditions (Goulet, 2006, 2007), although shuffling of the proportion of existing types may occur (Berkelmans and van Oppen, 2006), as well as transient or low level Symbiodiniaceae (Silverstein et al., 2012). Likewise, bacterial specificity exists in corals (Ainsworth et al., 2015; Shirur et al., 2016; van de Water et al., 2017, 2018; Huggett and Apprill, 2019; McCauley et al., 2020). Bacteria may consistently inhabit the holobiont ("core microbiome") or be transient (Hernandez-Agreda et al., 2017; van de Water et al., 2017; Leite et al., 2018) and/or vary geographically (Osman et al., 2020). Furthermore, the coral itself may host different bacteria in the surface mucus layer (SML), tissue, or skeleton (Ainsworth et al., 2010; Gajigan et al., 2017). The role of transient or low abundant entities is speculated. The Coral Probiotic Hypothesis, for example, relies on the premise that transient or low level bacteria become pronounced (Reshef et al., 2006). The concept of specificity commands attention since, whether the holobiont entity can change or not affects interpretation of coral acclimation, adaptation, resilience, and persistence (**Figure 1**).

DISCUSSION

A Holistic Approach Requires Evaluating the Entire Holobiont, Abandoning Interpretation Based on Only One of the Partners

Scientists approach the world through a personal prism formulated through research interests and academic experiences. Coral research may straddle multiple departments, either across taxonomic lines such as between departments of Zoology and Plant Sciences, or across resolution levels such as between Ecology vs. Cell and Molecular Biology departments. Departmental and training allegiances are nothing new. In 1931, Gardiner said "the investigator of the 'coral reef problem' to-day is usually either a geologist or a zoologist, for the botanist has not understood, up to the present, that he may claim an equal partnership" (Gardiner, 1931).

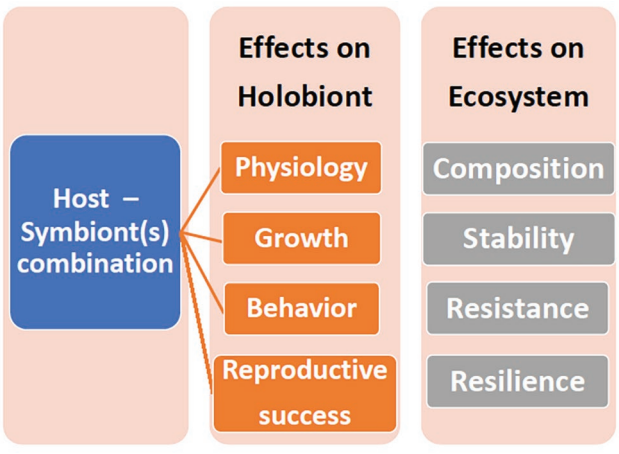

FIGURE 1 | The ramifications of different host-symbiont genotypic combinations on the holobiont and the ecosystem.

Terminology may also lead to biases in approaching holobiont related research questions. Since coral holobionts are often addressed in symbiotic terms, the coral is the host and the consortium constituents are referred to as the symbionts. The terms allude to size, the coral is the largest in the holobiont consortium; and to physical location, with the symbionts residing within or on the host. The words host and symbiont, however, are often extrapolated to include who controls whom. The dichotomy of interpretation was already articulated by Gardiner: "These special difficulties in respect to the nutrition of coral-building sedentary animals in tropical waters have been met by the 'taming' of unicellular green flagellates (Zooxanthellae) by the polyps – or the polyps being adopted by such plants-housing them as symbionts in their endoderm cells" (Gardiner, 1931).

Although data provide facts, an investigator's approach affects the interpretation of those facts. Often it is assumed that the host controls the symbionts. Even though endosymbionts reside within a host, they can affect the host. For instance, the scleractinian corals *Acropora millepora* and *A. tenuis* can host/be inhabited by two Symbiodiniaceae genera, *Cladocopium*, and *Durusdinium*. Juvenile corals with *Cladocopium* grew up to three times faster than juveniles that hosted *Durusdinium* (Little et al., 2004). In a benthic organism, growing faster may increase survivorship, and coral size affects the onset of reproduction (Rinkevich and Loya, 1979). Therefore, the symbiont's effect on coral growth affects holobiont survival and fitness.

Another example of how an approach affects interpretation pertains to corals and environmental perturbations. When corals encounter stressors, such as elevated seawater temperatures, a reduction of Symbiodiniaceae and/or their photosynthetic pigments can occur, a state termed "bleaching" (Glynn, 1996). Due to the obligate symbiosis between Symbiodiniaceae and many corals, bleaching may lead to holobiont death. It is still debated if algal loss is driven by the coral host expelling either dead algae or algae that impose a high metabolic demand (Weis, 2008), or if the algae instigate abandoning a sinking ship (Baird et al., 2009). Bleaching mechanisms may vary, and be holobiont-dependent and context-dependent. For example, in holobionts which host different Symbiodiniaceae genera and species, variation in conspecific bleaching may be attributed to the Symbiodiniaceae inhabiting the holobionts (Rowan, 2004; Goulet et al., 2005; Berkelmans and van Oppen, 2006; Sampayo et al., 2008). Conversely, in other coral species, no correlation exists between bleaching and the Symbiodiniaceae identity (Goulet et al., 2008), and the coral's response to the perturbation may affect the bleaching outcome for the holobiont (Baird et al., 2009).

Although coral bleaching is considered a consequence of stress, the Adaptive Bleaching Hypothesis (ABH) contemplated that bleaching may be beneficial (Buddemeier and Fautin, 1993). *Via* bleaching, Symbiodiniaceae not optimal for new environmental conditions could be lost. Novel Symbiodiniaceae,

better suited for the new conditions, could enter the holobiont from the environment. The ABH article recognized that holobiont physiology arises from "characteristics of the combination, rather than of the host or symbiotic algal partner alone" (Buddemeier and Fautin, 1993). Subsequent statements, however, such as "Bleaching provides an opportunity for the host to be repopulated with a different type of partner…" (Buddemeier and Fautin, 1993) turned this hypothesis into a coral-centric scenario. ABH being coral driven has been echoed in the literature (e.g., Baker et al., 2015). Although portraying phenomena with neutral, non-directional words (e.g., loss vs. expulsion of algae) is difficult, one needs to be cognizant of how word choice affects interpretation.

A Holistic Approach Requires the Realization That Holobionts Cannot Be Characterized Based Solely on One Component of the Holobiont

To achieve order, we label biological entities and try to assign them to categories. For example, scientists have termed certain coral species as hardier in their ability to withstand environmental perturbations than others (Loya et al., 2001). Likewise, blanket statements have been made about Symbiodiniaceae genera, such as that *Durusdinium* (previous clade D) is a thermally tolerant genus (Stat et al., 2013). *Durusdinium trenchii* is indeed heat tolerant (LaJeunesse et al., 2014; LaJeunesse, 2017). Overarching generalizations, however, such as if corals that host *Durusdinium* or acquire *Durusdinium* will preferentially survive climate change (Baker et al., 2004; Oliver and Palumbi, 2009; Stat and Gates, 2011; Stat et al., 2013), may lead to misconceptions. Not all *Durusdinium* are heat tolerant and some inhabit only certain specific coral hosts (LaJeunesse et al., 2014). Therefore, attributing characteristics such as "thermal tolerant" should be done at the holobiont level rather than focusing on partner attributes.

A Holistic Approach Requires Investigating Holobiont Characteristics and Holobiont Performance

The holobiont is a product of the interactions between the partners. Focusing on one partner, especially in isolation, is informative, although limited for understanding the holobiont. Cultured Symbiodiniaceae can provide information on the physiological range and attributes of Symbiodiniaceae and enable between- and within- Symbiodiniaceae comparisons (Banaszak et al., 2000; Tchernov et al., 2004; Robison and Warner, 2006; Brading et al., 2013). Culturable Symbiodiniaceae, however, may not represent the common Symbiodiniaceae found within the holobiont or may be a contaminant that does not occur in the holobiont (Goulet and Coffroth, 1997; Santos et al., 2001). Furthermore, *in hospite*, with the other partners present, the Symbiodiniaceae may exhibit a different physiology than what is observed in culture (Goulet et al., 2005). The host-symbiont genotypic combinations may also affect the physiology and ecology of the holobiont (**Figure 1**). The panmictic sea anemone *Exaiptasia pallida* (previously *Aiptasia pallida*) predominantly occurs with the Symbiodiniaceae genus *Breviolum*, although in Florida, it also hosts *Symbiodinium sensu stricto* and occasionally, *Cladocopium* (Thornhill et al., 2013). When exposed to elevated sea water temperatures, the Florida anemone – *Symbiodinium* holobionts had higher oxygen fluxes compared to Bermuda anemones with their natal *Breviolum* algae (Goulet et al., 2005). A lab produced host-symbiont genotypic combination of Bermuda anemones with *Symbiodinium* algae yielded a higher oxygen flux than either of the natal host-symbiont combinations at both 32 and 34°C (Goulet et al., 2005).

A Holistic Approach Requires Assessing Parameters of as Many of the Holobiont Participants as Possible

Studying corals from a holobiont perspective benefits from measuring parameters of multiple consortium members. Case in point, the definition of coral bleaching does not distinguish what drives the Symbiodiniaceae loss. Two potential, not mutually exclusive, scenarios may occur. Coral cells can lose the Symbiodiniaceae cells within them, or, the stressor may lead to loss of coral cells, and since the host cells contain Symbiodiniaceae, the end result is that the coral has less Symbiodiniaceae within it. The common approach of assessing Symbiodiniaceae density (Fitt et al., 2000; Siebeck et al., 2006; Johnson and Goulet, 2007) does not address the two scenarios. Conversely, quantifying both algal and host parameters can illuminate the route to the bleaching outcome. For example, branches of the octocorals *Eunicea tourneforti* and *Pseudoplexaura crucis* exposed in the summer to sea water temperatures 3°C above ambient, lost Symbiodiniaceae (McCauley et al., 2018). In *E. tourneforti*, Symbiodiniaceae density fell 26%, and the number of Symbiodiniaceae normalized to holobiont lipid content (Shirur et al., 2014) also differed between ambient and elevated temperatures (McCauley et al., 2018). In *P. crucis*, the 35% reduction in Symbiodiniaceae density occurred alongside a 19% reduction in the lipid amount, resulting in no significant changes to Symbiodiniaceae numbers normalized to holobiont lipid content (McCauley et al., 2018). Thus, in *E. tourneforti*, lower Symbiodiniaceae density was driven by less Symbiodiniaceae per host cells, while in *P. crucis*, the drop in Symbiodiniaceae was accompanied by a reduction in host cells. Without collecting data on both host and symbiont parameters, the different routes that led to the same outcome would have been missed.

A Holistic Approach Will Strive to Assess Whether Changes in the Holobiont Consortium Occurred During the Course of a Study

When attributes of conspecific holobionts differ temporally, spatially or due to perturbations, these differences may demonstrate acclimation and/or adaptation of the existing holobiont consortium. Alternatively, acclimation, and/or adaptation may manifest themselves in changes in a constituent of the genotypic complement of the holobiont. For example, in seven Caribbean octocoral species, sampled either seasonally or when exposed to perturbations, the Symbiodiniaceae did

not change, nor did the dominant bacterial operational taxonomic units, although shifts in bacterial abundances occurred (McCauley et al., 2020). Similarly, in thermal stress experiments on *Acropora digitifera* in the Philippines (Gajigan et al., 2017) and *Acropora muricata* in Taiwan (Lee et al., 2015), the overall microbial community remained stable, with shifts in bacterial abundance in the tissue and SML. In six Red Sea coral species, Symbiodiniaceae specificity occurred throughout latitudinal sampling, while the bacterial composition and diversity in the SML varied (Osman et al., 2020), illustrating the importance of identifying the holobiont consortium and its specificity.

FUTURE RESEARCH DIRECTIONS

The Role of the Partners in the Holobiont

Even though identifying the holobiont partners is important, identification is primarily descriptive and correlative. The next step, where feasible, is to decipher the role consortia members play in the holobiont, from investigating holobiont ecology and physiology, assessing metabolic products produced and exchanged, to gene expression. Furthermore, roles may vary depending on environment and interactions with other holobiont members (**Figure 1**). Although many studies manipulated environmental parameters, such as temperature, and evaluated the outcome for corals, often the Symbiodiniaceae are not identified (McLachlan et al., 2020). Studies on parameter effects on coral holobiont – bacterial and *archaea* interactions lag further behind. As the field moves beyond identifying the microbiota complement of the holobiont, more experimental studies will ensue.

Mechanisms Underlying Specificity and/or Flexibility of the Holobiont Consortium

In corals, a Symbiodiniaceae ontogenetic acquisition window appears to exist, after which Symbiodiniaceae specificity sets in (Coffroth et al., 2001; Weis et al., 2001). The mechanism that drives Symbiodiniaceae specificity and why coral species contain specific bacteria over other bacteria is unknown. The quandary of specificity vs. flexibility raises the issue of the definition of a holobiont from a different perspective, and that is whether entities that are transient in the coral consortium should be regarded as part of the holobiont? To address this point, what is considered transient needs to be defined.

Is the Coral Holobiont the Unit of Selection?

A coral holobiont exhibits characteristic physiological and ecological traits. These characteristics not only separate one coral species from another, but also conspecifics coral-symbiont genotypic combinations. The physiological performance of Symbiodiniaceae, for example, differs in different hosts. If the traits of a coral holobiont are driven by the holobiont consortium, is the holobiont the unit of selection? Does the holobiont depend on its specific consortia, or just on their physiological roles? And, does theoretical modeling, for example, coral survival under different climate conditions, require incorporating holobiont variables?

CONCLUSION

The coral holobiont is a consortium of phylogenetically disparate entities co-existing in a coral. The holobiont concept adds a level of complexity in deciphering the ecology and evolution of corals. To address research questions pertaining to coral holobionts, researchers need to leave research silos defined by research organisms, research training, and departmental affiliation. Although characterizing multiple aspects of a coral holobiont may not be feasible, considering that the data may arise from the myriad of participants in the holobiont may affect data interpretation. Due to the diversity of the coral holobiont consortium, collaborations of multiple investigators with multiple skill sets and knowledge about the multiple components of the coral holobiont will be key.

AUTHOR CONTRIBUTIONS

TLG, IE, MSA, SJF, and GTJ contributed to the conception of the review. TLG wrote the first draft of the manuscript. TLG, IE, MSA, SJF, and GTJ contributed to manuscript revision, read and approved the submitted version.

FUNDING

Funding was provided by the National Science Foundation (NSF, DEB, Grant No. 1839775) to TLG, and by a NSF grant administered by UCAR's Cooperative Programs for the Advancement of Earth System Science (CPAESS, Grant No. 1940791). Any opinions, findings, and conclusions or recommendations expressed in this material are those of the authors and do not necessarily reflect the views of the National Science Foundation.

ACKNOWLEDGMENTS

We thank the National Science Foundation for convening the Reintegrating Biology Jumpstart meeting and providing us the opportunity to brainstorm about reintegrating biology and the nature of holobionts. This is publication number 019 of the Center for Biodiversity and Conservation Research at The University of Mississippi.

REFERENCES

Ainsworth, T. D., Krause, L., Bridge, T., Torda, G., Raina, J. -B., Zakrzewski, M., et al. (2015). The coral core microbiome identifies rare bacterial taxa as ubiquitous endosymbionts. *ISME J.* 9, 2261–2274. doi: 10.1038/ismej.2015.39

Ainsworth, T. D., Thurber, R. V., and Gates, R. D. (2010). The future of coral reefs: a microbial perspective. *Trends Ecol. Evol.* 25, 233–240. doi: 10.1016/j.tree.2009.11.001

Arif, C., Daniels, C., Bayer, T., Banguera-Hinestroza, E., Barbrook, A., Howe, C. J., et al. (2014). Assessing *Symbiodinium* diversity in scleractinian corals via

next-generation sequencing-based genotyping of the ITS2 rDNA region. *Mol. Ecol.* 23, 4418–4433. doi: 10.1111/mec.12869

Baird, A. H., Bhagooli, R., Ralph, P. J., and Takahashi, S. (2009). Coral bleaching: the role of the host. *Trends Ecol. Evol.* 24, 16–20. doi: 10.1016/j.tree.2008.09.005

Baker, D. M., Freeman, C. J., Knowlton, N., Thacker, R. W., Kim, K., and Fogel, M. L. (2015). Productivity links morphology, symbiont specificity and bleaching in the evolution of Caribbean octocoral symbioses. *ISME J.* 9, 2620–2629. doi: 10.1038/ismej.2015.71

Baker, A. C., and Rowan, R. (1997). "Diversity of symbiotic dinoflagellates (zooxanthellae) in scleractinian corals of the Caribbean and Eastern Pacific." in *Proceedings of the 8th International Coral Reef Symposium*. *Vol. 2;* June 24–29, 1997; Panama, 1301–1306.

Baker, A. C., Rowan, R., and Knowlton, N. (1997). "Symbiosis ecology of two Caribbean acroporid corals." in *Proceedings of the 8th International Coral Reef Symposium*. *Vol. 2;* June 24–29, 1997; Panama, 1295–1300.

Baker, A. C., Starger, C. J., McClanahan, T. R., and Glynn, P. W. (2004). Coral reefs: corals' adaptive response to climate change. *Nature* 430:741. doi: 10.1038/430741a

Banaszak, A. T., LaJeunesse, T. C., and Trench, R. K. (2000). The synthesis of mycosporine-like amino acids (MAAs) by cultured, symbiotic dinoflagellates. *J. Exp. Mar. Biol. Ecol.* 249, 219–233. doi: 10.1016/S0022-0981(00)00192-1

Belda-Baillie, C. A., Sison, M., Silvestre, V., Villamor, K., Monje, V., Gomez, E. D., et al. (1999). Evidence for changing symbiotic algae in juvenile tridacnids. *J. Exp. Mar. Biol. Ecol.* 241, 207–221. doi: 10.1016/S0022-0981(99)00079-9

Benson, A. A., and Muscatine, L. (1974). Wax in coral mucus: energy transfer from corals to reef fishes. *Limnol. Oceanogr.* 19, 810–814. doi: 10.4319/lo.1974.19.5.0810

Berkelmans, R., and van Oppen, M. J. H. (2006). The role of zooxanthellae in the thermal tolerance of corals: a 'nugget of hope' for coral reefs in an era of climate change. *Proc. Biol. Sci.* 273, 2305–2312. doi: 10.1098/rspb.2006.3567

Blackall, L. L., Wilson, B., and van Oppen, M. J. (2015). Coral-the world's most diverse symbiotic ecosystem. *Mol. Ecol.* 24, 5330–5347. doi: 10.1111/mec.13400

Blank, R. J., and Trench, R. K. (1986). Nomenclature of endosymbiotic dinoflagellates. *Taxon* 35, 286–294. doi: 10.2307/1221270

Brading, P., Warner, M. E., Smith, D. J., and Suggett, D. J. (2013). Contrasting modes of inorganic carbon acquisition amongst *Symbiodinium* (*Dinophyceae*) phylotypes. *New Phytol.* 200, 432–442. doi: 10.1111/nph.12379

Buddemeier, R. W., and Fautin, D. G. (1993). Coral bleaching as an adaptive mechanism. *Bioscience* 43, 320–326. doi: 10.2307/1312064

Coffroth, M. A., Santos, S. R., and Goulet, T. L. (2001). Early ontogenetic expression of specificity in a cnidarian-algal symbiosis. *Mar. Ecol. Prog. Ser.* 222, 85–96. doi: 10.3354/meps222085

Douglas, A. E. (2010). *The symbiotic habit Princeton*. NJ: Princeton University Press.

Ellis, J. E. F. R. S. (1776). On the nature of the Gorgonia; that it is a real marine animal, and not of a mixed nature, between animal and vegetable. *Philos. Trans. R Soc. Lond.* 66, 1–17. doi: 10.1098/rstl.1776.0002

Fitt, W. K., McFarland, F. K., Warner, M. E., and Chilcoat, G. C. (2000). Seasonal patterns of tissue biomass and densities of symbiotic dinoflagellates in reef corals and relation to coral bleaching. *Limnol. Oceanogr.* 45, 677–685. doi: 10.4319/lo.2000.45.3.0677

Freudenthal, H. D. (1962). *Symbiodinium* gen. nov. and *Symbiodinium microadriaticum* sp. nov., a zooxanthella: taxonomy, life cycle, and morphology. *J. Protozool.* 9, 45–52. doi: 10.1111/j.1550-7408.1962.tb02579.x

Gajigan, A. P., Diaz, L. A., and Conaco, C. (2017). Resilience of the prokaryotic microbial community of *Acropora digitifera* to elevated temperature. *Microbiology* 6:e00478. doi: 10.1002/mbo3.478

Gardiner, J. S. (1931). Photosynthesis and solution in formation of coral reefs. *Nature* 127, 857–858. doi: 10.1038/127857a0

Glynn, P. W. (1980). Defense by symbiotic crustacea of host corals elicited by chemical cues from predator. *Oecologia* 47, 287–290. doi: 10.1007/BF00398518

Glynn, P. W. (1996). Coral reef bleaching: facts, hypotheses and implications. *Glob. Chang. Biol.* 2, 495–509. doi: 10.1111/j.1365-2486.1996.tb00063.x

Góes-Neto, A., Marcelino, V. R., Verbruggen, H., da Silva, F. F., and Badotti, F. (2020). Biodiversity of endolithic fungi in coral skeletons and other reef substrates revealed with 18S rDNA metabarcoding. *Coral Reefs* 39, 229–238. doi: 10.1007/s00338-019-01880-y

Goreau, T. F., and Goreau, N. I. (1959). The physiology of skeleton formation in corals. II. Calcium depostion by hermatypic corals under various conditions in the reef. *Biol. Bull.* 117, 239–250. doi: 10.2307/1538903

Goulet, T. L. (2006). Most corals may not change their symbionts. *Mar. Ecol. Prog. Ser.* 321, 1–7. doi: 10.3354/meps321001

Goulet, T. L. (2007). Most scleractinian corals and octocorals host a single symbiotic zooxanthella clade. *Mar. Ecol. Prog. Ser.* 335, 243–248. doi: 10.3354/meps335243

Goulet, T. L., and Coffroth, M. A. (1997). "A within colony comparison of zooxanthellae genotypes in the Caribbean gorgonian Plexaura kuna." in *Proceedings of the 8th International Coral Reef Symposium*. *Vol. 2;* June 24–29, 1997; Panama, 1331–1334.

Goulet, T. L., and Coffroth, M. A. (2004). The genetic identity of dinoflagellate symbionts in Caribbean octocorals. *Coral Reefs* 23, 465–472. doi: 10.1007/s00338-004-0408-8

Goulet, T. L., Cook, C. B., and Goulet, D. (2005). Effect of short-term exposure to elevated temperatures and light levels on photosynthesis of different host-symbiont combinations in the *Aiptasia pallida*/*Symbiodinium* symbiosis. *Limnol. Oceanogr.* 50, 1490–1498. doi: 10.4319/lo.2005.50.5.1490

Goulet, T. L., LaJeunesse, T. C., and Fabricius, K. E. (2008). Symbiont specificity and bleaching susceptibility among soft corals in the 1998 great barrier reef mass coral bleaching event. *Mar. Biol.* 154, 795–804. doi: 10.1007/s00227-008-0972-5

Goulet, T. L., Lucas, M. Q., and Nikolaos, V. S. (2019). "Symbiodiniaceae genetic diversity and symbioses with hosts from shallow to mesophotic coral ecosystems" in *Mesophotic coral ecosystems*. eds. Y. Loya, K. A. Puglise and T. C. L. Bridge (New York: Springer), 537–551.

Hernandez-Agreda, A., Gates, R. D., and Ainsworth, T. D. (2017). Defining the core microbiome in corals' microbial soup. *Trends Microbiol.* 25, 125–140. doi: 10.1016/j.tim.2016.11.003

Huggett, M. J., and Apprill, A. (2019). Coral microbiome database: integration of sequences reveals high diversity and relatedness of coral-associated microbes. *Environ. Microbiol. Rep.* 11, 372–385. doi: 10.1111/1758-2229.12686

Johannes, R. (1967). Ecology of organic aggregates in the vicinity of a coral reef. *Limnol. Oceanogr.* 12, 189–195. doi: 10.4319/lo.1967.12.2.0189

Johnson, C. E., and Goulet, T. L. (2007). A comparison of photographic analyses used to quantify zooxanthella density and pigment concentrations in cnidarians. *J. Exp. Mar. Biol. Ecol.* 353, 287–295. doi: 10.1016/j.jembe.2007.10.003

Knowlton, N., and Rohwer, F. (2003). Multispecies microbial mutualisms on coral reefs: the host as a habitat. *Am. Nat.* 162, S51–S62. doi: 10.1086/378684

LaJeunesse, T. C. (2001). Investigating the biodiversity, ecology, and phylogeny of endosymbiotic dinoflagellates in the genus *Symbiodinium* using the ITS region: in search of a "species" level marker. *J. Phycol.* 37, 866–880. doi: 10.1046/j.1529-8817.2001.01031.x

LaJeunesse, T. C. (2002). Diversity and community structure of symbiotic dinoflagellates from Caribbean coral reefs. *Mar. Biol.* 141, 387–400. doi: 10.1007/s00227-002-0829-2

LaJeunesse, T. C. (2017). Validation and description of *Symbiodinium microadriaticum*, the type species of *Symbiodinium* (Dinophyta). *J. Phycol.* 53, 1109–1114. doi: 10.1111/jpy.12570

LaJeunesse, T. C., Bhagooli, R., Hidaka, M., DeVantier, L., Done, T., Schmidt, G. W., et al. (2004a). Closely related *Symbiodinium* spp. differ in relative dominance in coral reef host communities across environmental, latitudinal and biogeographic gradients. *Mar. Ecol. Prog. Ser.* 284, 147–161. doi: 10.3354/meps284147

LaJeunesse, T. C., Bonilla, H. R., Warner, M. E., Wills, M., Schmidt, G. W., and Fitt, W. K. (2008). Specificity and stability in high latitude eastern Pacific coral-algal symbioses. *Limnol. Oceanogr.* 53, 719–727. doi: 10.4319/lo.2008.53.2.0719

LaJeunesse, T. C., Loh, W., van Woesik, R., Hoegh-Guldberg, O., Schmidt, G. W., and Fitt, W. K. (2003). Low symbiont diversity in southern great barrier reef corals, relative to those of the Caribbean. *Limnol. Oceanogr.* 48, 2046–2054. doi: 10.4319/lo.2003.48.5.2046

LaJeunesse, T. C., Parkinson, J. E., Gabrielson, P. W., Jeong, H. J., Reimer, J. D., Voolstra, C. R., et al. (2018). Systematic revision of Symbiodiniaceae highlights the antiquity and diversity of coral endosymbionts. *Curr. Biol.* 28, 2570–2580. doi: 10.1016/j.cub.2018.07.008

LaJeunesse, T. C., Thornhill, D. J., Cox, E. F., Stanton, F. G., Fitt, W. K., and Schmidt, G. W. (2004b). High diversity and host specificity observed among

symbiotic dinoflagellates in reef coral communities from Hawaii. *Coral Reefs* 23, 596–603. doi: 10.1007/s00338-004-0428-4

LaJeunesse, T. C., Wham, D. C., Pettay, D. T., Parkinson, J. E., Keshavmurthy, S., and Chen, C. A. (2014). Ecologically differentiated stress-tolerant endosymbionts in the dinoflagellate genus *Symbiodinium* (Dinophyceae) clade D are different species. *Phycologia* 53, 305–319. doi: 10.2216/13-186.1

Lee, S. T. M., Davy, S. K., Tang, S. -L., Fan, T. -Y., and Kench, P. S. (2015). Successive shifts in the microbial community of the surface mucus layer and tissues of the coral *Acropora muricata* under thermal stress. *FEMS Microbiol. Ecol.* 91:fiv142. doi: 10.1093/femsec/fiv142

Leggat, W., Gierz, S., Hernandez-Agreda, A., and Ainsworth, T. D. (2019). "The mesophotic coral microbial biosphere" in *Mesophotic coral ecosystems*. eds. Y. Loya, K. A. Puglise and T. C. L. Bridge (New York: Springer), 493–505.

Leite, D. C. A., Salles, J. F., Calderon, E. N., van Elsas, J. D., and Peixoto, R. S. (2018). Specific plasmid patterns and high rates of bacterial co-occurrence within the coral holobiont. *Ecol. Evol.* 8, 1818–1832. doi: 10.1002/ece3.3717

Liberman, T., Genin, A., and Loya, Y. (1995). Effects on growth and reproduction of the coral *Stylophora pistillata* by the mutualistic damselfish *Dascyllus marginatus*. *Mar. Biol.* 121, 741–746. doi: 10.1007/BF00349310

Little, A. F., van Oppen, M. J. H., and Willis, B. L. (2004). Flexibility in algal endosymbioses shapes growth in reef corals. *Science* 304, 1492–1494. doi: 10.1126/science.1095733

Loya, Y., Sakai, K., Yamazato, K., Nakano, Y., Sambali, H., and van Woesik, R. (2001). Coral bleaching: the winners and the losers. *Ecol. Lett.* 4, 122–131. doi: 10.1046/j.1461-0248.2001.00203.x

Margulis, L. (1991). "Symbiogenesis and symbionticism" in *Symbiosis as a source of evolutionary innovation: Speciation and morphogenesis*. Cambridge MA: MIT Press, 1–14.

McCauley, M., Banaszak, A. T., and Goulet, T. L. (2018). Species traits dictate seasonal-dependent responses of octocoral–algal symbioses to elevated temperature and ultraviolet radiation. *Coral Reefs* 37, 901–917. doi: 10.1007/s00338-018-1716-8

McCauley, M., Jackson, C. R., and Goulet, T. L. (2020). Microbiomes of Caribbean octocorals vary over time but are resistant to environmental change. *Front. Microbiol.* 11:1272. doi: 10.3389/fmicb.2020.01272

McDevitt-Irwin, J. M., Baum, J. K., Garren, M., and Vega Thurber, R. L. (2017). Responses of coral-associated bacterial communities to local and global stressors. *Front. Mar. Sci.* 4:262. doi: 10.3389/fmars.2017.00262

McLachlan, R. H., Price, J. T., Solomon, S. L., and Grottoli, A. G. (2020). Thirty years of coral heat-stress experiments: a review of methods. *Coral Reefs* 39, 885–902. doi: 10.1007/s00338-020-01931-9

Muscatine, L., and D'Elia, C. F. (1978). The uptake, retention, and release of ammonium by reef corals. *Limnol. Oceanogr.* 23, 725–734. doi: 10.4319/lo.1978.23.4.0725

Muscatine, L., and Porter, J. (1977). Reef corals: mutualistic symbioses adapted to nutrient-poor environments. *Bioscience* 27, 454–460. doi: 10.2307/1297526

Oliver, T. A., and Palumbi, S. R. (2009). Distributions of stress-resistant coral symbionts match environmental patterns at local but not regional scales. *Mar. Ecol. Prog. Ser.* 378, 93–103. doi: 10.3354/meps07871

Olson, J. B., and Kellogg, C. A. (2010). Microbial ecology of corals, sponges, and algae in mesophotic coral environments. *FEMS Microbiol. Ecol.* 73, 17–30. doi: 10.1111/j.1574-6941.2010.00862.x

Osman, E. O., Suggett, D. J., Voolstra, C. R., Pettay, D. T., Clark, D. R., Pogoreutz, C., et al. (2020). Coral microbiome composition along the northern Red Sea suggests high plasticity of bacterial and specificity of endosymbiotic dinoflagellate communities. *Microbiome* 8, 1–16. doi: 10.1186/s40168-019-0776-5

Pearse, V. B., and Muscatine, L. (1971). Role of symbiotic algae (zooxanthellae) in coral calcification. *Biol. Bull.* 141, 350–363. doi: 10.2307/1540123

Peixoto, R. S., Rosado, P. M., de Assis Leite, D. C., Rosado, A. S., and Bourne, D. G. (2017). Beneficial microorganisms for corals (BMC): proposed mechanisms for coral health and resilience. *Front. Microbiol.* 8:341. doi: 10.3389/fmicb.2017.00341

Putnam, H. M., Stat, M., Pochon, X., and Gates, R. D. (2012). Endosymbiotic flexibility associates with environmental sensitivity in scleractinian corals. *Proc. R Soc. Lond. B* 279, 4352–4361. doi: 10.1098/rspb.2012.1454

Reshef, L., Koren, O., Loya, Y., Zilber-Rosenberg, I., and Rosenberg, E. (2006). The coral probiotic hypothesis. *Environ. Microbiol.* 8, 2068–2073. doi: 10.1111/j.1462-2920.2006.01148.x

Rinkevich, B., and Loya, Y. (1979). The reproduction of the Red Sea coral *Stylophora pistillata*. II. Synchronization in breeding and seasonality of planulae shedding. *Mar. Ecol. Prog. Ser.* 1, 145–152. doi: 10.3354/meps001145

Robison, J. D., and Warner, M. E. (2006). Differential impacts of photoacclimation and thermal stress on the photobiology of four different phylotypes of *Symbiodinium* (Pyrrhophyta). *J. Phycol.* 42, 568–579. doi: 10.1111/j.1529-8817.2006.00232.x

Rohwer, F., Seguritan, V., Azam, F., and Knowlton, N. (2002). Diversity and distribution of coral-associated bacteria. *Mar. Ecol. Prog. Ser.* 243, 1–10. doi: 10.3354/meps243001

Rowan, R. (2004). Coral bleaching: thermal adaptation in reef coral symbionts. *Nature* 430:742. doi: 10.1038/430742a

Rowan, R., and Powers, D. A. (1991a). A molecular genetic classification of zooxanthellae and the evolution of animal-algal symbiosis. *Science* 251, 1348–1351. doi: 10.1126/science.251.4999.1348

Rowan, R., and Powers, D. A. (1991b). Molecular genetic identification of symbiotic dinoflagellates (zooxanthellae). *Mar. Ecol. Prog. Ser.* 71, 65–73. doi: 10.3354/meps071065

Rowan, R., and Powers, D. A. (1992). Ribosomal RNA sequences and the diversity of symbiotic dinoflagellates (zooxanthellae). *Proc. Natl. Acad. Sci. U. S. A.* 89, 3639–3643. doi: 10.1073/pnas.89.8.3639

Sampayo, E. M., Ridgway, T., Bongaerts, P., and Hoegh-Guldberg, O. (2008). Bleaching susceptibility and mortality of corals are determined by fine-scale differences in symbiont type. *Proc. Natl. Acad. Sci. U. S. A.* 105, 10444–10449. doi: 10.1073/pnas.0708049105

Santos, S. R., Taylor, D. J., and Coffroth, M. A. (2001). Genetic comparisons of freshly isolated versus cultured symbiotic dinoflagellates: implications for extrapolating to the intact symbiosis. *J. Phycol.* 37, 900–912. doi: 10.1046/j.1529-8817.2001.00194.x

Savage, A. M., Goodson, M. S., Visram, S., Trapido-Rosenthal, H., Wiedenmann, J., and Douglas, A. E. (2002). Molecular diversity of symbiotic algae at the latitudinal margins of their distribution: dinoflagellates of the genus *Symbiodinium* in corals and sea anemones. *Mar. Ecol. Prog. Ser.* 244, 17–26. doi: 10.3354/meps244017

Shashar, N., Cohen, Y., Loya, Y., and Sar, N. (1994). Nitrogen fixation (acetylene reduction) in stony corals: evidence for coral-bacteria interactions. *Mar. Ecol. Prog. Ser.* 111, 259–264. doi: 10.3354/meps111259

Shirur, K. P., Jackson, C. R., and Goulet, T. L. (2016). Lesion recovery and the bacterial microbiome in two Caribbean gorgonian corals. *Mar. Biol.* 163:238. doi: 10.1007/s00227-016-3008-6

Shirur, K. P., Ramsby, B. D., Iglesias-Prieto, R., and Goulet, T. L. (2014). Biochemical composition of Caribbean gorgonians: implications for gorgonian — *Symbiodinium* symbiosis and ecology. *J. Exp. Mar. Biol. Ecol.* 461, 275–285. doi: 10.1016/j.jembe.2014.08.016

Siebeck, U. E., Marshall, N. J., Klüter, A., and Hoegh-Guldberg, O. (2006). Monitoring coral bleaching using a colour reference card. *Coral Reefs* 25, 453–460. doi: 10.1007/s00338-006-0123-8

Silverstein, R. N., Correa, A. M. S., and Baker, A. C. (2012). Specificity is rarely absolute in coral–algal symbiosis: implications for coral response to climate change. *Proc. R Soc. Lond. B* 279, 2609–2618. doi: 10.1098/rspb.2012.0055

Stat, M., and Gates, R. D. (2011). Clade D *Symbiodinium* in scleractinian corals: a "nugget" of hope, a selfish opportunist, an ominous sign, or all of the above? *J. Mar. Biol.* 2011, 1–9. doi: 10.1155/2011/730715

Stat, M., Pochon, X., Franklin, E. C., Bruno, J. F., Casey, K. S., Selig, E. R., et al. (2013). The distribution of the thermally tolerant symbiont lineage (*Symbiodinium* clade D) in corals from Hawaii: correlations with host and the history of ocean thermal stress. *Ecol. Evol.* 3, 1317–1329. doi: 10.1002/ece3.556

Tchernov, D., Gorbunov, M. V., de Vargas, C., Yadav, S. N., Milligan, A. J., Häggblom, M., et al. (2004). Membrane lipids of symbiotic algae are diagnostic of sensitivity to thermal bleaching in corals. *Proc. Natl. Acad. Sci. U. S. A.* 101, 13531–13535. doi: 10.1073/pnas.0402907101

Thornhill, D. J., Xiang, Y., Pettay, D. T., Zhong, M., and Santos, S. R. (2013). Population genetic data of a model symbiotic cnidarian system reveal remarkable symbiotic specificity and vectored introductions across ocean basins. *Mol. Ecol.* 22, 4499–4515. doi: 10.1111/mec.12416

van de Water, J. A. J. M., Allemand, D., and Ferrier-Pagès, C. (2018). Host-microbe interactions in octocoral holobionts - recent advances and perspectives. *Microbiome* 6:64. doi: 10.1186/s40168-018-0431-6

van de Water, J. A. J. M., Melkonian, R., Voolstra, C. R., Junca, H., Beraud, E., Allemand, D., et al. (2017). Comparative assessment of mediterranean gorgonian-associated microbial communities reveals conserved core and locally variant bacteria. *Microb. Ecol.* 73, 466–478. doi: 10.1007/s00248-016-0858-x

van Oppen, M. J. H., Mieog, J. C., Sánchez, C. A., and Fabricius, K. E. (2005). Diversity of algal endosymbionts (zooxanthellae) in octocorals: the roles of geography and host relationships. *Mol. Ecol.* 14, 2403–2417. doi: 10.1111/j.1365-294X.2005.02545.x

Wegley, L., Edwards, R., Rodriguez-Brito, B., Liu, H., and Rohwer, F. (2007). Metagenomic analysis of the microbial community associated with the coral *Porites astreoides*. *Environ. Microbiol.* 9, 2707–2719. doi: 10.1111/j.1462-2920.2007.01383.x

Weis, V. M. (2008). Cellular mechanisms of cnidarian bleaching: stress causes the collapse of symbiosis. *J. Exp. Biol.* 211, 3059–3066. doi: 10.1242/jeb.009597

Weis, V. M., Reynolds, W. S., deBoer, M. D., and Krupp, D. A. (2001). Host-symbiont specificity during onset of symbiosis between the dinoflagellates *Symbiodinium* spp. and planula larvae of the scleractinian coral *Fungia scutaria*. *Coral Reefs* 20, 301–308. doi: 10.1007/s003380100179

Wilcox, T. P. (1998). Large-subunit ribosomal RNA systematics of symbiotic dinoflagellates: morphology does not recapitulate phylogeny. *Mol. Phylogenet. Evol.* 10, 436–448. doi: 10.1006/mpev.1998.0546

Ziegler, M., Arif, C., and Voolstra, C. R. (2019). "Symbiodiniaceae diversity in Red Sea coral reefs and coral bleaching" in *Coral reefs of the Red Sea*. Cham: Springer, 69–89.

Conflict of Interest: The authors declare that the research was conducted in the absence of any commercial or financial relationships that could be construed as a potential conflict of interest.

frontiers in Marine Science

ORIGINAL RESEARCH
published: 29 September 2020
doi: 10.3389/fmars.2020.565068

Increased Ammonium Assimilation Activity in the Scleractinian Coral *Pocillopora damicornis* but Not Its Symbiont After Acute Heat Stress

*Jia Tang[1], Xingzhen Ni[1], Jianqing Wen[1], Lingui Wang[1,2], Jian Luo[1,2,3] and Zhi Zhou[1,2,3]**

[1] Department of Marine Sciences, College of Marine Sciences, Hainan University, Haikou, China, [2] Key Laboratory of Tropical Hydrobiology and Biotechnology of Hainan Province, Hainan University, Haikou, China, [3] State Key Laboratory of Marine Resource Utilization in South China Sea, Hainan Aquaculture Breeding Engineering Research Center, Hainan University, Haikou, China

Ammonium is the main nitrogen resources for scleractinian coral-Symbiodiniaceae symbiotic association, and there is urgent need to investigate the involvement of ammonium assimilation in the heat acclimation of the symbiotic association to heat stress. In the present study, symbiont density and chlorophyll content, as well as redox and ammonium assimilation enzyme activities, in two symbiotic partners of the scleractinian coral *Pocillopora damicornis* were firstly investigated after acute heat stress (32°C). Symbiont density and chlorophyll content decreased significantly at 24 h (1.81×10^6 cell cm^{-2}, $p < 0.05$) and 36 h (23.25 pg $cell^{-1}$, $p < 0.05$) after heat stress, respectively. We observed significant activity increases of coral nitric oxide synthase, superoxide dismutase and catalase, and symbiont superoxide dismutase after heat stress, but no alterations in the activities of symbiont nitric oxide synthase and catalase during the whole experiment period. The activities of coral glutamine synthetase and glutamine oxoglutarate aminotransferase began to increase significantly at 24 h, and reached the peak at 36 h after heat stress. As for coral glutamate dehydrogenase activity, a significant increase was observed only at 36 h after heat stress. The activities of symbiont glutamine synthetase and glutamine oxoglutarate aminotransferase did not change significantly after heat stress. Secondly, symbiont density, chlorophyll content, apoptosis rate, coral total antioxidant capacity, and caspase3 activation level were determined after glufosinate (glutamine synthetase inhibitor) treatment. Symbiont density decreased significantly at 6 h (1.25×10^6 cell cm^{-2}, $p < 0.05$) after glufosinate treatment, and symbiont chlorophyll content also decreased significantly during 12–24 h after glufosinate treatment, with the lowest level at 12 h (16.69 pg $cell^{-1}$, $p < 0.05$). Furthermore, the coral total antioxidant capacity and caspase3 activation level both increased significantly at 12 h (0.57 U mg^{-1}, 2.08-fold, $p < 0.05$) after glufosinate treatment, while no significant change was observed for the symbiont apoptosis rate. These results suggest that the ammonium assimilation activity in the coral host *P. damicornis*, not its symbiont, was induced by acute heat stress, which might contribute to the acclimatization of the symbiotic association to high temperature through regulating coral antioxidant capacity and apoptosis.

Keywords: nitrogen nutrient, nitrogen limitation, heat acclimation, symbiosis breakdown, scleractinian coral

OPEN ACCESS

Edited by:
Hajime Kayanne,
The University of Tokyo, Japan

Reviewed by:
Daniel Aagren Nielsen,
University of Technology Sydney, Australia
Anthony William Larkum,
University of Technology Sydney, Australia

***Correspondence:**
Zhi Zhou
zhouzhi@hainanu.edu.cn

Specialty section:
This article was submitted to Coral Reef Research, a section of the journal Frontiers in Marine Science

Received: *23 May 2020*
Accepted: *11 September 2020*
Published: *29 September 2020*

Citation:
Tang J, Ni X, Wen J, Wang L, Luo J and Zhou Z (2020) Increased Ammonium Assimilation Activity in the Scleractinian Coral Pocillopora damicornis but Not Its Symbiont After Acute Heat Stress. Front. Mar. Sci. 7:565068. doi: 10.3389/fmars.2020.565068

INTRODUCTION

Scleractinian corals are main builders of coral reef, which provide habitats for one-quarter to one-third of all marine species (Plaisance et al., 2011). In order to thrive in oligotrophic reef environment, scleractinian corals have evolved the symbiotic relationship with unicellular, photosynthetic dinoflagellate algae of the family Symbiodiniaceae that are harbored within corals' endodermal cells (Dubinsky and Jokiel, 1994). Scleractinian corals provide shelter and inorganic nutrients for their symbiotic Symbiodiniaceae. In return, Symbiodiniaceae supply the coral host with photosynthates and other organic nutrients, which can meet up to 95% of the corals' energy requirements (Muscatine and Porter, 1977). The mutual nutrient exchange determines the stability and maintenance of the coral-Symbiodiniaceae symbiosis (Liu et al., 2018; Wall et al., 2020). However, it has been considered that the coral-Symbiodiniaceae symbiosis is vulnerable to environmental changes, especially for elevated seawater temperature (Vidal-Dupiol et al., 2011).

The rise of the mean annual sea surface temperature due to global warming has been threating the symbiosis between scleractinian corals and Symbiodiniaceae (Wooldridge, 2013). The typical physiological response of the symbiotic association to high temperature is the loss of symbiotic Symbiodiniaceae from coral host or the degradation of symbiont's photosynthetic pigments, which will lead to the collapse of coral-Symbiodiniaceae symbiosis (Coles and Brown, 2003; Hughes et al., 2017). It has been considered that the symbiosis collapse can attribute to excessive oxidative pressure in the symbiotic association owing to induced production of oxygen free radicals under heat stress, which is able to result in the damage of D1 protein (a crucial component of the photosynthetic electron transport chain) in symbiont chloroplast PSII system and the activation of apoptosis in coral host (Lesser, 1997; Roberty et al., 2015). Subsequently, symbionts are expelled from the coral host, and photosynthates will reduce dramatically, causing the coral host not to get sufficient nutrient and energy supply from their symbionts (Pernice et al., 2011; Wein et al., 2019). The imbalance of the nutrient exchanges under heat stress finally results in the collapse of the symbiosis, coral bleaching, and even death.

Nitrogen nutrient can also be exchanged between scleractinian corals and symbiotic Symbiodiniaceae, which is of importance for the maintenance of their symbiosis (Radecker et al., 2015). Coral host takes up and assimilates limited ammonium as main nitrogen resource from oligotrophic seawater environment through two key pathways including glutamine synthetase (GS)/glutamine oxoglutarate aminotransferase (GOGAT) pathway, and glutamate dehydrogenase (GDH) pathway, and symbiotic Symbiodiniaceae assimilate ammonium from coral host through GS/GOGAT pathway (Pernice et al., 2012; Roberty et al., 2020). The assimilated ammonium is used to synthesize amino acid and protein in the symbiotic association, and further symbionts can provide coral host with essential amino acid and other nitrogen-containing organics (Shinzato et al., 2011). Generally, symbiotic Symbiodiniaceae requires more ammonium nutrient than the coral host, and therefore are under nitrogen limitation (Peng et al., 2012). It has been believed that nitrogen limitation of symbionts is beneficial for the maintenance of the symbiosis because it obliges symbionts to produce and translocate more photosynthates and restrain their own reproduction (Radecker et al., 2015; Morris et al., 2019; Xiang et al., 2020). However, the role of nitrogen nutrient exchange, especially ammonium assimilation, in the acclimation of the coral-Symbiodiniaceae symbiotic association to high temperature, is still not well understood.

Scleractinian coral *Pocillopora damicornis* belongs to the family Pocilloporidae and is widely distributed in the tropical and subtropical areas of the Indian and Pacific Oceans. In the present study, *P. damicornis* was employed as a model of scleractinian corals to explore the involvement of ammonium assimilation in the acclimation of coral-Symbiodiniaceae symbiosis to high temperature. Firstly, the symbiont density, chlorophyll content, redox and ammonium assimilation enzyme activities in two symbiotic partners after acute heat stress were measured to investigate the response of ammonium assimilation in the coral-Symbiodiniaceae symbiotic association to high temperature. Secondly, GS inhibitor was used to repress ammonium assimilation ability of the coral-Symbiodiniaceae symbiotic association to further explore the potential regulation of heat acclimation by ammonium assimilation. Our results will provide insights into the effect of ammonium assimilation on the maintenance of coral-Symbiodiniaceae symbiosis and the environment acclimation of scleractinian corals.

MATERIALS AND METHODS

Coral

Three *P. damicornis* colonies were collected from a fringing reef at a depth 1.5 m in Wenchang, China, and have been shown to harbor Symbiodiniaceae within the genus *Cladocopium* as dominant symbionts (unpublished work). The branches in the colonies were split as nubbins, and these nubbins were attached on the plastic mesh plate located in the bottom of flow-through aquaria (ca. 500 L) filled with natural seawater (26°C). All nubbins were illuminated with white and blue cool fluorescent bulbs (Philips T5HO Activiva Active 54 W) at a light intensity of about 500 μmol photons m^{-2} s^{-1} in a 12 h/12 h light–dark cycle for 1 month to acclimatize to laboratory conditions.

Acute Heat Treatment Experiment

Forty-eight coral nubbins from three colonies (16 nubbins each colony) were employed in the heat treatment experiment. Twenty-four nubbins were transferred into the heated seawater (32°C), which were employed as the heat group. The rest of 24 nubbins were kept in 26°C seawater as the control group. Coral nubbins were randomly sampled in the heat and control groups after 0, 12, 24, and 36 h of incubation. Six nubbins (2 nubbins each colony, 3 colonies giving rise to 6 biological replicates) were sampled from each group at each time point to measure the density and chlorophyll content of the symbionts, as well as the enzyme activities of the two symbiotic partners.

Glufosinate Treatment Experiment

Water-soluble glufosinate was used to inhibit GS activity in the coral-Symbiodiniaceae symbiotic association under high temperature (32°C). A total of 48 coral nubbins from three colonies (16 nubbins each colony) were used in the glufosinate treatment experiment and divided into two groups, including glufosinate and control groups. Twenty-four nubbins in the glufosinate group were transferred into glufosinate-containing and heated seawater (final concentration 10 μmol L^{-1}, 32°C), and 24 nubbins in the control group were only placed into the heated seawater (32°C). To measure the density, apoptosis and chlorophyll content of the symbionts and enzyme activities of the two symbiotic partners, 6 nubbins (2 nubbins each colony, 3 colonies giving rise to 6 biological replicates) were sampled randomly from the glufosinate and control groups at 0, 6, 12, and 24 h after the treatment.

Determination of Symbiont Density

The density variation of symbionts was measured following a previous method with few modifications (Higuchi et al., 2008; Higuchi et al., 2015). Briefly, coral tissues were homogenized in 10 mL phosphate buffered saline (PBS, 377 mmol L^{-1} NaCl, 2.7 mmol L^{-1} KCl, 8.09 mmol L^{-1} Na_2HPO_4, 1.47 mmol L^{-1} KH_2PO_4, pH 7.4); 1-mL homogenates were then centrifuged at 5000 rpm, 4°C for 15 min, and the symbiont pellets were resuspended in PBS and counted using a Neubauer hemocytometer (QIUJING, China). The surface area of the nubbins was determined using the aluminum foil method (Johannes et al., 1970). The symbiont density was defined as its number per unit surface area of the coral nubbins (cells cm^{-2}).

Measurement of Chlorophyll Content

Chlorophyll content of symbionts was determined as previously reported (Hedouin et al., 2016). Briefly, 2-mL homogenates were centrifuged at 12,000 rpm, 4°C for 3 min. The harvested symbionts were resuspended in PBS and further centrifuged at 12,000 rpm, 4°C for 3 min. Chlorophyll *a* and c_2 were extracted for 24 h at 4°C in 2 mL of 100% acetone, followed by the centrifugation at 12,000 rpm, 4°C for 3 min. The absorbance values of the extracts were measured at 630 and 663 nm. The total content of chlorophyll $a + c_2$ was computed according to the equations of Jeffrey and Humphrey (1975). The total quantity of chlorophyll $a + c_2$ was divided by the number of symbionts to yield chlorophyll content (pg $cell^{-1}$).

Activity Assays of Ammonium Assimilation Enzymes in Coral and Symbiont

Six-milliliter homogenates were centrifuged at 5,000 rpm, 4°C for 15 min to collect the supernatants for the activity determination of enzymes in the coral host. The symbiont pellets were resuspended in 6 mL of PBS, following by a homogenate. After the centrifugation at 12,000 rpm, 4°C for 3 min, the supernatants were harvested for the activity detection of symbiont enzymes.

GS (BC0915, Solarbio, China), GDH (A125, JIANCHENG, China), and GOGAT (BC0070, Solarbio, China) kits were employed to determine their activities in the coral and symbiont supernatants according to manufacturer's protocol. After the total enzyme activities were obtained, the concentrations of total protein in the supernatants were quantified using bicinchoninic acid assay (BCA) method (Zhou et al., 2018) and used to normalize the measured activities of GS, GDH, and GOGAT to U mg^{-1} protein.

Determination of the Redox Parameters in Coral and Symbiont

The activities of superoxide dismutase (SOD), catalase (CAT), nitric oxide synthetase (NOS), and total antioxidant capacity in the coral and symbiont supernatants were measured using commercial kits (A001, A007, A014, and A015, JIANCHENG, China), following the manufacturer's recommendations. The measured enzyme activity or capacity was divided by the total protein to yield specific activity expressed as U mg^{-1} protein.

Detection of Caspase3 Activation Level in Coral

The caspase3 activity in the coral supernatant was measured by Caspase-3 Colorimetric Assay Kit (KeyGEN, China) according to the instruction. Briefly, the supernatants of all nubbin samples were diluted firstly to the same protein concentration. Then, 50 μL supernatant was added in the reaction mixture containing 50 μL reaction buffer and 5 μL substrate, following incubation for 4 h in the dark at 37°C. Finally, the color change of the mixture was detected spectrophotometrically at the wavelength of 405 nm. The activity of caspase3 was defined as the absorbance of the reaction solution at 405 nm (A_{405}), and the activation level of caspase3 in the coral was defined as the ratio of A_{405} in samples to that of the control group at 0 h.

Symbiont Apoptosis Assay

The apoptosis of symbionts was detected using the Apoptosis-Hoechst staining kit and the Tubulin-Tracker Red fluorescent probe (C0003, C1050, Beyotime, China). Briefly, about 3.0×10^5 symbionts were fixed by the fixative supplied in the apoptosis kit for 10 min, following by washing three times with PBS containing 0.05% Tween-20 (PBS-T). Then, 0.5 mL Hoechst 33258 staining solution was added to incubate for 5 min, and the symbionts were washed three times with PBS-T. After incubation with 200 μL Tubulin-tracker Red staining solution in the dark for 30 min and three washing, the double-stained symbionts were transferred to a glass slide and observed under a fluorescence microscope. The cell nucleus of healthy symbionts was stained blue, whereas the nucleus of apoptotic symbionts was not stained blue. Symbiont apoptosis rate was evaluated by counting the number of apoptotic symbionts in 100 cells, and each counting was repeated three times.

Statistical Analysis

All data was presented as means ± standard deviation (SD) from biological replicates. A paired samples t-test was applied using SPSS v22.0 (SPSS Inc., Chicago, Illinois) to determine significant differences of physiological parameters between the treatment

and control groups in the acute heat and glufosinate treatment experiments at each time point. Differences were considered significant at $p < 0.05$.

RESULTS

Symbiont Density and Chlorophyll Content After Acute Heat Treatment

The density and chlorophyll $a + c_2$ content of symbionts were determined in *P. damicornis* after heat treatment. The symbiont density decreased significantly at 24 h ($1.81 \pm 0.65 \times 10^6$ cell cm^{-2}, $p < 0.05$), in comparison with that in the control group, and returned to the control level at 36 h after heat treatment (**Figure 1A**). The content of symbiont chlorophyll $a + c_2$ also declined significantly after heat treatment, and it reached the lowest level at 36 h of treatment (23.25 ± 8.37 pg $cell^{-1}$, $p < 0.05$) (**Figure 1B**).

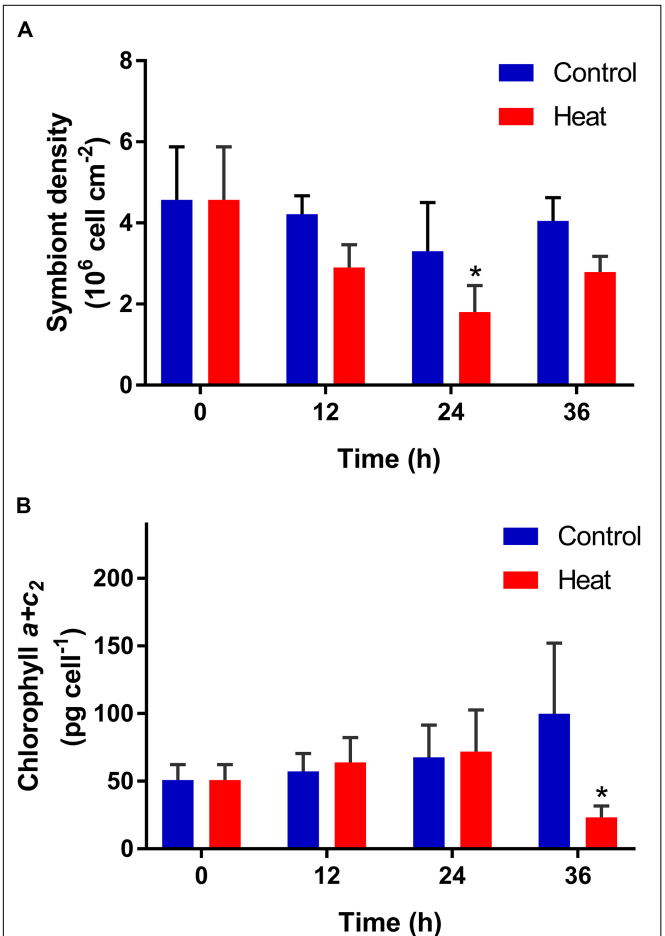

FIGURE 1 | Temporal variation of symbiont density **(A)** and chlorophyll content **(B)** in the scleractinian coral *Pocillopora damicornis* after heat treatment. Data points represent means, and error bars represent standard deviations ($N = 6$). Asterisks depict significant differences between the heat and control groups ($p < 0.05$).

Temporal Alterations of Redox Parameters in the Symbiotic Association After Acute Heat Treatment

Coral NOS, SOD, and CAT activities in the heat group all showed significant increases, compared to those in the control group. NOS activity began to increase significantly at 12 h (2.27 ± 0.57 U mg^{-1}, $p < 0.05$), and reached the peak at 36 h (5.64 ± 0.21 U mg^{-1}, $p < 0.05$) after heat treatment (**Figure 2A**). SOD and CAT activities both increased significantly during 24–36 h after heat treatment, with the highest level at 36 h (329.90 ± 94.68 U mg^{-1} and 22.22 ± 5.48 U mg^{-1}, respectively, $p < 0.05$) (**Figures 2B,C**).

Symbiont SOD activity underwent a significant rise during 24–36 h and peaked at 24 h after heat treatment (88.68 ± 5.63 U mg^{-1}, $p < 0.05$) (**Figure 2E**). However, symbiont NOS and CAT activities in the heat group showed no significant changes throughout the experiment process, compared to those in the control group (**Figures 2D,F**).

Temporal Activities of Ammonium Assimilation Enzymes in the Symbiotic Association After Acute Heat Treatment

GS, GDH and GOGAT activities also increased significantly in the coral host after heat treatment, in comparison with those in the control group. GS and GOGAT both began to increase significantly at 24 h (2.73 ± 1.32 U mg^{-1}, 131.27 ± 16.53 U mg^{-1}, $p < 0.05$), and reached the peak level at 36 h (5.03 ± 1.48 U mg^{-1}, 167.13 ± 51.39 U mg^{-1}, $p < 0.05$) after heat treatment (**Figures 3A,C**). For GDH activity, a significant increase was observed only at 36 h (17.31 ± 6.82 U mg^{-1}, $p < 0.05$) after heat treatment (**Figure 3B**). The activities of symbiont GS and GOGAT both did not change significantly after heat treatment during the whole treatment process (**Figures 3D,E**).

Symbiont Density and Chlorophyll Content After Glufosinate Treatment

The density and chlorophyll $a + c_2$ content of symbiont were determined after glufosinate treatment. The symbiont density decreased significantly at 6 h ($1.25 \pm 0.28 \times 10^6$ cell cm^{-2}, $p < 0.05$) after glufosinate treatment, compared by that in the control group (**Figure 4A**). The content of chlorophyll $a + c_2$ per symbiont cell decreased significantly during 12–24 h after glufosinate treatment, with the lowest level at 12 h (16.69 ± 3.66 pg $cell^{-1}$, $p < 0.05$) (**Figure 4B**).

Antioxidant Capacity and Apoptosis of the Symbiotic Association After Glufosinate Treatment

The total antioxidant capacity of the coral host increased significantly at 12 h (0.57 ± 0.18 U mg^{-1}, $p < 0.05$) after glufosinate treatment (**Figure 5A**), and its caspase3 activation level also rise significantly at 12 h (2.08 ± 0.37-fold, $p < 0.05$) after glufosinate treatment (**Figure 5B**), compared by those in the control group. In addition, no significant change was observed for the symbiont apoptosis rate in the glufosinate group at 12 and 24 h after the treatment of glufosinate (**Figure 5C**).

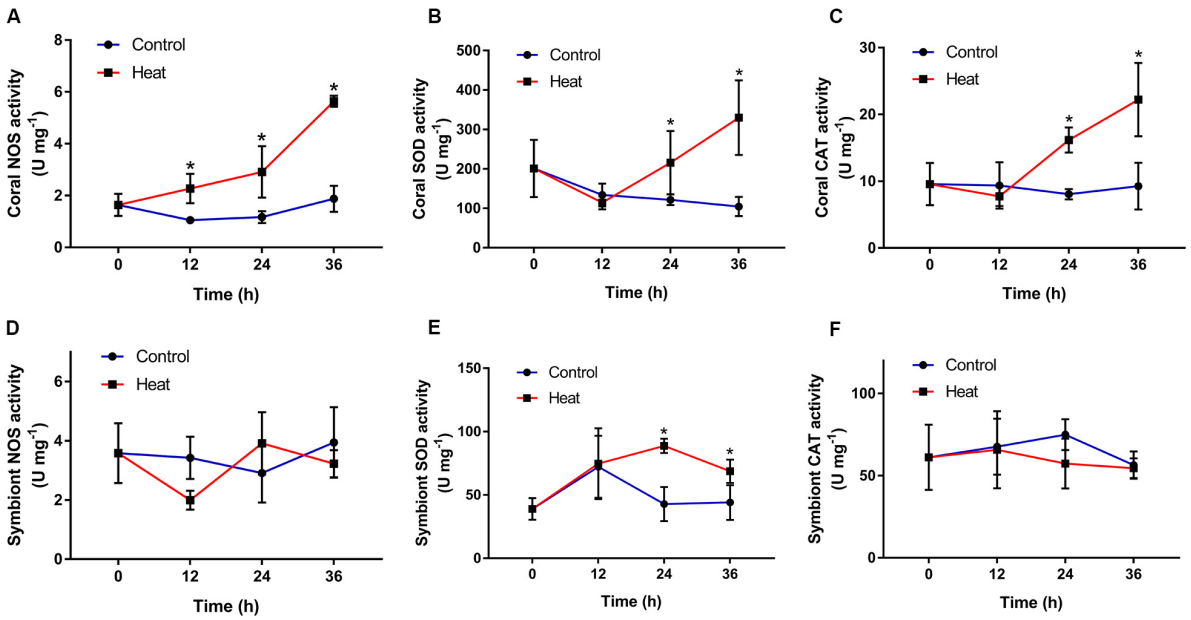

FIGURE 2 | Temporal patterns of redox-related enzyme activities in the scleractinian coral *Pocillopora damicornis* and its symbionts after heat treatment. **(A)** Nitric oxide synthetase (NOS) in the coral. **(B)** Superoxide dismutase (SOD) in the coral. **(C)** Catalase (CAT) in the coral. **(D)** NOS in the symbionts. **(E)** SOD in the symbionts. **(F)** CAT in the symbionts. Data points represent means and error bars represent standard deviations ($N = 6$). Asterisks depict significant differences between the heat and control groups ($p < 0.05$).

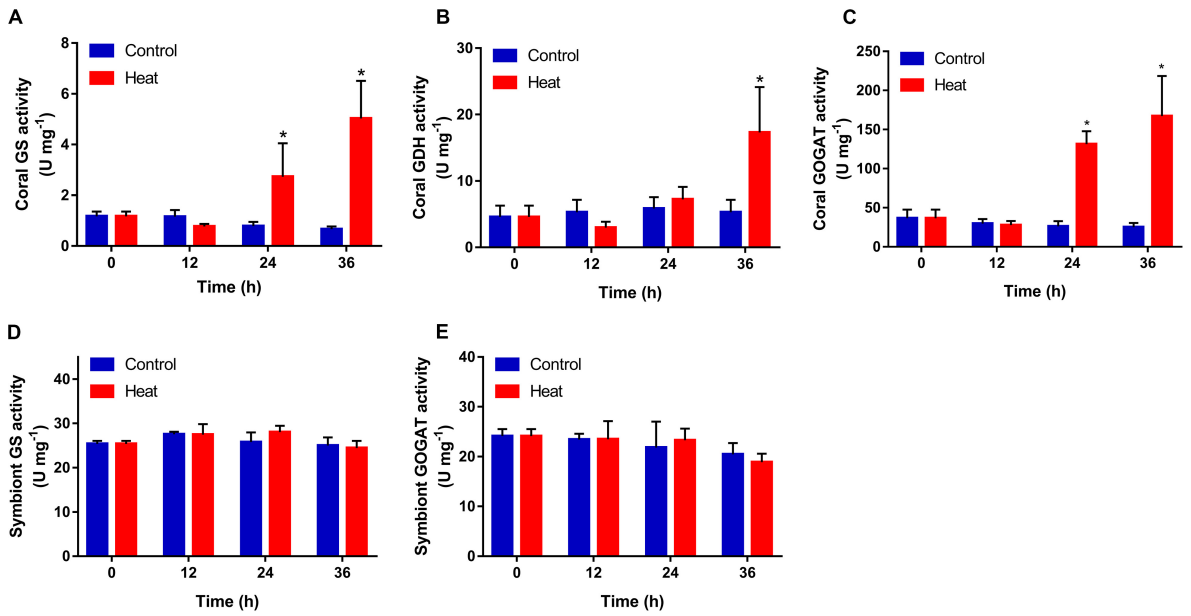

FIGURE 3 | Temporal activities of ammonium assimilation enzymes in the scleractinian coral *Pocillopora damicornis* and its symbionts after heat treatment. **(A)** Glutamine synthetase (GS) in the coral. **(B)** Glutamate dehydrogenase (GDH) in the coral. **(C)** Glutamine oxoglutarate aminotransferase (GOGAT) in the coral. **(D)** GS in the symbionts. **(E)** GOGAT in the symbionts. Data points represent means and error bars represent standard deviations ($N = 6$). Asterisks depict significant differences between the heat and control groups ($p < 0.05$).

DISCUSSION

Coral-Symbiodiniaceae symbiotic association assimilates ammonium as main inorganic nitrogen resource, which further forms a nitrogen cycling to sustain the symbiosis (Pernice et al., 2012; Radecker et al., 2015). However, little is known about the role of ammonium assimilation in heat acclimation of the coral-Symbiodiniaceae symbiotic association.

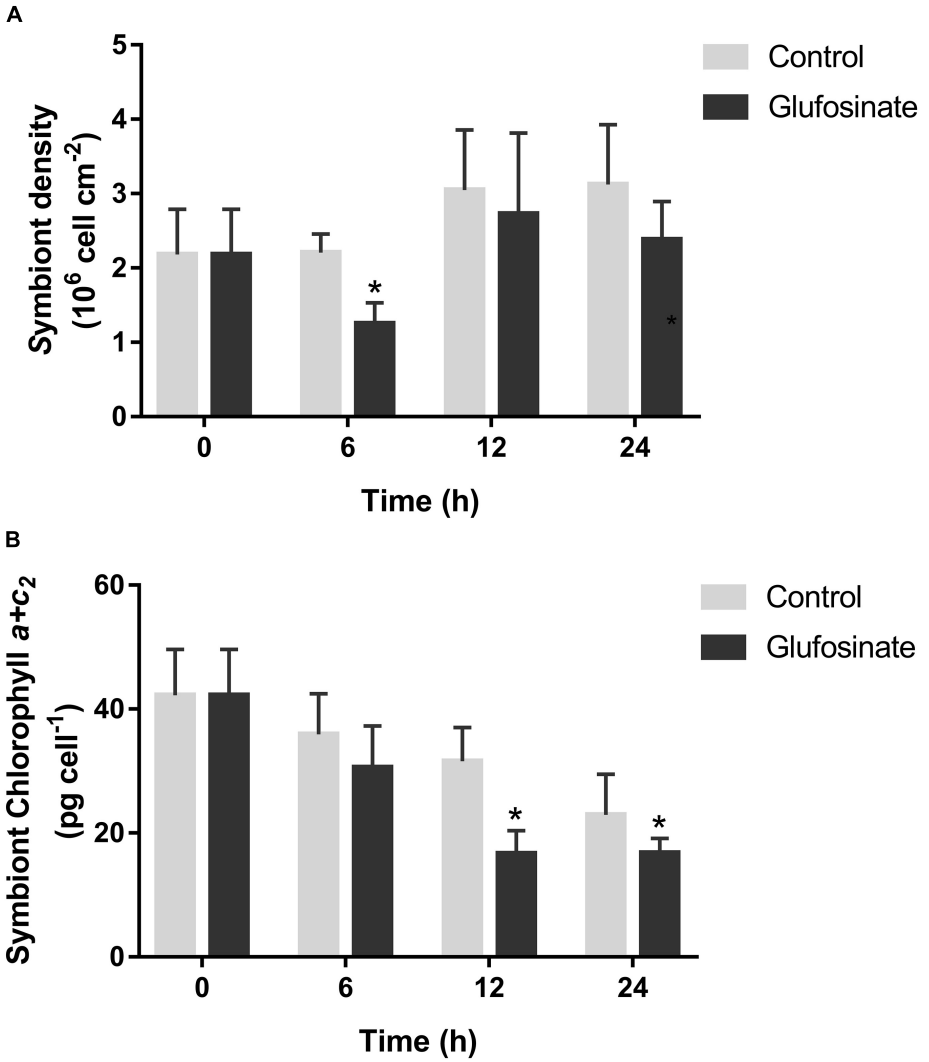

FIGURE 4 | Temporal symbiont density **(A)** and chlorophyll content **(B)** in the scleractinian coral *Pocillopora damicornis* after glufosinate treatment. Data points represent means and error bars represent standard deviations ($N = 6$). Asterisks depict significant differences between the glufosinate and control groups ($p < 0.05$).

In the present study, we found that the activities of GS, GDH, and GOGAT in the coral host *P. damicornis* all increased significantly under high temperature, along with the decrease of symbiont density and chlorophyll content. Furthermore, the treatment of glufosinate (GS inhibitor) under high temperature also caused the decline of density and chlorophyll content in the symbionts and the rise of total antioxidant capacity and apoptosis level in the coral host.

We employed firstly the exposure of the scleractinian coral *P. damicornis* to high temperature to simulate its acute heat stress, and subsequently determined the density and chlorophyll content of symbiotic Symbiodiniaceae. The symbiont density and chlorophyll $a + c_2$ content decreased significantly at 24 and 36 h after the exposure to high temperature, respectively. The results revealed that high temperature (32°C) induced the decline of symbiont density and chlorophyll content in the scleractinian coral *P. damicornis*. The loss of symbionts and the degradation of its photosynthetic pigments are both typical characterizations of coral bleaching (Coles and Brown, 2003), and therefore, the present results demonstrated that the heat exposure could activate the heat stress response of the symbiotic association, and therefore impair the symbiotic relationship between the coral host and symbionts. These results could also attribute to the excessive oxidative pressure in symbiotic association and subsequent D1 protein damage in symbiont chlorophyll PSII system under high temperature (Flores-Ramirez and Linan-Cabello, 2007; Weis, 2008; Lesser, 2011). However, the symbiont density reverted to the control level at 36 h after heat exposure, indicating the possible real-time regulation of heat acclimatization of the symbiotic association through the symbiont acquisition of the coral host from seawater environment and/or the propagation of symbionts in the coral's endodermal cells. It suggests that the acute heat stress induced the loss of symbionts and the degradation of

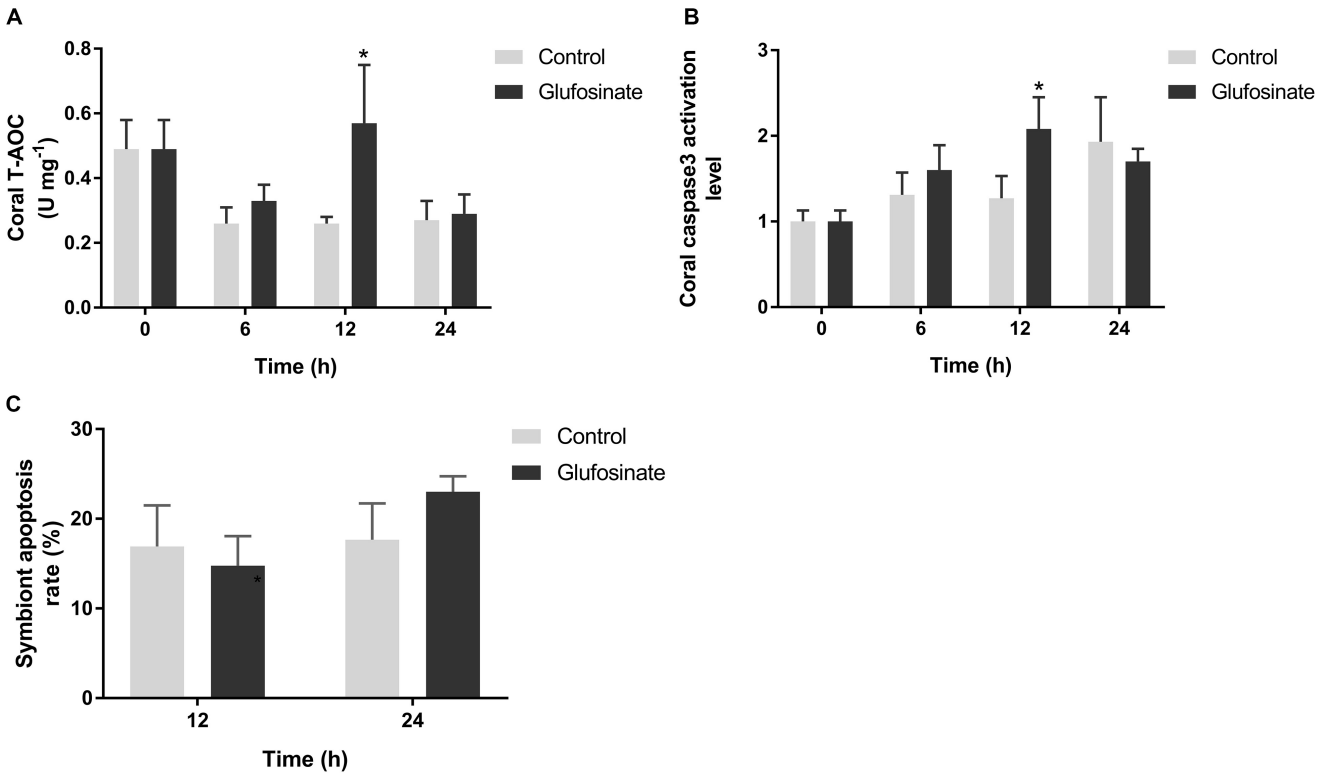

FIGURE 5 | Total antioxidant capacity (T-AOC) **(A)** and caspase3 activation level **(B)** in *Pocillopora damicornis* and symbiont apoptosis rate **(C)** after glufosinate treatment. Data points represent means and error bars represent standard deviations ($N = 6$). Asterisks depict significant differences between the glufosinate and control groups ($p < 0.05$).

its symbiont chlorophyll, and further resulted in the collapse of coral-Symbiodiniaceae symbiosis in the scleractinian coral *P. damicornis*.

To ascertain the mediation of redox system to the above symbiosis collapse, we monitored the activities of several enzymes including NOS, SOD, and CAT in the symbiotic association of *P. damicornis* after acute heat stress. The activities of NOS, SOD, and CAT in the coral host all increased significantly, while only SOD activity showed significant increase in the symbionts after heat stress. Because SOD and CAT are main antioxidases in the redox system of most organisms such as coral and Symbiodiniaceae (Levy et al., 2006), and their significant increases in the present study demonstrated that the acute heat stress induced the antioxidant capacity of the coral host and its symbionts. The rise of antioxidant capacity in the symbiotic association could result from elevated production of reactive oxygen species (ROS) owing to their heat stress response (Yakovleva et al., 2004; Levy et al., 2006; Teixeira et al., 2013). Furthermore, the significant increase of NOS activity in the coral host revealed the upregulation of nitric oxide (NO) production, which could bind with ROS to form reactive nitrogen species (RNS) with stronger oxidation ability, hinting excessive oxidative stress in the symbiotic association after heat stress. The excessive oxidative stress would activate the apoptosis of the coral host through the mediation of caspase3, damage the D1 protein in symbionts, and induce the substantial reduction of symbiont density and chlorophyll content after heat stress to trigger the collapse of coral-Symbiodiniaceae symbiosis (Lesser, 1997; Downs et al., 2002; Hawkins et al., 2014). These results might further suggest the collapse of coral-Symbiodiniaceae symbiosis in the scleractinian coral *P. damicornis*, owing to excessive oxidative pressure after heat stress.

Meanwhile, the activities of GS, GDH, and GOGAT in the two symbiotic partners were determined to understand the involvement of ammonium assimilation in their acute heat stress response. In the present study, the activities of GS, GDH and GOGAT all increased significantly in the coral host *P. damicornis*, whereas its symbiont GS and GOGAT activities did not change significantly after heat stress. The results demonstrated that heat stress induced the ability of ammonium assimilation in the coral host, not the symbionts. The induction of GS expression by heat stress was also observed in the Pacific oyster *Crassostrea gigas* (Meistertzheim et al., 2007), and similar results were reported that elevated temperature did not change significantly the expression level of GS gene in the symbiont of the scleractinian coral *P. damicornis* (Hoadley et al., 2015). Therefore, the activity rises of the three enzymes related to ammonium assimilation could also result from the upregulation of their gene expression level in the coral host. Furthermore, the rises of ammonium assimilation ability revealed

that coral host could need more inorganic nitrogen for the repair of heat damage and the acclimatization of high temperature. However, it was reported that heat stress decreased ammonium uptake of the scleractinian coral *Stylophora pistillata* (Godinot et al., 2011). Because symbiotic Symbiodiniaceae was reported to increase nitrogen availability from host coral under heat stress (Radecker et al., 2015; Cui et al., 2019), there was a contradiction among the increased nitrogen availability of symbionts, the increased ammonium assimilation ability and decreased ammonium uptake of coral host when suffering from high temperature. We speculated that the contradiction could be resolved by different expression and activity of ammonium transporter in the interface of coral/seawater and coral/symbiont interface, because ammonium transporter in thermotolerant symbiont *Durusdinium trenchii* was expressed differentially under heat stress (Bellantuono et al., 2019). However, more experimental evidences are needed to confirm the speculation and uncover the detailed mechanism in future study. Together, these results suggest that acute heat stress could induce the ability of ammonium assimilation in the coral host *P. damicornis*, which might be involved in the heat acclimation of the coral-Symbiodiniaceae symbiotic association of *P. damicornis*.

To further reveal the effect of ammonium assimilation on the coral-Symbiodiniaceae symbiosis under acute heat stress, the alteration of symbiont density and chlorophyll content were detected after the glufosinate (GS inhibitor) treatment to the scleractinian coral *P. damicornis*. The symbiont density and chlorophyll content decreased significantly after glufosinate treatment, which was earlier than that only under heat stress. It demonstrated that glufosinate treatment accelerated the collapse of coral-Symbiodiniaceae symbiosis after acute heat stress. Glufosinate is a GS inhibitor, and also functions in the scleractinian coral (Su et al., 2018). In the present study, glufosinate could repress the GS activities and corresponding ammonium assimilation ability in the coral host and symbionts, and caused inadequate acquisition of inorganic nitrogen resource for the symbiotic association and earlier collapse of the symbiosis under heat stress, which implied that available ammonium could contribute to the acclimatization of the symbiotic association to heat stress. This was also manifested in some observation that ammonium availability could reduce the negative effect of heat stress on scleractinian corals (Beraud et al., 2013; Zhou et al., 2017; Fernandes de Barros Marangoni et al., 2020). However, the significant decline of symbiont density was only observed at 6 h after the treatment, which could result from the compensation effect of GDH pathway in the coral host. We will explore the compensation effect and regulation mechanism in our further studies. To further understand the potential effect of ammonium assimilation under heat stress, we determined the total antioxidant capacity and caspase3 activation level in the coral host and symbiont apoptosis rate after glufosinate treatment. The total antioxidant capacity and caspase3 activation level of the coral host increased significantly, while symbiont apoptosis did not change significantly. It revealed that the repression of ammonium assimilation could facilitate the collapse of the coral-Symbiodiniaceae symbiosis through the induction of excessive oxidative pressure and apoptosis in the coral host after heat stress. All results imply that ammonium assimilation might be involved in the response and acclimatization of the coral-Symbiodiniaceae symbiosis to high temperature, and the effect of high temperate on scleractinian coral might depend on the nitrogen nutrient status of its symbiotic association.

DATA AVAILABILITY STATEMENT

The raw data supporting the conclusions of this article will be made available by the authors, without undue reservation.

ETHICS STATEMENT

All animal-involving experiments of this study were approved by the Ethics Committee of Hainan University and local government.

AUTHOR CONTRIBUTIONS

JT and ZZ conceived and designed the experiments. JT, XN, and JW performed the experiments. JT and ZZ analyzed the data. LW and JL contributed to the reagents, materials, and analysis tools. JT and ZZ contributed to the discussion and wrote the manuscript. All authors read and approved the final manuscript.

FUNDING

This research was supported by the National Key R&D Program of China (Grant 2018YFC1406504), the National Natural Science Foundation of China (Grants 31772460 and 42076145), the Major Science and Technology Program (ZDKJ2019011), and Natural Science Foundation of Hainan Province (2019RC067).

ACKNOWLEDGMENTS

The authors were grateful to all of the laboratory members for their continuous technical advice and helpful discussions.

REFERENCES

Bellantuono, A. J., Dougan, K. E., Granados-Cifuentes, C., and Rodriguez-Lanetty, M. (2019). Free-living and symbiotic lifestyles of a thermotolerant coral endosymbiont display profoundly distinct transcriptomes under both stable and heat stress conditions. *Mol. Ecol.* 28, 5265–5281. doi: 10.1111/mec.15300

Beraud, E., Gevaert, F., Rottier, C., and Ferrier-Pages, C. (2013). The response of the scleractinian coral Turbinaria reniformis to thermal stress depends on the nitrogen status of the coral holobiont. *J. Exp. Biol.* 216, 2665–2674. doi: 10.1242/jeb.085183

Coles, S. L., and Brown, B. E. (2003). Coral bleaching–capacity for acclimatization and adaptation. *Adv. Mar. Biol.* 46, 183–223. doi: 10.1016/s0065-2881(03)46004-5

Cui, G., Liew, Y. J., Li, Y., Kharbatia, N., Zahran, N. I., Emwas, A. H., et al. (2019). Host-dependent nitrogen recycling as a mechanism of symbiont control in Aiptasia. *PLoS Genet.* 15:e1008189. doi: 10.1371/journal.pgen.1008189

Downs, C. A., Fauth, J. E., Halas, J. C., Dustan, P., Bemiss, J., and Woodley, C. M. (2002). Oxidative stress and seasonal coral bleaching. *Free Radic. Biol. Med.* 33, 533–543. doi: 10.1016/s0891-5849(02)00907-3

Dubinsky, Z., and Jokiel, P. L. (1994). Ratio of energy and nutrient fluxes regulates symbiosis between zooxanthellae and corals. *Pacific Sci.* 48, 313–324.

Fernandes de Barros Marangoni, L., Ferrier-Pages, C., Rottier, C., Bianchini, A., and Grover, R. (2020). Unravelling the different causes of nitrate and ammonium effects on coral bleaching. *Sci. Rep.* 10:11975.

Flores-Ramirez, L. A., and Linan-Cabello, M. A. (2007). Relationships among thermal stress, bleaching and oxidative damage in the hermatypic coral, Pocillopora capitata. *Comp. Biochem. Physiol. C. Toxicol Pharmacol* 146, 194–202. doi: 10.1016/j.cbpc.2006.09.008

Godinot, C., Houlbreque, F., Grover, R., and Ferrier-Pages, C. (2011). Coral uptake of inorganic phosphorus and nitrogen negatively affected by simultaneous changes in temperature and pH. *PLoS One* 6:e25024. doi: 10.1371/journal.pone.0025024

Hawkins, T. D., Krueger, T., Becker, S., Fisher, P. L., and Davy, S. K. (2014). Differential nitric oxide synthesis and host apoptotic events correlate with bleaching susceptibility in reef corals. *Coral Reefs* 33, 141–153. doi: 10.1007/s00338-013-1103-4

Hedouin, L. S., Wolf, R. E., Phillips, J., and Gates, R. D. (2016). Improving the ecological relevance of toxicity tests on scleractinian corals: influence of season, life stage, and seawater temperature. *Environ. Pollut.* 213, 240–253. doi: 10.1016/j.envpol.2016.01.086

Higuchi, T., Fujimura, H., Arakaki, T., and Oomori, T. (2008). "Activities of antioxidant enzymes (SOD and CAT) in the coral *Galaxea fascicularis* against increased hydrogen peroxide concentrations in seawater," in *Proceeding of the 11th International Coral Reef Symposium*, Ft. Lauderdale, FLA.

Higuchi, T., Yuyama, I., and Nakamura, T. (2015). The combined effects of nitrate with high temperature and high light intensity on coral bleaching and antioxidant enzyme activities. *Reg. Stud. Mar. Sci.* 2, 27–31. doi: 10.1016/j.rsma.2015.08.012

Hoadley, K. D., Pettay, D. T., Grottoli, A. G., Cai, W. J., Melman, T. F., Schoepf, V., et al. (2015). Physiological response to elevated temperature and pCO2 varies across four Pacific coral species: understanding the unique host+symbiont response. *Sci. Rep.* 5:18371.

Hughes, T. P., Kerry, J. T., Alvarez-Noriega, M., Alvarez-Romero, J. G., Anderson, K. D., and Baird, A. H. (2017). Global warming and recurrent mass bleaching of corals. *Nature* 543, 373–377.

Jeffrey, S. W., and Humphrey, G. F. (1975). New spectrophotometric equations for determining chlorophylls a, b, c1 and c2 in higher plants, algae and natural phytoplankton. *Biochem. Physiol. Pflanzen* 167, 191–194. doi: 10.1016/s0015-3796(17)30778-3

Johannes, R. E., Coles, S. L., and Kuenzel, N. T. (1970). The role of zooplankton in the nutrition of some scleractinian Corals1. *Limnol. Oceanogr.* 15, 579–586. doi: 10.4319/lo.1970.15.4.0579

Lesser, M. P. (1997). Oxidative stress causes coral bleaching during exposure to elevated temperatures. *Coral Reefs* 16, 187–192. doi: 10.1007/s003380050073

Lesser, M. P. (2011). "Coral bleaching: causes and mechanisms," in *Coral Reefs: An Ecosystem in Transition*, eds Z. Dubinsky and N. Stambler (Dordrecht: Springer Netherlands), 405–419. doi: 10.1007/978-94-007-0114-4_23

Levy, O., Achituv, Y., Yacobi, Y. Z., Stambler, N., and Dubinsky, Z. (2006). The impact of spectral composition and light periodicity on the activity of two antioxidant enzymes (SOD and CAT) in the coral Favia favus. *J. Exp. Mar. Biol. Ecol.* 328, 35–46. doi: 10.1016/j.jembe.2005.06.018

Liu, H., Stephens, T. G., Gonzalez-Pech, R. A., Beltran, V. H., Lapeyre, B., Bongaerts, P., et al. (2018). Symbiodinium genomes reveal adaptive evolution of functions related to coral-dinoflagellate symbiosis. *Commun. Biol.* 1:95.

Meistertzheim, A. L., Tanguy, A., Moraga, D., and Thebault, M. T. (2007). Identification of differentially expressed genes of the Pacific oyster *Crassostrea gigas* exposed to prolonged thermal stress. *FEBS J.* 274, 6392–6402. doi: 10.1111/j.1742-4658.2007.06156.x

Morris, L. A., Voolstra, C. R., Quigley, K. M., Bourne, D. G., and Bay, L. K. (2019). Nutrient availability and metabolism affect the stability of coral-symbiodiniaceae symbioses. *Trends Microbiol.* 27, 678–689. doi: 10.1016/j.tim.2019.03.004

Muscatine, L., and Porter, J. W. (1977). Reef corals: mutualistic symbioses adapted to nutrient-poor environments. *BioScience* 27, 454–460. doi: 10.2307/1297526

Peng, S. E., Chen, C. S., Song, Y. F., Huang, H. T., Jiang, P. L., Chen, W. N., et al. (2012). Assessment of metabolic modulation in free-living versus endosymbiotic Symbiodinium using synchrotron radiation-based infrared microspectroscopy. *Biol. Lett.* 8, 434–437. doi: 10.1098/rsbl.2011.0893

Pernice, M., Dunn, S. R., Miard, T., Dufour, S., Dove, S., and Hoegh-Guldberg, O. (2011). Regulation of apoptotic mediators reveals dynamic responses to thermal stress in the reef building coral *Acropora millepora*. *PLoS One* 6:e16095. doi: 10.1371/journal.pone.0016095

Pernice, M., Meibom, A., Van Den Heuvel, A., Kopp, C., Domart-Coulon, I., Hoegh-Guldberg, O., et al. (2012). A single-cell view of ammonium assimilation in coral-dinoflagellate symbiosis. *ISME J.* 6, 1314–1324. doi: 10.1038/ismej.2011.196

Plaisance, L., Caley, M. J., Brainard, R. E., and Knowlton, N. (2011). The diversity of coral reefs: what are we missing? *PLoS One* 6:e25026. doi: 10.1371/journal.pone.0025026

Radecker, N., Pogoreutz, C., Voolstra, C. R., Wiedenmann, J., and Wild, C. (2015). Nitrogen cycling in corals: the key to understanding holobiont functioning? *Trends Microbiol.* 23, 490–497. doi: 10.1016/j.tim.2015.03.008

Roberty, S., Beraud, E., Grover, R., and Ferrier-Pages, C. (2020). Coral productivity is Co-limited by bicarbonate and ammonium availability. *Microorganisms* 8:640. doi: 10.3390/microorganisms8050640

Roberty, S., Fransolet, D., Cardol, P., Plumier, J. C., and Franck, F. (2015). Imbalance between oxygen photoreduction and antioxidant capacities in Symbiodinium cells exposed to combined heat and high light stress. *Coral Reefs* 34, 1063–1073. doi: 10.1007/s00338-015-1328-5

Shinzato, C., Shoguchi, E., Kawashima, T., Hamada, M., Hisata, K., Tanaka, M., et al. (2011). Using the *Acropora digitifera* genome to understand coral responses to environmental change. *Nature* 476, 320–323. doi: 10.1038/nature10249

Su, Y., Zhou, Z., and Yu, X. (2018). Possible roles of glutamine synthetase in responding to environmental changes in a scleractinian coral. *Mol. Biol. Rep.* 45, 2115–2124. doi: 10.1007/s11033-018-4369-3

Teixeira, T., Diniz, M., Calado, R., and Rosa, R. (2013). Coral physiological adaptations to air exposure: heat shock and oxidative stress responses in *Veretillum cynomorium*. *J. Exp. Mar. Biol. Ecol.* 439, 35–41. doi: 10.1016/j.jembe.2012.10.010

Vidal-Dupiol, J., Ladriere, O., Destoumieux-Garzon, D., Sautiere, P. E., Meistertzheim, A. L., Tambutte, E., et al. (2011). Innate immune responses of a scleractinian coral to vibriosis. *J. Biol. Chem.* 286, 22688–22698. doi: 10.1074/jbc.m110.216358

Wall, C. B., Kaluhiokalani, M., Popp, B. N., Donahue, M. J., and Gates, R. D. (2020). Divergent symbiont communities determine the physiology and nutrition of a reef coral across a light-availability gradient. *ISME J.* 14, 945–958. doi: 10.1038/s41396-019-0570-1

Wein, T., Romero Picazo, D., Blow, F., Woehle, C., Jami, E., Reusch, T. B. H., et al. (2019). Currency, exchange, and inheritance in the evolution of symbiosis. *Trends Microbiol.* 27, 836–849. doi: 10.1016/j.tim.2019.05.010

Weis, V. M. (2008). Cellular mechanisms of Cnidarian bleaching: stress causes the collapse of symbiosis. *J. Exp. Biol.* 211, 3059–3066. doi: 10.1242/jeb.009597

Wooldridge, S. A. (2013). Breakdown of the coral-algae symbiosis: towards formalising a linkage between warm-water bleaching thresholds and the growth rate of the intracellular zooxanthellae. *Biogeosciences* 10, 1647–1658. doi: 10.5194/bg-10-1647-2013

Xiang, T., Lehnert, E., Jinkerson, R. E., Clowez, S., Kim, R. G., Denofrio, J. C., et al. (2020). Symbiont population control by host-symbiont metabolic interaction in Symbiodiniaceae-cnidarian associations. *Nat. Commun.* 11:108.

Yakovleva, I., Bhagooli, R., Takemura, A., and Hidaka, M. (2004). Differential susceptibility to oxidative stress of two scleractinian corals: antioxidant

functioning of mycosporine-glycine. *Comp. Biochem. Physiol. B. Biochem. Mol. Biol* 139, 721–730. doi: 10.1016/j.cbpc.2004.08.016

Zhou, Z., Zhang, G., Chen, G., Ni, X., Guo, L., Yu, X., et al. (2017). Elevated ammonium reduces the negative effect of heat stress on the stony coral *Pocillopora damicornis*. *Mar. Pollut. Bull.* 118, 319–327. doi: 10.1016/j.marpolbul.2017.03.018

Zhou, Z., Zhao, S., Ni, J., Su, Y., Wang, L., and Xu, Y. (2018). Effects of environmental factors on C-type lectin recognition to zooxanthellae in the stony coral *Pocillopora damicornis*. *Fish Shellfish Immunol.* 79, 228–233. doi: 10.1016/j.fsi.2018.05.026

Conflict of Interest: The authors declare that the research was conducted in the absence of any commercial or financial relationships that could be construed as a potential conflict of interest.

frontiers in Physiology

ORIGINAL RESEARCH
published: 19 November 2020
doi: 10.3389/fphys.2020.574654

Transcriptome Reprogramming of Symbiodiniaceae *Breviolum minutum* in Response to Casein Amino Acids Supplementation

Andrea L. Kirk[1†], Sophie Clowez[2†], Fan Lin[3], Arthur R. Grossman[2] and Tingting Xiang[1]*

[1] Department of Biological Sciences, The University of North Carolina at Charlotte, Charlotte, NC, United States, [2] Department of Plant Biology, Carnegie Institution for Science, Stanford, CA, United States, [3] Brightseed Inc., San Francisco, CA, United States

Dinoflagellates in the family Symbiodiniaceae can live freely in ocean waters or form a symbiosis with a variety of cnidarians including corals, sea anemones, and jellyfish. Trophic plasticity of Symbiodiniaceae is critical to its ecological success as it moves between environments. However, the molecular mechanisms underlying these trophic shifts in Symbiodiniaceae are still largely unknown. Using *Breviolum minutum* strain SSB01 (designated SSB01) as a model, we showed that Symbiodiniaceae go through a physiological and transcriptome reprogramming when the alga is grown with the organic nitrogen containing nutrients in hydrolyzed casein, but not with inorganic nutrients. SSB01 grows at a much faster rate and maintains stable photosynthetic efficiency when supplemented with casein amino acids compared to only inorganic nutrients or seawater. These physiological changes are driven by massive transcriptome changes in SSB01 supplemented with casein amino acids. The levels of transcripts encoding proteins involved in altering DNA conformation such as DNA topoisomerases, histones, and chromosome structural components were all significantly changed. Functional enrichment analysis also revealed processes involved in translation, ion transport, generation of second messengers, and phosphorylation. The physiological and molecular changes that underlie *in vitro* trophic transitions in Symbiodiniaceae can serve as an orthogonal platform to further understand the factors that impact the Symbiodiniaceae lifestyle.

Keywords: transcriptomics, topoisomerase, histone, DNA conformation, transport, phosphorylation, Symbiodiniaceae, symbiosis

OPEN ACCESS

Edited by:
Kefu Yu,
Guangxi University, China

Reviewed by:
Jiayuan Liang,
Guangxi University, China
Yanjie Zhang,
Hong Kong Baptist University, Hong Kong

***Correspondence:**
Tingting Xiang
txiang@uncc.edu

† These authors have contributed equally to this work

Specialty section:
This article was submitted to Aquatic Physiology, a section of the journal Frontiers in Physiology

Received: *20 June 2020*
Accepted: *18 September 2020*
Published: *19 November 2020*

Citation:
Kirk AL, Clowez S, Lin F, Grossman AR and Xiang T (2020) Transcriptome Reprogramming of Symbiodiniaceae Breviolum minutum in Response to Casein Amino Acids Supplementation. Front. Physiol. 11:574654. doi: 10.3389/fphys.2020.574654

INTRODUCTION

Endosymbiotic dinoflagellates from the family Symbiodiniaceae enter symbiosis with cnidarians, which include corals, sea anemones, and jellyfish (Davy et al., 2012; Fransolet et al., 2012; Bucher et al., 2016); this association is fundamental to the survival of coral-reef ecosystems. Cnidarian hosts benefit from the photosynthetically fixed carbon received from the alga (Muscatine and Porter, 1977; Burriesci et al., 2012), utilizing it to meet its energy requirements and enhance calcification rates (Pearse and Muscatine, 1971). The endosymbiotic alga gains access to inorganic nutrients

from the host, establishes a stable location in the water column, and is protected from grazers (Davy et al., 2012). The breakdown of the symbiotic relationship between corals and its endosymbiotic alga, or "coral bleaching," occurs under stress conditions, including elevated temperature and pollution of reef habitats (Hoegh-Guldberg, 1999; Weis and Allemand, 2009). Coral bleaching plays a major role in the global decline of reef communities (Hughes et al., 2017), and yet we still know little about the molecular mechanisms that govern the establishment, maintenance and breakdown of the symbiotic association (Davy et al., 2012).

Symbiodiniaceae and corals often must acclimate to diverse environments with different availabilities of nutrients (Leal et al., 2015; Fox et al., 2019; Morris et al., 2019; Conti-Jerpe et al., 2020). The trophic flexibility of the Symbiodiniaceae algae is essential for survival during both free-living and intracellular growth, especially when environmental conditions challenge growth and physiological processes in both the animal and alga (Xiang et al., 2018; Morris et al., 2019). Free-living Symbiodiniaceae in the ocean have been shown to directly take up nutrients from their surroundings (D'Elia et al., 1983; Brading et al., 2013), although the waters around coral reefs are typically oligotrophic (low-nutrient) (Cook and D'elia, 1987). Recent work has shown that some Symbiodiniaceae algae can thrive under different trophic conditions; autotrophy, heterotrophy, and mixotrophy (Xiang et al., 2013, 2018). For instance, two Symbiodiniaceae algae, both formerly considered clade E (classifications have recently been updated), that were cultured from environmental samples and from the tissues of the coral *Alveopora japonica*, were able to survive through the acquisition of fixed carbon by heterotrophic feeding (Jeong et al., 2012). Low levels of nutrients, such as nitrogen (N), arrest cell division and elicit transcriptional and physiological responses that help the organism cope with the limited nutrient availability (Dagenais-Bellefeuille and Morse, 2013; Jiang et al., 2014; Li et al., 2020; Xiang et al., 2020), while excess inorganic N could impair processes in the alga and host and weaken the symbiotic association (Morris et al., 2019).

We previously reported that the Symbiodiniaceae alga *Breviolum minutum* strain SSB01 (designated SSB01 throughout), formerly placed in clade B (Lajeunesse et al., 2012; Xiang et al., 2013; Lajeunesse et al., 2018), grew rapidly under mixotrophic conditions (minimal medium supplemented with organic nutrients in the light), with slower growth in the absence of organic nutrients (Xiang et al., 2013). SSB01 is one of the well-studied species with available genome and transcriptome resources (Shoguchi et al., 2013; Xiang et al., 2015; Parkinson et al., 2016). It readily forms symbiosis with cnidarian hosts (Xiang et al., 2013; Hambleton et al., 2014; Maor-Landaw et al., 2020) and has been shown to grow under various trophic conditions (Xiang et al., 2013, 2018). This ability to accommodate different nutrient resources (organic and inorganic) affords the alga trophic flexibility within its host where nutrient conditions may fluctuate (Xiang et al., 2013); for example, the dynamic changes in nutrient availability may reflect both the level of various nutrients in the environment and changes in the density of the algal population within the host tissue (Xiang et al., 2020). The cnidarian host may also feed and transport ingested organic nutrients, such as amino acids, lipids and fatty acids to the endosymbiont, potentially creating a mixotrophic interaction for the algae (Steen, 1986; Wang and Douglas, 1999; Imbs et al., 2014). However, the physiological responses and molecular mechanisms that guide metabolic acclimation to changes in the types and levels of available nutrients are not well understood.

In this study, to explore the physiological and molecular mechanisms that underlie trophic shifts in the Symbiodiniaceae, we analyzed the physiology and transcriptome profiles of axenic SSB01 cultured under various nutrient conditions: Artificial Sea Water (ASW), ASW supplemented with inorganic nutrients (IMK), and IMK supplemented with casein amino acids (CAS), which contains a variety of organic nutrients. Inclusion of CAS in IMK improved growth, allowed sustained photosynthetic function, and caused extensive transcriptome changes relative to cells maintained in either ASW or IMK media. Furthermore, there were only minor changes in the transcriptome of the algae grown in IMK compared to ASW. An understanding of the physiological and molecular features that underlie trophic transitions in the Symbiodiniaceae can provide insights into trophic changes associated with the growth of Symbiodiniaceae algae within their cnidarian hosts and help establish more general "rules" that govern symbiotic associations.

MATERIALS AND METHODS

Strain and Growth Conditions

The clonal, axenic Symbiodiniaceae *B. minutum* (formerly *Symbiodinium minutum*) strain SSB01 (Xiang et al., 2013) was used throughout this study. Liquid cultures of SSB01 were grown either in ASW, ASW supplemented with 0.252 g L^{-1} of Daigo's IMK medium for marine microalgae (Wako Pure Chemicals, Osaka, Japan) as recommended in the manufacturer's instructions (IMK medium), or in IMK medium supplemented with 4 gL^{-1} casein hydrolysate (CAS; Affymetrix USB) (Xiang et al., 2013). Cultures were maintained at 27°C on a 12 h-light/12 h-dark cycle with an irradiance of ∼10 μmol photons m^{-2} s^{-1} provided by Philips ALTO II 25-W bulbs. To assess the effects of different nutrients on SSB01, approximately 2×10^7 SSB01 cells from an IMK culture in log growth were collected by centrifugation at 100 *g* for 5 min in an Eppendorf 5810R centrifuge at room temperature. Cells were washed once with 50 mL autoclave-sterilized ASW and resuspended in 50 mL of either ASW medium, IMK medium or IMK + CAS medium in 250-mL flasks. For the recovery experiments, SSB01 cells were grown in ASW for 20 days. On day 20, the cells were pelleted by centrifugation at 100 *g* for 5 min at room temperature (RT) in an Eppendorf 5810R centrifuge and then resuspended in IMK + CAS and allowed to grow for an additional 20 days.

Analysis of Photosynthetic Function

The cultures were prepared as described in Xiang et al. (2018, 2020) for measuring photosynthetic function. Maximum quantum yields of photosystem II (PSII) (calculated as $F_v/F_m = (F_m - F_0)/F_m$) were determined for cell cultures

using a JTS-10 spectrophotometer (Bio-Logic) (Joliot and Delosme, 1974) after ∼10 min of dark adaptation.

Growth Studies

SSB01 stock cultures were grown in IMK medium at 27°C on a 12 h-light/12 h-dark cycle with an irradiance of ∼10 μmol photons m^{-2} s^{-1}. Approximately 6 × 10^6 cells in log phase growth were pelleted by centrifugation at 100 *g* for 5 min at RT. Cells were washed twice with 20 mL sterile ASW medium, and resuspended in 30 mL of liquid ASW, IMK, or IMK + CAS media. SSB01 cells were quantified using a Countess™ II Automated Cell Counter following the manufacturer's instructions. Three biological replicates were performed for the growth experiments; they all yielded similar results.

RNA-Seq Analyses

Cultured SSB01 cells grown in different nutrient conditions were prepared as described in "growth studies" (above). Approximately 5 × 10^7 mid-log phase SSB01 cells grown in ASW, IMK, and IMK + CAS were collected by centrifugation and extracted with phenol/chloroform to prepare total RNA (Xiang et al., 2015; Xiang, 2018). RNA was prepared from three biological replicates for cells grown in IMK and IMK + CAS, and two biological replicates for cells grown in ASW. ASW cultures were transferred from IMK precultures and allowed to grow for 2 weeks before proceeding to RNA extraction. Approximately 1 μg of total RNA from each sample was used to construct libraries with the TruSeq RNA Sample Prep Kit (Illumina FC-122–1001) following the manufacturer's instructions. The resulting libraries were sequenced on an Illumina HiSeq 2000 sequencer (2 × 101 bp) at the Stanford Center for Genomics and Personalized Medicine. All raw sequencing reads are available in the Sequence Read Archive[1] with SRA accession numbers SRS5754975 (CAS samples) in the BioProject PRJNA591730 (Xiang et al., 2020), and SRS6837549 (IMK samples) and SRS6837550 (ASW samples) in the BioProject PRJNA639352. RNA-seq reads for populating symbiotic SSB01 samples (that were populating *Aiptasia* for 12 days and 30 days) were obtained from SRA, Project PRJNA261862 (Baumgarten et al., 2015). Differential expression analysis was performed as previously described (Xiang et al., 2020). Briefly, RNA-seq raw reads of each SSB01 sample grown in ASW, IMK, or CAS were aligned to the SSB01 transcriptome assembly Symb6 that we established previously (Xiang et al., 2015) [deposited at SRA, Project PRJNA591070[2] using BWA (Li and Durbin, 2009)]. The number of reads aligned to transcripts with a cutoff mapping quality score of 30 was counted using SAMtools. Differential expression from different nutrient conditions was further analyzed using the DESeq2 Bioconductor package (Love et al., 2014), with the transcripts comparing IMK vs. ASW, and IMK + CAS vs. ASW. Expression levels were analyzed as transcripts per kilobase million (TPM) (Wagner et al., 2012). Differential expression of transcripts was called based on the cutoff of a false-discovery rate (Benjamini-Hochberg method) adjusted *p*-value of ≤0.001. GO-term enrichment was analyzed using the BiNGO plugin for Cytoscape (Maere et al., 2005).

Amino Acid-Sequence Alignment

Amino acid sequence alignments for topoisomerases in SSB01 was conducted using MUSCLE (Edgar, 2004). 11 topoisomerase protein sequences predicted in symb6 and a total of 17 topoisomerase protein sequences from Arabidopsis (*Arabidopsis thaliana*; TOP1A, TOP1B, TOP2, TOP3A, TOP3B, TOP6A, TOP6B, TOP6BL, and GYRA), yeast (*Saccharomyces cerevisiae*, TOP1, TOP2, and TOP3), and human (*Homo sapiens*, TOP1, TOP2A, TOP2B, TOP3A, and TOP3B) were aligned. Protein sequences from the model systems were retrieved from the UniProt database with identifier IDs shown in **Supplementary Table S1**. The phylogenetic tree was constructed using the neighbor-joining method of Geneious tree builder in Geneious 9.1[3].

RESULTS AND DISCUSSION

IMK + CAS Medium Allows Faster Growth and Sustains Photosynthetic Function

To assess the impacts of inorganic and organic nutrients on the physiology of SSB01, we grew the cells in three different media with different nutrient compositions: (1) ASW; (2) IMK, which includes nitrate and ammonium; and (3) IMK + CAS. SSB01 cells were transferred from IMK medium to ASW, IMK, and IMK + CAS, respectively, and the growth characteristics and measurements of maximum quantum efficiency of PSII (F_v/F_m) were monitored.

Growth of SSB01 was significantly more rapid in IMK + CAS (*p*-value is 3.05E-05 based on two-sided *t*-test) and cells were able to reach much higher densities compared to ASW (during the 20 days of growth), while the difference between growth rates in IMK and ASW was small (*p*-value is 0.06 based on two-sided *t*-test) (**Figure 1**). The F_v/F_m remained stable over a growth period of 30 days in IMK + CAS but exhibited a significant decrease when the cells were grown in ASW (*p*-value = 0.004, two-sided *t*-test) or IMK (*p*-value = 0.006, two-sided *t*-test) for the same period of time (**Figure 2**). Interestingly, the decline in F_v/F_m was fully reversed in 2 days following supplementation of ASW-grown SSB01 cells with CAS; it remained stable for the additional 20 days of the experiment (**Figure 3**).

Extensive Transcriptome Changes in Response to IMK + CAS

To determine the changes in gene expression potentially associated with the physiological observations and to gain new insights into the acclimation of the cells to different trophic conditions, RNA-Seq was conducted for SSB01 grown

[1]http://www.ncbi.nlm.nih.gov/sra

[2]https://www.ncbi.nlm.nih.gov/bioproject/PRJNA591070

[3]https://www.geneious.com

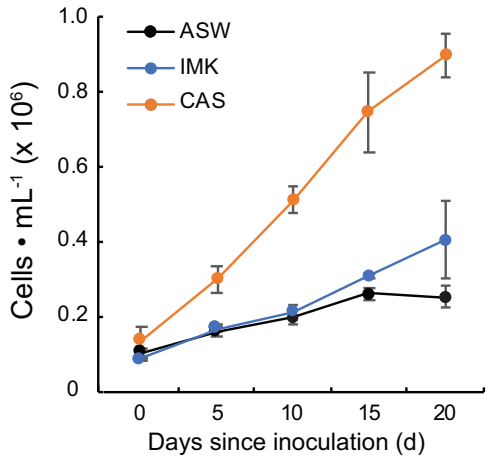

FIGURE 1 | Growth of SSB01 cells in ASW, IMK, and IMK + CAS. Growth of SSB01 was assessed in ASW (black line), IMK (blue line), and IMK + CAS (CAS, orange line) medium for 20 days. Error bars show standard errors derived from three replicate experiments.

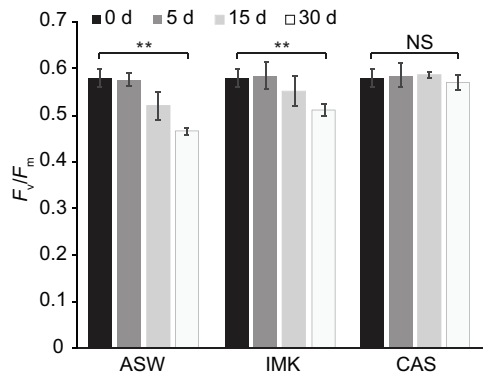

FIGURE 2 | Stability of PSII efficiency for SSB01 cells grown in ASW, IMK, and IMK + CAS (CAS). The F_v/F_m was measured (see "Materials and Methods") at 0, 5, 15, and 30 days when SSB01 cells were grown in ASW, IMK, and IMK + CAS, respectively. *p*-values (two sided *t*-test) for the significance of the 0 vs. 30 days differences are indicated (**p-value < 0.01, NS, not significant).

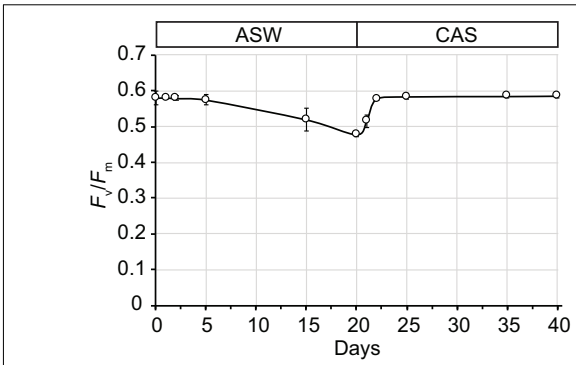

FIGURE 3 | Recovery of F_v/F_m after transfer of ASW-grown SSB01 cells to IMK + CAS medium (CAS). Cells were grown in seawater for 20 days and then transferred to IMK + CAS medium; the F_v/F_m was measured for cells before and after the transfer. Error bars show standard errors derived from three replicate experiments.

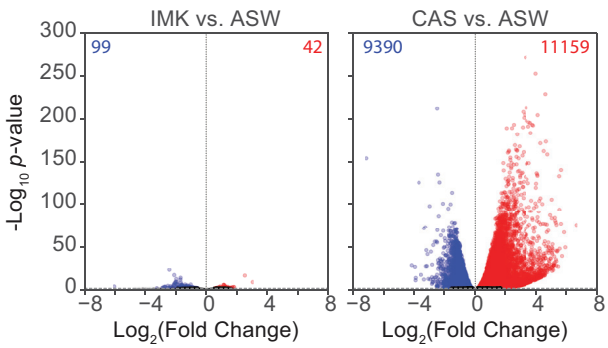

FIGURE 4 | Expression in SSB01 in IMK + CAS or IMK compared to ASW. Volcano plot of relative abundances of individual transcripts in IMK vs. ASW and IMK + CAS vs. ASW. *x*-axis, fold-changes; *y*-axis, adjusted *p*-values based on Benjamini-Hochberg correction; red dots indicate transcripts more abundant in IMK (left) or in IMK + CAS (right). Blue dots indicate transcripts more abundant in ASW. Both axes use log scales. The horizontal line indicates adjusted *p*-values = 0.001, the cutoff used for considering differences to be significant.

in ASW, IMK, and IMK + CAS, with comparisons of transcript abundances of IMK + CAS relative to ASW, and IMK relative to ASW. Based on a cutoff of adjusted *p*-values (based on Benjamini-Hochberg correction) ≤0.001, we identified 20,549 transcripts (approximately 34.4%) that were differentially expressed when comparing cells grown in IMK + CAS relative to ASW (**Figure 4**). In contrast, only 141 transcripts (approximately 0.2%) were scored as differentially expressed when comparing SSB01 cells grown in IMK relative to ASW (**Figure 4**).

We applied a Gene Ontology (GO) enrichment analysis and further analyzed the functional categories of the differentially expressed genes. GO terms for the proteins encoded by the transcripts enriched in IMK + CAS relative to ASW were represented by a wide variety of processes including "translation," "DNA conformation change" ("DNA topological change" in particular), "ion transport," cytoskeleton such as "microtubule-based movement," "phosphorylation" (mostly "protein amino acid phosphorylation"), "oxygen transport" which is fundamental to aerobic respiration, "nucleotide biosynthetic process," "cyclic nucleotide biosynthetic process," "signaling pathway," "neuropeptide signaling pathway," and "cellular glucan metabolic process." By contrast, few GO terms were enriched for the proteins encoded by transcripts expressed in IMK relative to ASW, but those terms that were slightly enriched include "generation of precursor metabolites and energy," "purine transport," and "meiosis" (**Figure 5**).

CAS May Modulate Translation and Protein Synthesis

The greatest number of genes that showed differential regulation in IMK + CAS relative to ASW medium encode proteins

associated with translation. The transcript (s6_33548) encoding the General Control Non-derepressible 2 (GCN2) exhibited an ∼18-fold increase in IMK + CAS. GCN2 is a serine/threonine-protein kinase that acts as an amino acid sensor in *S. cerevisiae* and can affect expression of genes encoding enzymes involved in amino acid synthesis (Castilho et al., 2014). Symbiodiniaceae GCN2 may perform similar functions in amino-acid sensing. Interestingly, the expression levels of *GCN2* in symbiotic SSB01 increased gradually when the algal symbiont population increased (**Supplementary Figure S1**). This data suggests that sensing and controlling the biosynthesis of amino acids in the symbiont may be integral to host-symbiont interactions as the symbiont populates the host.

Elongation factor thermo unstable (EF-Tu) is an essential component of translation that places the aminoacyl-tRNA complex at the A-site of the ribosome (Rodnina et al., 2005). The transcript encoding EF-Tu (s6_1943) increased in abundance by more than 3-fold in IMK + CAS. The transcript encoding valine tRNA ligase also showed a >2-fold change in abundance. In addition, expression of 15 transcripts involved in translation initiation were significantly changed in IMK + CAS. For example, the abundance of the transcript (s6_51857) encoding the eukaryotic translation initiation factor 3 subunit B protein (eIF-3B) increased by almost 3-fold in IMK + CAS. This translation initiation factor is an RNA-binding component of the eukaryotic translation initiation factor 3 (eIF-3) complex, which specifically initiates translation of a subset of mRNAs involved in cell proliferation (Lee et al., 2015). In contrast, the level of the transcript (s6_38195) encoding translation initiation factor 5A decreased by almost 3 fold in IMK + CAS (**Supplementary Table S3**). This translation initiation factor was recently reported to be involved in polypeptide elongation rather than initiation (Gregio et al., 2009; Saini et al., 2009) and was shown to stimulate protein synthesis in *S. cerevisiae* (Henderson and Hershey, 2011). The precise meaning of these results is unclear, although measuring the intracellular levels of amino acids in both ASW and IMK + CAS grown cells may provide insights into potential feedback signals that might be involved in modulating protein homeostasis through the controlled expression of genes related to translation and protein synthesis.

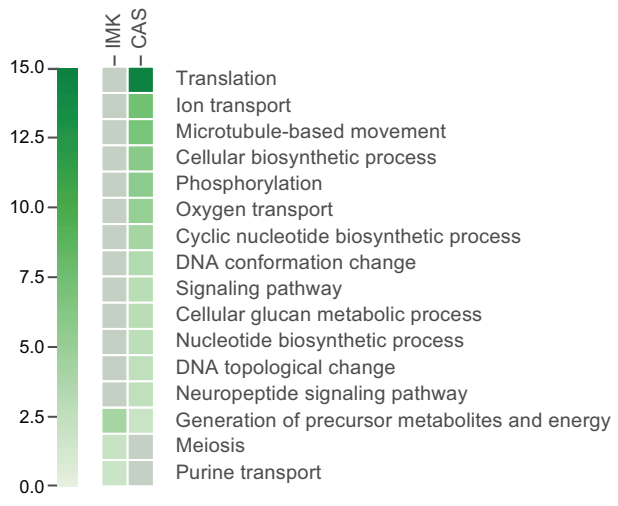

FIGURE 5 | The GO categories enriched (based on adjusted hypergeometric *p*-value < 0.1) in the transcripts showing significant differential expression. Heatmap showing the *p*-value for the enrichment of each category. Gray colored boxes indicate not significant.

Changes in Transcripts Encoding Transporters Associated With Limiting Nutrient Availability

Many changes in expression were observed for transcripts related to ion transporters, with 402 transcripts differentially expressed when SSB01 cells were grown in IMK + CAS (**Supplementary Table S6**). Of those differentially expressed in IMK + CAS, 279 showed elevated transcript accumulation while 123 showed reduced transcript levels (**Supplementary Table S6**). Transcripts encoding voltage-gated sodium channel and voltage-gated ion channel superfamily proteins were some of the most highly expressed in IMK + CAS. For example, the level of the transcript (s6_2946) encoding a voltage-gated sodium channel increased by more than 7-fold. Additionally, four transcripts (s6_9034, s6_3890, s6_2386, s6_1118) encoding chloride channel proteins increased in abundances by more than 2-fold. Voltage-gated ion channels are transmembrane proteins that function in action potential generation in animal, plant, and algal cells (Ward et al., 2009). Levels of transcripts encoding calcium channels were also elevated in IMK + CAS, with 15 of these transcripts exhibiting ∼2-fold increase in abundance relative to ASW (**Supplementary Table S6**). Calcium is an essential micronutrients and calcium signaling is critical for the cells to decode internal and external stimuli, and transduce them into changes in gene expression that modulates physiological processes (Demidchik et al., 2018). In addition, many transcripts involved in nitrogen transport including ammonium transporters and nitrate transporters were significantly changed in IMK + CAS. 20 transcripts encoding ammonium transporters were preferentially expressed in ASW while three were elevated (s6_7783, s6_5492, s6_32551) in IMK + CAS. However, only one transcript encoding an ammonium transporter (s6_51578), and one transcript involved in purine transport (s6_1521) were differentially expressed in IMK relative to ASW. The abundance of the transcript s6_51578 decreased >4-fold in both IMK and IMK + CAS relative to ASW. Similarly, we found seven transcripts encoding nitrate transporters that were expressed at higher levels in ASW (**Supplementary Table S6**). Symbiodiniaceae increases the level of transcripts encoding most transporters associated with the uptake of nitrogen compounds when the cells become limited for nitrogen (Li et al., 2020; Xiang et al., 2020). Previous studies have also shown that members of the former clade B Symbiodiniaceae displayed decreased growth rates under nitrogen-deprivation (Jiang et al., 2014). The elevation of transcripts encoding ammonium and nitrate transporters observed for cells maintained on ASW medium suggests that SSB01 is experiencing nitrogen limitation, which is consistent with its slow growth (**Figure 1**) and the decreased maximum

efficiency of photosystem II (**Figure 2**) in ASW medium. The presence of organic nutrients along with appropriate amounts of ammonium and nitrate were suggested to increase the health of the holobiont (Morris et al., 2019). The transcriptome responses observed for SSB01 cells grown in IMK + CAS compared to ASW medium also suggests that ASW-grown cells are experiencing nitrogen deprivation and that the amino acids of CAS may provide the alga with a sufficient supply of nitrogen; this also suggests that when necessary, organic nutrients, including amino acids, may be provided by the host to the symbiont (Steen, 1986; Wang and Douglas, 1999; Imbs et al., 2014).

IMK + CAS May Elevate the Synthesis of Cyclic Nucleotides

The cyclic nucleotides cAMP and cGMP are important second messengers that modulate many fundamental cellular processes including metabolism, development and differentiation, cell proliferation, and cell survival under adverse conditions (Scheib et al., 2018). Transcripts encoding adenylyl cyclase and guanylate cyclases, enzymes that synthesize cAMP and cGMP (Steer, 1975; Potter, 2011), respectively, were differentially expressed in SSB01 cells grown in IMK + CAS relative to ASW and IMK (**Supplementary Table S4**). Of the 21 transcripts encoding adenylyl and guanylate cyclases, 19 increased while only two decreased in IMK + CAS relative to ASW or IMK. The potential increase in the synthesis of adenylyl and guanylate cyclases in IMK + CAS raises the possibility that organic nutrients/amino acids may trigger the production of second messengers such as cGMP and cAMP (Carucci et al., 2000), which in turn might regulate aspects of Symbiodiniaceae cell growth, proliferation and/or might enable the cells to better cope with suboptimal environmental conditions. Two decades ago cAMP was shown to regulate cell cycle progression and growth of the dinoflagellate *Crypthecodinium cohnii* (Lam et al., 2001).

Massive Changes in Abundances of Transcripts for Enzymes Involved in Protein Phosphorylation

Dinoflagellates appear to have permanently condensed chromosomes and transcriptional control may be limited (e.g., transcript levels rarely become very high during acclimation processes), suggesting that post-translational modifications play important roles in dinoflagellates responses to environmental change (Leggat et al., 2007; Krueger et al., 2015; Rosic et al., 2015; Xiang et al., 2015; Gierz et al., 2016). Quantification of transcripts encoding enzymes involved in protein phosphorylation strongly suggest that phosphorylation may be modulating many cellular processes in response to different nutrient conditions. There are 64 transcripts encoding calcium-dependent protein kinases that are differentially expression in IMK + CAS relative to IMK (and ASW) (**Supplementary Table S5**); 50 of these differentially expressed transcripts were elevated while 14 were diminished in IMK + CAS. For example, a transcript encoding a calcium dependent protein kinase (s6_33927) increased by almost 10-fold in IMK + CAS relative to ASW. Furthermore, 17 transcripts related to cGMP-dependent protein kinases increased in IMK + CAS while only one decreased. The largest change in abundance for cGMP-dependent kinases was for cGMP-dependent protein kinase isozyme 1 (s6_7176), which exhibited a greater than 16-fold elevation in IMK + CAS relative to ASW (**Supplementary Table S5**). The increase observed for transcripts related to cGMP-dependent protein kinases is congruent with changes in the levels of transcripts associated with cyclic nucleotide metabolism. Overall, our results indicate that growth of SSB01 in a source of organic nitrogen elicits an increase in the synthesis of adenylyl and guanylate cyclases and cyclic nucleotide dependent kinases, which likely promotes signal transductions through cGMP and cAMP second messengers.

Changes in the Levels of Transcripts for DNA Topoisomerases and Histones Suggest That the Chromosomes Experience Nutrient Driven Changes in DNA Conformation

Some notable differences in cells maintained in IMK + CAS relative to IMK or ASW involves transcripts encoding proteins associated with DNA topography. Dinoflagellate chromosomes are permanently condensed and maintain a liquid crystalline state that does not appear to rely on histones (Wisecaver and Hackett, 2011). Differences in mechanisms controlling DNA replication and transcription in dinoflagellates may occur as a consequence of their permanently condensed chromosomes and the absence of nucleosomes or the presence of divergent nucleosomes. It has been suggested that extrachromosomal loops protruding from the condensed chromatin structure may allow access of the DNA to the cell's transcriptional machinery (Wisecaver and Hackett, 2011). However, analysis of the 3-dimensional organization of the *B. minutum* genome revealed large topological domains demarcated by convergent gene array boundaries ["dinoTADs," topologically associating domains (TADs) in dinoflagellates], possibly formed as a consequence of transcription-induced supercoiling (Marinov et al., 2020).

Many transcripts encoding DNA topoisomerases were elevated in IMK + CAS relative to ASW medium. We identified 22 transcripts encoding topoisomerases I, II, and III in SSB01. These enzymes change the topology of DNA by overwinding or underwinding the polynucleotide strands and have been implicated in critical cellular functions including DNA replication, DNA repair, and transcription (Levin et al., 1993; Champoux, 2001). Topoisomerase I functions in DNA replication and transcription by creating a single-strand break that allows relief of strain caused by DNA supercoiling (Champoux, 2001). Type II topoisomerases, which can form dimers with Type III topoisomerases, similarly relieve supercoiling strain through the generation of double-stranded DNA breaks (Hartung et al., 2008; Ahmad et al., 2016). The atypical type II topoisomerase, DNA gyrase, is essential for negative supercoiling during replication and transcription (Kampranis and Maxwell, 1996).

The transcripts for 11 topoisomerases, marked with an asterisk in **Supplementary Table S2**, had significantly increased mRNA

abundances in IMK + CAS relative to ASW (**Supplementary Table S2**). Of the 11 topoisomerase transcripts, one was type I, five were type II, and five were type III (**Figure 6**). The transcript for the DNA gyrase (s6_445) increased by more than 3-fold in IMK + CAS and also showed increased levels when symbiotic SSB01 algae populate the *Aiptasia* host (**Supplementary Figure S1**). Elevated transcripts for five Type II topoisomerases in *B. minutum* suggest that they may form a complex and participate in unwinding of DNA that relieves topological stresses and allows access of the genome to transcription factors.

Topoisomerases have been detected in various dinoflagellates (Mínguez et al., 1994; Mak et al., 2005) and it was suggested that *C. cohnii* type II topoisomerase unwinds condensed chromosomes of the G1 phase of the cell cycle for transcription (Mak et al., 2006). Our results also raise the possibility that these topoisomerases may be important for exposing regions of the chromosomal DNA during replication and transcription in the Symbiodiniaceae.

Previously it was thought that dinoflagellate histones play limited roles in DNA packaging, supercoiling and transcriptional changes, even though both conserved and divergent histones and the histone code were found in these organisms, including in *B. minutum*, through genomics analysis (Marinov and Lynch, 2015). Symbiodiniaceae possess transcripts for all core histones, but these histones do not appear to play major roles in the organization and packaging of nuclear DNA (Wisecaver and Hackett, 2011; Gornik et al., 2012). We identified several transcripts encoding core histones and histone protein variants that were differentially expressed when SSB01 was grown on IMK + CAS. Interestingly, the level of the transcript encoding a protein similar to the H3-like centromeric protein A (CENP-A, s6_36342) increased by more than 3-fold. Transcripts encoding Histone H3 (s6_4125 and s6_16949) and Histone H2A (s6_34360) were modestly downregulated. In

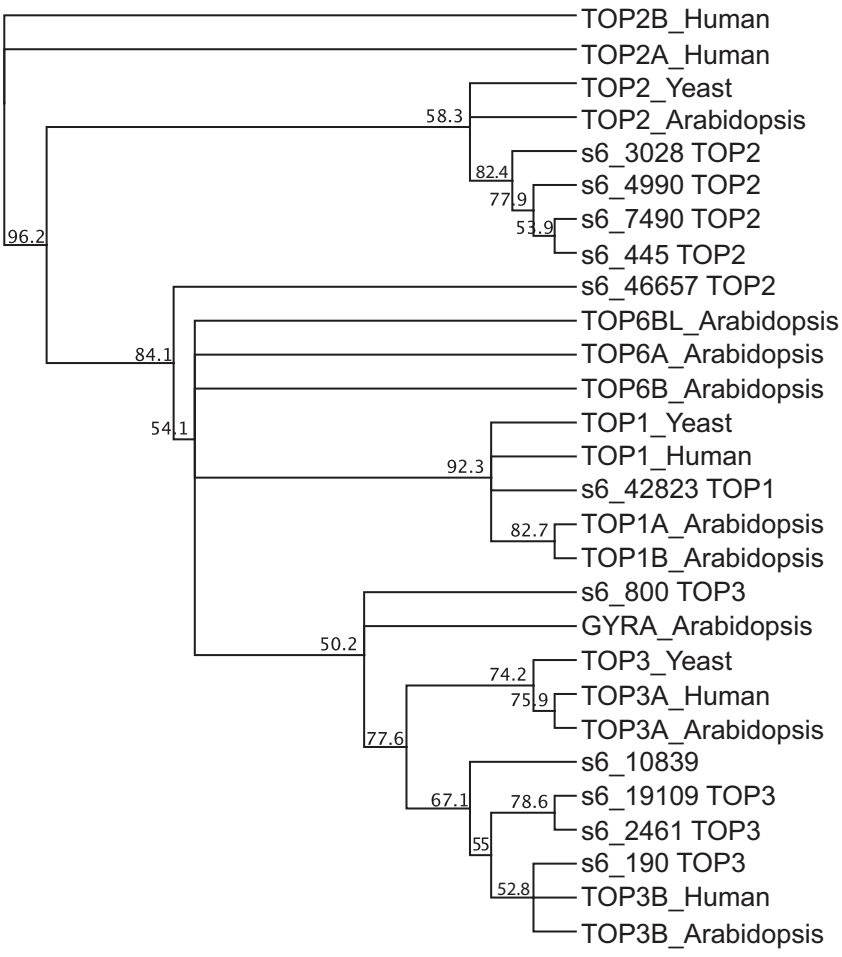

FIGURE 6 | Phylogenetic analysis of DNA topoisomerase sequences in SSB01. Protein polypeptide sequences of 11 DNA topoisomerases in SSB01, 9 in Arabidopsis (*Arabidopsis thaliana*; TOP1A, TOP1B, TOP2, TOP3A, TOP3B, TOP6A, TOP6B, TOP6BL, and GYRA), 3 in yeast (*S. cerevisiae*, TOP1, TOP2, and TOP3), and 5 in human (*Homo sapiens*, TOP1, TOP2A, TOP2B, TOP3A, and TOP3B) were aligned using the MUSCLE program. The phylogenetic tree was built using the neighbor-joining method by Geneious tree builder. The numbers on the nodes indicate the percentage of bootstrap *p*-values obtained from 1,000 replicates.

addition, the expression levels of the transcript for CENP-A increased when SSB01 algae were populating the *Aiptasia* host (**Supplementary Figure S1**). CENP-A, a histone H3 variant, confers epigenetic identity to centromeres and promotes the assembly of kinetochores, chromosome segregation, and cell division (Black et al., 2007; McKinley and Cheeseman, 2016). Tight regulation of CENP-A is critical for proper centromere assembly. It is possible that histones and histone variants could play similar roles in Symbiodiniaceae in modulating chromatin structures and accessibility during cell proliferation. CENP-A has also been shown to prevent the binding of H1 and modify the wrapping of DNA in the nucleosome (Roulland et al., 2016). The elevation of the CENP-A transcripts and the decline of the H3 transcripts in SSB01 cells grown in IMK + CAS may allow for DNA to become more accessible for replication and transcription. These changes may reprogram cell metabolism with respect to its nutrient status.

We also observed massive changes in the levels of transcripts encoding motor proteins. Kinesins are microtubule-bound molecular motors that hydrolyze ATP to perform a range of functions, including the transport of organelles, modulation of cellular organization, mitosis, and signal transduction (Hirokawa et al., 2009; Marx et al., 2009). Many transcripts (53) encoding kinesin family proteins were differentially expressed in SSB01 cells grown in IMK + CAS (**Supplementary Table S7**). The most significantly upregulated transcript encoding a chromosome-associated kinesin (s6_51770) showed more than 6-fold elevation in IMK + CAS relative to ASW. These results suggest that the nutrient status of the medium could significantly impact the levels and functions of microtubule bound motors which may play essential roles in cell division and cellular organization and would be a critical point for control during growth *in hospite*.

Interestingly, the level of the transcript for nucleosome assembly protein-1 (NAP1, s6_2729) is also elevated in IMK + CAS. NAP1 functions in shuttling histones into the nucleus, assembling nucleosomes, and promoting chromatin fluidity, thereby regulating transcription. The loss of NAP1 in yeast resulted in prolonged delays in mitosis, and it is hypothesized that the stimulation of transcription factor binding by NAP1 could result in greater DNA accessibility (Park and Luger, 2006).

Structural maintenance of chromosomes (SMC) proteins are part of a large family of ATPases that form dimers at the core of the condensin complexes (Löwe et al., 2001; Hirano, 2002). As key organizers of chromosome architecture, SMC proteins play major roles in higher-order chromosome organization and dynamics, including chromosome condensation, cohesion of sister chromatids, DNA repair, and gene expression (Harvey et al., 2002). The levels of transcripts encoding SMC1-like protein (s6_5945) and SMC2 (s6_3357) increased in IMK + CAS, whereas another transcript encoding SMC1 (s6_638) decreased in abundance (**Supplementary Table S2**). In addition, the transcript encoding condensin complex subunit 1 (s6_5055), which is a regulatory subunit of the condensin complex, increased in abundance by almost 3-fold in IMK + CAS. Together, our results raise the possibility that the supplementation of IMK medium with CAS impacts Symbiodiniaceae chromosome architecture through the core histone proteins, histone chaperones, topoisomerases, and SMC ATPases.

CONCLUSION

The study presented here provides insights into the responses of Symbiodiniaceae to organic and inorganic nutrients. When IMK medium is supplemented with CAS, a mixture of organic nitrogen containing compounds (mostly amino acids), SSB01 cells grow faster and maintain their photosynthetic apparatus; maximum quantum yield of photosystem II was diminished in cells cultivated for long periods in IMK or ASW. Analysis of differentially expressed transcripts showed that SSB01 grown in ASW and IMK showed few differences in transcript accumulation. In contrast, SSB01 cells grown in IMK + CAS exhibited significant differences in the abundances of transcripts that encode proteins associated with ion transport, translation, cyclic nucleotide biosynthesis, phosphorylation, and DNA conformation. Many of the changes appear to be related to rapid growth and cell division which may be coupled to the nutrient status of the cells. ASW is not conducive to rapid algal growth and may not provide the cells with adequate nutrients, as indicated by activation of nutrient scavenging pathways. Experiencing a scarcity of nutrients may also drive Symbiodiniaceae into establishing a symbiotic association with a cnidarian host, where nutrients may be more readily available and also play a major role in regulating host-symbiont interactions. More detailed physiological and molecular analyses of Symbiodiniaceae algae exposed to various conditions in culture may define the impact of light, temperature and nutrients (e.g., nitrogen, fixed carbon, phosphate) on growth and photosynthesis, suggest metabolic pathways associated with stress conditions and the different trophic life-styles (e.g., autotrophic, mixotrophic, heterotrophic), and provide a detailed picture of the ways in which these algae accommodate environmental change. Ultimately, by comparing transcriptional responses observed in culture with those associated with algae growing *in hospite* may help elucidate the *in hospite* conditions experienced by the endosymbiotic alga and identify key genes that are specifically involved in symbiosis. One important example of this is the elevation in levels of transcripts encoding GCN2 protein kinases, which may act as an amino acid/organic nitrogen sensor in SSB01, similar to its function in *S. cerevisiae* (Castilho et al., 2014).

DATA AVAILABILITY STATEMENT

The raw RNA-Seq reads datasets for this study can be found in the NCBI SRA with the accession number PRJNA639352.

AUTHOR CONTRIBUTIONS

TX conceived and planned the research. TX, SC, AK, FL, and AG analyzed the data. SC measured photosynthetic activities. AK, TX, and AG wrote the manuscript, with contributions

from all the authors. All authors contributed to the article and approved the submitted version.

FUNDING

This study was supported in part by The University of North Carolina at Charlotte start-up funds, the Gordon and Betty Moore Foundation, Grant No. 2629.01, and the NSF IOS EDGE Award 1645164.

ACKNOWLEDGMENTS

We thank Drs. Robert Jinkerson and Georgi Marinov for their helpful comments on the manuscript. High-throughput sequencing was performed by the Stanford Genome Sequencing Service Center of the Stanford Center for Genomics and Personalized Medicine (supported by NIH grant S10OD020141).

SUPPLEMENTARY MATERIAL

The Supplementary Material for this article can be found online at: https://www.frontiersin.org/articles/10.3389/fphys.2020.574654/full#supplementary-material

Supplementary Figure 1 | SSB01 transcripts for GCN2, TOP2, and CENP-A under different culturing and symbiotic conditions. Transcript levels for General Control Nonderepressible 2 (GCN2, s6_33548), topoisomerase II (TOP2, s6_445) and histone h3-like centromeric protein a-like (CENP-A, s6_36342) expressed as transcripts per kilobase million (TPM) from *in vitro* cultures (ASW, IMK and CAS) and populating symbiotic SSB01 (12 d, 30 d, and steady state) in the Aiptasia host. Results of symbiotic SSB01 were obtained by analyzing the data from Baumgarten et al., 2015; and Xiang et al., 2020. Shown are means ± SDs from at least three biological replicates.

Supplementary Table 1 | UniProt IDs of protein sequences used for amino acid-sequence alignment and phylogenetic tree.

Supplementary Table 2 | Annotations and expression levels of transcripts involved in DNA conformation change in IMK and IMK + CAS relative to ASW.

Supplementary Table 3 | Annotations and expression levels of transcripts involved in translation in IMK and IMK + CAS relative to ASW.

Supplementary Table 4 | Annotations and expression levels of transcripts involved in cyclic nucleotide metabolic process in IMK and IMK + CAS relative to ASW.

Supplementary Table 5 | Annotations and expression levels of transcripts involved in phosphorylation in IMK and IMK + CAS relative to ASW.

Supplementary Table 6 | Annotations and expression levels of transcripts for ion transporters in IMK and IMK + CAS relative to ASW.

Supplementary Table 7 | Annotations and expression levels of transcripts involved in microtubule-based movement in IMK and IMK + CAS relative to ASW.

REFERENCES

Ahmad, M., Xue, Y., Lee, S. K., Martindale, J. L., Shen, W., Li, W., et al. (2016). RNA topoisomerase is prevalent in all domains of life and associates with polyribosomes in animals. *Nucl. Acids Res.* 44, 6335–6349. doi: 10.1093/nar/gkw508

Baumgarten, S., Simakov, O., Esherick, L. Y., Liew, Y. J., Lehnert, E. M., Michell, C. T., et al. (2015). The genome of Aiptasia, a sea anemone model for coral symbiosis. *Proc. Natl. Acad. Sci. U S A.* 112, 11893–11898. doi: 10.1073/pnas.1513318112

Black, B. E., Jansen, L. E. T., Maddox, P. S., Foltz, D. R., Desai, A. B., Shah, J. V., et al. (2007). Centromere identity maintained by nucleosomes assembled with histone H3 containing the CENP-A targeting domain. *Mol. Cell* 25, 309–322. doi: 10.1016/j.molcel.2006.12.018

Brading, P., Warner, M. E., Smith, D. J., and Suggett, D. J. (2013). Contrasting modes of inorganic carbon acquisition amongst Symbiodinium (Dinophyceae) phylotypes. *New Phytol.* 200, 432–442. doi: 10.1111/nph.12379

Bucher, M., Wolfowicz, I., Voss, P. A., Hambleton, E. A., and Guse, A. (2016). Development and symbiosis establishment in the cnidarian endosymbiosis model Aiptasia sp. *Sci. Rep.* 6:19867.

Burriesci, M. S., Raab, T. K., and Pringle, J. R. (2012). Evidence that glucose is the major transferred metabolite in dinoflagellate-cnidarian symbiosis. *J. Exp. Biol.* 215, 3467–3477. doi: 10.1242/jeb.070946

Carucci, D. J., Witney, A. A., Muhia, D. K., Warhurst, D. C., Schaap, P., Meima, M., et al. (2000). Guanylyl cyclase activity associated with putative bifunctional integral membrane proteins in Plasmodium falciparum. *J. Biol. Chem.* 275, 22147–22156. doi: 10.1074/jbc.m001021200

Castilho, B. A., Shanmugam, R., Silva, R. C., Ramesh, R., Himme, B. M., and Sattlegger, E. (2014). Keeping the eIF2 alpha kinase Gcn2 in check. *Biochim. Biophys. Acta* 1843, 1948–1968. doi: 10.1016/j.bbamcr.2014.04.006

Champoux, J. J. (2001). DNA topoisomerases: structure, function, and mechanism. *Annu. Rev. Biochem.* 70, 369–413. doi: 10.1146/annurev.biochem.70.1.369

Conti-Jerpe, I. E., Thompson, P. D., Wong, C. W. M., Oliveira, N. L., Duprey, N. N., Moynihan, M. A., et al. (2020). Trophic strategy and bleaching resistance in reef-building corals. *Sci. Adv.* 6:eaaz5443. doi: 10.1126/sciadv.aaz5443

Cook, C. B., and D'elia, C. F. (1987). Are natural populations of zooxanthellae ever nutrient-limited? *Symbiosis* 4, 199–212.

D'Elia, C. F., Domotor, S. L., and Webb, K. L. (1983). Nutrient uptake kinetics of freshly isolated zooxanthellae. *Mar. Biol.* 75, 157–167. doi: 10.1007/bf00405998

Dagenais-Bellefeuille, S., and Morse, D. (2013). Putting the N in dinoflagellates. *Front. Microbiol.* 4:369. doi: 10.3389/fmicb.2013.00369

Davy, S. K., Allemand, D., and Weis, V. M. (2012). Cell biology of cnidarian-dinoflagellate symbiosis. *Microbiol. Mol. Biol. Rev.* 76, 229–261. doi: 10.1128/mmbr.05014-11

Demidchik, V., Shabala, S., Isayenkov, S., Cuin, T. A., and Pottosin, I. (2018). Calcium transport across plant membranes: mechanisms and functions. *New Phytol.* 220, 49–69. doi: 10.1111/nph.15266

Edgar, R. C. (2004). MUSCLE: a multiple sequence alignment method with reduced time and space complexity. *BMC Bioinformatics* 5:113. doi: 10.1186/1471-2105-5-113

Fox, M. D., Smith, EaE, Smith, J. E., and Newsome, S. D. (2019). Trophic plasticity in a common reef-building coral: Insights from delta C-13 analysis of essential amino acids. *Funct. Ecol.* 33, 2203–2214. doi: 10.1111/1365-2435.13441

Fransolet, D., Roberty, S., and Plumier, J.-C. (2012). Establishment of endosymbiosis: The case of cnidarians and Symbiodinium. *J. Exp. Mar. Bio. Ecol.* 42, 1–7. doi: 10.1016/j.jembe.2012.03.015

Gierz, S. L., Gordon, B. R., and Leggat, W. (2016). Integral light-harvesting complex expression in Symbiodinium within the coral Acropora aspera under thermal stress. *Sci. Rep.* 6:25081.

Gornik, S. G., Ford, K. L., Mulhern, T. D., Bacic, A., McFadden, G. I., and Waller, R. F. (2012). Loss of nucleosomal DNA condensation coincides with appearance of a novel nuclear protein in dinoflagellates. *Curr. Biol.* 22, 2303–2312. doi: 10.1016/j.cub.2012.10.036

Gregio, A. P. B., Cano, V. P. S., Avaca, J. S., Valentini, S. R., and Zanelli, C. F. (2009). eIF5A has a function in the elongation step of translation in yeast. *Biochem. Biophys. Res. Commun.* 380, 785–790. doi: 10.1016/j.bbrc.2009.01.148

Hambleton, E. A., Guse, A., and Pringle, J. R. (2014). Similar specificities of symbiont uptake by adults and larvae in an anemone model system

for coral biology. *J. Exper. Biol.* 217, 1613–1619. doi: 10.1242/jeb.095679

Hartung, F., Suer, S., Knoll, A., Wurz-Wildersinn, R., and Puchta, H. (2008). Topoisomerase 3α and RMI1 suppress somatic crossovers and are essential for resolution of meiotic recombination intermediates in Arabidopsis thaliana. *PLoS Genet* 4:e1000285. doi: 10.1371/journal.pgen.1000285

Harvey, S. H., Krien, M. J. E., and O'Connell, M. J. (2002). Structural maintenance of chromosomes (SMC) proteins, a family of conserved ATPases. *Genome Biol.* 3:REVIEWS3003.

Henderson, A., and Hershey, J. W. (2011). Eukaryotic translation initiation factor (eIF) 5A stimulates protein synthesis in *Saccharomyces cerevisiae*. *Proc. Natl. Acad. Sci. U S A.* 108, 6415–6419. doi: 10.1073/pnas.1008150108

Hirano, T. (2002). The ABCs of SMC proteins: two-armed ATPases for chromosome condensation, cohesion, and repair. *Genes Dev.* 16, 399–414. doi: 10.1101/gad.955102

Hirokawa, N., Noda, Y., Tanaka, Y., and Niwa, S. (2009). Kinesin superfamily motor proteins and intracellular transport. *Nat. Rev. Mol. Cell Biol.* 10, 682–696. doi: 10.1038/nrm2774

Hoegh-Guldberg, O. (1999). Climate change, coral bleaching and the future of the world's coral reefs. *Mar. Freshwater Res.* 50, 839–866.

Hughes, T. P., Barnes, M. L., Bellwood, D. R., Cinner, J. E., Cumming, G. S., Jackson, J. B., et al. (2017). Coral reefs in the Anthropocene. *Nature* 546, 82–90. doi: 10.1038/nature22901

Imbs, A. B., Yakovleva, I. M., Dautova, T. N., Bui, L. H., and Jones, P. (2014). Diversity of fatty acid composition of symbiotic dinoflagellates in corals: evidence for the transfer of host PUFAs to the symbionts. *Phytochemistry* 101, 76–82. doi: 10.1016/j.phytochem.2014.02.012

Jeong, H. J., Yoo, Y. D., Kang, N. S., Lim, A. S., Seong, K. A., Lee, S. Y., et al. (2012). Heterotrophic feeding as a newly identified survival strategy of the dinoflagellate *Symbiodinium*. *Proc. Natl. Acad. Sci. U S A.* 109, 12604–12609. doi: 10.1073/pnas.1204302109

Jiang, P. L., Pasaribu, B., and Chen, C. S. (2014). Nitrogen-deprivation elevates lipid levels in *Symbiodinium* spp. by lipid droplet accumulation: morphological and compositional analyses. *PLoS One* 9:e87416. doi: 10.1371/journal.pone.0087416

Joliot, P., and Delosme, R. (1974). Flash-induced 519 nm absorption change in green algae. *Biochim. Biophys. Acta* 357, 267–284. doi: 10.1016/0005-2728(74)90066-8

Kampranis, S. C., and Maxwell, A. (1996). Conversion of DNA gyrase into a conventional type II topoisomerase. *Proc. Natl. Acad. Sci. U. S. A.* 93, 14416–14421. doi: 10.1073/pnas.93.25.14416

Krueger, T., Fisher, P. L., Becker, S., Pontasch, S., Dove, S., Hoegh-Guldberg, O., et al. (2015). Transcriptomic characterization of the enzymatic antioxidants FeSOD. *MnSOD, APX and KatG in the dinoflagellate genus Symbiodinium*. *BMC Evol. Biol.* 15:48. doi: 10.1186/s12862-015-0326-0

Lajeunesse, T. C., Parkinson, J. E., and Reimer, J. D. (2012). A genetics-based description of Symbiodinium minutum sp. nov. and S. psygmophilum sp. nov. (dinophyceae), two dinoflagellates symbiotic with cnidaria. *J. Phycol.* 48, 1380–1391. doi: 10.1111/j.1529-8817.2012.01217.x

Lajeunesse, T. C., Parkinson, J. E., Gabrielson, P. W., Jeong, H. J., Reimer, J., Voolstra, C., et al. (2018). Systematic revision of Symbiodiniaceae highlights the antiquity and diversity of coral endosymbionts. *Curr. Biol.* 28, 2570–2580. doi: 10.1016/j.cub.2018.07.008

Lam, C. M. C., New, D. C., and Wong, J. T. Y. (2001). cAMP in the cell cycle of the dinoflagellate *Crypthecodinium cohnii* (Dinophyta). *J. Phycol.* 37, 79–85. doi: 10.1046/j.1529-8817.2001.037001079.x

Leal, M. C., Hoadley, K., Pettay, D. T., Grajales, A., Calado, R., and Warner, M. E. (2015). Symbiont type influences trophic plasticity of a model cnidarian-dinoflagellate symbiosis. *J. Exp. Biol.* 218, 858–863. doi: 10.1242/jeb.115519

Lee, A. S. Y., Kranzusch, P. J., and Cate, J. H. D. (2015). eIF3 targets cell-proliferation messenger RNAs for translational activation or repression. *Nature* 522, 111–114. doi: 10.1038/nature14267

Leggat, W., Hoegh-Guldberg, O., Dove, S., and Yellowlees, D. (2007). Analysis of an EST library from the dinoflagellate (*Symbiodinium* sp.) symbiont of reef-building corals 1. *J. Phycol.* 43, 1010–1021. doi: 10.1111/j.1529-8817.2007.00387.x

Levin, N. A., Bjornsti, M. A., and Fink, G. R. (1993). A novel mutation in DNA topoisomerase I of yeast causes DNA damage and RAD9-dependent cell cycle arrest. *Genetics* 133, 799–814.

Li, H., and Durbin, R. (2009). Fast and accurate short read alignment with Burrows-Wheeler transform. *Bioinformatics* 25, 1754–1760. doi: 10.1093/bioinformatics/btp324

Li, T., Chen, X., and Lin, S. (2020). Physiological and transcriptomic responses to N-deficiency and ammonium: nitrate shift in *Fugacium kawagutii* (Symbiodiniaceae). *BioRxiv* 2020:077719. doi: 10.1101/2020.05.04.077719

Love, M. I., Huber, W., and Anders, S. (2014). Moderated estimation of fold change and dispersion for RNA-seq data with DESeq2. *Genome Biol.* 15:550.

Löwe, J., Cordell, S. C., and van den Ent, F. (2001). Crystal structure of the SMC head domain: an ABC ATPase with 900 residues antiparallel coiled-coil inserted. *J. Mol. Biol.* 306, 25–35. doi: 10.1006/jmbi.2000.4379

Maere, S., Heymans, K., and Kuiper, M. (2005). BiNGO: a Cytoscape plugin to assess overrepresentation of gene ontology categories in biological networks. *Bioinformatics* 21, 3448–3449. doi: 10.1093/bioinformatics/bti551

Mak, C. K. M., Hung, V. K. L., and Wong, J. T. Y. (2005). Type II topoisomerase activities in both the G1 and G2/M phases of the dinoflagellate cell cycle. *Chromosoma* 114, 420–431. doi: 10.1007/s00412-005-0027-3

Mak, C. K. M., Hung, V. K. L., and Wong, J. T. Y. (2006). Type II topoisomerase activities in both the G1 and G2/M phases of the dinoflagellate cell cycle. *Chromosoma* 115, 341–341. doi: 10.1007/s00412-006-0054-8

Maor-Landaw, K., van Oppen, M. J. H., and McFadden, G. I. (2020). Symbiotic lifestyle triggers drastic changes in the gene expression of the algal endosymbiont *Breviolum minutum* (Symbiodiniaceae). *Ecol. Evol.* 10, 451–466. doi: 10.1002/ece3.5910

Marinov, G. K., and Lynch, M. (2015). Diversity and Divergence of Dinoflagellate Histone Proteins. *G3* 6, 397–422. doi: 10.1534/g3.115.023275

Marinov, G. K., Trevino, A. E., Xiang, T., Kundaje, A., Grossman, A. R., and Greenleaf, W. J. (2020). Transcription-dependent domain-scale 3D genome organization in dinoflagellates. *BioRxiv* doi: 10.1101/2020.07.01.181685

Marx, A., Hoenger, A., and Mandelkow, E. (2009). Structures of kinesin motor proteins. *Cell Motil. Cytoskeleton* 66, 958–966. doi: 10.1002/cm.20392

McKinley, K. L., and Cheeseman, I. M. (2016). The molecular basis for centromere identity and function. *Nat. Rev. Mol. Cell Biol.* 17, 16–29. doi: 10.1038/nrm.2015.5

Mínguez, A., Franca, S., and Moreno Díaz de la Espina, S. (1994). Dinoflagellates have a eukaryotic nuclear matrix with lamin-like proteins and topoisomerase II. *J. Cell Sci.* 107(Pt 10), 2861–2873.

Morris, L. A., Voolstra, C. R., Quigley, K. M., Bourne, D. G., and Bay, L. K. (2019). Nutrient Availability and Metabolism Affect the Stability of Coral-Symbiodiniaceae Symbioses. *Trends Microbiol.* 27, 678–689. doi: 10.1016/j.tim.2019.03.004

Muscatine, L., and Porter, J. W. (1977). Reef Corals: Mutualistic symbioses adapted to nutrient-poor environments. *Bioscience* 27, 454–460. doi: 10.2307/1297526

Park, Y.-J., and Luger, K. (2006). The structure of nucleosome assembly protein 1. *Proc. Natl. Acad. Sci. U S A.* 103, 1248–1253.

Parkinson, J. E., Baumgarten, S., Michell, C. T., Baums, I. B., Lajeunesse, T. C., and Voolstra, C. R. (2016). Gene Expression Variation Resolves Species and Individual Strains among Coral-Associated Dinoflagellates within the Genus Symbiodinium. *Genome Biol. Evol.* 8, 665–680. doi: 10.1093/gbe/evw019

Pearse, V. B., and Muscatine, L. (1971). Role of symbiotic algae (zooxanthellae) in coral calcification. *Biol. Bull.* 141, 350–363. doi: 10.2307/1540123

Potter, L. R. (2011). Guanylyl cyclase structure, function and regulation. *Cell. Signal.* 23, 1921–1926. doi: 10.1016/j.cellsig.2011.09.001

Rodnina, M. V., Gromadski, K. B., Kothe, U., and Wieden, H.-J. (2005). Recognition and selection of tRNA in translation. *FEBS Lett.* 579, 938–942. doi: 10.1016/j.febslet.2004.11.048

Rosic, N., Ling, E. Y. S., Chan, C.-K. K., Lee, H. C., Kaniewska, P., Edwards, D., et al. (2015). Unfolding the secrets of coral-algal symbiosis. *ISME J.* 9, 844–856. doi: 10.1038/ismej.2014.182

Roulland, Y., Ouararhni, K., Naidenov, M., Ramos, L., Shuaib, M., Syed, S. H., et al. (2016). The flexible ends of CENP-A nucleosome are required for mitotic fidelity. *Mol. Cell* 63, 674–685. doi: 10.1016/j.molcel.2016.06.023

Saini, P., Eyler, D. E., Green, R., and Dever, T. E. (2009). Hypusine-containing protein eIF5A promotes translation elongation. *Nature* 459, 118–121. doi: 10.1038/nature08034

Scheib, U., Broser, M., Constantin, O. M., Yang, S., Gao, S., Mukherjee, S., et al. (2018). Rhodopsin-cyclases for photocontrol of cGMP/cAMP and 2.3 Å structure of the adenylyl cyclase domain. *Nat. Commun.* 9:2046.

Shoguchi, E., Shinzato, C., Kawashima, T., Gyoja, F., Mungpakdee, S., Koyanagi, R., et al. (2013). Draft assembly of the Symbiodinium minutum nuclear genome reveals dinoflagellate gene structure. *Curr. Biol.* 23, 1399–1408. doi: 10.1016/j.cub.2013.05.062

Steen, R. G. (1986). Evidence for Heterotrophy by Zooxanthellae in Symbiosis with *Aiptasia pulchella*. *Biol. Bull.* 170, 267–278. doi: 10.2307/1541808

Steer, M. L. (1975). Adenyl cyclase. *Ann. Surg.* 182, 603–609. doi: 10.1097/00000658-197511000-00012

Wagner, G. P., Kin, K., and Lynch, V. J. (2012). Measurement of mRNA abundance using RNA-seq data: RPKM measure is inconsistent among samples. *Theory Biosci.* 131, 281–285. doi: 10.1007/s12064-012-0162-3

Wang, J. T., and Douglas, A. E. (1999). Essential amino acid synthesis and nitrogen recycling in an alga-invertebrate symbiosis. *Mar. Biol.* 135, 219–222. doi: 10.1007/s002270050619

Ward, J. M., Mäser, P., and Schroeder, J. I. (2009). Plant ion channels: gene families, physiology, and functional genomics analyses. *Annu. Rev. Physiol.* 71, 59–82. doi: 10.1146/annurev.physiol.010908.163204

Weis, V. M., and Allemand, D. (2009). Physiology. What determines coral health? *Science* 324, 1153–1155. doi: 10.1126/science.1172540

Wisecaver, J. H., and Hackett, J. D. (2011). Dinoflagellate genome evolution. *Annu. Rev. Microbiol.* 65, 369–387. doi: 10.1146/annurev-micro-090110-102841

Xiang, T. (2018). Total RNA extraction from dinoflagellate *Symbiodinium* cells. *Bio. Protoc.* 8:e2866. doi: 10.21769/BioProtoc.2866

Xiang, T., Hambleton, E. A., DeNofrio, J. C., Pringle, J. R., and Grossman, A. R. (2013). Isolation of clonal axenic strains of the symbiotic dinoflagellate *Symbiodinium* and their growth and host specificity. *J. Phycol.* 49, 447–458. doi: 10.1111/jpy.12055

Xiang, T., Jinkerson, R. E., Clowez, S., Tran, C., Krediet, C. J., Onishi, M., et al. (2018). Glucose-induced trophic shift in an endosymbiont dinoflagellate with physiological and molecular consequences. *Plant Physiol.* 176, 1793–1807. doi: 10.1104/pp.17.01572

Xiang, T., Lehnert, E., Jinkerson, R. E., Clowez, S., Kim, R. G., DeNofrio, J. C., et al. (2020). Symbiont population control by host-symbiont metabolic interaction in Symbiodiniaceae-cnidarian associations. *Nat. Commun.* 11:108.

Xiang, T., Nelson, W., Rodriguez, J., Tolleter, D., and Grossman, A. R. (2015). Symbiodinium transcriptome and global responses of cells to immediate changes in light intensity when grown under autotrophic or mixotrophic conditions. *Plant J.* 82, 67–80. doi: 10.1111/tpj.12789

Conflict of Interest: FL was employed by the company Brightseed Inc.

The remaining authors declare that the research was conducted in the absence of any commercial or financial relationships that could be construed as a potential conflict of interest.

frontiers in Physiology

ORIGINAL RESEARCH
published: 18 January 2021
doi: 10.3389/fphys.2020.621111

Monoclonal Culture and Characterization of Symbiodiniaceae C1 Strain From the Scleractinian Coral *Galaxea fascicularis*

*Jun Wang†, Jiaqi Chen†, Shaoyu Wang†, Fuyu Li, Chengchong Fu and Yan Wang**

State Key Laboratory of Marine Resource Utilization in South China Sea, College of Marine Sciences, Hainan University, Haikou, China

The symbiosis between cnidarian hosts and photosynthetic dinoflagellates of the family Symbiodiniaceae (i.e., zooxanthellae) provides the energy foundation of coral reef ecosystems in oligotrophic waters. The structure of symbiont biota and the dominant species of algal symbiont partly shape the environmental adaptability of coral symbiotes. In this study, the algal symbiont cells were isolated from the tentacles of *Galaxea fascicularis*, a hermatypic coral with obvious differentiation in heat resistance, and were cultured *in vitro* with an improved L1 medium. An algal monoclonal cell line was established using separated algal culture drops and soft agar plating method, and named by GF19C1 as it was identified as *Cladocopium* sp. C1 (Symbiodiniaceae) based on its ITS1, ITS2, and the non-coding region of the plastid psbA minicircle (*psbA*^{ncr}) sequences. Most GF19C1 cells were at the coccoid stage of the gymnodinioid, their markedly thickened (ca. two times) cell wall suggests that they developed into vegetative cysts and have sexual and asexual reproductive potential. The average diameter of GF19C1 cells decreased significantly, probably due to the increasing mitotic rate. The chloroplasts volume density of GF19C1 was significantly lower than that of their symbiotic congeners, while the surface area density of thylakoids relative to volumes of chloroplasts was not significantly changed. The volume fraction of vacuoles increased by nearly fivefold, but there was no significant change in mitochondria and accumulation bodies. Light-temperature orthogonal experiments showed that, GF19C1 growth preferred the temperature 25 ± 1°C (at which it is maintained post-isolation) rather than 28 ± 1°C under the light intensity of 42 ± 2 or 62 ± 2 μmol photons m^{-2} s^{-1}, indicating an inertia for temperature adaptation. The optimum salinity for GF19C1 growth ranged between 28–32 ppt. The monoclonal culture techniques established in this study were critical to clarify the physiological and ecological characteristics of various algal symbiont species, and will be instrumental to further reveal the roles of algal symbionts in the adaptive differentiation of coral-zooxanthellae holobionts in future studies.

Keywords: *Cladocopium* sp. C1, monoclonal strain, *Galaxea fascicularis*, ultrastructure, stereology, growth rate

OPEN ACCESS

Edited by:
Kefu Yu,
Guangxi University, China

Reviewed by:
Biao Chen,
Guangxi University, China
Fiorella Prada,
University of Bologna, Italy

***Correspondence:**
Yan Wang
ywang@hainanu.edu.cn

†These authors have contributed equally to this work

Specialty section:
This article was submitted to Aquatic Physiology, a section of the journal Frontiers in Physiology

Received: *25 October 2020*
Accepted: *31 December 2020*
Published: *18 January 2021*

Citation:
Wang J, Chen J, Wang S, Li F, Fu C and Wang Y (2021) Monoclonal Culture and Characterization of Symbiodiniaceae C1 Strain From the Scleractinian Coral Galaxea fascicularis. Front. Physiol. 11:621111. doi: 10.3389/fphys.2020.621111

INTRODUCTION

The establishment of specialized intracellular symbiotic relationship between reef-building corals and photosynthetic dinoflagellates (Symbiodiniaceae, also known as zooxanthellae) is the primary energy source for reef ecosystems to flourish in oligotrophic tropical shallow waters. Photosynthesis of symbiotic algae can supply more than 95% of the nutritional needs of the corals and contribute to the calcification of reef corals to form the carbonate framework of coral reefs (Mallela, 2013). However, due to the essential differences in metabolic rates and nutritional requirements between corals and algal symbionts, the precise homeostasis necessary to maintain the symbiotic relationship is highly sensitive to environmental stresses (Obura, 2009), especially to the synergistic stress of light intensity and temperature variations (Lesser and Farrell, 2004; Ferrier-Pages et al., 2007; Hawkins et al., 2015). A thermal perturbation as little as 1°C above the average summer maxima could cause the breakdown of this symbiosis and lead to coral bleaching (Hume et al., 2015). Since 1980s, worldwide coral bleaching events caused by global warming have become more and more frequent, with too short intervals allowing for a full recovery of mature assemblages. As a result, mass coral mortality and the severe degradation of the coral reefs structure and ecological functions occurred (Hoegh-Guldberg et al., 2007; Hughes et al., 2017). Even more worrying, as global warming in progression, local extreme weather conditions are more frequently seen, and the coral reef ecosystems are likely to further decline (Hughes et al., 2018). Therefore, analyzing the adaptation and resilience of reef-building coral holobionts has become the focus of coral reef protection and resilience. This is bound to start with the two symbiotic parties, respectively, to clarify the physiological and ecological characteristics and environmental adaptation potentials of reef-building corals (Shinzato et al., 2011; Ying et al., 2018) and symbiotic algae (Lin et al., 2015; Aranda et al., 2016). And then, bring it to the level of holobiont as a unique biological entity of evolutionary selection for integrated research (Rosenberg, 2013).

The algal symbiont used to belong to *Symbiodinium*, a genus with obscure morphological and taxonomic characteristics with complex phylogenetic lineages (LaJeunesse et al., 2018). The species of this genus formed a complex symbiotic relationship with numerous categories of marine invertebrates (Trench, 1993). In the past 30 years, DNA sequences and molecular biology techniques have been used to establish a comprehensive phylogenetic relationship for algal symbionts derived from various marine invertebrates. Based on nuclear 18S-rDNA and restriction fragment length polymorphisms (RFLPs) (Rowan and Powers, 1991a,b), chloroplast 23S-rDNA gene sequence (Santos et al., 2002; Pochon et al., 2006; Pochon and Gates, 2010), *Symbiodinium* was classified into nine (A–I) genetically distinctive clades. And each clade is further divided into multiple subclades based on the nuclear internal transcribed spacer (ITS) regions (LaJeunesse, 2001; Van Oppen et al., 2005). Recently, LaJeunesse et al. (2018) systematically revised the evolutionarily divergent *Symbiodinium* Clade A–G to seven genera in the family Symbiodiniaceae, and some subclades or genetic strains are described as species within those genera. With increasing phylogenetic, ecological, and biogeographic evidences available, more novel genera and species will be likely uncovered and classified in the family Symbiodiniaceae (LaJeunesse et al., 2018). The host species associated with algal symbionts are highly diverse, even when spoken of reef-building coral hosts, they are also miscellaneous. Since the existence of symbiont-host specificity at the species level (Trench, 1993), the lineages of genetic differentiation of symbiotic algae, combining with that of coral hosts, have indicated much greater genetic and functional diversities in the algal symbionts of reef-building corals (Barshis et al., 2014). Certainly, the establishment of *in vitro* monoclonal culture of host-associated algal symbiont strains would be necessary to elucidate the species identification and characterization through collecting and analyzing their physiological and ecological data. In addition, such efforts could facilitate to reveal the roles of algal symbionts in building, maintaining, breaking down and reconstruction of the symbiosis. Nevertheless, due to the numerous difficulties in the establishment of *in vitro* culture strains (Schoenberg and Trench, 1980a), the studies on the host-associated monoclonal algal symbiont cultures are still limited (Chakravarti and Van Oppen, 2018).

Galaxea fascicularis, a massive coral with large polyps, is mainly distributed in the tropical and subtropical coral reef areas of the Indian- Pacific Ocean (Veron, 2000). It is also the dominant species on the fringing reefs of Hainan Island (Chen et al., 2013; Wang et al., 2013). *G. fascicularis* species includes two morphologically and genetically differentiated lineages characterized by the microbasic p-mastigophores (MpM) types of tentacular nematocyst (Hidaka, 1992) and mitochondrial genotypes (Watanabe et al., 2005) around Hainan Island (Wu, 2018; Wepfer et al., 2020). These two lineages demonstrate significant differences in heat resistance (Xu, 2019), indicating the potential of *G. fascicularis* as an ideal model for exploring the genetic basis of heat resistance differentiation of corals. Thus, the establishment of *in vitro* monoclonal cultures of *G. fascicularis* associated algal symbiont species, followed by characterization of their morphological, physiological and ecological traits, would be necessary and helpful to reveal the symbiosis flexibility behind the differentiations in environmental adaptability between the two lineages, as well as the interaction between corals and symbionts within the holobiont. In this study, we conceived and developed the techniques for successful isolation and cultivation of the monoclonal symbiotic algal strain of *G. fascicularis*. and then characterized the first monoclonal algal strain GF19C1 (**Supplementary Figure 1**).

MATERIALS AND METHODS

Coral Samples and Algal Symbiont Identification

The scleractinian coral *Galaxea fascicularis* (GF) samples (one piece/colony, 23 pieces in total) were collected from West Island (18°14′16″ N, 109°21′54″ E, Sanya, Hainan, China) in April, 2018. The sample collection was approved and assisted by

the Management Office of Sanya National Coral Reef Nature Reserve. Two polyps were taken down from each coral piece, and fixed in triplicate 95% alcohol. The living samples were brought back to the laboratory and maintained in the aquaria at the College of Marine Science, Hainan University under the following conditions: seawater renewal rate at 1,000 L h^{-1}; temperature at 26 ± 1°C; salinity of 32–34 ppt; light intensity of 160 μmol photons m^{-2} s^{-1} and photoperiod at 12 h light: 12 h dark.

The GF symbiote DNA were extracted using modified CTAB method (Mieog et al., 2009). In brief, freshly fixed tissue filaments were cut into pieces and suspended in 800 μL CTAB extract (2% CTAB, 1.4 M NaCl, 20 mM EDTA, 100 mM Tris–HCl, 20 μg/mL proteinase K, pH 8). After adding 3–5 glass beads (diameter 3 mm) in the tube, the tissue pieces were grinded for 5 min in Tissuelyser-48 grinder (Shanghai JingXin Industrial Development Co., Ltd.), and then incubated overnight at 60°C. The total DNA was extracted with 800 μL chloroform/isopentanol (24:1), and precipitated with isopropanol at −20°C. The DNA pellets was washed by 70% ethanol and air-dried, followed by suspended at 200 μL 0.01M TE (pH 8). Subsequently, the algal symbiont nuclear small subunit (n18S)-rDNA was amplified by PCR using the primers ss5 and ss3z (Rowan and Powers, 1991b). PCR solution (10 μL) contained 1 × Taq-HS PCR Master Mix [Mona (Wuhan) Biotechnology Co., Ltd.], ∼20 ng template DNA, 5 pmol of each primer. Cycling profiles were 94°C for 5 min followed by 30 cycles of 94°C for 1 min, annealing at 55°C for 2 min, extension at 72°C for 3 min, and a final extension at 72°C for 10 min. The PCR products were digested with *TaqI* restriction enzyme to generate RFLPs (restriction fragment length polymorphism) and visualized by electrophoresis separated on 2.5% agarose gels. The clade (genus) was identified according to the RFLP patterns (Santos et al., 2002). Accordingly, the coral individual 5gw14, associated with clade C symbiont, were selected for the following isolation of algal symbiont.

Isolation and Monoclonal Culture of Algal Symbionts

The ordinary tentacles were sampled with sterilized tweezers, and were rinsed with sterilized sea water to remove the broken septa (**Supplementary Figure 2A**). Each tentacle was put in an eppendorf tube, and then break the tentacle with pipette tip to release the symbiotic algae. Tissue fragments were precipitated by inching centrifugation, and the suspending algal cells were transferred into a new tube (**Supplementary Figure 2B**, 1st tube) containing the modified L1 medium (Z1 medium, **Supplementary Table 1**). In suspensions, adjust the cell density to 500 cells/mL, then sample several 5 μL droplets onto microscopy slides and observe cells under a microscopy. Transfer 4–5 algal cells into fresh tubes (2nd, 3rd, and 4th tube, **Supplementary Figure 2B**), and then culture them with Z1 medium. In 6 weeks or so, adjust the cell density to 2,000 cells/mL and spread 50 μL algal liquid on a soft agar plate containing antibiotics to obtain clonal axenic culture, until the microscopic confirmation of the absence of contamination and monoclonal algal colonies appeared on the plate (ca. 10–12 weeks later, **Supplementary Figure 2C**). The well-developed, clearly isolated and dense colonies were then transferred into Z1 liquid medium for extended cultivation. Finally, the axenic algal cells were inoculated into fresh Z1 medium every 2 weeks and cultured continuously (**Supplementary Figure 2D**) under the following conditions: temperature at 25 ± 1°C, light intensity of 45 ± 5 μmol photons m^{-2} s^{-1}, photoperiod at 14 h light: 10 h dark. The soft agar plate medium contains: 1.5 × Z1, plus 75 mg/L $NaNO_3$, 35 mg/L NH_4Cl, penicillin (final concentration 200 μg mL^{-1}), streptomycin 100 μg mL^{-1}, kanamycin 100 μg mL^{-1} (Lin et al., 2015), and 0.5% (w/v) agar powder (Becton, Dickinson and Company, United States).

Identification of the Monoclonal Algal Strains

The genomic DNA of *in vitro* cultured algae was extracted as mentioned above. The ITS1 and ITS2 regions were amplified by primer symITS1 (Van Oppen et al., 2001), ITSintfor2 (LaJeunesse and Trench, 2000) and ITS-Reverse (Coleman et al., 1994). PCR was conducted in a 35 μL reaction solution containing ca. 50 ng template DNA, and 1 × MonAmp HS Taq Mix [Mona (Wuhan) Biotechnology Co., Ltd.], 17.5 pmol of each primer. The PCR profile was: 94°C for 5 min followed by 40 cycles of 94°C for 30 s, annealing for 30 s at 59°C (for ITS1) or 51°C (for ITS2), extension at 72°C for 30 s, and a final extension at 72°C for 5 min. For further confirming the phylogenetic identity of the algal strain, sequences of the non-coding region of the plastid psbA minicircle ($psbA^{ncr}$) were amplified using primers 7.4-Forw and 7.8-Rev (Moore et al., 2003). The PCR conditions are as followed as: 94°C for 2 min; then 40 cycles at 94°C 10 s, 55°C for 30 s, and 72°C for 2 min; followed by a final extension at 72°C for 10 min (LaJeunesse and Thornhill, 2011). The purified PCR amplicons were directly (Sanger) sequenced in both directions (ABI 3730XL DNA Sequencer) by Tsingke Company (Guangzhou, China). Mega X (Kumar et al., 2018) were used to align those sequences (**Supplementary Material 1**) with the associated homologous sequences of ITS1 (AF380530-AF380565, Van Oppen et al., 2001), ITS2 (GU111863-GU111905, LaJeunesse et al., 2010) and $psbA^{ncr}$ (JQ043677-JQ043719, LaJeunesse and Thornhill, 2011), and then Neighbor-Joining phylogeny trees were constructed (**Supplementary Material 1**).

Ultrastructure and Stereometry of the Monoclonal Algal Cells

The *in vitro* algal cells were collected from 2 mL culture by centrifugation and then fixed using 1 mL 2.5% (v/v) glutaraldehyde. For the *in situ* symbiont control, a few inner tissues from a polyp of 5gw14 were sampled and fixed with 1 mL 2.5% (v/v) glutaraldehyde. Upon fixation at room temperature for 2 h, the tissues or algae were embedded in 1% (w/v) agarose, and rinsed with 0.1 M phosphate buffer (pH 7.4). The agar blocks were post-fixed in 1% osmium tetroxide for 2 h at room temperature followed by rinsing with 0.1 M phosphate buffer (pH 7.4), and then dehydrated sequentially with 50–100% gradient alcohol, replaced with 100% acetone, and embedded in Epon

812. Leica EM UC7 ultramicrotome was used to make the thin sections (60–80 nm), which were stained with 2% (w/v) saturated uranium acetate alcohol solution and lead citrate. Images of *in situ* control and *in vitro* cultured algal cells were processed under a HT7700 transmission electron microscopy (Hitachi, Japan).

Randomly selected ten section micrographs showing typical features of algal organelles from both cultured and tissue sections (15–20 K final magnification) were used to assess the volume fractions of chloroplasts, mitochondria, accumulations and vacuoles by Adobe Photoshop CC software based on principles of stereology (Elias and Hyde, 1980). The ratio of chloroplast/mitochondrion/accumulation/vacuole to total cell area of each cell was calculated by the respective corresponding numbers of pixels. In order to avoid the effect of differential image resolutions, we used the image scale tool to measure the central width of three random chloroplasts in each cell and counted the number of thylakoid lamellae. The mean number of thylakoid lamellae per unit width represents the surface density of thylakoid lamellae relative to chloroplast volume (SDTL) (Lesser and Shick, 1990). Similarly, the mean thickness of cell wall from those 10 algal cells of each group was determined. For each cell, three clear cell wall locations were randomly measured.

To analyze the volume changes of *in vitro* cultured algae, the diameters of 50 algal cells (both *in vitro* and *in situ* from tentacles of the coral 5gw14) were measured by using objective micrometer (40×) under a light microscope, respectively. Meanwhile, the cell division ratio of the two groups were also calculated. Total of randomly selected 50 cells were counted each time, and the mean measure was obtained by three counts. The criteria for cells in division was based on the evidence that there is a distinct cleavage furrow in the center, and the two dividing cells are wrapped in one maternal wall.

Orthogonal Experimental Analysis of Suitable Light and Temperature

Since isolation, the algae have been cultured under the conditions of 25 ± 1°C and 42 ± 2 μmol photons m^{-2} s^{-1}. Preliminary experiments showed they are sensitive to the increase of temperature and light intensity and the growth rate is low during 8 months after isolation. Therefore, when testing the suitable photo-temperature conditions for its growth with orthogonal experiments, the parameters were set slightly higher: temperature (T1: 25 ± 1°C, T2: 28 ± 1°C), light intensity (L1: 42 ± 2, L2: 62 ± 2 μmol photons m^{-2} s^{-1}). Other conditions are as follows: salinity 28 ppt, pH 8.05, and 12 h photoperiod, batch culture in small chambers. Each set of treatments has three replicates ($n = 3$). The algal cell density and growth rate were measured in 7 and 14 days, respectively. The specific growth rate (K, doubling/day) was calculated as:

$$K = (\ln Z_t - \ln Z_0)/t$$

Where Z_0 is the cell density at the starting point of the experiment, and Z_t is the cell density at day 7 and 14, respectively, t is the duration of cultures in days.

Test of Optimum Salinity for Growth

The test was performed at 12 months after isolation. Considering that the algae were transferred from coral cells to the external environment, they may be more sensitive to salinity changes. Therefore, a dense salinity gradient was set to determine the optimum salinity: 10, 15, 20, 24, 26, 28, 30, 32, 35, and 40 ppt. Each salinity has three culture replicates ($n = 3$). The salinity gradients of cultures were obtained by diluting 0.2 μm filtered seawater (FSW) with distilled water or amended with NaCl (pH = 8.05). According to the results of orthogonal experiment and preliminary experiments, the temperature was set at 25 ± 1°C and light condition was under 62 ± 2 μmol photons m^{-2} s^{-1} with 12 h photoperiod. Batch culture in small chambers. The algal cell densities and growth rates were measured on days 7, 21, and 28, respectively, as above-mentioned.

Statistical Analyses

Statistical analysis was carried out with IBM SPSS Statistics 26.0. Kruskal–Wallis Test was used to evaluate the significance of differences in morphological and structural parameters between GF19C1 and its symbiotic congeners (SC). One way ANOVA was used to investigate the salinity (ten levels) on the growth rate of GF19C1, with Tukey *post hoc* comparisons to locate significant differences. Similar analytical methods are used to compare the effects of temperature (two levels) and illumination (two levels) on the algal growth rates. The growth rate data of 7 days in the orthogonal experiment of light and temperature were log-transformed before analysis, because they did not conform to the homogeneity of variance. Differences with $P < 0.05$ were considered as significant for all analysis.

RESULTS

Identification of the Algal Symbionts of *Galaxea fascicularis*

The electrophoretogram of n18S-rDNA *Taq*I-generated RFLPs from a *Galaxea fascicularis* population ($n = 23$) showed that, only the fingerprint patterns of individuals 5gw14 and 5gw15 were identical to that of type C coral (Santos et al., 2002; two bands, 700 bp and 1,000 bp as shown in **Figure 1**), and 18 individuals were associated simultaneously with type C and D, while the other three samples were associated with type D only. The individual 5gw14 was then chosen to isolate the algal symbionts.

Phylogenetic Identity of the Monoclonal Algal Strains

The internal transcribed spacer (ITS1 and ITS2) sequences obtained from monoclonal cultured algae were all identical to *Cladocopium* sp. C1 ITS1 (AF380551, Van Oppen et al., 2001) and *Cladocopium* sp. C1 ITS2 (GU111864, LaJeunesse et al., 2010), respectively. The algal $psbA^{ncr}$ sequence is identical to *Cladocopium* sp. C1 isolate 152 clone 16 $psbA^{ncr}$ (JQ043704), which differs from *Cladocopium goreaui* (JQ043677) by one base transversion and four insertion-deletions over the entire non-coding region (999 aligned bases) and therefore

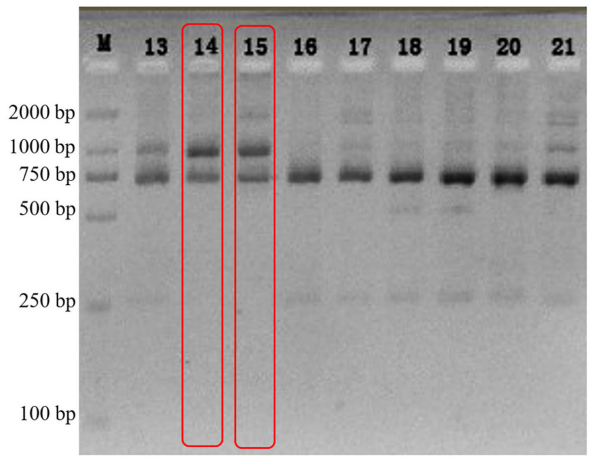

FIGURE 1 | The electrophoretogram of n18S-rDNA *Taq*I-generated RFLPs from *G. fascicularis* DNA.

represents a distinct haplotype variant of *C. goreaui* (LaJeunesse and Thornhill, 2011). The phylogenetic tree (**Supplementary Material 1**) based on $psbA^{ncr}$ regions (1,013 bp in total) show that, GF19C and *Cladocopium goreaui* belong to two closest sister clades, while the entire *Cladocopium* sp. C1 isolates roughly divided into three clades. In sum, the algal strain isolated from *Galaxea fascicularis* and cultured *in vitro* in this study were *Cladocopium* sp. C1 (family: Symbiodiniaceae). We designated this strain as GF19C1.

Morphology and Ultrastructure of GF19C1

Most of GF19C1 cells were on the coccoid stage of gymnodinioid dinoflagellate, with smaller mean size than their symbiotic congeners (SC). The average long diameter and short diameter of GF19C1 were 9.65 ± 1.07 μm and 8.92 ± 1.18 μm (**Table 1**), respectively, which were significantly smaller than those of their SC (**Table 1**, 10.32 ± 0.97 μm and 9.83 ± 0.93 μm, respectively, $P = 0.003$, Kruskal–Wallis test, same below). Contrastingly, the average division ratio of GF19C1 was 17.6 ± 3.7%, significantly higher than that of its SC (9.7 ± 1.7%, $P = 0.010$, **Table 1**).

The ultrastructure pattern of coccoid stage of GF19C1 (**Figure 2**) is similar to that of algal symbionts from other coral hosts (Berner and Izhaki, 1994; Wham et al., 2017). The cell walls of GF19C1 (**Figure 2B-1/-2**) are composed of an electron-translucent material, showing the homogeneous fine granular structure as described by Palincsar et al. (1988) and Lesser and Shick (1990), while the cell wall of their SC (**Figure 2A**) is dark and thin, lacking the granular layer presented in GF19C1. In addition, the mean thickness of cell walls of GF19C1 is 0.178 ± 0.042 μm, which is significantly thicker than that of its SC (0.061 ± 0.022 μm, $P = 0.000$, **Table 1**, also see **Figures 2A,B-1/-2**, coupled arrows).

The symbiont cells of *G. fascicularis* have several well-developed and long-striped chloroplasts that are connected with each other and surround continuously the outer layer of cytoplasm in 1–2 layers (**Figure 2A**), whereas in GF19C1 cells, the chloroplasts are short and discontinuous (**Figures 2B-1/-2**). The chloroplast volume fraction of symbiont cells was 56.4 ± 10.1%, which is significantly higher ($P = 0.000$) than that of GF19C1 (12.9 ± 3.9%, **Table 1**), but there is no discernable difference in the surface density of thylakoid lamellae (SDTL) relative to chloroplast volume (**Table 1**, 10.27 ± 0.91 vs. 10.79 ± 1.66, $P = 0.602$). The vacuoles are often small and numerous in symbiont cells, with regular shapes of round or ellipse (**Figure 2A**), while in GF19C1 cells, the vacuole usually presents an irregular large cavity (**Figures 2B-1/-2**). The vacuole volume fraction of GF19C1 was significantly higher than that of its SC (16.8 ± 8.14% vs. 3.5 ± 1.44%, $P = 0.009$, **Table 1**). Compared to the symbionts *in hospite*, more freshly divided cells were observed in GF19C1 (**Figure 2B-1**) and the newly formed cell wall is thin and membranous, instead of vesicular (**Figure 2B-1**, triangle).

In addition, no significant differences were found in both the volume fractions of mitochondria and accumulation bodies between GF19C1 cells and their SC (**Table 1**, 1.3 ± 0.18% vs. 1.2 ± 0.18% $P = 0.456$ and 4.4 ± 2.06% vs. 9.5 ± 6.13% $P = 0.347$, respectively).

Effect of Light and Temperature on the Growth Rate of GF19C1

The results of orthogonal experiments in 8 months post-isolation showed that, at day 7, the growth rates (K) of T1L1 (low temperature/weak light) and T1L2 (low temperature/strong light) groups were the highest (both are 0.099, **Figure 3** and **Supplementary Table 2**), which was significantly higher than that of T2L1 (high temperature/weak light) and T2L2 (high temperature/strong light) groups (ANOVA, $P < 0.05$). At day 14, the growth rate of T1L1 and T1L2 were 0.024 and 0.022 (**Figure 3** and **Supplementary Table 2**), respectively, which were also notably higher than that of T2L1 (0.010) and T2L2 (0.010) ($P < 0.01$), indicating that GF19C1 prefers the lower temperature (T1, 25 ± 1 vs. 28 ± 1°C) at which it was consistently maintained ever since the isolation. On the other hand, the impact of light intensities (42 ± 2/62 ± 2 μmol photons m^{-2} s^{-1}) in this experiment showed no significant difference on algal growth.

Effect of Salinity on the Growth Rate of GF19C1

The effects of different salinity (S) on the growth rate of GF19C1 (12 months post-isolation) were shown in **Figure 4** and **Supplementary Table 3**.

The cell numbers of all salinity groups increased during the first 7-day period. Where the salinity ranging from 10 to 28 ppt, the growth rates increased with the increasing salinities. That is, when $S = 10$, the growth rate (K_{10}) was the minimum (0.080), while K_{28} was the highest (0.108, and the cell density reached to 33.85 × 10^4 cells/mL) while K_{30} is the second (0.107, the cell density was 33.64 × 10^4 cells/mL). On the contrast, the growth rates decreased with the increase of salinity from 28 to 40 ppt, as K_{40} decreased to 0.096. Nonetheless, the variance analysis indicated no significant difference in growth rates when the salinity ranging from 26 to 32 ppt ($P > 0.05$).

TABLE 1 | Comparison of the morphology and structure of GF19C1 and its symbiotic congeners (SC).

Morphology/structure		GF19C1	SC	Significance
Cell size	long diameter	9.65 ± 1.07 μm	10.32 ± 0.97 μm	***P* = 0.003**
	short diameter	8.92 ± 1.18 μm	9.83 ± 0.93 μm	***P* = 0.008**
Cell wall thickness		0.178 ± 0.042 μm	0.061 ± 0.022 μm	***P* = 0.000**
Chloroplast volume density		12.9 ± 3.9%	56.4 ± 0.1%	***P* = 0.000**
Surface density of thylakoid lamellae		10.27 ± 0.91	10. 79 ± 1.66	*P* = 0.602
Volume fraction (VF) of vacuole		16.80 ± 8.14%	3.50 ± 1.44%	***P* = 0.009**
VF of accumulation bodies		4.40 ± 2.06%	9.50 ± 6.13%	*P* = 0.347
VF of mitochondria		1.30 ± 0.18%	1.20 ± 0.18%	*P* = 0.456
Cell division ratio		17.6 ± 3.7%	9.7 ± 1.7%	***P* = 0.010**

P values are obtained from Kruskal–Wallis test. Data are mean ± standard deviation. The significant P values are indicated in bold.

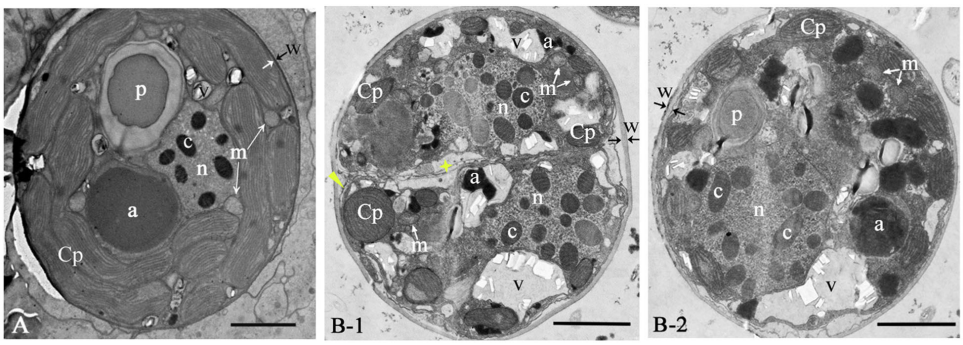

FIGURE 2 | The ultrastructure of *Cladocopium* sp. C1 from coral *G. fascicularis*. **(A)** *in situ*; **(B-1/B-2)** GF19C1, *in vitro* cultured. Panel **(B-1)** is the newly divided cell, showing new cell membranes (star) and cell wall forming (triangle). a, accumulation body; c, chromosome; Cp, chloroplast; m, mitochondrion; n, Nucleus; p, pyrenoid; v, vacuole; w, cell wall, paired arrows indicate the thickness of the cell wall. Scale bars = 2 μm.

At day 21, K_{30}, and K_{32} reached the peak (0.059), where the cell densities were 54.93 × 10^4 and 55.14 × 10^4 cells/mL, respectively. Besides, it was observed that the cytochrome gradually faded in the groups of salinity lower than 28 ppt.

At day 28, the cell density declined in all salinity groups. However, the decline in groups $S \leq 30$ are still higher than that of groups $S = 32$ and 35, which had the highest cell density (50.92 × 10^4 and 50.71 × 10^4 cells/mL). Hence, we concluded that the GF19C1 strain can grow normally in the salinity ranging from 26–40 ppt, and the optimum salinity is between 28–32 ppt.

Overall, the growth rate K in this test (12 months post-isolation, **Figure 4** and **Supplementary Table 3**) are significantly higher than that of light-temperature orthogonal experiment (8 months post-isolation; **Figure 3** and **Supplementary Table 2**).

DISCUSSION

The symbiosis between algal symbionts and reef-building corals were thought to emerge in the mid-Triassic period (Stanley, 1981). In the ensuing 230 million years of intense differentiation and speciation of the hermatypic corals (Shepard, 1964), the two mutualistic sides, corals and their endosymbiotic algae, have undergone precise coordination or a series of synergistic mutations and formed obligate interdependence (Antonelli et al., 2016). The photosynthetic symbionts have established relatively stable and complex communities in specific coral species and geographic regions (Lewis et al., 2019), and the symbiont biota also changed with the persistence and periodicity of environmental stress (Lee et al., 2016; Lewis et al., 2019). On the other hand, adapted to the life in coral cells, symbionts and their host have reached a delicate metabolic balance (Lin et al., 2019) and physiological compromises (such as abandoning sexual reproduction and being compatible with the coral's immune system) (Antonelli et al., 2016). Therefore, when we attempt to isolate the symbionts from coral cells and establish genetically and physiologically consistent strains, the algae should experience drastic morphological and physiological changes so as to adapt to the new artificial culture environment.

Isolation and *in vitro* Culture of GF19C1

The isolation of algal symbionts from *Galaxea fascicularis* and the establishment of monoclonal strain GF19C1 have undergone a tedious process for more than 1 year, while many efforts have been taken for optimization, including culture medium components, light intensity managements, and contamination control etc. We found that the common medium (e.g., f/2 and L1 medium) could be applied to GF19C1 *in vitro* culture upon minor modification. One of the greatest challenges was to eliminate the contamination of diatoms, protozoa, and fungi in the culture system. Although the use of triple antibiotics (penicillin, streptomycin and kanamycin, final concentration of

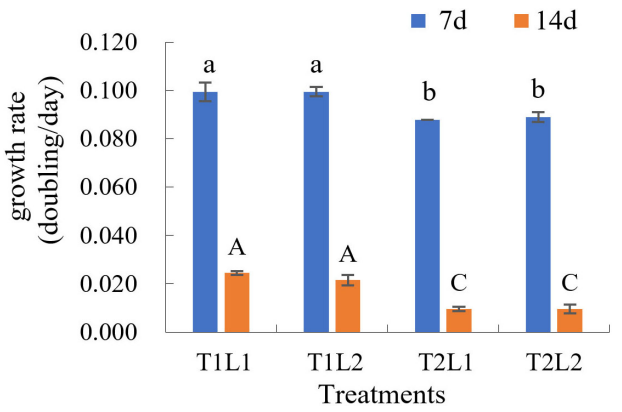

FIGURE 3 | The growth rate (*K*, doubling/day) of GF19C1 in the orthogonal experiments of illumination (weak L1/strong L2) and temperature (low T1/high T2). Each set of treatments has three replicates ($n = 3$). The error bars stand for standard deviation (SD). Superscripts in lowercase and uppercase letters denote twice ANOVA multiple comparisons, followed by Tukey *post hoc* to locate the significant differences. Different letters within the same comparison group mean significant difference (ANOVA, $P < 0.05$).

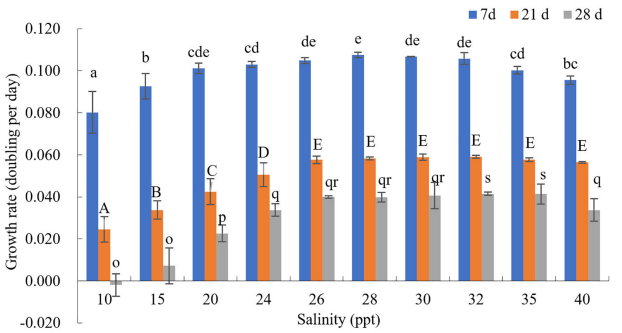

FIGURE 4 | The growth rate (*K*, doubling/day) of GF19C1 under a series of salinity (ppt) gradient. Superscripts in a-e, A-E, and o-s denote three ANOVA multiple comparisons, followed by Tukey *post hoc* to locate the significant differences. Different letters within the same comparison group mean significant difference (ANOVA, $P < 0.05$). Each salinity has three replicates ($n = 3$). The error bars stand for standard deviation (SD).

200, 100, and 100 μg/mL, respectively, Lin et al., 2015) can effectively inhibit the bacteria growth in the cultures, however, contaminants like fungi, diatoms and protozoa that originated from the coral exoskeleton or internal polyps during isolation, were difficult to eliminate. Chakravarti and Van Oppen (2018) used an antifungal cocktail (consisting of nystatin, amphotericin, and GeO_2, final concentration 100 μg/mL, 2.5 μg/mL and 50 μM, respectively) to inhibit the contamination of fungi and other organisms during the centrifugal collection of symbiotic algae from plenty of broken tissues. As reported here, we used a different strategy to reduce the sources of contamination. We selected the tentacles of *Galaxea fascicularis*, which were easily sampled and cleaned for symbiont isolation. Meanwhile, we also gently teared down the tissue to avoid the damage of symbiont cells. The algal colonies were then cultured by the soft agar plates containing triple antibiotics. We eventually obtained the stable and passaged algal -strain GF19C1 cell line. The protocol of the established GF19C1 strain mainly followed the monoclonal culture procedure from Schoenberg and Trench (1980a), which is a rather rigorous and tedious approach with the process involving the rejection of the dominant alga to achieve culture purification during the algae culture (Chakravarti and Van Oppen, 2018).

The symbiotic phylotypes associated with *G. fascicularis* were mainly dominated by Symbiodiniaceae ITS2-C1, D1, and C21a, along with numerous of other background clade C phylotypes (Xu, 2019; Wepfer et al., 2020). Even identified as clade C phylotype by n18S-rDNA and *Taq*I-generated RFLPs (Santos et al., 2002), the symbiotic biota in *G. fascicularis* could also possess multiple composition of both dominant and background symbionts when probed with ITS2 sequence tagging. Thus, a more rigorous strategy of isolation and purification process is necessary to achieve the pure cell line.

Ultrastructural Changes of GF19C1

Our study revealed that the cell wall of *in vitro* cultured GF19C1 could be significantly thicker (about twofold) than that of their symbiotic congeners (SC). This phenomenon is rather common (Lesser and Shick, 1990), but there are several aspects to account for its causes and results. One probable explanation is that, the thinner cell wall of symbionts *in hospite* is an adaptation to live inside coral cells, which may facilitate the transport of nutrients between coral cell and symbiont (Schoenberg and Trench, 1980b). Freudenthal (1962) noted that, the algal symbiont in coral cell is haplontic and autotrophic vegetative cell. When cultured *in vitro*, they become vegetative cyst by thickening the cell wall, which could restore both sexual and asexual reproductive potential through producing autospores, aplanospores, or motile gymnodinioid zoospores, or possible gametes, so that they can adapt to the outside environment (Freudenthal, 1962). Palincsar et al. (1988) also observed the phenomenon of cell wall thickening of algae during growth outside the host sea anemone *Aiptasia pallida*. This was thought to be related to an increase in mitotic rate after isolation, because during the division the entire new cell walls were synthesized resulting thickened newly produced cells (Palincsar et al., 1988). In addition, the mitotic rate of GF19C1 also increased by 8% higher than that of its SC, which was similar to that (10%) of *in vitro* cultured algal symbiont isolated from *A. pallida* (Palincsar et al., 1988).

The volume fraction (VF) of chloroplast of GF19C1 cells was significantly lower than that of their SC, whereas the surface density of thylakoid lamellae (SDTL) showed no obvious change. Unlike their SC, *in vitro* cultured algal symbionts don't have to provide photosynthetic nutrients for coral cells in exchange for their protection (Davies, 1993). Therefore, their photosynthetic burden is reduced and they don't need to possess so many photosynthetic apparatuses. Especially when cultured *in vitro*, the light intensity is usually greater than that in host cells. Interestingly, for the algal strain isolated from sea anemone *Aiptasia pallida*, its VF of chloroplast didn't change but SDTL remarkably decreased, when compared to their SC (Lesser and Shick, 1990). Perhaps, that is another photo-adaptive strategy to a greater outside (*in vitro*) light intensity.

With the notable reduction in chloroplast VF, the vacuoles of GF19C1 cells could join together and merge into one or two larger irregular vacuoles. And the volume density of vacuoles increases significantly, which may favor frequent mitosis in GF19C1. Freudenthal (1962) also found *in vitro* cultured symbiont cells have 1–2 large vacuoles, meanwhile, contain intact chloroplasts and accumulation bodies. Such cells not only do not mean aging, but extensively appear in the culture medium containing actively-reproducing algae. The appearance of these big vacuoles could imply some unknown factors on regulating cell physiology. We speculate that it is likely to be associated with the increased demand for processing metabolic wastes and more flexibility in space as cell division accelerating.

Suitable Light, Temperature and Salinity Conditions of GF19C1 Growth

Light and temperature are critical environmental factors for algae growth. We found that the initially isolated algal cells show a high sensitivity to light intensity, and might bleach to death in 3 days under 50 μmol photons m^{-2} s^{-1}, with 12:12 light/dark cycle. If the light intensity was reduced to 40 μmol photons m^{-2} s^{-1}, the survival time of the algal cells could be significantly prolonged. Even within coral cells, a sudden increase in light intensity could also reduce the pigment content rather than decrease the density of symbionts, and result in coral bleaching (Hoegh-Guldberg and Smith, 1989). Generally, light intensity has a greater effect on algal growth than temperature (Sakami, 2000). The appropriate light intensity range for GF19C1 increased from 40 to 64 μmol photons m^{-2} s^{-1} in 8 months post-isolation, when the cell growth rate at 25 ± 1°C was significantly higher ($P < 0.05$) than that at 28 ± 1°C. This may be due to the fact that GF19C1 have been kept consistently at 25 ± 1°C since isolation, which result in an inertia of temperature preference for its growth and division so that they could not adapt to the sudden increase of temperature. The growth rate K on 8 months post-isolation was rather low. This may be because, on the one hand, GF19C1 hasn't adapted to the extracellular environment yet, or on the other hand, the restrained influence of host cytokines is still present (Cunning et al., 2015). When GF19C1 was cultured for 12 months *in vitro*, the growth rate K increased to 0.108, and showed more rapid evolution than the coral host (Chakravarti and Van Oppen, 2018). Although this K value was still low compared with other free-living dinoflagellates (Liang et al., 2011), it is comparable to that of other algal symbionts cultured *in vitro* (Chakravarti and Van Oppen, 2018).

Given that when GF19C1 were transferred from coral cells to the external environment, they may be more sensitive to salinity changes. Therefore, a dense gradient (ten gradients. from 10 to 40 ppt) was set to determine the optimum salinity *in vitro*. The effect of salinity on aquatic organisms is mainly manifested in the regulation of osmotic pressure in cells (Sakami, 2000). At day 7, the density of GF19C1 increased in all salinity groups (10–40 ppt, **Supplementary Table 3**). As the experiment went on, comparing with the high salinity groups, the growth of low salinity groups (10–24 ppt) decreased more significantly (**Figure 4** and **Supplementary Table 3**) because of the accumulation of osmotic pressure (Maboloc et al., 2015), at day 21, we can observe that the cytochrome gradually faded in the low salinity groups. Compared with the algal symbionts on mantle of juvenile giant clam *Tridacna gigas*, which display acclimation response to salinity of 25 ppt (Maboloc et al., 2015), GF19C1 was more sensitive to low salinity stress. In addition, we also observed that, the cell density declined in all salinity groups at 28 days post-experiment, that is because the batch culture model was applied during the test and at that time the algae was at the Death/Lysis phase (Farag and Price, 2013).

GF19C1 cells can grow normally in a salinity range of 26–40 ppt, and its optimum salinity is 28–32 ppt, comparable to the suitable salinity (32–40 ppt) of most corals (Veron, 1986). In suitable ranges, the effects of salinity on algal growth are not as obvious as that of light and temperature (Hoegh-Guldberg and Smith, 1989).

To sum up, GF19C1 is the first *in vitro* cultivated monoclonal strain isolated from the endosymbiotic biota of the scleractinian coral *Galaxea fascicularis*. When cultured *in vitro*, GF19C1 cells show morphological changes, preparation for the recovery of sexual reproduction, rapid adaptation to light intensity, and rapid evolution of growth rate. Symbiodiniaceae C1 are the most widespread algal symbiont in reef-building corals (Stat et al., 2008), their distribution ranged from high latitude region e.g., Korea-Jeju Island and Japan, to tropical region e.g., South China Sea (Reimer et al., 2006; Ng and Ang, 2016; Chen et al., 2019, 2020; Wepfer et al., 2020), thus they have experienced large sea surface temperature variations and high turbidity (Ng and Ang, 2016; Wepfer et al., 2020). Therefore, in future study it is necessary to further explore the adaptive potential of GF10C1 to multiple environmental factors and high gradient changes. The establishment of monoclonal culture technology will make it possible for the isolation and *in vitro* culture of *G. fascicularis* and other hermatypic corals-associated algal symbiont species, which is important to elucidate the physiological and ecological characteristics of various species of symbiont, and their cooperative mechanisms within coral hosts, and will help to further clarify their role and function in the environment adaptation of scleractinian corals.

DATA AVAILABILITY STATEMENT

The original contributions presented in the study are included in the article/**Supplementary Material**, further inquiries can be directed to the corresponding author/s.

AUTHOR CONTRIBUTIONS

JW, JC, and SW contributed equally to this study. YW was responsible for conceptualization, funding acquisition, and resources. JW, JC, FL, CF, and SW were responsible for experimental investigation. JW and JC were mainly responsible for data processing and picture modification. YW, JW, and JC were responsible for the draft preparation. YW proofread the final manuscript before submission. All authors have read and approved the final manuscript.

FUNDING

This work was supported by the National Key R&D Program of China (2018YFC1406500) and the Hainan Provincial Key R&D Program (ZDYF2018108).

SUPPLEMENTARY MATERIAL

The Supplementary Material for this article can be found online at: https://www.frontiersin.org/articles/10.3389/fphys.2020.621111/full#supplementary-material

REFERENCES

Antonelli, P. L., Rutz, S. F., Sammarco, P. W., and Strychar, K. B. (2016). Evolution of symbiosis in hermatypic corals: a model of the past, present, and future. *Nonlinear Anal. Real World Appl.* 32, 389–402. doi: 10.1016/j.nonrwa.2016.05.004

Aranda, M., Li, Y., Liew, Y. J., Baumgarten, S., Simakov, O., Wilson, M. C., et al. (2016). Genomes of coral dinoflagellate symbionts highlight evolutionary adaptations conducive to a symbiotic lifestyle. *Sci. Rep.* 6:39734. doi: 10.1038/srep39734

Barshis, D. J., Ladner, J. T., Oliver, T. A., and Palumbi, S. R. (2014). Lineage-specific transcriptional profiles of *Symbiodinium* spp. unaltered by heat stress in a coral host. *Mol. Biol. Evol.* 31, 1343–1352. doi: 10.1093/molbev/msu107

Berner, T., and Izhaki, I. J. U. O. H. P. (1994). Effect of exogenous nitrogen levels on ultrastructure of zooxanthellae from the hermatypic coral *Pocillopora damicornis*. *Pac. Sci.* 48, 254–262.

Chakravarti, L., and Van Oppen, M. (2018). Experimental evolution in coral photosymbionts as a tool to increase thermal tolerance. *Front. Mar. Sci.* 5:227.

Chen, B., Yu, K., Liang, J., Huang, W., Wang, G., Su, H., et al. (2019). Latitudinal variation in the molecular diversity and community composition of *Symbiodiniaceae* in coral from the South China sea. *Front. Microbiol.* 10:1278. doi: 10.3389/fmicb.2019.01278

Chen, B., Yu, K., Qin, Z., Liang, J., Wang, G., Huang, X., et al. (2020). Dispersal, genetic variation, and symbiont interaction network of heat-tolerant endosymbiont *Durusdinium trenchii*: insights into the adaptive potential of coral to climate change. *Sci. Total Environ.* 723:138026. doi: 10.1016/j.scitotenv.2020.138026

Chen, D., Wang, D., Zhu, J., Li, Y., Wu, X., and Wang, Y. (2013). Identification and characterization of microsatellite markers for scleractinian coral *Galaxea fascicularis* and its symbiotic zooxanthellae. *Conserv. Genet. Resour.* 5, 741–743. doi: 10.1007/s12686-013-9895-7

Coleman, A. W., Suarez, A., and Goff, L. J. (1994). Molecular delineation of species and syngens in volvocacean green algae (chlorophyta). *J. Phycol.* 30, 80–90. doi: 10.1111/j.0022-3646.1994.00080.x

Cunning, R., Vaughan, N., Gillette, P., Capo, T., Mate, J., and Baker, A. (2015). Dynamic regulation of partner abundance mediates response of reef coral symbioses to environmental change. *Ecology* 96, 1411–1420. doi: 10.1890/14-0449.1

Davies, P. S. (1993). "Endosymbiosis in marine cnidarians," in *Plant-Animal Interactions in the Marine Benthos*, eds D. M. John, S. J. Hawkins, and J. H. Price (England: Clarendon, Oxford), 511–540.

Elias, H., and Hyde, D. M. (1980). An elementary introduction to stereology (quantitative microscopy). *Am. J. Anat.* 159, 411–446. doi: 10.1002/aja.1001590407

Farag, I., and Price, K. (2013). Resources Conservation in Microalgae Biodiesel Production. *Int. J. Eng. Tech. Res.* 1, 49–56.

Ferrier-Pages, C., Richard, C., Forcioli, D., Allemand, D., Pichon, M., and Shick, J. M. (2007). Effects of temperature and UV radiation increases on the photosynthetic efficiency in four scleractinian coral species. *Biol. Bull.* 213, 76–87. doi: 10.2307/25066620

Freudenthal, H. D. (1962). *Symbiodinium* gen. nov. and *Symbiodinium* microadriaticum sp. nov., a Zooxanthella: taxonomy, life cycle, and morphology. *J. Protozool.* 9, 45–52. doi: 10.1111/j.1550-7408.1962.tb02579.x

Hawkins, T. D., Krueger, T., Wilkinson, S. P., Fisher, P. L., and Davy, S. K. (2015). Antioxidant responses to heat and light stress differ with habitat in a common reef coral. *Coral Reefs* 34, 1229–1241. doi: 10.1007/s00338-015-1345-4

Hidaka, M. (1992). Use of nematocyst morphology for taxonomy of some related species of scleractinian corals. *Galaxea* 11, 21–28.

Hoegh-Guldberg, O., Mumby, P. J., Hooten, A. J., Steneck, R. S., Greenfield, P., Gomez, E., et al. (2007). Coral reefs under rapid climate change and ocean acidification. *Science* 318, 1737–1742. doi: 10.1126/science.1152509

Hoegh-Guldberg, O., and Smith, G. J. (1989). The effect of sudden changes in temperature, light and salinity on the population density and export of zooxanthellae from the reef corals *Stylophora pistillata* Esper and *Seriatopora hystrix* Dana. *J. Exp. Mar. Biol. Ecol.* 129, 279–303. doi: 10.1016/0022-0981(89)90109-3

Hughes, T. P., Anderson, K. D., Connolly, S. R., Heron, S. F., Kerry, J. T., Lough, J. M., et al. (2018). Spatial and temporal patterns of mass bleaching of corals in the Anthropocene. *Science* 359, 80–83. doi: 10.1126/science.aan8048

Hughes, T. P., Kerry, J. T., lvarez-Noriega, M., lvarez-Romero, J. G., Anderson, K. D., Baird, A. H., et al. (2017). Global warming and recurrent mass bleaching of corals. *Nature* 543, 373–377. doi: 10.1038/nature21707

Hume, B. C. C., D'angelo, C., Smith, E. G., Stevens, J. R., Burt, J., and Wiedenmann, J. (2015). *Symbiodinium thermophilum* sp. nov., a thermotolerant symbiotic alga prevalent in corals of the world's hottest sea, the Persian/Arabian Gulf. *Sci. Rep.* 5:8562. doi: 10.1038/srep08562

Kumar, S., Stecher, G., Li, M., Knyaz, C., and Tamura, K. (2018). MEGA X: molecular evolutionary genetics analysis across computing platforms. *Mol. Biol. Evol.* 35, 1547–1549. doi: 10.1093/molbev/msy096

LaJeunesse, T., Pettay, D., Sampayo, E., Phongsuwan, N., Brown, B., Obura, D., et al. (2010). Long-standing environmental conditions, geographic isolation and host-symbiont specificity influence the relative ecological dominance and genetic diversification of coral endosymbionts in the genus *Symbiodinium*. *J. Biogeogr.* 37, 785–800. doi: 10.1111/j.1365-2699.2010.02273.x

LaJeunesse, T., and Trench, R. (2000). Biogeography of two species of *Symbiodinium* (Freudenthal) inhabiting the intertidal sea anemone *Anthopleura elegantissima* (Brandt). *Biol. Bull.* 199, 126–134. doi: 10.2307/1542872

LaJeunesse, T. C. (2001). Investigating the biodiversity, ecology, and phylogeny of endosymbiotic dinoflagellates in the genus *symbiodinium* using the its region: in search of a "species" level marker. *J. Phycol.* 37, 866–880. doi: 10.1046/j.1529-8817.2001.01031.x

LaJeunesse, T. C., Parkinson, J. E., Gabrielson, P. W., Jeong, H. J., Reimer, J. D., Voolstra, C. R., et al. (2018). Systematic revision of *Symbiodiniaceae* highlights the antiquity and diversity of coral endosymbionts. *Curr. Biol.* 28, 2570–2580.e2576. doi: 10.1016/j.cub.2018.07.008

LaJeunesse, T. C., and Thornhill, D. J. (2011). Improved resolution of reef-coral endosymbiont (*Symbiodinium*) species diversity, ecology, and evolution through psbA non-coding region genotyping. *PLoS One* 6:e29013. doi: 10.1371/journal.pone.0029013

Lee, M. J., Jeong, H. J., Jang, S. H., Lee, S. Y., Kang, N. S., Lee, K. H., et al. (2016). Most low-abundance "Background" *Symbiodinium* spp. Are transitory and have minimal functional significance for symbiotic corals. *Microb. Ecol.* 71, 771–783. doi: 10.1007/s00248-015-0724-2

Lesser, M. P., and Farrell, J. H. (2004). Exposure to solar radiation increases damage to both host tissues and algal symbionts of corals during thermal stress. *Coral Reefs* 23, 367–377. doi: 10.1007/s00338-004-0392-z

Lesser, M. P., and Shick, J. M. (1990). Effects of visible and ultraviolet radiation on the ultrastructure of zooxanthellae (*Symbiodinium* sp.) in culture and in situ. *Cell Tissue Res.*261, 501–508. doi: 10.1007/bf00313529

Lewis, C., Neely, K. L., and Rodriguez-Lanetty, M. (2019). Recurring episodes of thermal stress shift the balance from a dominant host-specialist to a background host-generalist zooxanthella in the threatened pillar coral, *Dendrogyra cylindrus*. *Front. Mar. Sci.* 6:1–15. doi: 10.3389/fmars.2019.00005

Liang, J. L., Long, L. J., Zhang, S., and Wu, J. (2011). Influence of trace elements, Fe, Mn, and Co, on growth and toxin-producing of toxic marine dinoflagellate *Coolia monotis*. *J. Trop. Oceanogr.* 30, 119–123.

Lin, M.-F., Takahashi, S., Forêt, S., Davy, S. K., and Miller, D. J. (2019). Transcriptomic analyses highlight the likely metabolic consequences of colonization of a cnidarian host by native or non-native *Symbiodinium* species. *Biol. Open* 8:bio038281. doi: 10.1242/bio.038281

Lin, S., Cheng, S., Song, B., Zhong, X., Lin, X., Li, W., et al. (2015). The Symbiodinium kawagutii genome illuminates dinoflagellate gene expression and coral symbiosis. *Science* 350, 691–694. doi: 10.1126/science.aad0408

Maboloc, E. A., Puzon, J. J. M., and Villanueva, R. D. (2015). Stress responses of zooxanthellae in juvenile *Tridacna gigas* (Bivalvia, Cardiidae) exposed to reduced salinity. *Hydrobiologia* 762, 103–112. doi: 10.1007/s10750-015-2341-y

Mallela, J. (2013). Calcification by reef-building sclerobionts. *PLoS One* 8:e60010. doi: 10.1371/journal.pone.0060010

Mieog, J. C., Van Oppen, M. J., Berkelmans, R., Stam, W. T., and Olsen, J. L. (2009). Quantification of algal endosymbionts (*Symbiodinium*) in coral tissue using real-time PCR. *Mol. Ecol. Res.* 9, 74–82. doi: 10.1111/j.1755-0998.2008.02222.x

Moore, R. B., Ferguson, K. M., Loh, W. K. W., Hoegh-Guldberg, O., and Carter, D. A. (2003). Highly organized structure in the non-coding region of the psbA minicircle from clade C *Symbiodinium*. *Int. J. Syst. Evol. Micr.* 53, 1725–1734. doi: 10.1099/ijs.0.02594-0

Ng, T. Y., and Ang, P. (2016). Low symbiont diversity as a potential adaptive strategy in a marginal non-reefal environment: a case study of corals in Hong Kong. *Coral Reefs* 35, 941–957. doi: 10.1007/s00338-016-1458-4

Obura, D. O. (2009). Reef corals bleach to resist stress. *Mar. Pollut. Bull.* 58, 206–212. doi: 10.1016/j.marpolbul.2008.10.002

Palincsar, J. S., Jones, W. R., and Palincsar, E. E. (1988). Effects of isolation of the endosymbiont *Symbiodinium microadriaticum* (Dinophyceae) from its host Aiptasia pallida (Anthozoa) on cell wall ultrastructure and mitotic rate. *Trans. Am. Microsc. Soc.* 107, 53–66. doi: 10.2307/3226408

Pochon, X., and Gates, R. D. (2010). A new Symbiodinium clade (Dinophyceae) from soritid foraminifera in Hawai'i. *Mol. Phylogenet. Evol.* 56, 492–497. doi: 10.1016/j.ympev.2010.03.040

Pochon, X., Montoya-Burgos, J. I., Stadelmann, B., and Pawlowski, J. (2006). Molecular phylogeny, evolutionary rates, and divergence timing of the symbiotic dinoflagellate genus *Symbiodinium*. *Mol. Phylogenet. Evol.* 38, 20–30. doi: 10.1016/j.ympev.2005.04.028

Reimer, J. D., Takishita, K., and Maruyama, T. (2006). Molecular identification of symbiotic dinoflagellates (*Symbiodinium* spp.) from *Palythoa* spp. (Anthozoa: Hexacorallia) in Japan. *Coral Reefs* 25, 521–527. doi: 10.1007/s00338-006-0151-4

Rosenberg, E. Z.-R. (2013). *The Hologenome Concept: Human, Animal and Plant Microbiota*. New York, NY: Springer International Publishing. doi: 10.1007/978-3-319-04241-1

Rowan, R., and Powers, D. A. (1991a). A molecular genetic classification of zooxanthellae and the evolution of animal-algal symbioses. *Science* 251, 1348–1351. doi: 10.1126/science.251.4999.1348

Rowan, R., and Powers, D. A. (1991b). Molecular genetic identification of symbiotic dinoflagellates(zooxanthellae). *Mar. Ecol. Prog. Ser. Oldendorf.* 71, 65–73. doi: 10.3354/meps071065

Sakami, T. (2000). Effects of temperature, irradiance, salinity and inorganic nitrogen concentration on coral zooxanthellae in culture. *Fish. Sci.* 66, 1006–1013. doi: 10.1046/j.1444-2906.2000.00162.x

Santos, S. R., Taylor, D. J., Kinzie, I. I. I. R. A., Hidaka, M., Sakai, K., and Coffroth, M. A. (2002). Molecular phylogeny of symbiotic dinoflagellates inferred from partial chloroplast large subunit (23S)-rDNA sequences. *Mol. Phylogenet. Evol.* 23, 97–111. doi: 10.1016/s1055-7903(02)00010-6

Schoenberg, D., and Trench, R. (1980a). Genetic variation in *Symbiodinium* (= *Gymnodinium*) microadriaticum Freudenthal, and specificity in its symbiosis with marine invertebrates. I. Isoenzyme and soluble protein patterns of axenic cultures of *Symbiodinium microadriaticum*. *Proc. R. Soc. Lond. B Biol. Sci.* 207, 405–427. doi: 10.1098/rspb.1980.0031

Schoenberg, D. A., and Trench, R. K. (1980b). Genetic Variation in *Symbiodinium* (=*Gymnodinium*) microadriaticum Freudenthal, and specificity in its symbiosis with marine invertebrates. II. Morphological variation in *Symbiodinium microadriaticum*. *Proc. R. Soc. B Biol. Sci.* 207, 429–444. doi: 10.1098/rspb.1980.0032

Shepard, F. P. J. S. (1964). Sea level changes in the past 6000 years: Possible archeological significance. *Science* 143, 574–576. doi: 10.1126/science.143.3606.574

Shinzato, C., Shoguchi, E., Kawashima, T., Hamada, M., Hisata, K., Tanaka, M., et al. (2011). Using the *Acropora digitifera* genome to understand coral responses to environmental change. *Nature* 476, 320–323. doi: 10.1038/nature10249

Stanley, G. Jr. (1981). Early history of scleractinian corals and its geological consequences. *Geology* 9, 507–511. doi: 10.1130/0091-7613(1981)9<507:ehosca>2.0.co;2

Stat, M., Morris, E., and Gates, R. D. (2008). Functional diversity in coral-dinoflagellate symbiosis. *Proc. Natl. Acad. Sci. U.S.A.* 105, 9256–9261. doi: 10.1073/pnas.0801328105

Trench, R. K. (1993). Microalgal-invertebrate symbiosis, a review. *Endocytobiosis Cell Res.* 9, 135–175.

Van Oppen, M. J., Mieog, J. C., Sanchez, C. A., and Fabricius, K. E. (2005). Diversity of algal endosymbionts (zooxanthellae) in octocorals: the roles of geography and host relationships. *Mol. Ecol.* 14, 2403–2417. doi: 10.1111/j.1365-294x.2005.02545.x

Van Oppen, M. J., Palstra, F. P., Piquet, A. M., and Miller, D. J. (2001). Patterns of coral-dinoflagellate associations in *Acropora*: significance of local availability and physiology of *Symbiodinium* strains and host-symbiont selectivity. *Proc. R. Soc. B Biol. Sci.* 268, 1759–1767. doi: 10.1098/rspb.2001.1733

Veron, J. E. N. (1986). *Corals of Australia and the Indo-Pacifc*. North Ryde, NSW: Angus & Robertson Publishers.

Veron, J. E. N. (2000). *Corals of the World*. Townsville, QLD: Australian Institute of Marine Science and CRR Qld Pty Ltd.

Wang, D. R., Wu, R., Li, Y. C., and Wu, Z. J. (2013). *Study on Tropical Typical Marine Ecosystem in Hainan Province*. Beijing: Ocean Press.

Watanabe, T., Nishida, M., Watanabe, K., Wewengkang, D. S., and Hidaka, M. (2005). Polymorphism in nucleotide sequence of mitochondrial intergenic region in scleractinian coral (*Galaxea fascicularis*). *Mar. Biotechnol.* 7, 33–39. doi: 10.1007/s10126-004-3200-4

Wepfer, P. H., Nakajima, Y., Hui, F. K., Mitarai, S., and Economo, E. P. (2020). Metacommunity ecology of *Symbiodiniaceae* hosted by the coral *Galaxea fascicularis*. *Mar. Ecol. Prog. Ser.* 633, 71–87. doi: 10.3354/meps13177

Wham, D. C., Ning, G., and Lajeunesse, T. C. (2017). *Symbiodinium glynnii* sp. nov., a species of stress-tolerant symbiotic dinoflagellates from pocilloporid and montiporid corals in the Pacific Ocean. *Phycologia* 56, 396–409. doi: 10.2216/16-86.1

Wu, Y. (2018). *Comparative Analysis of Growth and Structure Characteristics of the Two Types Stony Coral Galaxea Fascicularis*. Master of Fishery Science, Thesis, Hainan University, haikou.

Xu, T. (2019). *Community Structure Change of Symbiotic Zooxanthellae Responsing to High Temperature and Internal Symbiotic Bacterial Community Change in the Stony Coral Galaxea Fascicularis*. Master of Aquaculture, Thesis, Hainan University, haikou.

Ying, H., Cooke, I., Sprungala, S., Wang, W., Hayward, D. C., Tang, Y., et al. (2018). Comparative genomics reveals the distinct evolutionary trajectories of the robust and complex coral lineages. *Genome Biol.* 19:175. doi: 10.1186/s13059-018-1552-8

Conflict of Interest: The authors declare that the research was conducted in the absence of any commercial or financial relationships that could be construed as a potential conflict of interest.

frontiers in Marine Science

ORIGINAL RESEARCH
published: 01 April 2021
doi: 10.3389/fmars.2021.657348

Photophysiological Tolerance and Thermal Plasticity of Genetically Different Symbiodiniaceae Endosymbiont Species of Cnidaria

*Vanessa Russnak[1], Mauricio Rodriguez-Lanetty[2] and Ulf Karsten[1]**

[1] Institute of Biological Sciences, Applied Ecology and Phycology, University of Rostock, Rostock, Germany, [2] Department of Biological Sciences, Institute of Environment, Florida International University, Miami, FL, United States

Coral reefs are endangered by constantly rising water temperature due to global warming. This triggers a breakdown of the nutritional symbiosis between cnidarian hosts and their Symbiodiniaceae symbionts, resulting in the loss of the algal partner. In the Symbiodiniaceae exists a high genetic diversity with broad physiological plasticity within and between species, resulting in large thermal tolerance. While these variations have been studied in individual taxa, comprehensive comparative experimental data on numerous species are still rare. In the present study, the photosynthetic performance and tolerance as function of light and temperature of nine Symbiodiniaceae genetic types of four different clades were determined. The data indicate significant differences in the response patterns. Almost all algal isolates exhibited low to moderate light requirements for photosynthesis without photoinhibition, and a photosynthetic efficiency between 20 and 80% in the temperature range 20–34°C, indicating a broad thermal tolerance to temperature fluctuations in tropical regions. The presented data clearly point to a broad photophysiological tolerance and thermal plasticity of genetically different Symbiodiniaceae, which contributes as an important finding to a better understanding of host-symbiont response to an increasing sea surface temperature.

Keywords: irradiance, photosynthesis, respiration, Symbiodiniaceae, temperature, tolerance

OPEN ACCESS

Edited by:
Kefu Yu,
Guangxi University, China

Reviewed by:
Biao Chen,
Guangxi University, China
Anthony William Larkum,
University of Technology Sydney, Australia

***Correspondence:**
Ulf Karsten
ulf.karsten@uni-rostock.de

Specialty section:
This article was submitted to Coral Reef Research, a section of the journal Frontiers in Marine Science

Received: *22 January 2021*
Accepted: *15 March 2021*
Published: *01 April 2021*

Citation:
Russnak V, Rodriguez-Lanetty M and Karsten U (2021) Photophysiological Tolerance and Thermal Plasticity of Genetically Different Symbiodiniaceae Endosymbiont Species of Cnidaria. Front. Mar. Sci. 8:657348. doi: 10.3389/fmars.2021.657348

INTRODUCTION

Coral reefs are one of the most important ecosystems in the marine environment, as they are highly diverse and productive ecosystems (Connell, 1978; Moberg and Folke, 1999). The high productivity of coral reef systems is based on a mutualistic symbiosis between unicellular dinoflagellates (Symbiodiniaceae) and different invertebrate reef species, including corals, sea anemones and sponges among many others (Trench, 1993; Coffroth and Santos, 2005; Decelle et al., 2018).

The success of this symbiosis depends on complementary intracellular solute exchange such as nutrients and carbon compounds. The symbionts can provide up to 95% of photosynthetically fixed organic carbon in the form of glycerol, glucose and alanine to the host (Muscatine and Porter, 1977; Burriesci et al., 2012; Davy et al., 2012). In exchange the host offers protection against environmental stresses (e.g., herbivory) and delivers inorganic nitrogen

(Davies, 1984; Steen and Muscatine, 1984). Despite their immense ecological importance, coral reefs are diminishing worldwide due to various environmental stressors (Hoegh-Guldberg et al., 2007; Hughes et al., 2018, 2020). There are several factors, such as low salinity, water pollution, unusually high or low water temperatures or high solar irradiance causing coral bleaching (Van Oppen and Lough, 2018). When, for instance, the local temperature exceeds the upper physiological threshold of the host, the symbiosis collapses and "bleaching" occurs as a result of the loss of algal endosymbionts (Glynn and D'Croz, 1990). This impact has already been observed globally, with an increasing frequency of these "bleaching events" due to more frequent El-Nino events, particularly in recent years (Glynn, 1993; Eakin et al., 2010; Hughes et al., 2017, 2018, 2020). However, the probability of bleaching depends either on the host characteristics (Baird et al., 2009), on the symbiont ecophysiological traits (Rowan, 2004) or on the prevailing environmental conditions (Hoegh-Guldberg, 1999; Anthony et al., 2009). The flexibility of the coral host, in particular, to associate with different photosymbiont strains at the same time could be critical to cope with rapid environmental fluctuations (Baker, 2001; Berkelmans and Van Oppen, 2006; Abrego et al., 2008; Lewis et al., 2019; Qin et al., 2019).

Several studies suggested that the host might be able to acclimate to higher water temperatures by switching to more temperature-tolerant symbiont species or strains from the local environment or by distributing temperature-tolerant symbionts to make them more abundant (Buddemeier and Fautin, 1993; Baker, 2003; Fautin and Buddemeier, 2004; Correa and Baker, 2011; Cunning et al., 2018). Nevertheless, some investigations revealed that altered host-symbiont pairings often return to their original composition when sufficient time elapsed after a bleaching event (Thornhill et al., 2006; Sampayo et al., 2008). For example, this was found in several coral species at the Great Barrier Reef after a bleaching event in 2002. During bleaching, corals harbored the same Symbiodiniaceae as before and after the thermal stress events (Stat et al., 2009). This suggests that not all symbiotic strains are beneficial to the respective host (Stat et al., 2008; Starzak et al., 2014; Gabay et al., 2018) or that the competitive advantage varies with the environment (Thornhill et al., 2006; Jones et al., 2008; LaJeunesse et al., 2009). The Symbiodiniaceae are highly diverse and combine at least seven different genera, which were recently taxonomically revised (LaJeunesse et al., 2018). The six genera are *Breviolum*, *Cladocopium*, *Durusdinium*, *Effrenium*, *Fugacium*, and *Gerakladium*. Members of the Symbiodiniaceae have a different sensitivity to solar radiation and temperature fluctuations. The underlying mechanisms can be explained by biochemical and molecular processes of the photosynthetic machinery (Takahashi et al., 2008). The key pigments peridinin, chlorophyll *a* and *c*2 are integrated into the chloroplast membrane as the two major antennas *a*-chlorophyll *c*2-peridinin protein complex (acpPC) and peridinin-chlorophyll *a*-binding protein (PCP) (Brown et al., 1999; Takahashi et al., 2008; Niedzwiedzki et al., 2014; Hennige et al., 2019).

High irradiances and temperatures are factors contributing to the phenomenon of coral bleaching. High temperature contributes to an increased production of harmful reactive oxygen molecules (ROS), such as hydrogen peroxide (H_2O_2), singlet oxygen $^1O_2$ or superoxide O_2. ROS originate as a metabolic byproduct and are primarily produced by photosystem I and in parts of photosystem II (Szabó et al., 2020). ROS are chemically highly reactive and hence can, for example, mutate DNA, denature proteins and oxidize lipids as well as cell membranes (Takahashi et al., 2008, 2009; Venn et al., 2008; Lesser et al., 2010). As a result of ROS production and the cellular cascade, this can lead to a disruption of communication and interaction between the host and symbiont. ROS production is considered as the key element for the bleaching process (Weis, 2008; Baird et al., 2009; Szabó et al., 2020). Evidence suggests that the ROS leakage varies between species, as well as depending on temperature and salinity (Gegner et al., 2019). Various species of the Symbiodiniaceae acclimate their photosynthetic performance to different light conditions (Iglesias-Prieto and Trench, 1994; Hennige et al., 2009; Suggett et al., 2015). With elevated temperatures, various Symbiodiniaceae did not grow (Lesser, 1996), while other investigations reported the opposite (Sakami, 2000; Karim et al., 2015; Klueter et al., 2017). Karim et al. (2015), for example, that growth and photochemical efficiency of PSII remained unchanged between 25 and 30°C in various Symbiodiniaceae genera. At temperatures above 33°C, however, the thermal tolerance was exceeded. Further reports point to different genotypes of Symbiodiniaceae which are tolerant to specific temperatures and radiation conditions (Robison and Warner, 2006). Consequently, the tolerance width and upper survival temperature varies from species to species and genotype to genotype (Berkelmans and Van Oppen, 2006; Van Oppen et al., 2009). The genetic identity and ecophysiological capability of Symbiodiniaceae species play a major role in acclimation and adaptation to thermal stress. Several studies identified significant differences in heat tolerance both within a single Symbiodiniaceae genus (Díaz-Almeyda et al., 2017; Bayliss et al., 2019) and between genera (Grégoire et al., 2017). In addition, there are several species, such as *Durusdinum trenchii* (Rowan, 2004; Jones et al., 2008; Bellantuono et al., 2019) and *Cladocopium thermophilum* (formerly Class C, ITS2-"Golf C3") (Hume et al., 2015) which are considered thermotolerant. A genetic subtype of ITS2-D1a (LaJeunesse et al., 2018) within Clade D, gives coral hosts a 1–1.5°C increase in thermal tolerance (Rowan, 2004; Berkelmans and Van Oppen, 2006). A culture of *Cladocopium* C1 in a laboratory selection exhibited better photophysiology and growth at high temperature (31°C) compared to wild type cells (Chakravarti et al., 2017). However, alternating heat-resistant host-symbiont assemblages are associated with metabolic "costs," since the growth rates of the corals often decrease (Abrego et al., 2008).

The objective of this study was to examine the photosynthetic performance [net primary production], hyperthermal tolerance, acclimation capacity of several genotypes (strains), species, and genera of Symbiodiniaceae using oxygen optodes. Based on previous studies (Rowan, 2004; Jones et al., 2008; Bellantuono et al., 2019), in which *Durusdinium trenchii* exhibited a pronounced heat tolerance, we hypothesized that *D. trenchii* outperforms the other strains in terms of photosynthetic

efficiency as no loss of photosynthetic function occurs at higher temperature. A total of nine algal strains belonging to four genera and four species of Symbiodiniaceae were comparatively examined under controlled manipulative conditions: *Breviolum minutum* (4 strains), *Breviolum psygmophilum* (2 strains), *D. trenchii* (one strain), *Effrenium voratum* (one strain), and *Symbiodinium linucheae* (one strain).

MATERIALS AND METHODS

Origin and Maintenance of Symbiodiniaceae

The photophysiological properties and thermal tolerance of clonal cultures under controlled conditions were investigated in nine different Symbiodiniaceae genetic types from four different clades (A, B, D, and E) (LaJeunesse et al., 2018). These strains originated from the culture collection of the IMaGeS Lab (Dr. Rodriguez-Lanetty; originally started by Dr. Mary Alice Coffroth) of Florida International University Miami. The investigated isolates were isolated from four host species (seven individual hosts) collected in three biogeographic regions [Hawaii (Pacific), Florida (Caribbean), and Panama (Caribbean)]. In addition, *Effrenium voratum* was utilized as a free-living species from New Zealand waters (West Pacific) (**Table 1**). These lineages originate from locations with distinct thermal profiles and thus, have likely acquired specific adaptations to their local environments. For example, the strain *Breviolum minitum* SSB 01 from Hawaii (Pacific) is more temperature sensitive (Dang et al., 2019) compared to heat tolerant *Durusdinium trenchii* CCMP2556 (Bellantuono et al., 2019) from the Caribbean. All Symbiodiniaceae strains were kept as unialgal cultures under controlled conditions (21° ± 0.6°C, approx. 35–40 μmol photons m^{-2} s^{-1} at 16:8 h light dark cycle, provided by Lumilux Cool Daylight L18W/865; OSRAM, Munich, Germany) for at least 6 months in Rostock. The clonal cultures were grown in natural, filtered (0.2 μm, Sartorius, Germany) Baltic Sea water (absolute salinity, 14 S_A), where the salinity was adjusted to 33 S_A by adding artificial sea salt (hw Marinemix professional–HW Wiegandt Aquaristik, Krefeld, Germany) and enriched with f/2 medium (Guillard's Medium, type G0154, Sigma Aldrich, Germany). The stock culture media were refreshed monthly. The medium was refreshed 3–4 days prior each experiment to ensure always growth in the log phase.

Genetic Identity

Genetic identity of the Symbiodiniaceae cultures was confirmed and evaluated by amplification and sequencing of the hypervariable region of domain V of the chloroplast 23S ribosomal DNA gene (cpr23S), which is considered as a *Symbiodinium*-specific molecular marker (Granados-Cifuentes et al., 2015; Bonthond et al., 2018). This region was identified with the forward primer 23S_F-Forward_Overhang (TCGTCGGCAGCGTCAGATGTGTATAAGAGACAGAATAA CGACCTGCATGAAAC, Invitrogen) and reverse primer 23S_R-Reverse_Overhang (GTCTCGTGGCTCGGAGATGTGTATA AGAGACAGGCCTGTTATCCGTAGAGTAGC, Invitrogen). The PCR profile was as follows: initial denaturation for 2 min at 95°C, 35 cycles at 95°C for 35 s, 35 cycles 55°C for 30 s, 35 cycles 72°C for 60 s, followed by a final extension of 5 min at 72°C. The PCRs contained 1X GoTaq GreenMaster Mix (Promega), 0.625 μl per primer and nuclease-free water in a final volume of 25 μl. For each sample 1 μl of template DNA was used. Purified PCR product were sent to Eurofins for sequencing using the Sanger-O Primer. Received dinoflagellates sequences were adjusted and aligned with the program SnapGene Viewer. Sequences were BLASTn search against the GenBank from National Center for Biotechnology Information (NCBI) for species identification.

Photosynthesis and Respiration Measurements

The photosynthesis irradiance curves (PI curve) reflect the measured relationship of oxygen production per chlorophyll *a* as function of increasing photon fluence densities (PFD). For this purpose, the PI curves were generated in four separate water-surrounded oxygen electrode chambers (Hansatech Instruments, King's Lynn, United Kingdom), each filled on top of a magnetic stirrer (Hansatech Instruments, King's Lynn, United Kingdom). The chambers were connected to a water supply (K10, Thermo Haake, Karlsruhe, Germany) and a thermostat (DC10, Thermo Haake, Karlsruhe, Germany) to keep the temperature constant (± 0.1°C). LEDs (LUXEON Rebel1 LXML-PWN1-0100, neutral white, Phillips, Amsterdam) were used as light sources, which were implemented in the PI-Box. To reduce the photon flux densities (PFD), neutral density filters were placed between the

TABLE 1 | Culture and taxonomic assignment of the investigated Symbiodiniaceae genotypes, along with information on origin, lifestyle, and isolator.

Culture	Symbiodiniaceae type	Host	origin	Lifestyle	Isolated by	18S rDNA	cp-type
Mf 1.05 b	*Breviolum minutum*	*Orbicella faveolata*	Caribbean	Symbiotic	M.A. Coffroth	B	B184
SSB 01	*Breviolum minutum*	*Aiptasia pulchella*	Pacific	Symbiotic	Xiang	B	
RT-002	*Breviolum minutum*	*Aiptasia pallida*	Caribbean	Symbiotic	R.K. Trench	B	
MAC 703	*Breviolum minutum*	*Plexaura kuna*	Caribbean	Symbiotic	M.A. Coffroth	B	B211
CCMP 421	*Effrenium voratum*	–	W. Pacific	Free-living	Bigelow	E	E202
MAC HIAP	*Breviolum psygmophilum*	*Aiptasia pulchella*	Pacific	Symbiotic	R.A. Kinzie	B	B224
1046	*Breviolum psygmophilum*	–		Symbiotic		B	
CCMP 2556	*Durusdinium trenchii*	*Orbicella faveolata*	Caribbean	Symbiotic	M.A. Coffroth	D	D206
SSA 01	*Symbiodinium linucheae*	*Aiptasia pallida*	Caribbean	Symbiotic	T. Bieri	A	

LEDs and the cuvette to generate different PFDs (0–1,400 μmol photons m^{-2} s^{-1}). Each cuvette was equipped with an integrated oxygen immersion probe (optode) (PreSens Precision Sensing GmbH, Regensburg) and connected via a fiber optic to an oxygen transmitter (Oxy 4-Mini, PreSens Precision Sensing GmbH, Regensburg). For each cuvette, the oxygen concentrations were displayed and recorded with the computer program OXY4v2_30 (PreSens Precision Sensing GmbH, Regensburg) and later calculated based on the chlorophyll *a* content. To calibrate the oxygen dip probes, each cuvette was treated at 0 and 100% oxygen saturation at 20°C. Oxygen saturation at 100% was done by aeration of the culture media for 15 min. Sodium dithionite ($Na_2S_2O_4$) was used to achieve oxygen free media.

In each measurement, four replicates of 3 ml pre-incubated log-phase suspension of Symbiodiniaceae were loaded into the cuvette. All replicates were enriched with sodium bicarbonate ($NaHCO_3$, 2 mM final concentration) before the measurements to ensure sufficient carbon supply. Each PI measurement started with a 30 min respiration phase in darkness, followed by an always 10 min photosynthesis phase at each of 10 different light level, at a constant temperature of 20°C. After each PI curve measurement, the algal suspension was filtered from each cuvette onto an individual Whatman GF/6 glass fiber filter (Ø 25 mm) for chlorophyll *a* determination. Chlorophyll *a* was extracted with 3 ml 96% ethanol (v/v), thoroughly vortexed and incubated in the dark for 24 h at 4°C. Afterward the extracts were centrifuged at 5,000 rpm for 10 min (Heraeus Megafuge, Hanau, Germany) to reduce turbidity. The extinction of the supernatants were measured at 665 and 750 nm in a spectrophotometer (Shimadzu UV-2401 PC, Kyoto, Japan). The concentration of chlorophyll *a* was calculated according to a protocol of the Baltic Marine Environment Protection Commission (1988) (Helcom, 1988).

To generate the PI curve, the chlorophyll *a* content and the measured data were fitted using the mathematical photosynthesis model of Platt et al. (1980). Several photosynthesis parameters were estimated from the least square's regression curves, which were adjusted to the measured values using the solver function of MS Office excel 2013. Based on these curves, the maximum rate of net primary production (NPP_{max}), respiration (R), light utilization coefficient (α), photoinhibition coefficient (ß), light saturation point (I_k) and light compensation point (I_c) were calculated.

Temperature Dependent Photosynthesis and Respiration

To investigate the temperature requirements of photosynthesis and respiration, two different temperature treatments were applied. The first and broader experiment aimed to define the upper and lower temperature tolerance along with the optimum for each strain in the temperature range from 10°C up to 40°C and down to 10°C in 5°C increments.

The second temperature experiment was carried out based on the previously gained data with smaller temperature range and steps to precisely identify the upper temperature limits for both photosynthesis and respiration. The responses between the temperatures 20°C up to 34°C in 2°C steps were measured. Both experiments were performed using the oxygen-optode system described above with four replicates of 3 ml pre-incubated log-phase suspension of Symbiodiniaceae at the same time. Each sample was incubated in the dark for 20 min at each experimental temperature, starting at the respective starting temperature (10°C/20°C), before respiration was monitored for an additional 10 min. This was followed by the photosynthesis phase for an additional 10 min at an exposure of ∼340 μmol photons m^{-2} s^{-1}. This light level was held constant for all photosynthesis measurements. After determining photosynthetic oxygen evolution, the temperature was increased by 5°C/2°C and a new incubation period was started after reaching the new temperature in the thermostat chamber. The O_2 consumption and production per unit time were related to the concentration of total Chl *a* per sample as described above.

Statistics

All values shown represent mean values and standard deviation (n = 4), unless otherwise stated. For statistical analysis, IBM's SPSS Statistics 25 computer program was applied. Significance levels were calculated using one-way ANOVAs with *post hoc* Tukey tests to show significant differences between the different temperature levels. For the assumptions, normality was previously tested with the Shapiro-Wilk test and for homogeneity of variances, the Levene's test ($p > 0.05$) was applied. For violation of assumptions, if Levene's test was significant, Welch-ANOVA and Games-Howell *post hoc* test were performed instead of a one-way ANOVA. For all ANOVAS, "photosynthesis" and "respiration" were used as independent variables (= levels).

RESULTS

Photosynthesis and Respiration Measurements

Photosynthetic oxygen production in all Symbiodiniaceae cultures at 20°C showed a similar PI curve shape with increasing PFD, followed by rarely perceived photoinhibition (**Figure 1**). The average respiration rate at 20°C ranged from −38.33 μmol O_2 mg^{-1} Chl *a* h^{-1} in strain SSB 01 to −127.40 μmol O_2 mg^{-1} Chl *a* h^{-1} in strain SSA 01, while the maximum photosynthesis rate NNP_{max} in the light saturated range was between 47.21 μmol O_2 mg^{-1} Chl *a* h^{-1} in strain SSA 01 and 233.45 μmol O_2 mg^{-1} Chl *a* h^{-1} in strain 1,046 (**Figure 1**). Even under the highest tested photon fluence density (1,400 μmol photons m^{-2} s^{-1}), only in SSB 01 small photoinhibition could be demonstrated (**Figure 1B**). The Symbiodiniaceae genotypes showed an alpha value (photosyntethic efficiency) between 2.66 and 6.09 μmol O_2 mg^{-1} Chl *a* h^{-1} (μmol photons m^{-2} s^{-1}) $^{-1}$, whereas SSA 01 exhibited a very high alpha value with 39 μmol O_2 mg^{-1} Chl *a* h^{-1} (μmol photons m^{-2} s^{-1}) $^{-1}$. The values of the light saturation point (I_k) ranged from 4.48 μmol photons m^{-2} s^{-1} in strain SSA 01–110.26 μmol photons m^{-2} s^{-1} in strain MAC HIAp, and those of the light compensation point (I_c) between 5.84 (strain SSA 01) and 35.73 μmol photons m^{-2} s^{-1} (strain 1,046) (**Figure 1** and **Table 2**). All these values indicate low to moderate light requirements for photosynthesis at 20°C, with the

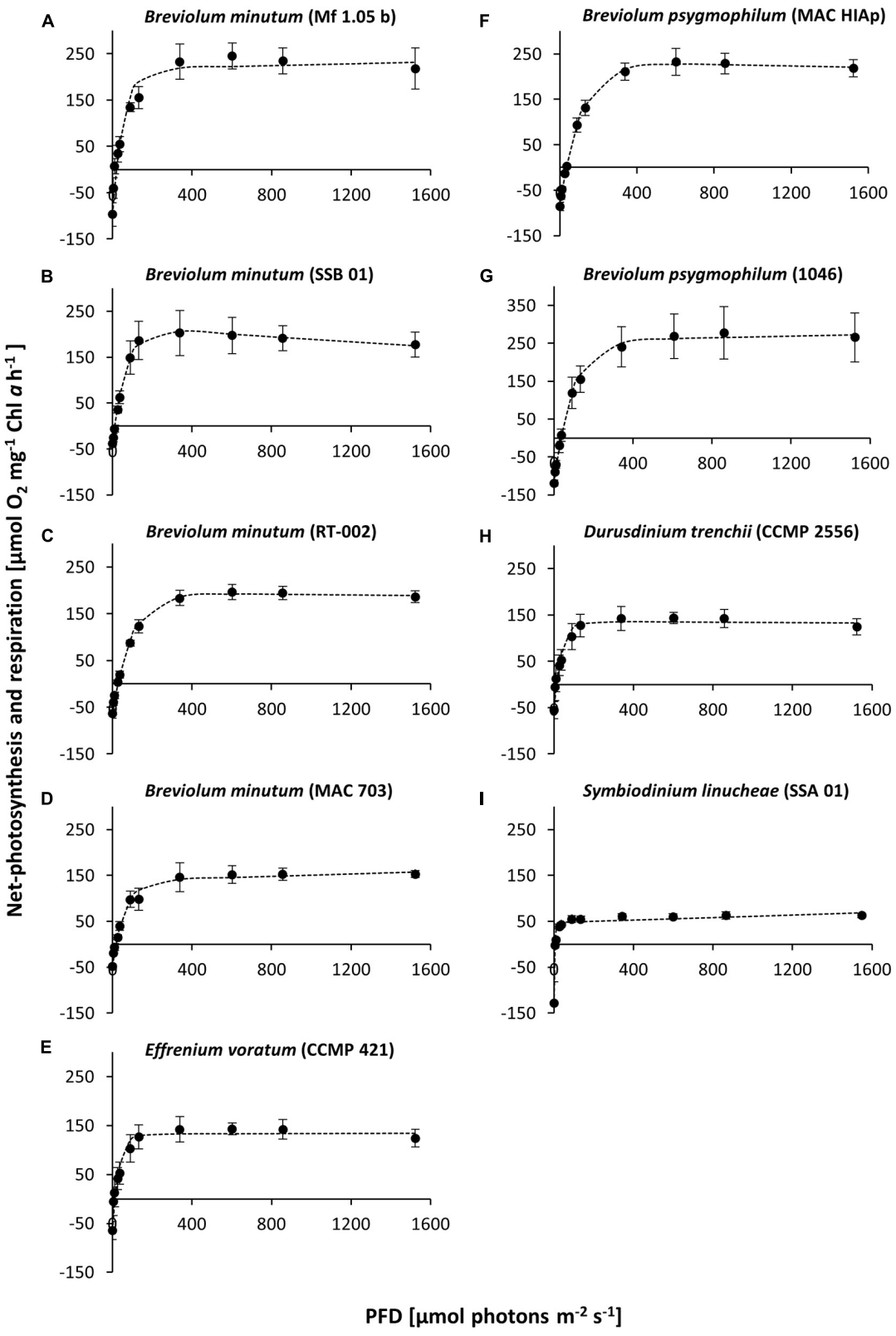

FIGURE 1 | Net primary production [NPP] rates [µmol O_2 mg^{-1} Chl *a* h^{-1}] in relation to increasing photon fluence density (PFD) [µmol photons m^{-2} s^{-1}] of nine Symbiodiniaceae cultures at 20°C, kept in f/2 Baltic Sea water medium, $33S_A$, measured by oxygen production with optodes. Data represent a mean value ± SD (*n* = 4). Dotted line: fitted according to Platt et al. (1980). **(A–I)** represent the studied Symbiodiniaceae genotypes as shown in **Table 1**.

TABLE 2 | Parameter of respective PI-curves (**Figures 1A–I**) of nine Symbiodiniaceae cultures (n = 4, mean value ± SD) at 20°C kept in a f/2 Baltic Sea water medium, $33S_A$.

Strains	NPP max [μmol O_2 mg^{-1} Chl *a* h^{-1}]	Respiration [μmol O_2 mg^{-1} Chl *a* h^{-1}]	α [μmol O_2 mg^{-1} Chl *a* h^{-1} [μmol photons m^{-2} s^{-1}]$^{-1}$]	β [μmol O_2 mg^{-1} Chl *a* h^{-1} [μmol photons m^{-2} s^{-1}]$^{-1}$]	I_k [μmol photons m^{-2} s^{-1}]	I_c [μmol photons m^{-2} s^{-1}]
Mf 1.05b	212.56 ± 46.98	−97.17 ± 25.78	5.73 ± 1.72	−0.01 ± 0.04	54.08 ± 16.99	20.36 ± 3.12
SSB01	218.28 ± 57.05	−38.33 ± 5.90	3.73 ± 0.45	0.03 ± 0.03	68.79 ± 11.69	11.02 ± 2.30
RT-002	194.92 ± 23.41	−63.36 ± 9.93	2.66 ± 0.24	0.00 ± 0.01	97.06 ± 9.94	27.26 ± 3.67
MAC 703	133.34 ± 38.73	−47.56 ± 4.39	3.01 ± 0.26	−0.01 ± 0.02	60.05 ± 11.41	18.34 ± 3.10
CCMP 421	132.49 ± 21.37	−64.51 ± 18.07	6.09 ± 1.15	0.00 ± 0.01	32.35 ± 5.06	12.83 ± 5.47
MAC HIAp	233.45 ± 29.59	−85.69 ± 9.33	2.89 ± 0.48	0.01 ± 0.01	110.26 ± 8.78	34.34 ± 3.21
1046	249.35 ± 57.35	−119.19 ± 5.47	4.03 ± 1.05	−0.01 ± 0.01	91.53 ± 17.85	35.73 ± 5.08
CCMP 2556	136.30 ± 16.26	−55.14 ± 18.22	5.16 ± 2.64	0.00 ± 0.01	37.07 ± 17.85	12.59 ± 5.08
SSA01	47.21 ± 7.93	−127.40 ± 19.36	39.00 ± 19.38	−0.01 ± 0.01	4.48 ± 1.49	5.84 ± 1.03

NPP_{max} represents the maximum oxygen production rate, alpha (α) the initial slope of oxygen production in the light limited range, beta (β) the final slope of oxygen production in the light saturated range (photoinhibition), I_c the light compensation point where respiration and photosynthesis are equal, I_k the light saturation point.

exception of *Symbiodinium linucheae* which revealed a strong increase with a rather low maximum oxygen production rate (NNP_{max}) (**Figure 1I**).

Overall, the data document genotype-specific similarities and differences between the nine Symbiodiniaceae isolates. While, for example, similar PI curves concerning the NNP_{max} values were recorded for members of the different genera *B. minutum*, *D. trenchii,* and *E. voratum* (MAC 703, CCMP 2556, and CCMP 421), the PI curves within the genus *Breviolum* varied widely. Both isolates of *B. psygmophilum* showed a remarkably similar NNP_{max}, as well as light compensation and light saturation point. On the other hand, all *Breviolum minutum* strains exhibited a wide range of NNP_{max} values. In addition, SSB 01 showed a slight photoinhibition (β). Furthermore, *S. linucheae* (SSA 01) had the lowest NNP_{max}, while *B. psygmophilum* (1046) showed the highest NNP_{max} (**Figures 1I,G**).

Temperature Dependent Photosynthesis and Respiration

The effects of temperature on the production of photosynthetic oxygen and respiratory oxygen consumption in Symbiodiniaceae cultures displayed strong differences within and between the strains with an increasing temperature gradient.

A broad temperature experiment (**Figure 2**) was conducted from 10°C up to 40°C, with a recovery phase decreasing the temperature back to 10°C. All isolates showed a weak photosynthetic and respiratory rate at 10°C. Increasing temperature stimulated photosynthesis and respiration to a species-specific maximum, followed by a decrease under the highest temperature conditions. While optimal photosynthesis was measured between 20 and 30°C in all investigated strains, the highest respiration occurred between 30 and 40°C (**Figure 2**). Furthermore, after a complete inhibition of photosynthesis at 40°C, no recovery was observed when the temperature was subsequently lowered, indicating a damage to the photosynthesis apparatus. This was illustrated by a two-color triangle in the graph (A-I). All cultures showed still respiration in the dark at 40°C (**Figure 2**). Subsequently, four (**Figures 2B,E,I,H**) out of nine cultures exhibited a complete inhibition of photosynthesis along with high respiration rates from 30 to 35°C. The remaining five strains (**Figures 2A,C,D,F,G**) showed still a partly functioning photosynthesis at 35°C. Both strains of *B. psygmophilum* reached the highest values in photosynthetic oxygen evolution (MAC HIAp: ∼264.76 μmol O_2 mg^{-1} Chl *a* h^{-1}; strain 1046: ∼201.70 μmol O_2 mg^{-1} Chl *a* h^{-1}) (F, G). In contrast, *B. minutum* (SSB 01) showed the lowest maximum value at 20°C with ∼59.98 μmol O_2 mg^{-1} Chl *a* h^{-1} (B). Therefore, SSB 01 was the only strain with maximum photosynthetic oxygen evolution at 20–25°C, while all other isolates had their maxima between 25 and 30°C (**Figure 2**). At 35°C photosynthesis of *E. voratum* was completely inhibited. In contrast, the other eight cultures showed only slightly decreased or constant respiration during the light phase at 35°C (**Figures 2A–I**).

A second experiment was carried out to identify more precisely the temperature requirements of photosynthesis and respiration in the critical range between 20 and 34°C (**Figures 3A–I**). The data confirmed in principle the previous experiment. Eight out of nine strains showed photosynthesis and respiration between 20 and 34°C, although at the highest temperature some inhibition in oxygen production could be observed. *B. minutum* (SSB 01) was the only exception as photosynthesis >28°C was fully inhibited (**Figure 3B**). To determine the optimum temperature for photosynthesis, we applied the widely used model of Blanchard et al. (1996) (**Figure 4** and **Table 3**). It shows the species-specific tolerance range of temperature for photosynthesis and respiration in both temperature experiments. For all cultures percentiles of <20%, 20–80%, and >80% were determined. In the broad temperature approach, all Symbiodiniaceae exhibited a wide temperature tolerance, with almost all values above the 20% percentile. At the lowest tested temperature (10°C), four isolates (Mf 1.05 b, MAC 703, MAC HIAp, CCMP 2556) showed efficiency below 20%. All other strains had efficiency between 20 and 80%. Four isolates (Mf 1.05 b, 1046, SSA 01, CCMP 421) exhibited the largest temperature range in the upper percentile by covering three temperature levels from 20 to 30°C. In comparison,

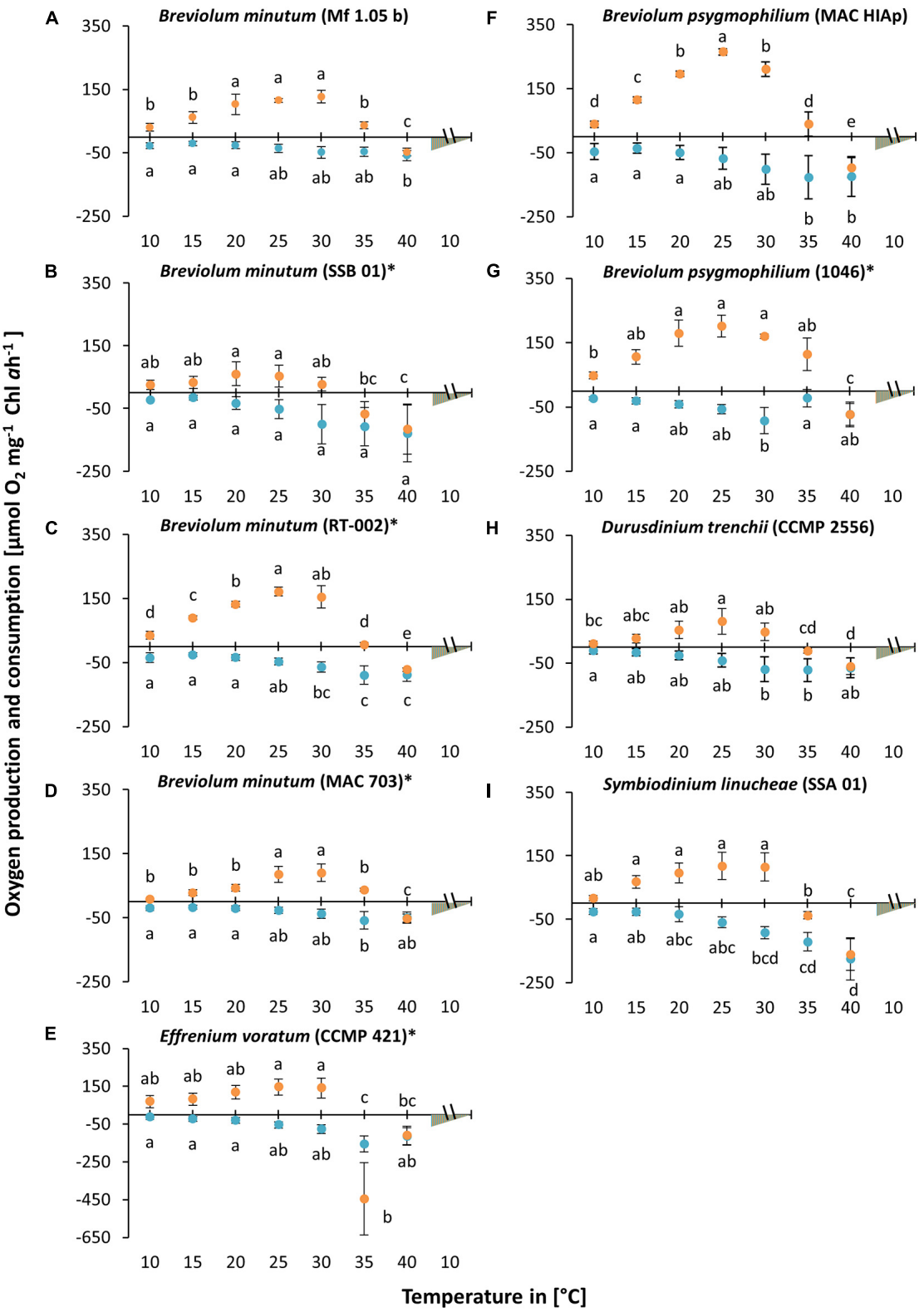

FIGURE 2 | Oxygen production (orange) and consumption rates (blue) [µmol O_2 mg^1 Chl *a* h^1] in relation to increasing temperature [10–40°C] at a saturating photon fluence density (PFD) of approx. 350 µmol photons m^{-2} s^{-1} in nine Symbiodiniaceae cultures **(A–I)**, kept in f/2 Baltic Sea water medium, ~ 33 S_A, measured by oxygen evolution with optodes. Data represent a mean value ± SD (n = 4). Lowercase letters at photosynthesis and respiration indicate significantly means ($p < 0.05$; one-way ANOVA with *post hoc* Tukey-HSD test; * indicate Welch-ANOVA (significant: $p < 0.05$) with Games-Howell *post hoc* test).

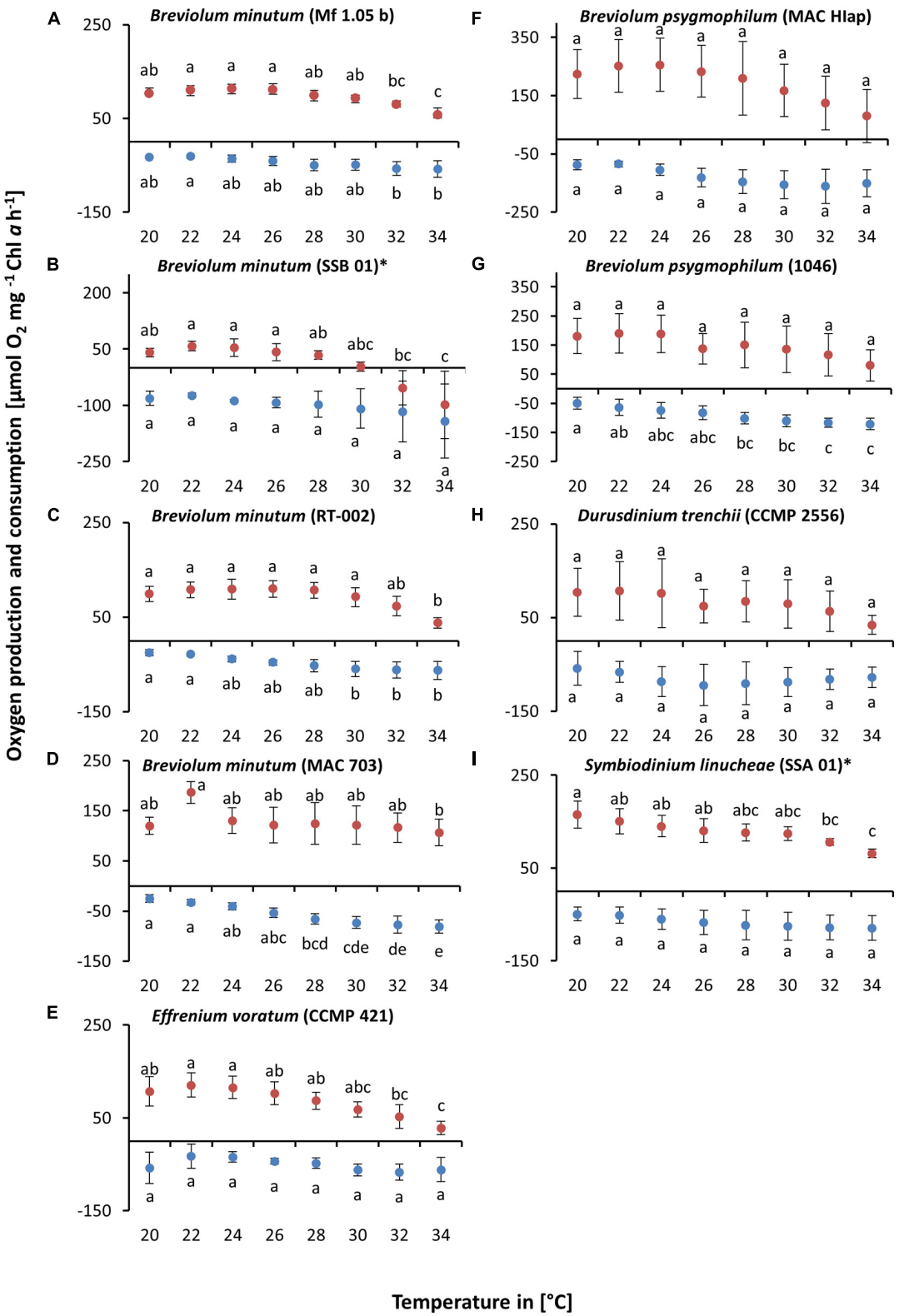

FIGURE 3 | Oxygen production (red) and consumption rates (dark blue) [µmol O_2 mg^{-1} Chl *a* h^{-1}] in relation to increasing temperature [20–34°C] at a saturating photon fluence density (PFD) of approx. 350 µmol photons m^{-2} s^{-1} in nine Symbiodiniaceae cultures **(A–I)**, kept in f/2 Baltic Sea water medium, ~ 33 S_A, measured by oxygen evolution with optodes. Data represent a mean value ± SD (n = 4). Lowercase letters at photosynthesis and respiration indicate significantly means ($p < 0.05$; one-way ANOVA with *post hoc* Tukey-HSD test; * indicate Welch-ANOVA (significant: $p < 0.05$) with Games-Howell *post hoc* test).

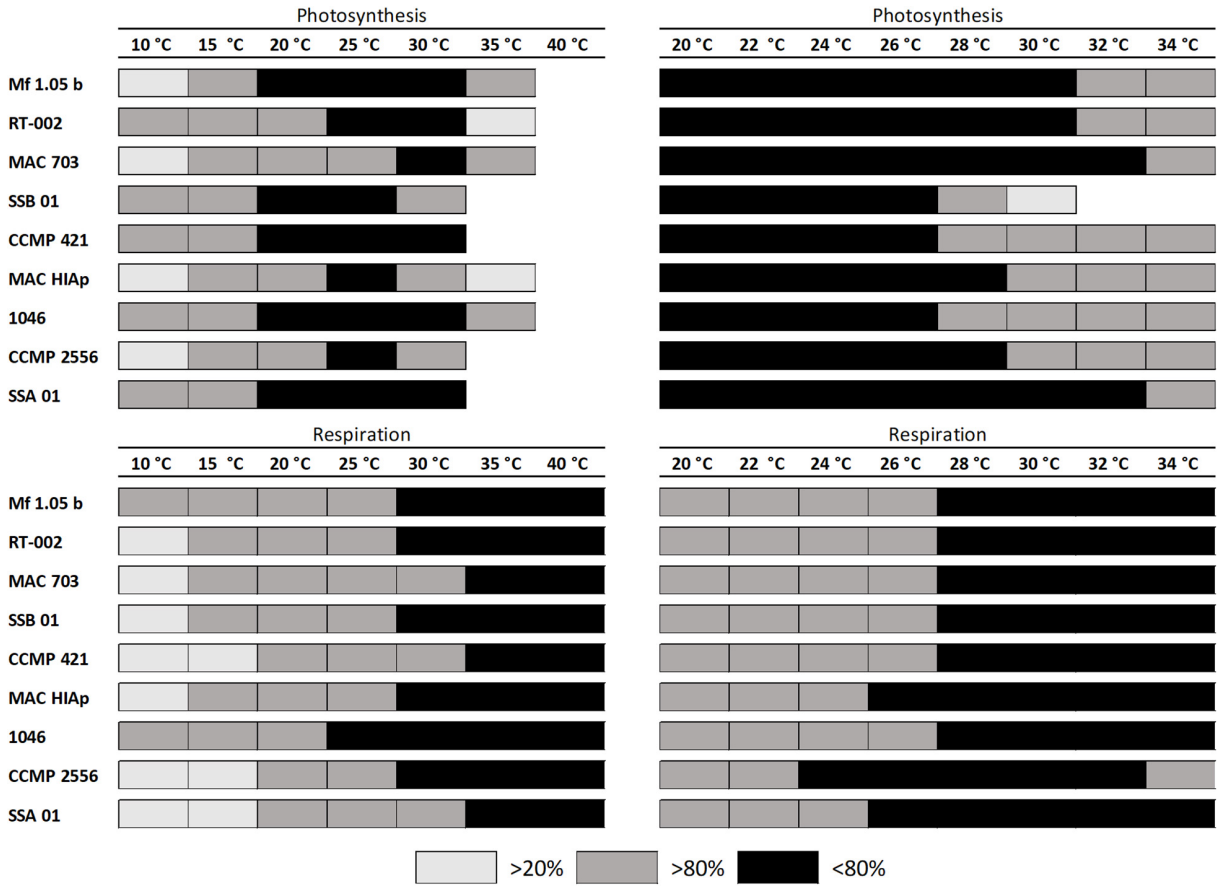

FIGURE 4 | Influence of temperature on photosynthetic oxygen production and respiratory oxygen consumption of nine tested Symbiodiniaceae strains using the fit of Blanchard et al. (1996). The black box represents area of highest photosynthesis more than >80% percentile, dark gray symbols within 20 and 80% percentile light gray symbols <20% percentile and white spaces no photosynthesis or respiratory signal. The data represent mean values (n = 4).

several strains showed a small range for photosynthetic efficiency, MAC HIAp and CCMP 2556 at 25°C and MAC 703 at 30°C. Photosynthesis was not detectable at 35°C in four of nine strains (SSB 01, CCMP 2556, SSA 01, CCMP 421). At 35°C the other cultures showed different efficiencies, for RT-002 and MAC HIAp the efficiency ranged below 20%, for the remaining isolates the efficiency reached 20–80%. The highest respiration values were measured between 30 and 40°C. The respiration increased above the 80% for different strains at different temperatures (**Figure 4** and **Table 3**).

The critical temperature levels from the experiments were analyzed in more detail and all cultures without a "cold stress" had a photosynthetic efficiency in the upper percentile of over 80% from 20°C up to 26°C. MAC 703 and SSA 01 exhibited largest temperature tolerance as reflected in the upper percentile >80% up to 32°C. In contrast, SSB 01, 1046, and CCMP 421 showed highest photosynthetic efficiency in the upper percentile up to the 26°C range. The different strains tested showed an increased respiration at 28°C with more than >80%, while CCMP 2556, MAC HIAp, and SSA 01 exhibited lower temperature values (24 and 26°C, respectively) (**Figure 4** and **Table 3**). The results indicate that all investigated strains have a broad temperature tolerance for photosynthesis and respiration.

DISCUSSION

The susceptibility of corals is influenced by a variety of abiotic factors such as increased light and temperature conditions, and the physiological and genetic diversity of the endosymbionts strongly contribute to different response patterns of the host (Berkelmans and Van Oppen, 2006; Robison and Warner, 2006; Baird et al., 2009). In the present study the experiments focused on the physiological tolerance and plasticity of genetically different Symbiodiniaceae strains in response to elevated temperatures for a better understanding of their photosynthetic traits as a function of light and temperature.

The Symbiodiniaceae used were grown as unialgal cultures under identical and controlled conditions for at least 1 year, which might explain relatively similar alpha, I_c and I_k values derived from the respective PI curves. Symbiodiniaceae species acclimate their photosynthetic performance to various light levels (Iglesias-Prieto and

TABLE 3 | Calculation of temperature effects on photosynthetic oxygen production and respiratory oxygen consumption in nine tested Symbiodiniaceae strains using the fit of Blanchard et al. (1996).

		Photosynthesis			Respiration		
		Temperature [°C]			Temperature [°C]		
	Strains	100%	>80%	>20%	100%	>80%	>20%
10–40°C	Mf 1.05 b	24.7	19.4–30.1	10.4–35.4	38.7	27.0–(49.9)	(5.9)–(67.9)
	RT-002	26.4	20.6–31.2	(8.3)–37.3	40	30.0–(49.0)	10.9–(61.9)
	MAC 703	28.5	24.0–32.1	14.1–36.3	38.9	30.5–(47.9)	13.1–(62.2)
	SSB 01	22.4	17.7–26.8	(6.2)–32.4	36.4	27.5–(44.9)	12–(58.6)
	CCMP 421	28.2	19.0–34.9	(4.6)–(41.6)	38.9	32.7–(44.9)	21.7–(54.5)
	MAC HIAp	25.9	21.0–29.8	10.7–34.5	38.2	29.5–(46.0)	13.2–(57.7)
	1046	25.1	19.0–31.1	(8.9)–41.2	32.9	22.9–(42.8)	(6)–(59.4)
	CCMP 2556	24.2	20.2–28.2	13.5–35.0	35.4	28.8–(40.9)	15–(47.8)
	SSA 01	27.2	19.9–33.8	(5.8)–(43.5)	40	33.2–(46.5)	21.2–(56.9)
20–34°C	Mf 1.05 b	24	17.9–30.1	(7.4)–(40.0)	34	26.6–(41)	(13.1)–(51.9)
	RT-002	25.2	16.9–30.6	(4.9)–(36.7)	33	27.2–(37.9)	(15.3)–(42.2)
	MAC 703	26	4.6–33.9	(−71)–(35.2)	33.7	28–(39.2)	(17.8)–(47.8)
	SSB 01	23.1	18.8–26.4	(9.7)–29	34	26.9–(40.7)	(14)–(51)
	CCMP 421	22.6	17–27.6	(6.3)–(36.8)	32.5	27.8–(37.2)	(19.9)–(45.1)
	MAC HIAp	23	19.1–28.8	(10.7)–(36.8)	33.5	25.6–(41.1)	(11.4)–(53)
	1046	20.3	20.0–27.9	(−0.4)–(40.4)	33.6	27.2–(40.7)	(15.5)–(51.8)
	CCMP 2556	20.8	13.3–28.1	(10.6)–(40.2)	27.5	22.2–32.7	(13)–(41.1)
	SSA 01	21.9	18–32.8	(−81)–(35)	34	25–(43.4)	(8.5)–(58)

The data represent mean values (n = 4) of maximum photosynthesis and respiration (100%) and the upper 80 and 20% percentiles. The data in brackets represent temperature calculations that exceed the measured temperature.

Trench, 1994; Anthony and Hoegh-Guldberg, 2003; Roth, 2014). The applied light conditions under which the cultures were grown are comparable to the shady *in vivo* conditions inside the coral tissue (Anthony et al., 2005). Furthermore, Symbiodiniaceae maximize light absorption and utilization under low light conditions by increasing the concentration of photosynthetic pigments thereby improving photosynthetic efficiency (Anthony and Hoegh-Guldberg, 2003).

The photosynthetic optimum under the prevailing environmental conditions is represented by the maximum rate of photosynthesis (NPP_{max}) (Raven and Geider, 2003). The Symbiodiniaceae cultures investigated in this study revealed different type-specific eco-physiological response patterns regarding NPP_{max} and respiration. These patterns are mainly caused by type-specific traits rather than as a result of the stable cultivation conditions. The data displayed a similar NPP_{max} for various genera (MAC 703, CCMP 2556, and CCMP 421), which was distinct to both genotypes of *Breviolum psygmophilum* MAC HIAp and 1046. Furthermore, the NPP_{max} of *Symbiodinium linucheae* SSA 01 was much lower in contrast to the other eight strains. This strain is also considered "heat tolerant" (Swain et al., 2017; LaJeunesse et al., 2018; Gegner et al., 2019) but might not be so beneficial for the coral host (Stat et al., 2008; Herrera et al., 2020). Although only minor photoinhibition was detected in the studied strains we cannot completely exclude an experimental effect as longer exposure to high irradiances could have resulted in a stronger photoinhibitory response. The data from this study, clearly indicate that SSA 01 has a much lower photosynthetic rate compared to the other strains than, for example, strain *B. psygmophilum* (1046), which had the highest average photosynthetic rates per chlorophyll *a*. Therefore, SSA 01 likely transfers less important photosynthetically fixed organic carbon to the host (Stat et al., 2008). The photosynthetic rates of the present study are in agreement with data of Grégoire et al. (2017), who used two identical genotypes for their experiments. The photosynthesis performance between the species were different under the same cultivation conditions (Iglesias-Prieto and Trench, 1994), pointing to genotypic traits. Previous studies indicate an important role of the genetic identity of Symbiodiniaceae strains as well as their respective eco-physiological capabilities in acclimation and adaptation to thermal stress in the reef environment (Baker, 2003; Abrego et al., 2008; Frade et al., 2008a,b). Both the endosymbiont and the host are affected by elevated temperatures. Host genetics have been identified as an important trait in the response of the symbionts (Cunning et al., 2015; Howells et al., 2016). In order to determine how the genetic identity of the symbiont is affected by elevated temperatures, the cultures were exposed to different thermal stress scenarios.

The results of this study indicated a clear species-specific threshold of upper temperature tolerance, in the range of 30°–40°C for all tested species, and the Symbiodiniaceae cultures demonstrated the strongest stress response with a reduced or an inhibition of photosynthesis and strongly increased respiration rate. At 35°C, only five of nine species showed a reduced but measurable photosynthesis (**Figure 4**). Above 35°C, none of the

strains exhibited any photosynthetic activity. It can be assumed that the Symbiodiniaceae were not dead due to the continuing respiratory activity. Moreover, the results of the Symbiodiniaceae cultures showed clearly a tolerance to short-term cold stress at 10°C and the most efficient photosynthesis performance was measured on average at 25°C (**Figure 4**). The different Symbiodiniaceae species are classified based on a variation in thermal tolerances, which is also reflected in the results of this study (Robison and Warner, 2006; Suggett et al., 2008; Díaz-Almeyda et al., 2017; Bellantuono et al., 2019). While any oxygen production at 35°C was not traceable in the isolates SSB 01, CCMP 2556, SSA 01, and CCMP 421, the other strains still showed a reduced activity. *Durusdinium trenchii* is described as heat tolerant species (Bellantuono et al., 2019) but demonstrated in culture a similar pattern as the other tested isolates up to 34°C. The hypothesis that *D. trenchii* is more heat tolerant than the other tested strains could not be confirmed in this experiment. Thus, all tested Symbiodiniaceae exhibited quite similar temperature tolerance with an optimal photosynthetic performance between 20° and 26°C. In addition, the strains MAC 703 and SSA 01 showed an "optimal" photosynthetic capacity up to 32°C. The upper temperature tolerance for photosynthesis of the investigated strains was between 34 and 35°C, that of respiration even higher. Consequently, it is reasonable to assume that the increased consumption of oxygen under elevated temperatures might favor anoxic conditions within the holobiont, which can cause symbiont loss and bleaching. The results of the present study are comparable to those of other studies, which demonstrated a decrease in the maximum quantum yield of PSII and the rate of gross photosynthesis under heat stress in different zooxanthellae in culture. Impairment of photosynthesis was mainly measured at 32–34°C in cultivated zooxanthellae (Iglesias-Prieto et al., 1992; Warner et al., 1996; Iglesias-Prieto and Trench, 1997; Jones et al., 1998; Brown et al., 1999). In *Symbiodinium microadriaticum*, gradual inhibition of photosynthesis occurred at temperatures above 30°C, followed by complete inhibition at higher temperatures of 34–36°C (Iglesias-Prieto et al., 1992). The reason why so many zooxanthellae exhibit a similar upper temperature tolerance for photosynthesis might be related to the fact that dinoflagellates have a Type II Rubisco, which differs in many properties including heat sensitivity from Type I, the dominant form in other algal groups (Tabita et al., 2008).

In the second temperature experiment, it became clear that *Breviolum minutum* SSB 01 was much more susceptible to enhanced temperatures starting at 30°C. This demonstrates different temperature thresholds between strains of *B. minutum*, also within the genus *Breviolum* the species-specific tolerances differ. This is in line with another study, where closely related *Breviolum* species revealed significant functional variation against elevated temperature (Bayliss et al., 2019; Herrera et al., 2020). The different genotypes exhibited decreasing photosynthetic activity at elevated temperatures, which could be an important feature for the strength of the relationship between the symbiont and the host. Some studies concluded that thermotolerance is not species- or clade-specific but is widespread and diverse among members of the genus *Symbiodinium* (Suggett et al., 2008; Díaz-Almeyda et al., 2017). Considering the photosynthetic machinery of coral symbionts as very sensitive to changes in the environment, it was observed that exposure of Symbiodiniaceae to light and temperature caused an impairment of the photosynthetic apparatus by PSII photoinhibition (Iglesias-Prieto et al., 1992). The level of photoinhibition is partly determined by elevated temperatures or light, as these factors can accelerate PSII photodamage and inhibit repair processes (Brown et al., 1999; Takahashi et al., 2009). But other studies report that the temperature-induced inhibition of the dark reactions (Calvin-cycle) in zooxanthellae does not exclusively contribute to coral bleaching, while the concomitant ROS formation could be the main trigger (Hill et al., 2014).

The results of Mansour et al. (2018) found intra- and interspecific differences in the melting points of thylakoid membranes of Symbiodiniaceae species. Such process could explain the inhibition of photosynthetic oxygen production under elevated temperatures during the experiments. A still ongoing respiration was measured at higher temperatures, indicating that the repair mechanisms are working and that the experimental cooling time was too short to be used as proxy for recovery. However, in the experiment 20–34°C the thermal capacity of the photosynthetic membrane was probably not exceeded and hence significant differences between the strain-specific response patterns could be measured. A certain, genetically determined temperature threshold must be reached to harm the photosynthetic activity. The loss of photosynthetic function at extremely high temperatures occurs in a short time period in isolated Symbiodiniaceae cultures. The results of this study clearly indicated that the physiological properties of Symbiodiniaceae at elevated temperatures vary even within the same taxon, i.e., genotypic differentiation even on taxonomically lower rank levels plays a key role for temperature acclimation/adaptation, with consequences for the endosymbiont-host interactions (Bayliss et al., 2019). However, the physiological temperature response patterns of Symbiodiniaceae might differ between culture conditions and in symbiosis as documented for *D. trenchii* (Bellantuono et al., 2019). These authors compared *in hospite* and free-living transcriptomes, and reported strong alteration of transcriptional activity *in hospite* under increased temperature conditions, indicating that symbiotic interactions elicited an exacerbated stress response compared to free-living cells.

Although mainly vegetative (clonal) reproduction occurs within the Symbiodiniaceae, mutation rates can be high, resulting in new variants of individual genotypes. These genetic variations are further increased or maintained by transposons, retrotransposons, tandem repeats, or recombination during sexual reproduction (Shoguchi et al., 2013). Even hosts harboring only a single symbiont genotype can quickly accumulate genetic variation due to this high mutation rate in Symbiodiniaceae (van Oppen et al., 2011). Natural selection is likely to lead to a higher temperature tolerance in the symbiont population, since many temperature tolerance traits are inherited (Császár et al., 2010; Quigley et al., 2016). This selection in the symbiont population also strengthens the holobiont, allowing the host to survive periods of warming (Chakravarti and Van Oppen, 2018).

Nevertheless, previous work suggests that the physiology of symbionts actually differs in culture and host (Ralph et al., 2001; Bhagooli and Hidaka, 2003; Howells et al., 2012; Chakravarti et al., 2017; Ravelo and Conaco, 2018).

Intact relationships between host and symbionts are essential for the ecological health of coral reefs, as they represent one of the most important ecosystems in tropical marine waters. Coral reefs provide many ecosystem services such as high biodiversity and productivity, habitat, fishery, water quality and biogeochemical cycling, and coastal protection (Moberg and Folke, 1999), which are negatively influenced by anthropogenic global warming.

CONCLUSION

In this study we demonstrate a necessity for a comprehensive comparative eco-physiological analysis at intra-specific taxonomic level to fully understand the underlying genetic traits responsible for the variation in thermotolerance. The results clearly demonstrate that there are significant eco-physiological differences among the tested species but also within a species, regarding light affinity and temperature tolerance. Although the short-term responses shown here do not necessarily reflect the long-term response of corals in the reef, this study highlights that symbionts play an important role in the response of holobionts to temperature increases within their average summer maxima. The results showed clearly that *B. minutum* (SSB 01) is much more sensitive to heat in comparison to the strain *B. minutum* (MAC 703) and to the species *S. linucheae* (SSA 01). Furthermore, *S. linucheae* (SSA 01) exhibited a lower photosynthetic rate, suggesting that this strain in symbiosis probably transfers less photosynthetically fixed organic carbon to the host (Stat et al., 2008). Therefore, future studies in which specific symbiont genotypes are introduced into the same host (e.g., Starzak et al., 2014; Hoadley et al., 2015; Herrera et al., 2020) are required to determine the role of host and symbiont in the response patterns. The different response patterns suggest that in symbiosis with a host, the carbon supply from the symbiont to the host might be affected by light and temperature. Presumably, thermal stress leads to an unbalanced bi-directional flow of metabolites between host and endosymbiont which should be further investigated in future studies.

DATA AVAILABILITY STATEMENT

The original contributions presented in the study are included in the article/**Supplementary Materials**, further inquiries can be directed to the corresponding author/s.

AUTHOR CONTRIBUTIONS

VR and UK planned and designed the ecophysiological experiments. VR conducted the ecophysiological characterization of the algal strains, and processed the data. MR-L and VR planned molecular analysis, which was conducted by VR. VR wrote the first draft of the manuscript, which was edited by MR-L and UK. All authors edited and approved the final version of this manuscript.

FUNDING

This work was supported by the DAAD Promos Fellowship to VR.

ACKNOWLEDGMENTS

We are thankful for laboratory support of photosynthesis measurements by Lara Prelle and Angelika Graiff, as well as to Juliane Müller for helping with the culture work. This Master project was funded in the frame of the DAAD Promos scheme.

SUPPLEMENTARY MATERIAL

The Supplementary Material for this article can be found online at: https://www.frontiersin.org/articles/10.3389/fmars.2021.657348/full#supplementary-material

REFERENCES

Abrego, D., Ulstrup, K. E., Willis, B. L., and Van Oppen, M. J. H. (2008). Species-specific interactions between algal endosymbionts and coral hosts define their bleaching response to heat and light stress. *Proc. R. Soc. B Biol. Sci.* 275, 2273–2282. doi: 10.1098/rspb.2008.0180

Anthony, K. R. N., and Hoegh-Guldberg, O. (2003). Kinetics of photoacclimation in corals. *Oecologia* 134, 23–31. doi: 10.1007/s00442-002-1095-1

Anthony, K. R. N., Hoogenboom, M. O., and Connolly, S. R. (2005). Adaptive variation in coral geometry and the optimization of internal colony light climates. *Funct. Ecol.* 19, 17–26. doi: 10.1111/j.0269-8463.2005.00925.x

Anthony, K. R. N., Hoogenboom, M. O., Maynard, J. A., Grottoli, A. G., and Middlebrook, R. (2009). Energetics approach to predicting mortality risk from environmental stress: A case study of coral bleaching. *Funct. Ecol.* 23, 539–550. doi: 10.1111/j.1365-2435.2008.01531.x

Baird, A. H., Bhagooli, R., Ralph, P. J., and Takahashi, S. (2009). Coral bleaching: the role of the host. *Trends Ecol. Evol.* 24, 16–20. doi: 10.1016/j.tree.2008.09.005

Baker, A. C. (2001). Reef corals bleach to survive change. *Nature* 411, 765–766. doi: 10.1038/35081151

Baker, A. C. (2003). Flexibility and Specificity in Coral-Algal Symbiosis: Diversity, Ecology, and Biogeography of Symbiodinium. *Annu. Rev. Ecol. Evol. Syst.* 34, 661–689. doi: 10.1146/annurev.ecolsys.34.011802.132417

Bayliss, S. L. J., Scott, Z. R., Coffroth, M. A., and terHorst, C. P. (2019). Genetic variation in Breviolum antillogorgium, a coral reef symbiont, in response to temperature and nutrients. *Ecol. Evol.* 9, 2803–2813. doi: 10.1002/ece3.4959

Bellantuono, A. J., Dougan, K. E., Granados-Cifuentes, C., and Rodriguez-Lanetty, M. (2019). Free-living and symbiotic lifestyles of a thermotolerant coral endosymbiont display profoundly distinct transcriptomes under both stable and heat stress conditions. *Mol. Ecol.* 28, 5265–5281. doi: 10.1111/mec.15300

Berkelmans, R., and Van Oppen, M. J. H. (2006). The role of zooxanthellae in the thermal tolerance of corals: A "nugget of hope" for coral reefs in an era of climate change. *Proc. R. Soc. B Biol. Sci.* 273, 2305–2312. doi: 10.1098/rspb.2006.3567

Bhagooli, R., and Hidaka, M. (2003). Comparison of stress susceptibility of in hospite and isolated zooxanthellae among five coral species. *J. Exp. Mar. Bio. Ecol.* 291, 181–197. doi: 10.1016/S0022-0981(03)00121-7

Blanchard, G. F., Guarini, J.-M., Richard, P., Ph, G., and Mornet, F. (1996). Quantifying the short-term temperature effect on light-saturated photosynthesis of intertidal microphytobenthos. *Mar. Ecol. Prog. Ser.* 134, 309–313. doi: 10.3354/meps134309

Bonthond, G., Merselis, D. G., Dougan, K. E., Graff, T., Todd, W., Fourqurean, J. W., et al. (2018). Inter-domain microbial diversity within the coral holobiont *Siderastrea siderea* from two depth habitats. *PeerJ* 6:e4323. doi: 10.7717/peerj.4323

Brown, B. E., Ambarsari, I., Warner, M. E., Fitt, W. K., Dunne, R. P., Gibb, S. W., et al. (1999). Diurnal changes in photochemical efficiency and xanthophyll concentrations in shallow water reef corals: Evidence for photoinhibition and photoprotection. *Coral Reefs* 18, 99–105. doi: 10.1007/s003380050163

Buddemeier, R. W., and Fautin, D. G. (1993). Coral Bleaching as an Adaptive Mechanism. *Bioscience* 43, 320–326. doi: 10.2307/1312064

Burriesci, M. S., Raab, T. K., and Pringle, J. R. (2012). Evidence that glucose is the major transferred metabolite in dinoflagellate-cnidarian symbiosis. *J. Exp. Biol.* 215, 3467–3477. doi: 10.1242/jeb.070946

Chakravarti, L. J., and Van Oppen, M. J. H. (2018). Experimental Evolution in Coral Photosymbionts as a Tool to Increase Thermal Tolerance. *Front. Mar. Sci.* 5:227. doi: 10.3389/fmars.2018.00227

Chakravarti, L. J., Beltran, V. H., and van Oppen, M. J. H. (2017). Rapid thermal adaptation in photosymbionts of reef-building corals. *Glob. Chang. Biol.* 23, 4675–4688. doi: 10.1111/gcb.13702

Coffroth, M. A., and Santos, S. R. (2005). Genetic diversity of symbiotic dinoflagellates in the genus Symbiodinium. *Protist* 156, 19–34. doi: 10.1016/j.protis.2018.06.008

Connell, J. H. (1978). Diversity in Tropical Rain Forests and Coral Reefs. *Science* 199, 1302–1310. doi: 10.1126/science.199.4335.1302

Correa, A. M. S., and Baker, A. C. (2011). Disaster taxa in microbially mediated metazoans: How endosymbionts and environmental catastrophes influence the adaptive capacity of reef corals. *Glob. Chang. Biol.* 17, 68–75. doi: 10.1111/j.1365-2486.2010.02242.x

Császár, N. B. M., Ralph, P. J., Frankham, R., Berkelmans, R., and van Oppen, M. J. H. (2010). Estimating the Potential for Adaptation of Corals to Climate Warming. *PLoS One* 5:9751. doi: 10.1371/journal.pone.0009751

Cunning, R., Gillette, P., Capo, T., Galvez, K., and Baker, A. C. (2015). Growth tradeoffs associated with thermotolerant symbionts in the coral Pocillopora damicornis are lost in warmer oceans. *Coral Reefs* 34, 155–160. doi: 10.1007/s00338-014-1216-4

Cunning, R., Silverstein, R. N., and Baker, A. C. (2018). Symbiont shuffling linked to differential photochemical dynamics of Symbiodinium in three Caribbean reef corals. *Coral Reefs* 37, 145–152. doi: 10.1007/s00338-017-1640-3

Dang, K., Van, Pierangelini, M., Roberty, S., and Cardol, P. (2019). Alternative Photosynthetic Electron Transfers and Bleaching Phenotypes Upon Acute Heat Stress in Symbiodinium and Breviolum spp. (Symbiodiniaceae) in Culture. *Front. Mar. Sci.* 6:1–10. doi: 10.3389/fmars.2019.00656

Davies, P. S. (1984). The role of zooxanthellae in the nutritional energy requirements of Pocillopora eydouxi. *Coral Reefs* 2, 181–186. doi: 10.1007/BF00263571

Davy, S. K., Allemand, D., and Weis, V. M. (2012). Cell Biology of Cnidarian-Dinoflagellate Symbiosis. *Microbiol. Mol. Biol. Rev.* 76, 229–261. doi: 10.1128/mmbr.05014-11

Decelle, J., Carradec, Q., Pochon, X., Henry, N., Romac, S., Mahé, F., et al. (2018). Worldwide Occurrence and Activity of the Reef-Building Coral Symbiont Symbiodinium in the Open Ocean. *Curr. Biol.* 28, 3625.e–3633.e. doi: 10.1016/j.cub.2018.09.024

Díaz-Almeyda, E. M., Prada, C., Ohdera, A. H., Moran, H., Civitello, D. J., Iglesias-Prieto, R., et al. (2017). Intraspecific and interspecific variation in thermotolerance and photoacclimation in Symbiodinium dinoflagellates. *Proc. R. Soc. B Biol. Sci.* 284:1767. doi: 10.1098/rspb.2017.1767

Eakin, C. M., Morgan, J. A., Heron, S. F., Smith, T. B., Liu, G., Alvarez-Filip, L., et al. (2010). Caribbean Corals in Crisis: Record Thermal Stress, Bleaching, and Mortality in 2005. *PLoS One* 5:e13969. doi: 10.1371/journal.pone.0013969

Fautin, D. G., and Buddemeier, R. W. (2004). Adaptive bleaching: a general phenomenon. *Hydrobiologia* 530–531, 459–467. doi: 10.1007/s10750-004-2642-z

Frade, P. R., Bongaerts, P., Winkelhagen, A. J. S., Tonk, L., and Bak, R. P. M. (2008a). In situ photobiology of corals over large depth ranges: A multivariate analysis on the roles of environment, host, and algal symbiont. *Limnol. Oceanogr.* 53, 2711–2723. doi: 10.4319/lo.2008.53.6.2711

Frade, P. R., Englebert, N., Faria, J., Visser, P. M., and Bak, R. P. M. (2008b). Distribution and photobiology of Symbiodinium types in different light environments for three colour morphs of the coral Madracis pharensis: Is there more to it than total irradiance? *Coral Reefs* 27, 913–925. doi: 10.1007/s00338-008-0406-3

Gabay, Y., Weis, V. M., and Davy, S. K. (2018). Symbiont Identity Influences Patterns of Symbiosis Establishment, Host Growth, and Asexual Reproduction in a Model Cnidarian-Dinoflagellate Symbiosis. *Biol. Bull.* 234, 1–10. doi: 10.1086/696365

Gegner, H. M., Rädecker, N., Ochsenkühn, M., Barreto, M. M., Ziegler, M., Reichert, J., et al. (2019). High levels of floridoside at high salinity link osmoadaptation with bleaching susceptibility in the cnidarian-algal endosymbiosis. *Biol. Open* 8:45591. doi: 10.1242/bio.045591

Glynn, P. W. (1993). Coral reef bleaching: ecological perspectives. *Coral Reefs* 12, 1–17. doi: 10.1007/BF00303779

Glynn, P. W., and D'Croz, L. (1990). Experimental evidence for high temperature stress as the cause of El Niño-coincident coral mortality. *Coral Reefs* 8, 181–191. doi: 10.1007/BF00265009

Granados-Cifuentes, C., Neigel, J., Leberg, P., and Rodriguez-Lanetty, M. (2015). Genetic diversity of free-living Symbiodinium in the Caribbean: the importance of habitats and seasons. *Coral Reefs* 34, 927–939. doi: 10.1007/s00338-015-1291-1

Grégoire, V., Schmacka, F., Coffroth, M. A., and Karsten, U. (2017). Photophysiological and thermal tolerance of various genotypes of the coral endosymbiont Symbiodinium sp. (Dinophyceae). *J. Appl. Phycol.* 29, 1893–1905. doi: 10.1007/s10811-017-1127-1

Helcom (1988). *Declaration on the protection of the marine environment of the baltic sea*. Helsinki: HELCOM.

Hennige, S. J., Smith, D. J., Walsh, S. M. S. J., McGinley, M. P., Warner, M. E., Suggett, D. J., et al. (2019). Free-living and symbiotic lifestyles of a thermotolerant coral endosymbiont display profoundly distinct transcriptomes under both stable and heat stress conditions. *Ecol. Modell.* 163, 1–15. doi: 10.1007/978-94-007-0114-4

Hennige, S. J., Suggett, D. J., Warner, M. E., McDougall, K. E., and Smith, D. J. (2009). Photobiology of Symbiodinium revisited: Bio-physical and bio-optical signatures. *Coral Reefs* 28, 179–195. doi: 10.1007/s00338-008-0444-x

Herrera, M., Klein, S. G., Campana, S., Chen, J. E., Prasanna, A., Duarte, C. M., et al. (2020). Temperature transcends partner specificity in the symbiosis establishment of a cnidarian. *ISME J.* 15:768–y. doi: 10.1038/s41396-020-00768-y

Hill, R., Szabó, M., Rehman, A., Vass, I., Ralph, P. J., and Larkum, A. W. D. (2014). Inhibition of photosynthetic CO_2 fixation in the coral *Pocillopora damicornis* and its relationship to thermal bleaching. *J. Exp. Biol.* 217, 2150–2162. doi: 10.1242/jeb.100578

Hoadley, K. D., Pettay, D. T., Grottoli, A. G., Cai, W. J., Melman, T. F., Schoepf, V., et al. (2015). Physiological response to elevated temperature and pCO2 varies across four Pacific coral species: Understanding the unique host+symbiont response. *Sci. Rep.* 5, 1–15. doi: 10.1038/srep18371

Hoegh-Guldberg, O. (1999). Climate change, coral bleaching and the future of the world's coral reefs. *Mar. Freshw. Res.* 50, 839–866. doi: 10.1071/MF99078

Hoegh-Guldberg, O., Mumby, P. J., Hooten, A. J., Steneck, R. S., Greenfield, P., Gomez, E., et al. (2007). Coral Reefs Under Rapid Climate Change and Ocean Acidification. *Science* 318, 1737–1742. doi: 10.1126/science.1152509

Howells, E. J., Abrego, D., Meyer, E., Kirk, N. L., and Burt, J. A. (2016). Host adaptation and unexpected symbiont partners enable reef-building corals to tolerate extreme temperatures. *Glob. Chang. Biol.* 22, 2702–2714. doi: 10.1111/gcb.13250

Howells, E. J., Beltran, V. H., Larsen, N. W., Bay, L. K., Willis, B. L., and van Oppen, M. J. H. (2012). Coral thermal tolerance shaped by local adaptation of photosymbionts. *Nat. Clim. Chang.* 2, 116–120. doi: 10.1038/nclimate1330

Hughes, D. J., Alderdice, R., Cooney, C., Kühl, M., Pernice, M., Voolstra, C. R., et al. (2020). Coral reef survival under accelerating ocean deoxygenation. *Nat. Clim. Chang.* 10, 296–307. doi: 10.1038/s41558-020-0737-9

Hughes, T. P., Anderson, K. D., Connolly, S. R., Heron, S. F., Kerry, J. T., Lough, J. M., et al. (2018). Spatial and temporal patterns of mass bleaching of corals in the Anthropocene. *Science* 359, 80–83. doi: 10.1126/science.aan8048

Hughes, T. P., Barnes, M. L., Bellwood, D. R., Cinner, J. E., Cumming, G. S., Jackson, J. B. C., et al. (2017). Coral reefs in the Anthropocene. *Nature* 546, 82–90. doi: 10.1038/nature22901

Hume, B. C. C., D'Angelo, C., Smith, E. G., Stevens, J. R., Burt, J., and Wiedenmann, J. (2015). Symbiodinium thermophilum sp. nov., a thermotolerant symbiotic alga prevalent in corals of the world's hottest sea, the Persian/Arabian Gulf. *Sci. Rep.* 5:8562. doi: 10.1038/srep08562

Iglesias-Prieto, R., and Trench, R. (1994). Acclimation and adaptation to irradiance in symbiotic dinoflagellates. I. Responses of the photosynthetic unit to changes in photon flux density. *Mar. Ecol. Prog. Ser.* 113, 163–175. doi: 10.3354/meps113163

Iglesias-Prieto, R., and Trench, R. K. (1997). Acclimation and adaptation to irradiance in symbiotic dinoflagellates. II. Response of chlorophyll-protein complexes to different photon-flux densities. *Mar. Biol.* 130, 23–33. doi: 10.1007/s002270050221

Iglesias-Prieto, R., Matta, J. L., Robins, W. A., and Trench, R. K. (1992). Photosynthetic response to elevated temperature in the symbiotic dinoflagellate Symbiodinium microadriaticum in culture. *Proc. Natl. Acad. Sci. U S A.* 89, 10302–10305. doi: 10.1073/pnas.89.21.10302

Jones, A., Berkelmans, R., van Oppen, M. J., Mieog, J., and Sinclair, W. (2008). A community change in the algal endosymbionts of a scleractinian coral following a natural bleaching event: field evidence of acclimatization. *Proc. R. Soc. B Biol. Sci.* 275, 1359–1365. doi: 10.1098/rspb.2008.0069

Jones, R. J., Hoegh-Guldberg, O., Larkum, A. W. D., and Schreiber, U. (1998). Temperature-induced bleaching of corals begins with impairment of the CO2 fixation mechanism in zooxanthellae. *Plant Cell Environ.* 21, 1219–1230. doi: 10.1046/j.1365-3040.1998.00345.x

Karim, W., Nakaema, S., and Hidaka, M. (2015). Temperature Effects on the Growth Rates and Photosynthetic Activities of Symbiodinium Cells. *J. Mar. Sci. Eng.* 3, 368–381. doi: 10.3390/jmse3020368

Klueter, A., Trapani, J., Archer, F. I., McIlroy, S. E., and Coffroth, M. A. (2017). Comparative growth rates of cultured marine dinoflagellates in the genus Symbiodinium and the effects of temperature and light. *PLoS One* 12:e0187707. doi: 10.1371/journal.pone.0187707

LaJeunesse, T. C., Parkinson, J. E., Gabrielson, P. W., Jeong, H. J., Reimer, J. D., Voolstra, C. R., et al. (2018). Systematic Revision of Symbiodiniaceae Highlights the Antiquity and Diversity of Coral Endosymbionts. *Curr. Biol.* 28, 2570.e–2580.e. doi: 10.1016/j.cub.2018.07.008

LaJeunesse, T. C., Smith, R. T., Finney, J., and Oxenford, H. (2009). Outbreak and persistence of opportunistic symbiotic dinoflagellates during the 2005 Caribbean mass coral 'bleaching' event. *Proc. R. Soc. B Biol. Sci.* 276, 4139–4148. doi: 10.1098/rspb.2009.1405

Lesser, M. P. (1996). Elevated temperatures in symbiotic dinoflagellates stress and inhibit photosynthesis latitudes. *Limnol. Ocean.* 41, 271–283.

Lesser, M. P., Bailey, M. A., Merselis, D. G., and Morrison, J. R. (2010). Physiological response of the blue mussel Mytilus edulis to differences in food and temperature in the Gulf of Maine. *Comp. Biochem. Physiol. A Mol. Integr. Physiol.* 156, 541–551. doi: 10.1016/j.cbpa.2010.04.012

Lewis, C., Neely, K., and Rodriguez-Lanetty, M. (2019). Recurring episodes of thermal stress shift the balance from a dominant host-specialist to a background host-generalist zooxanthella in the threatened pillar coral, Dendrogyra cylindrus. *Front. Mar. Sci.* 6:1–15. doi: 10.3389/fmars.2019.00005

Mansour, J. S., Pollock, F. J., Díaz-Almeyda, E., Iglesias-Prieto, R., and Medina, M. (2018). Intra- and interspecific variation and phenotypic plasticity in thylakoid membrane properties across two Symbiodinium clades. *Coral Reefs* 37, 841–850. doi: 10.1007/s00338-018-1710-1

Moberg, F., and Folke, C. (1999). Ecological goods and services of coral reef ecosystems. *Ecol. Econ.* 29, 215–233. doi: 10.1016/S0921-8009(99)00009-9

Muscatine, L., and Porter, J. W. (1977). Reef Corals: Mutualistic Symbioses Adapted to Nutrient-Poor Environments. *Bioscience* 27, 454–460. doi: 10.2307/1297526

Niedzwiedzki, D. M., Jiang, J., Lo, C. S., and Blankenship, R. E. (2014). Spectroscopic properties of the Chlorophyll a–Chlorophyll c 2–Peridinin-Protein-Complex (acpPC) from the coral symbiotic dinoflagellate Symbiodinium. *Photosynth. Res.* 120, 125–139. doi: 10.1007/s11120-013-9794-5

Platt, T., Gallegos, C. L., and Harrison, W. (1980). Photoinhibiton of photosynthesis in natural assemblages of marine phytoplankton. *J. Mar. Res.* 38, 687–701.

Qin, Z., Yu, K., Chen, B., Wang, Y., Liang, J., Luo, W., et al. (2019). Diversity of Symbiodiniaceae in 15 Coral Species From the Southern South China Sea: Potential Relationship With Coral Thermal Adaptability. *Front. Microbiol.* 10:2343. doi: 10.3389/fmicb.2019.02343

Quigley, K. M., Willis, B. L., and Bay, L. K. (2016). Maternal effects and Symbiodinium community composition drive differential patterns in juvenile survival in the coral Acropora tenuis. *R. Soc. Open Sci.* 3:160471. doi: 10.1098/rsos.160471

Ralph, P., Gademann, R., and Larkum, A. (2001). Zooxanthellae expelled from bleached corals at 33°C are photosynthetically competent. *Mar. Ecol. Prog. Ser.* 220, 163–168. doi: 10.3354/meps220163

Ravelo, S. F., and Conaco, C. (2018). Comparison of the response of in hospite and ex hospite Symbiodinium to elevated temperature. *Mar. Freshw. Behav. Physiol.* 51, 93–108. doi: 10.1080/10236244.2018.1503935

Raven, J. A., and Geider, R. J. (2003). "Adaptation, Acclimation and Regulation in Algal Photosynthesis," in *Photosynthesis in Algae*, eds J. A. Raven, A. Larkum, S. Douglas (Berlin: Nature Publishing Group), 385–412. doi: 10.1007/978-94-007-1038-2_17

Robison, J. D., and Warner, M. E. (2006). Differential impacts of photoacclimation and thermal stress on the photobiology of four different phylotypes of Symbiodinium (Pyrrhophyta). *J. Phycol.* 42, 568–579. doi: 10.1111/j.1529-8817.2006.00232.x

Roth, M. S. (2014). The engine of the reef: Photobiology of the coral-algal symbiosis. *Front. Microbiol.* 5:1–22. doi: 10.3389/fmicb.2014.00422

Rowan, R. (2004). Thermal adaptation in reef coral symbionts. *Nature* 430, 742–742. doi: 10.1038/430742a

Sakami, T. (2000). Effects of temperature, irradiance, salinity and inorganic nitrogen concentration on coral zooxanthellae in culture. *Fish. Sci.* 66, 1006–1013. doi: 10.1046/j.1444-2906.2000.00162.x

Sampayo, E. M., Ridgway, T., Bongaerts, P., and Hoegh-Guldberg, O. (2008). Bleaching susceptibility and mortality of corals are determined by fine-scale differences in symbiont type. *Proc. Natl. Acad. Sci. U S A.* 105, 10444–10449. doi: 10.1073/pnas.0708049105

Shoguchi, E., Shinzato, C., Kawashima, T., Gyoja, F., Mungpakdee, S., Koyanagi, R., et al. (2013). Draft Assembly of the Symbiodinium minutum Nuclear Genome Reveals Dinoflagellate Gene Structure. *Curr. Biol.* 23, 1399–1408. doi: 10.1016/j.cub.2013.05.062

Starzak, D. E., Quinnell, R. G., Nitschke, M. R., and Davy, S. K. (2014). The influence of symbiont type on photosynthetic carbon flux in a model cnidarian-dinoflagellate symbiosis. *Mar. Biol.* 161, 711–724. doi: 10.1007/s00227-013-2372-8

Stat, M., Loh, W. K. W., LaJeunesse, T. C., Hoegh-Guldberg, O., and Carter, D. A. (2009). Stability of coral-endosymbiont associations during and after a thermal stress event in the southern Great Barrier Reef. *Coral Reefs* 28, 709–713. doi: 10.1007/s00338-009-0509-5

Stat, M., Morris, E., and Gates, R. D. (2008). Functional diversity in coral-dinoflagellate symbiosis. *Proc. Natl. Acad. Sci.* 105, 9256–9261. doi: 10.1073/pnas.0801328105

Steen, R. G., and Muscatine, L. (1984). Daily Budgets of Photosynthetically Fixed Carbon in Symbiotic Zoanthids. *Biol. Bull.* 167, 477–487. doi: 10.2307/1541292

Suggett, D. J., Goyen, S., Evenhuis, C., Szabó, M., Pettay, D. T., Warner, M. E., et al. (2015). Functional diversity of photobiological traits within the genus Symbiodinium appears to be governed by the interaction of cell size with cladal designation. *N. Phytol.* 208, 370–381. doi: 10.1111/nph.13483

Suggett, D. J., Warner, M. E., Smith, D. J., Davey, P., Hennige, S., and Baker, N. R. (2008). Photosynthesis and production of hydrogen peroxide by Symbiodinium (Pyrrhophyta) phylotypes with different thermal tolerances. *J. Phycol.* 44, 948–956. doi: 10.1111/j.1529-8817.2008.00537.x

Swain, T. D., Chandler, J., Backman, V., and Marcelino, L. (2017). Consensus thermotolerance ranking for 110 Symbiodinium phylotypes: an exemplar

utilization of a novel iterative partial-rank aggregation tool with broad application potential. *Funct. Ecol.* 31, 172–183. doi: 10.1111/1365-2435.12694

Szabó, M., Larkum, A. W. D., and Vass, I. (2020). "A Review: The Role of Reactive Oxygen Species in Mass Coral Bleaching," in *Photosynthesis in Algae: Biochemical and Physiological Mechanisms*, eds J. A. Raven, A. Larkum, A. R. Grossman (Basingstoke: Springer Nature), 459–488. doi: 10.1007/978-3-030-33397-3_17

Tabita, R. F., Satagopan, S., Hanson, T. E., Kreel, N. E., and Scott, S. S. (2008). Distinct form I, II, III, and IV Rubisco proteins from the three kingdoms of life provide clues about Rubisco evolution and structure/function relationships. *J. Exp. Bot.* 59, 1515–1524. doi: 10.1093/jxb/erm361

Takahashi, S., Whitney, S. M., and Badger, M. R. (2009). Different thermal sensitivity of the repair of photodamaged photosynthetic machinery in cultured Symbiodinium species. *Proc. Natl. Acad. Sci.* 106, 3237–3242. doi: 10.1073/pnas.0808363106

Takahashi, S., Whitney, S., Itoh, S., Maruyama, T., and Badger, M. (2008). Heat stress causes inhibition of the de novo synthesis of antenna proteins and photobleaching in cultured Symbiodinium. *Proc. Natl. Acad. Sci.* 105, 4203–4208. doi: 10.1073/pnas.0708554105

Thornhill, D. J., LaJeunesse, T. C., Kemp, D. W., Fitt, W. K., and Schmidt, G. W. (2006). Multi-year, seasonal genotypic surveys of coral-algal symbioses reveal prevalent stability or post-bleaching reversion. *Mar. Biol.* 148, 711–722. doi: 10.1007/s00227-005-0114-2

Trench, R. K. (1993). Microalgal-invertebrate symbiosis: a review. *Endocytobiosis Cell Res.* 9, 135–175.

Van Oppen, M. J. H., and Lough, J. M. (2018). *Coral Bleaching*. New York City: Springer International Publishing, doi: 10.1007/978-3-319-75393-5

van Oppen, M. J. H., Bongaerts, P., Underwood, J. N., Peplow, L. M., and Cooper, T. F. (2011), The role of deep reefs in shallow reef recovery: an assessment of vertical connectivity in a brooding coral from west and east Australia. *Mol. Ecol.* 20, 1647–1660. doi: 10.1111/j.1365-294X.2011.05050.x

Van Oppen, M. J. H., Baker, A. C., Coffroth, M. A., and Willis, B. L. (2009). Bleaching Resistance and the Role of Algal Endosymbionts. *Coral Bleaching* 2009, 83–102. doi: 10.1007/978-3-540-69775-6_6

Venn, A. A., Loram, J. E., and Douglas, A. E. (2008). Photosynthetic symbioses in animals. *J. Exp. Bot.* 59, 1069–1080. doi: 10.1093/jxb/erm328

Warner, M. E., Fitt, W. K., and Schmidt, G. W. (1996). The effects of elevated temperature on the photosynthetic efficiency of zooxanthellae in hospite from four different species of reef coral: a novel approach. *Plant Cell Environ.* 19, 291–299.

Weis, V. M. (2008). Cellular mechanisms of Cnidarian bleaching: stress causes the collapse of symbiosis. *J. Exp. Biol.* 211, 3059–3066. doi: 10.1242/jeb.009597

Conflict of Interest: The authors declare that the research was conducted in the absence of any commercial or financial relationships that could be construed as a potential conflict of interest.

frontiers in Marine Science

ORIGINAL RESEARCH
published: 13 January 2022
doi: 10.3389/fmars.2021.814124

Antibiotics Alter *Pocillopora* Coral-Symbiodiniaceae-Bacteria Interactions and Cause Microbial Dysbiosis During Heat Stress

Michael T. Connelly[1†], Crystal J. McRae[2,3], Pi-Jen Liu[4], Cecily E. Martin[1,5] and Nikki Traylor-Knowles[1]*

[1] Department of Marine Biology and Ecology, Rosenstiel School of Marine and Atmospheric Science, University of Miami, Coral Gables, FL, United States, [2] Department of Biological Sciences, Simon Fraser University, Burnaby, BC, Canada, [3] Department of Natural Resources and Environmental Studies, National Dong Hwa University, Hualien, Taiwan, [4] Graduate Institute of Marine Biology, National Dong Hwa University, Pingtung, Taiwan, [5] Department of Mechanical Engineering, Imperial College London, London, United Kingdom

OPEN ACCESS

Edited by:
Kefu Yu,
Guangxi University, China

Reviewed by:
Xiaopeng Yu,
Guangxi University, China
Danwei Huang,
National University of Singapore, Singapore

***Correspondence:**
Nikki Traylor-Knowles
ntraylorknowles@rsmas.miami.edu

† Present address:
Michael T. Connelly, Department of Invertebrate Zoology, National Museum of Natural History, Smithsonian Institution, Washington, DC, United States

Specialty section:
This article was submitted to Coral Reef Research, a section of the journal Frontiers in Marine Science

Received: *12 November 2021*
Accepted: *22 December 2021*
Published: *13 January 2022*

Citation:
Connelly MT, McRae CJ, Liu P-J, Martin CE and Traylor-Knowles N (2022) Antibiotics Alter Pocillopora Coral-Symbiodiniaceae-Bacteria Interactions and Cause Microbial Dysbiosis During Heat Stress. Front. Mar. Sci. 8:814124. doi: 10.3389/fmars.2021.814124

Symbioses between eukaryotes and their associated microbial communities are fundamental processes that affect organisms' ecology and evolution. A unique example of this is reef-building corals that maintain symbiotic associations with dinoflagellate algae (Symbiodiniaceae) and bacteria that affect coral health through various mechanisms. However, little is understood about how coral-associated bacteria communities affect holobiont heat tolerance. In this study, we investigated these interactions in four *Pocillopora* coral colonies belonging to three cryptic species by subjecting fragments to treatments with antibiotics intended to suppress the normal bacteria community, followed by acute heat stress. Separate treatments with only antibiotics or heat stress were conducted to compare the effects of individual stressors on holobiont transcriptome responses and microbiome shifts. Across all *Pocillopora* species examined, combined antibiotics and heat stress treatment significantly altered coral-associated bacteria communities and caused major changes in both coral and *Cladocopium* algal symbiont gene expression. Individually, heat stress impaired *Pocillopora* protein translation and activated DNA repair processes, while antibiotics treatments caused downregulation of *Pocillopora* amino acid and inorganic ion transport and metabolism genes and *Cladocopium* photosynthesis genes. Combined antibiotics-heat stress treatments caused synergistic effects on *Pocillopora* and *Cladocopium* gene expression including enhanced expression of oxidative stress response genes, programed cell death pathways and proteolytic enzymes that indicate an exacerbated response to heat stress following bacteria community suppression. Collectively, these results provide further evidence that corals and their Symbiodiniaceae and bacteria communities engage in highly coordinated metabolic interactions that are crucial for coral holobiont health, homeostasis, and heat tolerance.

Keywords: coral, holobiont, transcriptome, microbiome, antibiotics, bacteria, dysbiosis

INTRODUCTION

Microbial symbioses are fundamental to the structure and functioning of marine ecosystems, and influence marine organisms' ecology, evolution, and stress responses (O'Brien et al., 2019; Wilkins et al., 2019; Apprill, 2020). Healthy reef-building corals (Order Scleractinia) maintain associations with endosymbiotic algae (Family Symbiodiniaceae) and bacteria, and are popular models for the study of complex microbial symbioses that underpin marine ecosystem processes (Blackall et al., 2015; Thompson et al., 2015).

Coral-associated bacteria communities exhibit patterns of phylosymbiosis and cophylogeny (Pollock et al., 2018) and demonstrate genomic signatures that are suggestive of highly interdependent symbiotic relationships between corals and bacteria (Robbins et al., 2019). Recent studies have also uncovered evidence for intimate associations between bacteria and Symbiodiniaceae, indicating that diverse multi-partner symbiotic interactions are present in coral holobionts (Motone et al., 2020; Maire et al., 2021). Certain coral-associated bacteria have been investigated for their roles in affecting corals' responses to heat stress, with different bacteria taxa exerting either negative or positive effects on coral holobiont resistance and resilience (Tout et al., 2015; Zaneveld et al., 2016; Ziegler et al., 2017, 2019; Epstein et al., 2019; Avila-Magaña et al., 2021). Other environmental stressors such as nutrient enrichment can also alter coral bacteria communities (Pogoreutz et al., 2018; Ziegler et al., 2019), but the interactive effects of different stressors applied in combination and their effects on coral health are still the focus of much research (Maher et al., 2019).

In contrast to other environmental stressors, broad-spectrum antibiotics treatments have previously been used to directly suppress the coral-associated bacteria community and generate hypotheses about how bacteria might affect coral holobiont health and homeostasis (Hodgson, 1990; Gilbert et al., 2012; Sweet et al., 2014; Sweet and Bythell, 2015; Glasl et al., 2016). Altogether, these studies have documented negative effects of antibiotics on coral health and hypothesized that antibiotic suppression of the native microbiota enables the proliferation of potential pathogens. These results have led to concerns about antibiotics as environmental pollutants on coral reefs (Zhang R. et al., 2018, 2019), which merit special consideration as antibiotics treatments are now being broadly deployed as field interventions to combat stony coral tissue loss disease (SCTLD) in the Caribbean (Neely et al., 2020). Despite these novel applications and concerns over the use of antibiotics on coral reefs, the specific genes and pathways involved in coral holobiont responses to antibiotic suppression of the bacteria community have not been explored. The experimental study of these processes can inform our knowledge of risks that antibiotics pose to coral health in the field and can also improve our understanding of coral holobiont interactions under normal conditions.

The coral genus *Pocillopora* is among the most widespread and important reef-building coral taxa in the world, with a distribution from east Africa to western Central America. For this reason, *Pocillopora* corals have become popular experimental model species and *Pocillopora* holobiont responses to heat stress and other environmental stressors have been thoroughly studied (Traylor-Knowles et al., 2011; Mayfield et al., 2014; Vidal-Dupiol et al., 2014; Zhou et al., 2018; Poquita-Du et al., 2019; Li et al., 2020). These studies suggest that *Pocillopora* coral transcriptomes are generally more responsive to heat stress than their associated Symbiodiniaceae transcriptomes, and that expression of genes involved in metabolism, protein folding and immune pathways such as heat shock proteins (HSPs) and tumor necrosis factor receptors (TNFRs) are important components of the *Pocillopora* coral heat stress response (Zhou et al., 2017; Zhang Y. et al., 2018). Other studies have assessed *Pocillopora*-associated bacteria community shifts that occur during heat stress, nutrient enrichment, and treatment with putative beneficial microbes (Tout et al., 2015; Pogoreutz et al., 2018; Rosado et al., 2018; Maher et al., 2019; Ziegler et al., 2019; Li et al., 2020, 2021; Zhang Y. et al., 2021). However, despite the critical importance of coral-associated bacteria to holobiont health, no study has simultaneously assessed coral holobiont transcriptome and microbiome responses to acute heat stress following direct antibiotic suppression of the native bacteria community. These studies are needed to better understand the role of coral-associated bacteria in coral holobiont health and heat tolerance, and to inform ongoing efforts that seek to conserve and restore coral reef ecosystems by enhancing corals' natural resilience through the application of beneficial microbes (Peixoto et al., 2021; Voolstra et al., 2021).

To investigate how antibiotics treatments suppress the native coral bacteria community and affect coral holobiont interactions and acute heat stress responses, we performed an experiment with four *Pocillopora* coral colonies (genotypes) collected from Kenting National Park in southern Taiwan. These four distinct genotypes belonged to three morphologically cryptic *Pocillopora* species: *Pocillopora acuta* (n = 2) and *Pocillopora damicornis* (n = 1) (Schmidt-Roach et al., 2014), and the undescribed species *Pocillopora* type 8a (n = 1) (Gélin et al., 2017; Johnston et al., 2017). In this experiment we examined the effects of antibiotics, acute heat stress, and combined antibiotics-heat stress treatments on coral host and *Cladocopium* symbiont gene expression through RNAseq and bacteria composition through 16S gene amplicon sequencing. Through this work, we identified genes involved in coral-bacteria interactions to gain a better understanding of how coral-associated bacteria communities affect coral holobiont stress responses. We found that there were differences between the four *Pocillopora* genotypes from distinct cryptic species and sites, as expected. However, we also found that there were shared responses across all genotypes and species examined. Most notably, for all genotypes we found that both antibiotics and combined antibiotics-heat stress treatments altered *Pocillopora* coral bacteria community composition and affected *Pocillopora* coral and *Cladocopium* symbiont gene expression. We hypothesize that the changes in bacteria community composition exacerbated the holobiont heat stress responses causing microbial dysbiosis and the activation of programed cell death pathways. These results have implications for understanding how multi-partner interactions affect coral holobiont health and homeostasis and highlight the utility of

antibiotics treatments as an experimental tool to suppress and manipulate coral-associated bacteria communities.

MATERIALS AND METHODS

Coral Study Site, Collection, Fragmentation, and Acclimation

Colonies of *Pocillopora* corals were collected from two reefs within Kenting National Park in southern Taiwan (Kenting National Park Permit #10621218300) Houwan (22° 2′29″ N, 120°41′43″ E) and Wanglitung (21°59′43″ N, 120°42′22″ E) (**Supplementary Figure 1**). Two *Pocillopora* colonies with morphological similarity to *P. damicornis* were collected at each site, Houwan and Wanglitung, and colonies (hereafter referred to as HW1, HW2, WT1, and WT2) were collected in July 2017 (**Table 1**). Colonies were acclimated in a flow-through system receiving ambient seawater under natural sunlight at the National Museum of Marine Biology and Aquarium (NMMBA), and then split into a minimum of 12 replicate 2 cm^2 fragments per colony that were affixed to numbered plastic tags and allowed to recover for 3 weeks before the experiment.

Heat Stress, Antibiotics, and Antibiotics-Heat Stress Treatment Experiment

Three experimental treatments (heat stress, antibiotics, and antibiotics-heat stress) and a control were designed to examine the separate and interactive effects of acute heat stress and antibiotic bacteria suppression on the *Pocillopora* holobiont transcriptome and bacteria community composition (**Figure 1**). Triplicate fragments from each coral genotype were placed into individual autoclaved 400 mL glass jars filled with filtered seawater (1 μm) and randomly assigned to experimental or seawater control treatments (**Figure 1**). Jars were placed into two recirculating systems, one for the control and antibiotics treatment and another for the heat stress and antibiotics-heat stress treatments. Blue and white LED lights were operated on a 12 h:12 h light:dark cycle with even distribution across fragment jars. At 9:00 am in the morning of each day of the 3-day experiment, partial water changes were completed using 100 mL of filtered seawater (1 μm). The control system was maintained at 28°C for the full 72 h, to mimic the mean summer seawater temperature in Kenting National Park (Keshavmurthy et al., 2019).

TABLE 1 | Origin sites and species designations of the *Pocillopora* coral colonies used in the antibiotics and heat stress experiment.

Colony	Site	*Pocillopora* nominal species (*sensu* Schmidt-Roach et al., 2014)	*Pocillopora* mtORF type (*sensu* Pinzón et al., 2013)	*Pocillopora* ORF type (*sensu* Gélin et al., 2017)
HW1	Houwan	*Pocillopora* sp. type 8a	8a	ORF23
HW2	Houwan	*Pocillopora damicornis*	4a	ORF09
WT1	Wanglitung	*Pocillopora acuta*	5a	ORF18
WT2	Wanglitung	*Pocillopora acuta*	5a	ORF18

Acute Heat Stress Treatment

The acute heat stress treatment was maintained for 48 h at 32°C (∼0.9 DHWs) after an initial 24 h at 28°C and a 90-min temperature ramp to 32°C. Temperatures in the control system and heat stress system were recorded at 1-min intervals with HOBO® Pendant data loggers (Onset, MA, United States) (**Figure 1**). This acute heat stress was done to contrast the short-term transcriptomic responses of healthy corals with normal bacteria communities against those with bacteria communities that had been previously suppressed by antibiotics treatment.

Antibiotics Treatment

The antibiotics treatment consisted of a combined exposure to 100 μg/mL ampicillin (Sigma-Aldrich A9393) and 100 μg/mL streptomycin sulfate (Sigma-Aldrich 6501), which were administered together to each jar as 400 μL of 100 mg/mL stock solution. These antibiotics were selected for their broad-spectrum antibacterial activity and different modes of action against bacterial cell wall cross-linking and protein synthesis, respectively. Previous studies that have used ampicillin and streptomycin indicate that the chosen concentrations of these antibiotics are non-toxic to the coral host or associated Symbiodiniaceae, and preliminary experiments supported this observation (Soffer et al., 2008; Gilbert et al., 2012; Sweet et al., 2014). Coral fragments were exposed to the antibiotic solution for a total of 72 h before fragment sampling and preservation. For daily partial water changes, 100 mL of antibiotic-treated seawater was used to maintain consistent levels of antibiotic exposure.

Antibiotics-Heat Stress Treatment

A combined antibiotics-heat stress treatment was conducted to parse apart the relative importance of stability within the coral-associated bacteria community toward the holobiont heat stress response. The antibiotics-heat stress treatment consisted of the same combined ampicillin and streptomycin treatment as in the individual antibiotics treatment. Corals were incubated in the antibiotic cocktail for 24 h at 28°C before exposure to acute heat stress at 32°C for 48 h (**Figure 1**), to allow 24 h for the antibiotic suppression of the coral bacteria community to occur before the start of the heat stress. For daily partial water changes, 100 mL of antibiotic-treated seawater was used to maintain consistent levels of antibiotic exposure for a total of 72 h through the entire experiment (**Figure 1**).

Collection and Preservation of Coral Tissue Samples

After the experiment was completed, fragments were photographed, and 1 cm^2 coral fragments were cut using stainless steel bone cutters that were cleaned in 70% ethanol between samples (**Supplementary Figure 4**). These fragments were placed into tubes with 5 mL of RNA stabilization solution consisting of 70% w/v ammonium sulfate, 20 mM EDTA, and

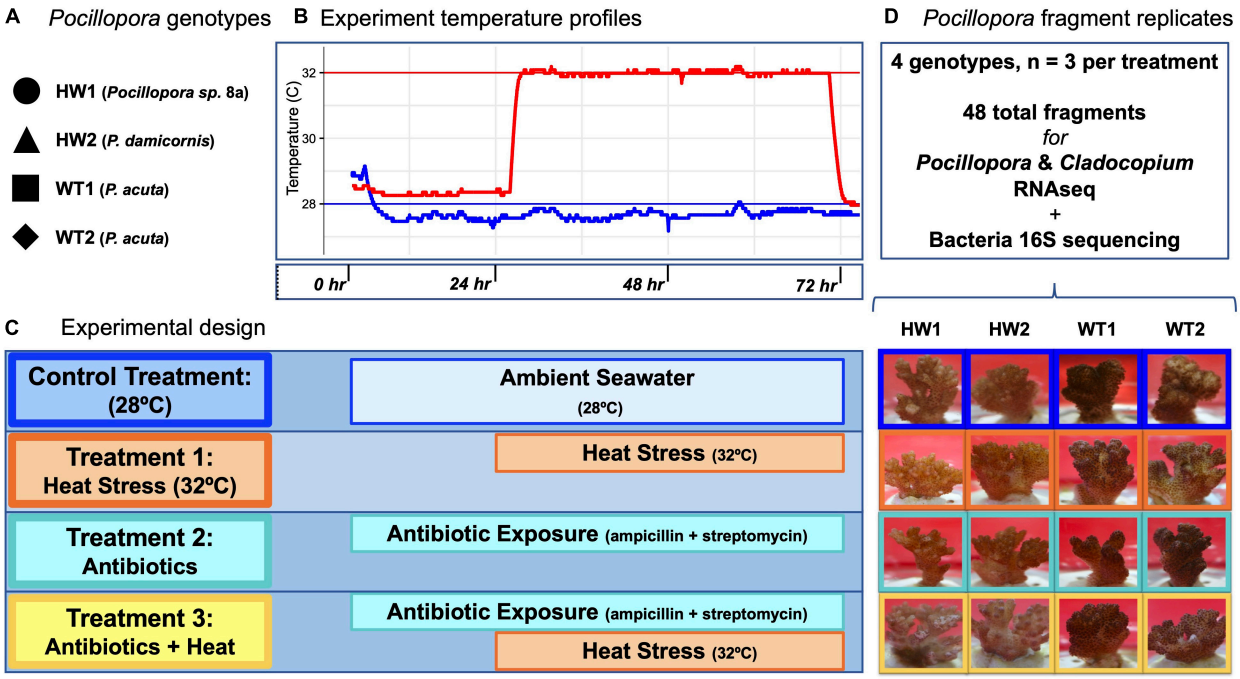

FIGURE 1 | Experimental design for heat stress, antibiotics, and antibiotics-heat stress treatments. **(A)** *Pocillopora* genotypes and species identifications used in the experiment. **(B)** Experiment temperature profiles for control (blue) and heat stress (red) aquarium systems. **(C)** Experimental design indicating the intensity and duration of the control, heat stress, antibiotics, and antibiotics-heat stress treatments. **(D)** Fragment replicates used for downstream sequencing analyses and representative photographs of *Pocillopora* coral fragments from each genotype in each treatment at the time of sampling. All fragments in the control, heat stress, and antibiotics treatment appeared visually healthy, while two fragments in the antibiotics-heat stress treatment showed early signs of tissue loss.

25 mM sodium citrate adjusted to pH 5.2 with 1.0 M H_2SO_4. Fragments were incubated at room temperature for 30 min and frozen at −80°C. Frozen samples were then transported to the University of Miami Rosenstiel School of Marine and Atmospheric Science in Miami, FL, United States, in coolers on dry ice for further processing.

RNA Extraction, cDNA Library Preparation and Sequencing

Total RNA was isolated from the coral tissue using the Qiagen RNeasy Kit and eluted in 30 μL of RNase-free water. RNA concentration and purity were quantified using a NanoDrop 2000 spectrophotometer (Thermo Fisher). cDNA libraries were then created using the Illumina TruSeq RNA Library Prep Kit v2 with Poly-A selection according to the manufacturer's protocol. cDNA concentrations were quantified using the Qubit fluorometer and Qubit dsDNA BR kit (Thermo Fisher Q32853). cDNA libraries were shipped overnight on dry ice to the University of Utah's Huntsman Cancer Center for 50 bp single-end sequencing on the Illumina HiSeq 2000.

Pocillopora Mitochondrial Open Reading Frame Type Determination and Symbiodiniaceae Community Profiling

Pocillopora mitochondrial open reading frame (mtORF) consensus sequences were extracted for each genotype and used to identify the closest mtORF haplotype in GenBank as described previously (Connelly et al., 2020), and these mtORF haplotypes were used to assign species designations following the most recent taxonomic revision to the genus *Pocillopora* (Schmidt-Roach et al., 2014). The genus-level composition of the Symbiodiniaceae community was assessed by aligning non-coral reads against reference sequences of Symbiodiniaceae clade-delineating loci (ITS1, ITS2, and cp23S) with BWA (Li and Durbin, 2009) as in Ladner et al. (2012) to show that all colonies were dominated by *Cladocopium goreauii* (**Supplementary Table 2**).

Pocillopora and *Cladocopium* Dual RNAseq Data Analysis

Raw FASTQ files were checked for base pair quality using the FASTQC program[1], then Illumina adapter sequences and reads with poor-quality bases were removed using Trimmomatic v0.36 (Bolger et al., 2014). Trimmed reads were aligned against the *P. damicornis* genome using the program STAR v2.5.3a in two-pass mode (Dobin et al., 2013; Cunning et al., 2018), and the remaining unaligned reads were then aligned against the *C. goreauii* genome (Liu et al., 2018). Unsorted BAM files containing the *Pocillopora* or *Cladocopium*-aligned transcripts were quantified at the gene level using the featureCounts command in the Subread program (Liao et al., 2014), with only

[1]https://www.bioinformatics.babraham.ac.uk/projects/fastqc/

transcripts that were assigned as accurately single-mapping being retained for gene expression analysis in R version 4.0.3 (R Core Team, 2020).

Pocillopora and *Cladocopium* gene counts were filtered to include only genes with counts ≥ 10 in at least 90% of samples, and counts were normalized using the variance-stabilizing transformation (vst) in the R package DESeq2 (Love et al., 2014). Principal coordinates analysis (PCoA) of Manhattan distances was used to visualize the overall transcriptome patterns of coral and symbiont normalized counts, and pairwise PERMANOVA tests in the R package vegan (Oksanen et al., 2019; Martinez Arbizu, 2020) were used to test for significant differences in transcriptome profiles between experimental treatments.

Statistical analysis of differential gene expression was conducted using generalized linear models implemented in DESeq2. Average log2 fold change (LFC) for each gene was estimated by comparing normalized gene expression counts between treatments, and significantly differentially expressed genes (DEGs) were identified based on a Benjamini–Hochberg false discovery rate-adjusted *p*-value cutoff of <0.05. The set properties of the DEGs lists produced by each experimental treatment contrasted against the control treatment were visualized using the R package VennDiagram (Chen and Boutros, 2011).

To identify modules of co-expressed *Pocillopora* and *Cladocopium* genes across all treatments, weighted gene co-expression network analysis (WGCNA) was performed. The R package WGCNA (Langfelder and Horvath, 2008) was used to construct a signed co-expression network using vst-normalized gene counts and the bi-weight mid-correlation statistic. The resulting adjacency matrix was transformed into connection strengths using a soft-thresholding power of 20 for *Pocillopora* and 5 for *Cladocopium*, based on a scale-free topology fit index. Modules were identified using a cut height of 0.99 on the topological overlap matrix and a minimum module size of 50 genes, and modules with >70.0% similar expression profiles were merged. The expression of each network module "eigengene" was correlated against a binary matrix containing categorical sample treatment information to identify modules with expression patterns linked to a given treatment.

Gene ontology (GO) and Eukaryotic Orthologous Group (KOG) class annotations were obtained for the *P. damicornis* and *C. goreauii* genome using the eggNOG-mapper online tool[2] (Huerta-Cepas et al., 2017). Fisher's exact tests for enrichment of GO terms and KOG categories associated with transcriptome changes among sets of differentially expressed genes and co-expression module genes were conducted using GO_MWU[3] and the R package KOGMWU (Wright et al., 2015; Barfield et al., 2018; Matz, 2019).

Bacteria DNA Extraction and 16S rRNA Gene Amplicon Sequencing

Total DNA was extracted using the Qiagen Dneasy PowerSoil kit from all coral fragment samples in the experiment (Weber et al., 2017). PCR amplification of the V4 region of the bacterial 16S gene was completed with the PCR primers 515F and 806R with single-indexed Illumina adapters according to the Earth Microbiome Project protocols (Apprill et al., 2015). PCR amplicons were checked for quality and size distribution on a 1.5% TE-agarose gel, and amplicon DNA concentration was determined using a Qubit fluorometer and Qubit dsDNA BR kit (Thermo Fisher Q32853). 16S amplicons from all samples and controls were purified using AMPure XP beads (Beckman Coulter A63881) and 80.0% ethanol washes to remove contaminants, then final DNA amplicon products were normalized to 4 nM concentration and pooled before submission to the University of Miami Center for Genome Technology (CGT) for 300 bp paired-end sequencing on the Illumina MiSeq.

Bacteria Community Data Analysis

Raw 16S sequence reads were processed using the QIIME2 pipeline version 2020.2 (Bolyen et al., 2018). The QIIME2 plugin q2-demux was used to visualize read quality and the plugin DADA2 (Callahan et al., 2016) was used to remove primer sequences, trim poor-quality bases, dereplicate reads, identify chimeric sequences and merge paired-end reads. The plugin q2-feature-table (McDonald et al., 2012) was used to generate sequence summary statistics based upon sample metadata. Bacterial 16S rRNA sequences were taxonomically classified using the plugin q2-feature-classifier (Bokulich et al., 2018) and a Naïve Bayes Classifier previously trained on the SILVA 16S rRNA database (Quast et al., 2013) version 132 QIIME2 release based on the 515F/806RB primer pair[4] at the 99.0% similarity amplicon sequence variant (ASV) level. The plugins q2-alignment (Katoh and Standley, 2013) and q2-phylogeny (Price et al., 2010) were used to create a phylogenetic tree for further downstream analyses, and the plugin q2-taxa was used to remove all mitochondria and chloroplast sequences from the dataset. The plugin q2-diversity was used to assess the core diversity metrics of the dataset and create sequence depth rarefaction plots in the QIIME2 environment. Finally, the output tables containing ASV counts, phylogenetic trees and sample metadata were exported from QIIME2 and imported into R for statistical analyses.

All bacteria community statistical analyses were conducted in R using the packages phyloseq (McMurdie and Holmes, 2013), CoDaSeq (Gloor and Reid, 2016), vegan (Oksanen et al., 2019), ggplot2 (Wickham, 2016), and the tidyverse (Wickham et al., 2019). ASVs with a mean count < 3 were filtered from the dataset and ASV abundances were adjusted with the package zCompositions before the centered log-ratio (clr) transformation was performed for compositional data analysis (Palarea-Albaladejo and Martín-Fernández, 2015; Gloor et al., 2017). Alpha-diversity metrics were calculated for the unfiltered dataset using the Chao1 richness, Simpson evenness and Shannon diversity indices, and non-parametric Kruskal–Wallis tests were used to test for significant differences between treatments, reef sites, and coral genotypes (Xia and Sun, 2017; Ziegler et al., 2019). Beta-diversity was calculated using Aitchison dissimilarity matrices and visualized using

[2]http://eggnog-mapper.embl.de/

[3]https://github.com/z0on/GO_MWU

[4]https://data.qiime2.org/2020.2/common/silva-132-99-515-806-nb-classifier.qza

principal coordinates analysis (PCA) (Gloor et al., 2017). Tests for homogeneity of multivariate dispersions (PERMDISP) and permutational analysis of molecular variance (PERMANOVA) (Anderson, 2017) were used to test for differences in bacteria community beta-diversity between treatments, reef sites and coral genotypes. Tests for differential abundance of bacteria ASVs between experimental treatments and the control treatment were completed with the R package ALDEx2 (Fernandes et al., 2013, 2014).

RESULTS

Pocillopora and *Cladocopium* Transcriptome Profiling Reveals Strong Species and Genotype Effects on Coral and Symbiont Gene Expression

RNAseq of 24 *Pocillopora* tissue samples yielded approximately 647.1 million raw reads ranging from 8.2 to 20.4 million reads per sample (**Supplementary Table 1** and **Supplementary Figure 5**). Approximately 69.3% of total reads aligned to the *P. damicornis* genome while 16.1% of total reads aligned to the *C. goreauii* genome (**Supplementary Figure 2**). This was supported by preliminary alignments of non-coral reads to algal ITS2 reference sequences that suggested that the symbiont community was dominated by *C. goreauii* (**Supplementary Table 2**) as has been previously observed for *Pocillopora* corals at these sites (Keshavmurthy et al., 2014; Brener-Raffalli et al., 2018). The 14.6% of total reads that did not align to either reference were discarded from downstream analysis. Filtering only genes with counts $\geq$ 10 in at least 90% of samples left 12,867 *Pocillopora* genes and 9,818 *Cladocopium* genes remaining for downstream expression analyses.

Principal coordinates analysis visualization of vst-normalized gene counts indicated that *Pocillopora* genotype accounted for the most variance in overall *Pocillopora* and *Cladocopium* gene expression (**Figures 2A,B**). PCoA visualization showed the different genotypes clustering separately along PC1 with HW1 (*Pocillopora* sp. 8a) as the most dissimilar from the other three genotypes and HW2 (*P. damicornis*) in between HW1 and the WT1 and WT2 genotypes (*P. acuta*). PERMANOVA tests revealed significant effects of coral genotype (*Pocillopora*: $F = 8.21$, $R^2 = 0.36$, $p < 0.001$; *Cladocopium*: $F = 8.36$, $R^2 = 0.37$, $p < 0.001$) and experimental treatment (*Pocillopora*: $F = 3.64$, $R^2 = 0.20$, $p < 0.001$; *Cladocopium*: $F = 2.36$, $R^2 = 0.14$, $p < 0.001$) on overall transcriptome patterns.

Differential Gene Expression Analysis Reveals Effects of Acute Heat Stress, Antibiotics, and Antibiotics-Heat Stress Treatments

In addition to *Pocillopora* host genotypic effects, PCoA and PERMANOVA revealed a combined effect of the antibiotics-heat stress treatment on *Pocillopora* and *Cladocopium* gene expression. Samples in the antibiotics-heat stress treatment grouped separately from samples in the control treatment and the individual heat stress or antibiotics treatments in the PCoA plot (**Figure 2**). Furthermore, pairwise PERMANOVA tests between treatments only identified significant differences ($p < 0.001$) in *Pocillopora* transcriptome profiles between the antibiotics-heat treatment and the individual control, antibiotics, and heat stress treatments, which were not significantly different from each other (**Supplementary Table 3**).

This pattern was confirmed via the DESeq2 differential gene expression analysis that identified *Pocillopora* and *Cladocopium* DEGs between each of the heat stress, antibiotics, and antibiotics-heat stress treatments versus the control treatment for each genotype and all genotypes analyzed together (**Table 1**). The all-genotypes analysis detected 702 coral DEGs (185 up and 517 down) and 35 symbiont DEGs (11 up and 24 down) between the heat stress treatment and the control treatment, 730 coral DEGs (369 up and 361 down) and 1,614 symbiont DEGs (804 up and 810 down) between the antibiotics treatment and control treatment, and 6,118 coral DEGs (3,117 up and 3,001 down) and 2,936 symbiont DEGs (1,558 up and 1,378 down) between the antibiotics-heat stress treatment and the control treatment (**Table 1** and **Supplementary Table 3**). Venn diagram analysis of the DEG set intersects revealed that many *Pocillopora* DEGs were uniquely differentially expressed in the antibiotics-heat stress treatment (5,044, 82.4%, **Figure 3A**), indicating a synergistic effect of antibiotics and heat stress on the *Pocillopora* transcriptome (Gunderson et al., 2016). This same pattern was also observed in the *Cladocopium* DEGs in the antibiotics-heat stress treatment (1,971, 67.1%, **Figure 3B**).

Eukaryotic Orthologous Group and Gene Ontology Enrichment Identifies *Pocillopora* and *Cladocopium* Biological Processes Affected by Heat Stress, Antibiotics, and Antibiotics-Heat Stress Treatments

Enrichment analysis of the *Pocillopora* and *Cladocopium* DEGs detected in treatment contrasts that had annotations to 23 non-overlapping KOG categories revealed distinct biological responses to the heat stress, antibiotics, and antibiotics-heat stress treatments (**Figure 3C**).

Pocillopora upregulated DEGs in the heat stress treatment were not significantly enriched ($p_{adj} < 0.05$) for any KOG categories or GO terms (**Figure 3C**). However, *Pocillopora* downregulated DEGs in the heat stress treatment were enriched for the KOG categories 'translation, ribosomal structure and biogenesis' and 'inorganic ion transport and metabolism' (**Figure 3C**) and this was supported by enriched biological process (BP) GO terms ($n = 36$, $p_{adj} < 0.05$), including 'protein localization to endoplasmic reticulum,' 'cytoplasmic translation,' and 'ribosome biogenesis' (**Supplementary Table 4**).

Pocillopora upregulated DEGs in the antibiotics treatment were enriched for the KOG categories 'intracellular trafficking, secretion, and vesicular transport' and 'posttranslational modification, protein turnover, chaperones' (**Figure 3C**), and were enriched for BP GO terms ($n = 20$, $p_{adj} < 0.05$)

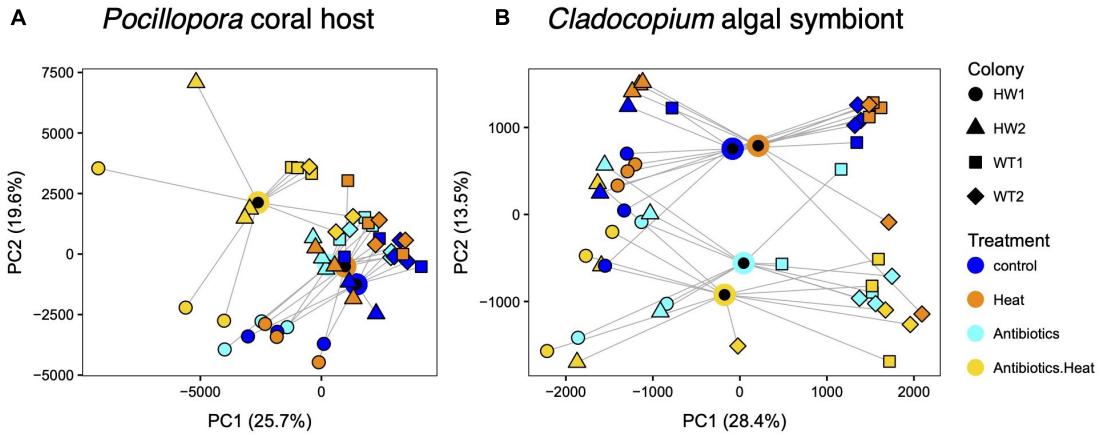

FIGURE 2 | Principal coordinates analysis (PCoA) of transcriptome patterns in **(A)** *Pocillopora* corals and **(B)** *Cladocopium* algal symbionts reveals coral host cryptic species variation and experimental treatment effects, including a synergistic effect of combined antibiotics-heat treatment on coral host and algal symbiont gene expression. Point shape represents the sample colony (genotype) and color represents the treatment, with blue for the control treatment, orange for the heat treatment, cyan for the antibiotics treatment, and yellow for the combined treatment. Treatment centroids are plotted as black circles outlined in each treatment color with lines connected to each sample within the treatment.

including 'endoplasmic reticulum to Golgi vesicle-mediated transport,' 'response to topologically incorrect protein,' 'canonical Wnt signaling pathway,' and 'regulation of hydrolase activity' (**Supplementary Table 4**). *Pocillopora* downregulated DEGs in the antibiotics treatment were enriched for the KOG categories 'inorganic ion transport and metabolism' and 'cytoskeleton' (**Figure 3C**), however no BP GO terms were significantly enriched at the $p_{adj} < 0.05$ level (**Supplementary Table 4**). Notable downregulated *Pocillopora* DEGs in the antibiotics treatments included five amino acid transporters (pdam_00001802, pdam_00001810, pdam_00011663, pdam_00012562, and pdam_00017019), one ammonium transporter (pdam_00014954), and several enzymes involved in amino acid biosynthetic pathways including glutamate carboxypeptidase 2 (pdam_00006146), adenosylhomocysteinase (pdam_00017020), *S*-adenosylmethionine synthase (pdam_00004044), and alanine aminotransferase 1 (pdam_00024643) (**Supplementary Table 3**).

Pocillopora upregulated DEGs in the antibiotics-heat stress treatment were enriched for the KOG categories 'energy production and conversion,' 'intracellular trafficking, secretion and vesicular transport,' 'posttranslational modification, protein turnover, chaperones,' and 'translation, ribosomal structure and biogenesis' (**Figure 3C**), as well as many BP GO terms ($n = 92$, $p_{adj} < 0.05$), among which the most significantly enriched were 'cellular respiration,' 'electron transport chain,' and 'establishment of protein localization to mitochondrion.' Other highly enriched terms included 'antigen processing and presentation,' 'generation of precursor metabolites and energy' 'oxidation-reduction process,' and 'proteolysis' (**Supplementary Table 4**).

Pocillopora downregulated DEGs in the antibiotics-heat stress treatment were enriched for the KOG categories 'inorganic ion transport and metabolism,' 'extracellular structures,' 'signal transduction mechanisms,' 'amino acid transport and metabolism,' 'replication, recombination and repair,' and 'cell wall/membrane/envelope biogenesis' (**Figure 3C**), and these processes were supported by the most highly enriched BP GO terms ($n = 154$, $p_{adj} < 0.05$) including 'sodium ion transport,' 'metal ion transport,' 'microtubule organizing center organization,' 'response to wounding,' and 'cell–cell adhesion via plasma-membrane adhesion molecules' (**Supplementary Table 4**).

The few *Cladocopium* upregulated DEGs in the heat stress treatment were not enriched for any KOG categories or BP GO terms, whereas *Cladocopium* downregulated DEGs in the heat stress treatment were enriched for the KOG category 'translation, ribosomal structure and biogenesis' and the BP GO terms ($n = 4$, $p_{adj} < 0.05$) 'cytoplasmic translation,' 'amide biosynthetic process,' 'maturation of LSU-rRNA,' and 'ribosomal large subunit biogenesis' (**Supplementary Table 4**).

Cladocopium upregulated DEGs in the antibiotics treatment were also not enriched for any KOG categories or BP GO terms. *Cladocopium* downregulated DEGs in the antibiotics treatment were enriched for the KOG categories 'energy production and conversion' and 'inorganic ion transport and metabolism' and BP GO terms ($n = 4$, $p_{adj} < 0.05$) 'cytoplasmic translational elongation,' 'photosynthesis,' 'cellular response to hydrogen peroxide,' and 'cellular response to toxic substance.' Among these *Cladocopium* downregulated DEGs was a chloroplastic aminomutase (SymbC1.scaffold4424.2), a chloroplastic delta-aminolevulinic acid dehydratase (SymbC1.scaffold548.4), six aminotransferases (SymbC1.scaffold31.2, SymbC1.scaffold2551.4, SymbC1.scaffold 2895.2, SymbC1.scaffold2898.1, SymbC1.scaffold2207.2, and SymbC1.scaffold1758.2), an amino acid permease (Symb C1.scaffold7668.1), a chloroplastic glutamate synthase (Sym bC1.scaffold1423.11), a type-3 glutamine synthase (SymbC1. scaffold371.1), a mitochondrial basic amino acid transporter (SymbC1.scaffold1251.1), and a fumarate reductase enzyme (SymbC1.scaffold10507.1).

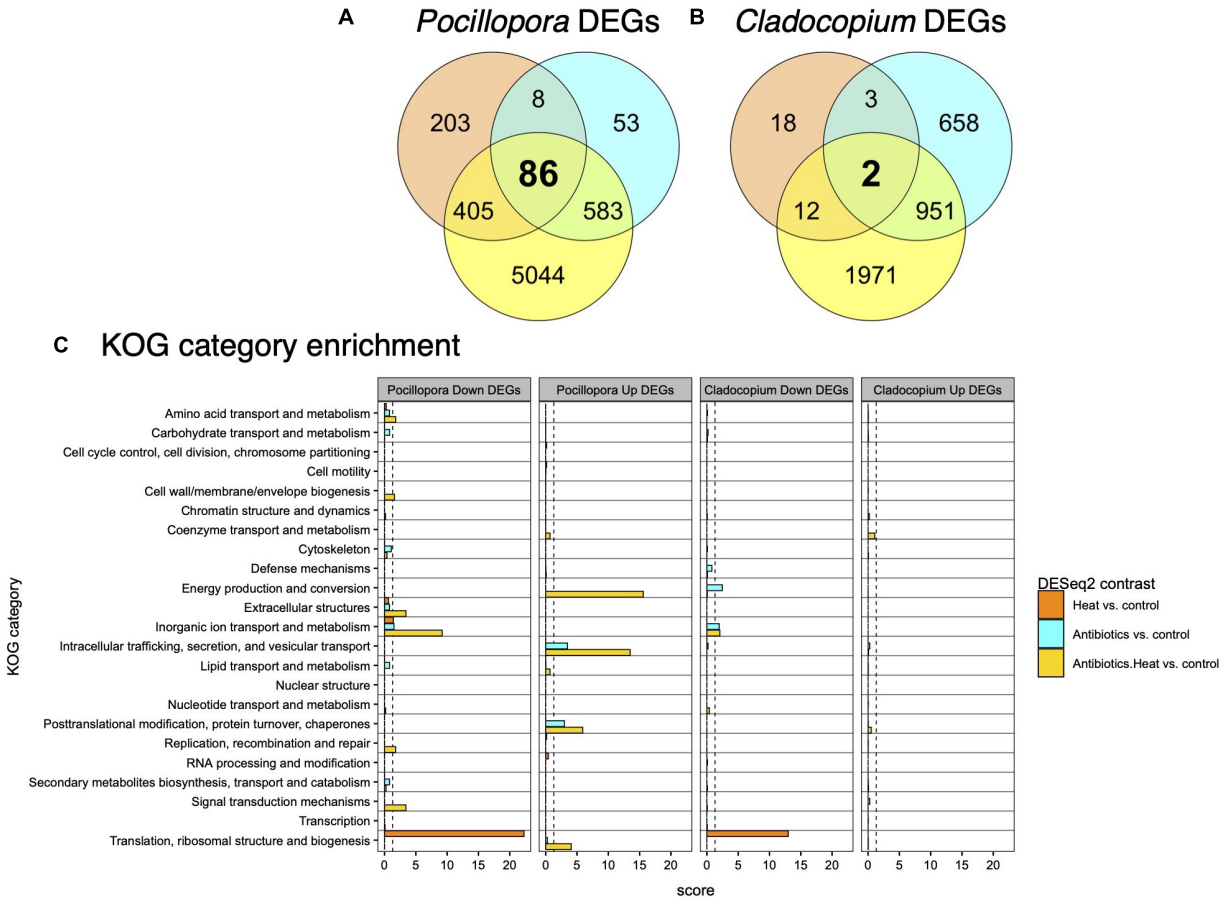

FIGURE 3 | The overall summary of shared and unique DEGs detected in *Pocillopora* and *Cladocopium*. Venn diagrams of the number of shared and unique DEGs detected among experimental treatments contrasted with the control treatment for **(A)** *Pocillopora* corals and **(B)** *Cladocopium* algal symbionts. Thousands more DEGs are detected in the antibiotics and heat combined treatment than the individual antibiotics or heat stress treatments for both coral host and algal symbiont. **(C)** Barplots of enriched KOG categories for *Pocillopora* and *Cladocopium* upregulated and downregulated DEGs reveals that heat stress, antibiotics, and combined treatments affect different functional classes of genes. KOG categories are shown on the *y*-axis, and the *x*-axis depicts the enrichment score [–log10(p_{adj})] for each KOG category within each set of upregulated or downregulated DEGs.

Cladocopium upregulated DEGs in the antibiotics-heat stress treatment were not enriched for any KOG categories or BP GO terms, whereas *Cladocopium* downregulated DEGs in the antibiotics-heat stress treatment were enriched for the KOG category 'inorganic ion transport and metabolism,' and no BP GO terms (**Supplementary Table 4**).

WCGNA Reveals Modules of Co-expressed Immunity, Symbiosis, and Stress Response Genes Correlated to Experimental Treatments

WGCNA based on vst-transformed counts identified 23 *Pocillopora* and 13 *Cladocopium* co-expressed gene modules that were labeled according to module size along a standard sequence of colors within the WGCNA R package (**Figure 4**). Of these, 12 *Pocillopora* modules and 8 *Cladocopium* modules displayed module eigengene expression that was significantly correlated to one or more treatments ($p < 0.05$).

For *Pocillopora*, there were 2 positively ('grey60' and 'mediumpurple3') and 4 negatively ('royalblue,' 'floralwhite,' 'orange,' and 'blue') correlated modules to the control treatment, 1 positively ('cyan') and 3 negatively ('bisque4,' 'lightsteelblue1,' and 'darkgreen') correlated modules to the heat stress treatment, 1 module positively correlated to the antibiotics treatment ('lightsteelblue1'), and 5 positively ('floralwhite,' 'royalblue,' 'orange,' 'bisque4,' and 'palevioletred3') and 4 negatively ('grey60,' 'cyan,' 'mediumpurple3,' and 'skyblue') correlated modules to the antibiotics-heat stress treatment (**Figure 4A**).

For *Cladocopium*, there was 1 positively ('green') and 1 negatively ('grey60') correlated modules to the control treatment, 2 positively ('magenta' and 'darkgrey') and 2 negatively ('grey60' and 'brown') correlated modules to the heat stress treatment, 1 positively ('purple') and 2 negatively ('darkturquoise' and 'green') correlated modules to the antibiotics treatment, and 3 positively ('grey60,' 'brown,' and 'darkgreen') and 3 negatively ('magenta,' 'darkgrey,' and 'green') correlated modules the antibiotics-heat stress treatment (**Figure 4B**).

Among all the significantly correlated *Pocillopora* modules, the 'lightsteelblue1' module (n = 104 genes) was the only module positively correlated to the antibiotics treatment and was also negatively correlated to the heat stress treatment. This module was enriched for the KOG category 'signal transduction mechanisms' and BP GO terms (n = 38, $p_{adj} < 0.05$) related to immune processes such as 'activation of immune response,' 'leukocyte activation,' and 'response to bacterium' (**Supplementary Tables 5, 6**). The module hub gene was an endoribonuclease (ZC3H12B, pdam_00012426) (**Table 2**) that may function as an RNase involved in immunomodulation via mRNA decay, and other co-expressed genes included the immune-related transcription factors ETS-related transcription factor Elf-4 (ELF4, pdam_00016137), ETS domain-containing protein Elk-1 (ELK1, pdam_00003296), baculoviral IAP repeat-containing protein 2 (BIRC2, pdam_00007333), and neural proliferation differentiation and control protein 1 (NPDC1, pdam_00019344).

The 'floralwhite' module was the largest module (n = 1,661 genes) and was negatively correlated to the control treatment and positively correlated to the antibiotic-heat treatment (**Figure 4A**). This module was highly enriched for the KOG categories 'energy production and conversion,' 'intracellular trafficking, secretion, and vesicular transport,' 'posttranslational modification, protein turnover, chaperones' and 'translation, ribosomal structure and biogenesis,' as well as the BP GO terms (n = 131, $p_{adj} < 0.05$) 'generation of precursor metabolites and energy,' 'protein polyubiquitination,' and 'proteasome assembly' (**Supplementary Tables 5, 6**). The 'floralwhite' module hub gene was a proteolytic subunit of the

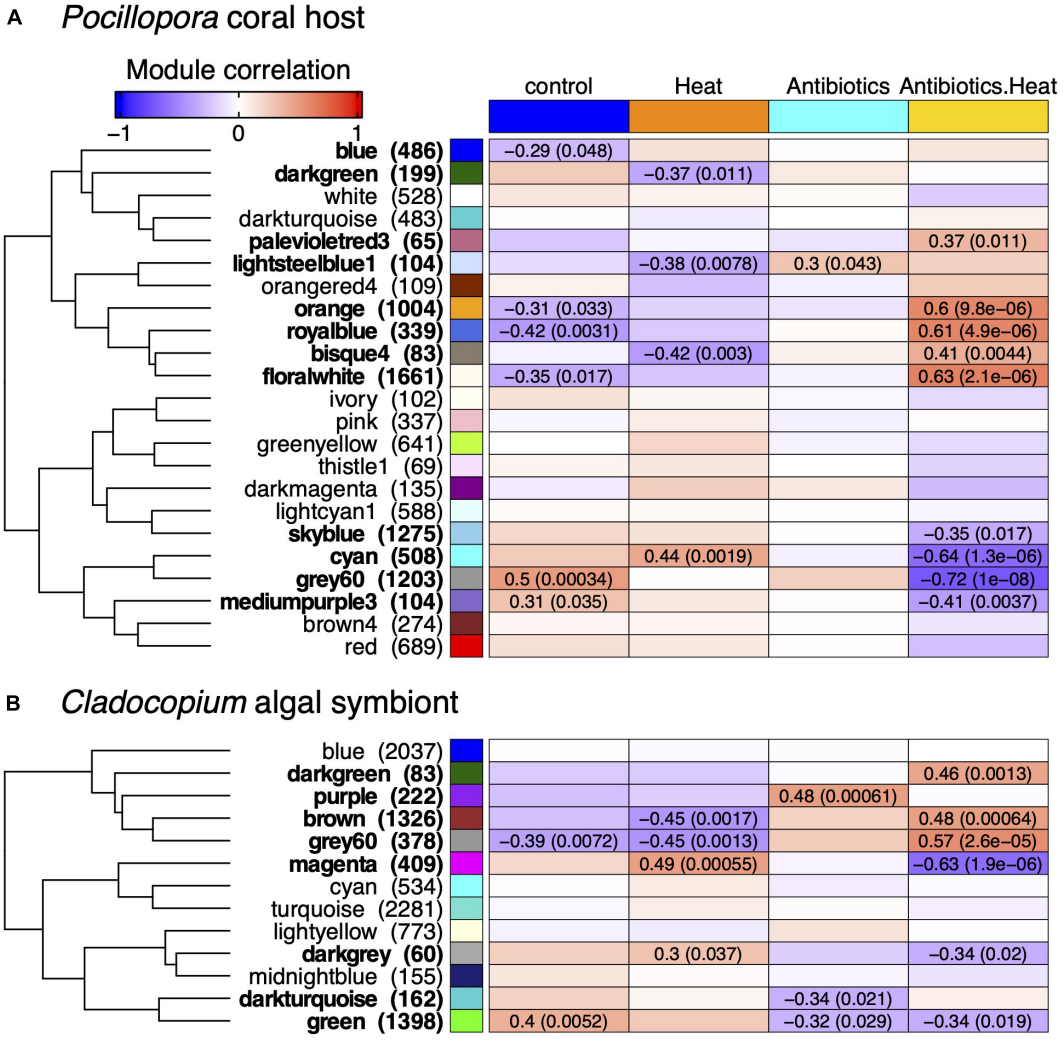

FIGURE 4 | WGCNA reveals **(A)** *Pocillopora* and **(B)** *Cladocopium* co-expressed gene modules correlated to experimental treatments. The heatmap color represents the correlation coefficient of module eigengene expression to each treatment ranging from blue for negative correlation (–1) to red for positive correlation (+1), and the Pearson correlation coefficient and p-value is listed in each cell with a significant correlation ($p < 0.05$). The eigengene hierarchical clustering dendrogram is depicted to the left of the heatmap, and the number of genes in each module is listed in parentheses next to the module label. There are 12 *Pocillopora* and 8 *Cladocopium* modules that are significantly correlated to one or more treatments.

TABLE 2 | Number of *Pocillopora* and *Cladocopium* DEGs (# of genes DESeq2 $p_{adj} < 0.05$ [up, down]) detected in contrasts between each experimental treatment and the control treatment for each genotype and all genotypes together.

Holobiont partner	DESeq2 contrast	HW1	HW2	WT1	WT2
Pocillopora	Heat vs. control	0 [0, 0]	2 [0, 2]	58 [12, 46]	71 [8, 63]
Pocillopora	Antibiotics vs. control	210 [96, 114]	75 [59, 16]	6 [4, 2]	14 [11, 3]
Pocillopora	Antibiotics heat vs. control	1124 [572, 552]	2677 [1315, 1362]	2000 [848, 1152]	929 [487, 442]
Cladocopium	Heat vs. control	0 [0, 0]	0 [0, 0]	6 [1, 5]	4 [2, 2]
Cladocopium	Antibiotics vs. control	1 [1, 0]	0 [0, 0]	10 [4, 6]	699 [346, 353]
Cladocopium	Antibiotics heat vs. control	144 [91, 53]	149 [86, 63]	701 [336, 365]	1453 [730, 723]

The increased number of DEGs for both the coral host and algal symbiont in the combined antibiotics and heat stress treatment relative to the separate treatments indicates that there is a synergistic effect of antibiotics and heat stress on both coral and algal symbiont gene expression.

mitochondrial ATP-dependent Clp protease complex (CLPP, pdam_00002241) (**Table 2**), and other co-expressed genes within the 'floralwhite' module were involved in immune-related processes including the master immune regulator NF-κB (pdam_00003205), tumor necrosis factor receptor-associated factor 6 (TRAF6, pdam_00017873), and mannan-binding lectin-associated serine protease 1 (MASP1, pdam_00000447). Additional upregulated and co-expressed genes were involved in pro-apoptosis pathways and protein degradation such as apoptosis regulator BAX (pdam_00019537), programed cell death 6-interacting protein (pcdip6, pdam_00015525), matrix metalloproteinase 25 (MMP25, pdam_00023163), and multiple 26S proteasome subunits.

The 'orange' module (n = 1,004 genes) was also negatively correlated to control treatment and positively correlated to antibiotics-heat stress treatment (**Figure 4A**). The 'orange' module was enriched for the KOG category 'cytoskeleton,' and the most highly enriched BP GO terms (n = 74, $p_{adj} < 0.05$) included 'response to oxidative stress,' 'cellular amino acid catabolic process,' and 'response to temperature stimulus' (**Supplementary Tables 5, 6**). Although the module hub gene (pdam_00024070) lacked annotation, other highly connected and upregulated genes were involved in the oxidative stress response, such as catalase (pdam_00001882), peroxidase (pdam_00000351), peroxiredoxin-6 (pdam_00009060) and apoptosis-inducing factor 2 (AIFM2, pdam_00001271), which is involved in directly triggering programed cell death pathways during oxidative stress.

Conversely, the 'grey60' (n = 1,203 genes) and 'mediumpurple3' (n = 104 genes) modules were both positively correlated to the control treatment and negatively correlated to the antibiotics-heat treatment. The 'grey60' module was enriched for the KOG categories 'extracellular structures,' 'inorganic ion transport and metabolism,' 'signal transduction mechanisms,' and 'transcription' as well as many BP GO terms (n = 305, $p_{adj} < 0.05$) related to cellular housekeeping functions and homeostasis maintenance (**Supplementary Tables 5, 6**). The 'mediumpurple3' module was enriched for the KOG category 'signal transduction mechanisms' and several BP GO terms (n = 25, $p_{adj} < 0.05$) involved in epithelial immune processes such as 'regulation of antibacterial peptide biosynthetic process,' 'positive regulation of humoral immune response,' 'cell–cell adhesion,' and 'columnar/cuboidal epithelial cell development.' The module hub gene was a fibroblast growth factor receptor (FGFR, pdam_00020781), and there were numerous other tyrosine kinase receptors within the module (**Supplementary Tables 5, 6**).

The 'cyan' module (n = 508 genes) was positively correlated to the control treatment and heat stress treatment and negatively correlated the antibiotics-heat treatment, and was enriched for the KOG categories 'cell cycle control, cell division, and chromosome partitioning,' 'chromatin structure and dynamics,' 'cytoskeleton,' 'nucleotide transport and metabolism,' 'replication, recombination, and repair,' and 'secondary metabolites biosynthesis, transport, and catabolism,' and the top enriched BP GO terms (n = 209, $p_{adj} < 0.05$) included numerous DNA damage response and repair processes (**Supplementary Tables 5, 6**).

For *Cladocopium*, only the 'purple' module (n = 222 genes) was positively correlated with antibiotics treatment, however, no KOG categories or BP GO terms were significantly enriched (**Figure 4B**). The module hub gene was a 26S proteasome regulatory subunit (SymbC1.scaffold7524.1) (**Table 2**), and other genes in the module that were also upregulated in the antibiotics treatment included a D-amino acid dehydrogenase small subunit protein (SymbC1.scaffold805.5), an isoleucine-tRNA ligase (SymbC1.scaffold2776.4), a vacuolar amino acid transporter associated with ATP-mediated isoleucine uptake (SymbC1.scaffold2075.3), and two sodium-dependent amino acid transporters (SymbC1.scaffold8224.5 and SymbC1.scaffold8948.3).

The largest significant *Cladocopium* module was the 'green' module (n = 1,398 genes), which was positively correlated to the control treatment and negatively correlated to both the antibiotics and antibiotics-heat stress treatment, and was enriched for the KOG category 'energy production and conversion' and BP GO terms 'photosynthesis' and 'nucleoside monophosphate biosynthetic process.' The 'darkturquoise' module (n = 162 genes) was also negatively correlated to the antibiotics treatment and had a chloroplastic hub gene of fucoxanthin-chlorophyll binding protein E (SymbC1.scaffold3718.1), an element of the light-harvesting complex associated with photosystem II.

Both the *Cladocopium* 'magenta' (n = 409 genes) and 'darkgrey' (n = 60 genes) modules were positively correlated to the heat stress treatment and negatively correlated to the antibiotics-heat stress treatment (**Figure 4B**). The 'magenta'

module was enriched for the KOG category 'signal transduction mechanisms,' however, no BP GO terms were enriched. Conversely, the 'brown' (n = 1,326 genes) and 'grey60' (n = 378 genes) modules were negatively correlated to the heat stress treatment and positively correlated to the antibiotics-heat stress treatment. The 'brown' module was enriched for the KOG category 'translation, ribosomal structure and biogenesis' and BP GO terms 'cytoplasmic translation,' 'membrane docking,' 'ncRNA metabolic process,' and 'RNA/ncRNA processing,' and its hub gene was autophagy-related protein 9 (ATG9, SymbC1.scaffold517.1), a protein involved in autophagic vesicle formation. Genes related to ncRNA metabolism and processing included piRNA biogenesis protein Exd1 (SymbC1.scaffold5866.5), an Elav-like RNA-binding protein associated with miRNA processing (SymbC1.scaffold526.10), and an insulin-like mRNA-binding protein capable of shielding target transcripts from microRNA-mediated degradation (SymbC1.scaffold2518.1).

Antibiotics Alters *Pocillopora*-Associated Bacteria Communities

Sequencing of bacteria 16S rRNA gene V4 region on the Illumina MiSeq at the University of Miami CGT was completed in April 2019. A total of 3,716,629 demultiplexed reads were obtained from all 48 samples, with an average sequence length of 300 bp (**Supplementary Figure 3**). After read denoising, classification against the SILVA database and filtering of mitochondria and chloroplast-derived sequences, 470 coral-associated ASVs were detected representing 17 phyla, 31 classes, 84 orders, and 135 bacterial and archaeal families. The most abundant bacterial phyla were Proteobacteria, Bacteroidetes, and Cyanobacteria, and the most abundant families within the phylum Proteobacteria were Endozoicomonadaceae, Rhodobacteraceae, and Alteromonadaceae (**Figure 5B**). Filtering out low-abundance taxa with mean counts < 3 left 36 high-abundance ASVs remaining for compositional data analysis of bacteria community alpha and beta-diversity. Antibiotics treatments caused significant changes in coral-associated bacteria community beta-diversity according to PCA visualization of center-log ratio transformed abundances, as PC1 separated samples in both antibiotics treatments from the control and heat stress treatment samples and explained 24.8% of the variance (**Figure 5A**). PC2 explained 20.8% of the variance and partially separated the *P. acuta* genotypes (WT1 and WT2) from the *P. damicornis* genotypes (HW1 and HW2), in part due to a higher relative abundance of *Endozoicomonas* bacteria (**Figures 5A,B**).

Non-parametric Kruskal–Wallis tests detected significant differences in bacteria community alpha-diversity metrics between experimental treatments (Chao1, Kruskal–Wallis chi-squared = 8.62, p = 0.035), with lower alpha-diversity observed in antibiotics-treated samples. PERMDISP tests revealed inhomogeneity of dispersions between treatments (F = 3.44, p = 0.027), and PERMANOVA tests also revealed significant differences between treatment centroids (F = 5.28, R^2 = 0.26, p < 0.001), indicating differences in bacteria community composition in antibiotics-treated samples.

Specifically, antibiotics treatments reduced the relative abundance of bacteria in the family Rhodobacteraceae while bacteria in the family Alteromonadaceae persisted and increased in relative abundance (**Figure 5B** and **Supplementary Figure 4**). Bacteria in the genus *Endozoicomonas* were also observed to persist through antibiotics treatment but did not increase in relative abundance (**Figure 5B** and **Supplementary Figure 4**).

Furthermore, paired ALDEx2 tests that contrasted each experimental treatment with the control identified specific differentially abundant ASVs. Three ASVs in the family Rhodobacteraceae and one ASV in the genus *Neptuniibacter* (family Nitrincolaceae) were significantly reduced in both antibiotics and antibiotics-heat stress treatment samples (**Supplementary Figure 5**). Two ASVs in the family Alteromonadaceae had increased relative abundance in the antibiotics treatment and antibiotics-heat stress treatment (**Supplementary Figure 5**). BLASTn searches of these ASVs against the NCBI 16S rRNA database uncovered 100% sequence similarity (e-values < $3e^{-123}$) to *Alteromonas aestuariivivens*, an ampicillin-resistant bacterium isolated from a South Korea tidal flat (Park et al., 2017) and *Aestuariibacter aggregatus*, another ampicillin-resistant bacterium isolated from Yellow Sea (Wang et al., 2010).

DISCUSSION

On coral reefs, antibiotics are increasingly being considered for use in coral disease intervention strategies and as environmental pollutants that are potentially damaging to coral health (Zhang R. et al., 2018; Zhang R. et al., 2019; Neely et al., 2020; Walker et al., 2021). Our experiment reveals that antibiotic suppression of coral-associated bacteria communities produces dramatic changes in *Pocillopora* coral and *Cladocopium* symbiont gene expression and bacteria community composition, resulting in microbial dysbiosis and diminished holobiont heat tolerance. These findings corroborate results from previous studies that documented negative effects of antibiotics on coral health (Gilbert et al., 2012; Glasl et al., 2016), and provide new insights into the complex multi-partner interactions that occur within *Pocillopora* coral holobionts (Brener-Raffalli et al., 2018; Pogoreutz et al., 2018; Geissler et al., 2021; Haydon et al., 2021; Li et al., 2021).

Antibiotics Treatment Disrupts Expression of Genes Involved in Coral Holobiont Metabolic Interactions

Pocillopora and *Cladocopium* transcriptome responses to antibiotics treatment revealed changes in intracellular trafficking and vesicular transport and inorganic ion transport and metabolism genes and upregulation of immune-related genes in the *Pocillopora* 'lightsteelblue1' module. These changes suggest that disruptions of the coral-associated bacteria community negatively affect coral holobiont metabolic exchanges and inter-partner signaling, resulting in immune

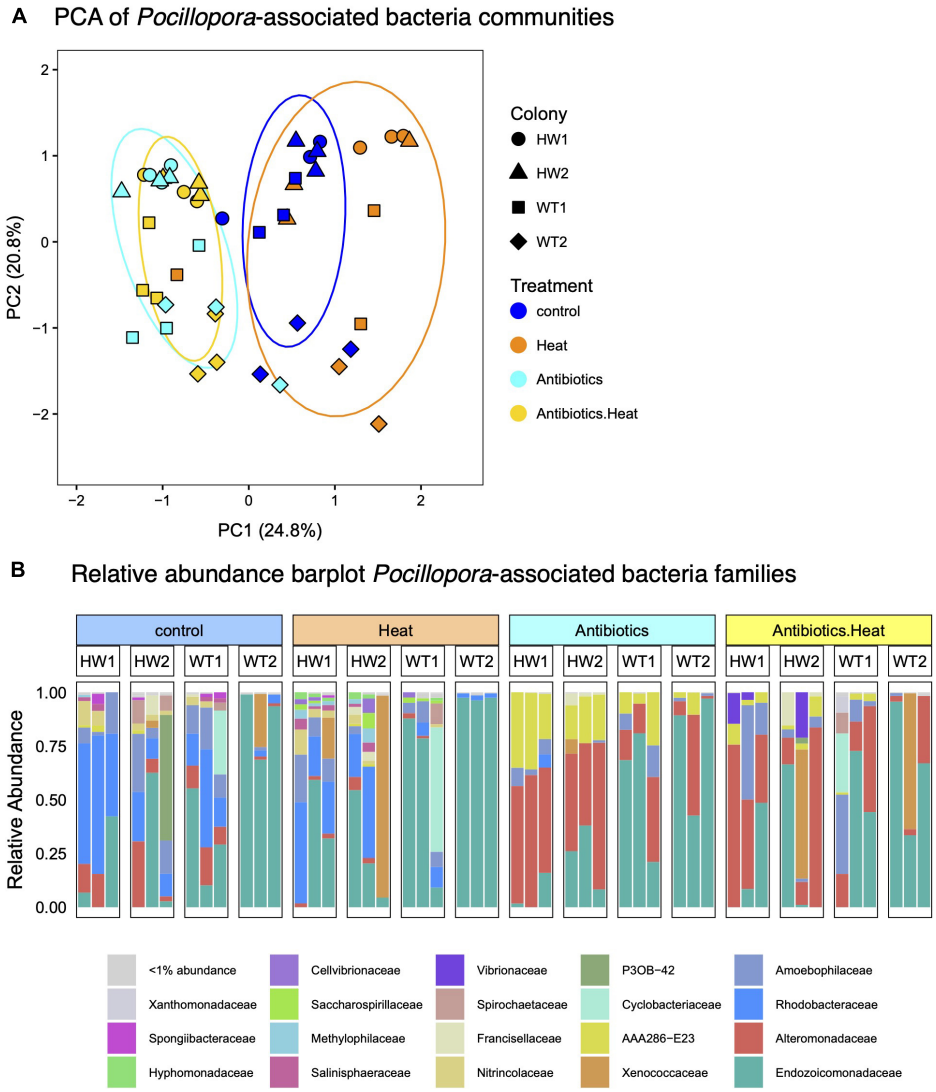

FIGURE 5 | Bacteria 16S sequencing demonstrates that antibiotics treatments alter coral-associated bacteria communities, and that certain coral-associated bacteria families exhibit differential susceptibility to antibiotics treatment. **(A)** Principal components analysis (PCA) plot of coral-associated bacteria communities reveals that antibiotics-treated samples (yellow and cyan) cluster separately from heat stress and control treatment samples (blue and orange). Point shape represents the sample colony (genotype) and color represents the treatment, with blue for the control treatment, orange for the heat treatment, cyan for the antibiotics treatment, and yellow for the combined treatment. Colored ellipses represent the 95% confidence interval. **(B)** Barplot of the relative abundance of bacteria families in each treatment reveals significant declines in the abundance of coral-associated Rhodobacteraceae bacteria (royal blue) and increases in Alteromonadaceae bacteria (red) in antibiotics-treated corals, while Endozoicomonadaceae bacteria (dark green) tend to dominate both WT genotypes and are not eliminated by antibiotics treatment.

inflammation and microbiome dysregulation (**Figures 4**, **5** and **Supplementary Table 3**). This transcriptomic evidence also supports the notion that these holobiont metabolic interactions entail the exchanges of amino acids, inorganic ions, and other secondary metabolites among the *Pocillopora* coral host, its *Cladocopium* algal symbionts and specific bacteria within the coral holobiont (Matthews et al., 2020; Peixoto et al., 2021). Previous studies have identified diazotrophic bacteria as a source of fixed nitrogen to coral holobionts (Olson et al., 2009; Benavides et al., 2017; Lesser et al., 2018; Rädecker et al., 2021), and have implicated coral-associated bacteria in dimethylsulfoniopropionate (DMSP) metabolism (Raina et al., 2010; Tandon et al., 2020) and the production of siderophores capable of alleviating iron and trace metal limitation (Hopkinson and Morel, 2009; Schalk et al., 2011; Amin et al., 2017; Reich et al., 2020; Peixoto et al., 2021). Importantly, while transcriptome read alignments suggest these *Pocillopora* genotypes were *Cladocopium*-dominated, direct measurement of Symbiodiniaceae community composition via ITS2 amplicon sequencing (Boulotte et al., 2016; Hume et al., 2019) in future studies would be preferred for assessing interactions of different Symbiodiniaceae genera with associated bacteria.

While the magnitude of *Pocillopora* gene expression changes were similar for the acute heat stress treatment and antibiotics treatment relative to the control treatment, *Cladocopium* gene expression had more DEGs in response to antibiotics treatment than to the heat stress treatment (**Figures 2B**, **3B**). This difference was driven in part by the downregulation of genes involved in energy production and photosynthesis in the *Cladocopium* 'green' and 'darkturquoise' modules that were negatively correlated to antibiotics treatment, such as the light-harvesting fucoxanthin-chlorophyll A–C binding proteins E and F, a carotenо-chlorophyll A-C-binding protein and several photosystem I proteins (**Figures 3C**, **4B** and **Supplementary Table 4**).

We hypothesize that the downregulation of *Cladocopium* photosynthesis and metabolism genes in the antibiotics treatment may be related to disruptions in nitrogen cycling and amino acid exchanges between the *Pocillopora* coral, *Cladocopium* symbionts and members of the associated bacteria community. Five *Pocillopora* amino acid transporters were downregulated in the antibiotics treatment (**Supplementary Table 3**), however, for *Cladocopium* three amino acid transporters and an isoleucine tRNA ligase were upregulated in the 'purple' module, and other genes involved in amino acid metabolism were downregulated in the 'green' and 'darkturquoise' modules. The role of amino acids in generating energy via the TCA cycle (Akram, 2014) or alternatively as metabolites in chlorophyll biosynthesis (Vavilin and Vermaas, 2002) could potentially play a role in *Cladocopium* photosynthetic impairment. This second hypothesis is consistent with observations of decreased chlorophyll a in nitrogen-starved *C. goreauii* (Zhou et al., 2021) and stable photochemical efficiency and dramatically increased growth rates in *Breviolium minutum* cultures supplemented with casein amino acids (Kirk et al., 2020). Although the *Pocillopora* and *Cladocopium* genomes possess pathways for synthesizing most amino acids and heterotrophic feeding may account for substantial input of essential amino acids to the coral holobiont (Fox et al., 2019; Ferrier-Pagès et al., 2021), these observations suggest that certain coral-associated and/or Symbiodiniaceae-associated bacteria may provide *in hospite* Symbiodiniaceae with additional nitrogenous compounds that benefit holobiont metabolism (Benavides et al., 2017; Geissler et al., 2021; Glaze et al., 2021; Rädecker et al., 2021). While more experimental evidence is required to validate this conclusion, *Cladocopium* symbionts were recently shown to associate with diverse bacteria located within algae cells and on external cell surfaces, which supports the idea that Symbiodiniaceae-bacteria metabolic exchanges may be more common than previously recognized (Camp et al., 2020; Matthews et al., 2020; Maire et al., 2021).

Antibiotics Treatment Alters *Pocillopora*-Associated Bacteria Communities

Treatments of *Pocillopora* corals with the broad-spectrum antibiotics ampicillin and streptomycin caused significant changes in coral-associated bacteria community composition (**Figure 5A**), as antibiotics treatment substantially reduced the relative abundance of bacteria in the family Rhodobacteraceae while bacteria in the family Alteromonadaceae persisted and increased in relative abundance (**Figure 5B**).

Bacteria community analysis of these *Pocillopora* corals from southern Taiwan revealed similar results to previous studies demonstrating that *P. acuta* corals in Taiwan and elsewhere in the Indo-Pacific have high relative abundances of *Endozoicomonas* bacteria (Brener-Raffalli et al., 2018; Epstein et al., 2019; Connelly et al., 2020), however, further studies on how variation in coral host species, site effects and environmental factors affect *Pocillopora* corals' associations with *Endozoicomonas* bacteria are needed to corroborate this trend. Furthermore, these results indicate that *Endozoicomonas*-dominated microbiomes may be more resistant to experimental antibiotic perturbation (**Figure 5B** and **Supplementary Figure 4**). The persistence of *Endozoicomonas* bacteria throughout multiple stressors suggests that these bacteria are either resistant to environmental perturbations or perhaps are effectively shielded from external stressors because of their location as cellular aggregates within *Pocillopora* coral tissues (Work and Aeby, 2014; Neave et al., 2017; Pogoreutz et al., 2018).

Furthermore, it appears that other bacteria that persist through antibiotics treatment, such as the bacteria ASVs similar to the ampicillin-resistant *Alteromonas* spp. and *A. aggregatus*, might act as opportunistic pathogens that activate coral immune responses and cause microbial dysbiosis during antibiotics-heat stress treatment (Wang et al., 2010; Park et al., 2017; Zaneveld et al., 2017). More in-depth research on the taxonomic diversity, localization, and metabolic functions of *Pocillopora* coral-associated bacteria communities is necessary to fully understand how interactions with specific bacteria influence coral holobiont health, and these results highlight the potential of antibiotics treatments as an experimental tool to manipulate these associations.

Antibiotics-Heat Stress Treatment Causes Microbial Dysbiosis and Exacerbates *Pocillopora* and *Cladocopium* Transcriptome Stress Responses

Despite the strong influence of coral genotype on both *Pocillopora* and *Cladocopium* gene expression, differential gene expression and gene co-expression network analyses revealed distinct effects of the separate acute heat stress and antibiotics treatments as well as a strong combined effect of the antibiotics-heat treatment (**Figure 2** and **Table 1**). Samples in the antibiotics-heat stress treatment clustered separately from the heat stress, antibiotics, and control treatment samples in PCoA, and thousands more DEGs were detected in the antibiotics-heat treatment than either individual heat stress or antibiotics treatment (**Table 1** and **Figures 2**, **3**). This dramatic transcriptional activation of *Pocillopora* and *Cladocopium* energy conversion and stress response genes suggest that in the antibiotics-heat stress treatment, bacteria community disruption negatively impacts *Pocillopora* coral holobiont metabolism and immune homeostasis such that opportunistic microbes flourish and the corals' ability to

collectively mount an efficient heat stress response and defend against infection is diminished (**Figures 3C**, **5B**). This is supported by functional enrichment analyses of *Pocillopora* DEGs and the co-expressed 'floralwhite,' 'orange,' 'grey60,' 'mediumpurple3,' and 'cyan' modules that indicate *Pocillopora* corals' responses to the antibiotics-heat stress treatment involved increases in energy production and conversion, immune inflammation, proteolysis and apoptosis at the expense of diminished holobiont metabolism, epithelial immune integrity, ion transport, inter-partner signal transduction, and DNA maintenance (**Figure 3C**). This suggests that in the antibiotics-heat treatment, oxidative damage signals together with a dysregulated bacteria community triggers programed cell death pathways through the activation of tumor necrosis factor and caspase pathways, and proteolytic effectors such as MMPs and the 26S proteasome (Wecker et al., 2018; Chuang, 2020; Jiang et al., 2020). Indeed, many of these energy conversion, oxidative stress response and proteolysis genes were co-expressed within the *Pocillopora* 'floralwhite' and 'orange' modules and the *Cladocopium* 'brown' module, making the hub genes of each of these modules appealing targets for future functional characterization, pharmacological inhibition and gene knockdown/knockout studies (**Table 3**) (Cleves et al., 2020a,b; Jiang et al., 2020).

Implications for Coral Conservation and Disease Intervention Strategies

The results on the effect of antibiotic suppression of coral bacteria community and host-microbe interactions lead us to warn coral reef conservation practitioners to be cautious in considering field-based applications of antibiotics treatments as potential disease therapies, as there may be numerous unintended consequences for coral health. Current mitigation strategies being used throughout the Caribbean for treating stony coral tissue loss disease (SCTLD) involve treatments with antibiotics-infused epoxies (Voss et al., 2019; Walker and Pitts, 2019; Neely et al., 2020; Shilling, 2020). Our results suggest that ampicillin and streptomycin based antibiotic treatments do not non-selectively eliminate pathogenic bacteria, and more investigation into the efficacy and safety of these approaches should be conducted.

Future laboratory work should attempt to carefully manipulate associations between different coral genotypes and microbial symbiotic partners (including Symbiodiniaceae and bacteria) to move toward the generation of gnotobiotic (i.e., known-microbiome) corals for use in functional experiments. This has been shown to be feasible in cnidarian model systems such as *Hydra*, *Nematostella*, and *Aiptasia* (Murillo-Rincon et al., 2017; Domin et al., 2018; Medrano et al., 2019; Costa et al., 2021; Dungan et al., 2021), but is only beginning to be explored in reef-building corals and other cnidarians (Lin et al., 2019; Cunning and Baker, 2020; Weiland-Bräuer et al., 2020). Experiments that apply a combination of antibiotics treatments followed by targeted probiotic delivery or "microbiome recovery" treatments will yield insights into whether disturbed coral-associated bacteria communities and host stress response phenotypes can be "rescued" by the re-introduction of one or several beneficial microbes (Peixoto et al., 2017, 2021; Rosado et al., 2018; Damjanovic et al., 2019; Assis et al., 2020; Santoro et al., 2021). Future work would also benefit from the inclusion of baseline samples and additional time points to track the temporal changes in bacteria community composition and transcriptome responses across coral colonies.

TABLE 3 | Hub genes of *Pocillopora* and *Cladocopium* WGCNA modules with significant correlations to experimental treatments.

Holobiont partner	Module	Hub gene	UniProt best match
Pocillopora	Blue	pdam_00016931	Cct6a: T-complex protein 1 subunit zeta (*Mus musculus*)
Pocillopora	Darkgreen	pdam_00015892	RPS11: 40S ribosomal protein S11 (*Canis lupus familiaris*)
Pocillopora	Palevioletred3	pdam_00006619	SAMD15: sterile alpha motif domain-containing protein 15 (*Macaca fascicularis*)
Pocillopora	Lightsteelblue1	pdam_00012426	ZC3H12B: probable ribonuclease ZC3H12B (*Homo sapiens*)
Pocillopora	Orange	pdam_00024070	Unknown function
Pocillopora	Royalblue	pdam_00014622	PPP2CA: serine/threonine-protein phosphatase 2A catalytic subunit alpha isoform (*Gallus gallus*)
Pocillopora	Bisque4	pdam_00010339	wnt8a: protein Wnt-8a (*Danio rerio*)
Pocillopora	Floralwhite	pdam_00002241	Clpp: ATP-dependent Clp protease proteolytic subunit%2C mitochondrial (*Mus musculus*)
Pocillopora	Skyblue	pdam_00015203	SYT11: synaptotagmin-11 (*Homo sapiens*)
Pocillopora	Cyan	pdam_00002625	ZP domain-containing protein (Acropora millepora)
Pocillopora	Grey60	pdam_00009922	Unknown function
Pocillopora	Mediumpurple3	pdam_00020781	FGFR: fibroblast growth factor receptor (*Strongylocentrotus purpuratus*)
Cladocopium	Darkgreen	SymbC1.scaffold9599.2	50S ribosomal protein L15 OS = *Prochlorococcus marinus* (strain MIT 9215) GN = rplO PE = 3 SV = 1
Cladocopium	Purple	SymbC1.scaffold7524.1	26S protease regulatory subunit 4 homolog OS = *Oryza sativa* subsp. *japonica* GN = TBP2 PE = 2 SV = 2
Cladocopium	Brown	SymbC1.scaffold517.1	Autophagy-related protein 9 OS = *Dictyostelium discoideum* GN = atg9 PE = 2 SV = 1
Cladocopium	Grey60	SymbC1.scaffold1162.13	Unknown function
Cladocopium	Magenta	SymbC1.scaffold4557.4	Glycine–tRNA ligase OS = *Symbiodinium microadriaticum* GN = glyQS PE = 4 SV = 1
Cladocopium	Darkgrey	SymbC1.scaffold2117.1	Unknown function
Cladocopium	Darkturquoise	SymbC1.scaffold3718.1	Fucoxanthin-chlorophyll a-c binding protein E, chloroplastic OS = *Macrocystis pyrifera* GN = FCPE PE = 2 SV = 1
Cladocopium	Green	SymbC1.scaffold36579.1	Twitchin OS = *Symbiodinium microadriaticum* GN = unc-22 PE = 4 SV = 1

Collectively, the results of this experiment highlight the vital importance of coral-associated bacteria communities to coral holobiont metabolism, immunity, and acute heat stress responses, and provide a basis for future mechanistic studies of how symbiotic interactions between multiple partners shape coral holobiont health, evolution, and ecological resilience (Engelberts et al., 2021; Voolstra et al., 2021).

DATA AVAILABILITY STATEMENT

The mRNA and 16S sequencing datasets generated for this study can be found in the NCBI Sequence Read Archive under accession PRJNA587509. All scripts used in the RNAseq and 16S data analysis are available on GitHub: https://github.com/michaeltconnelly/EAPSI_Pocillopora_AxH.

AUTHOR CONTRIBUTIONS

MC and NT-K designed the research. MC, CJM, and P-JL conducted the experiments. MC and CEM analyzed the data. MC, CEM, and NT-K wrote the manuscript. All authors participated in the editing of the manuscript.

FUNDING

This work was supported by the National Science Foundation East Asia and Pacific Summer Institute (EAPSI) Program Award #1713962 and the Taiwan Ministry of Science and Technology (MOST) S.I.T. program 2017 awarded to MC.

ACKNOWLEDGMENTS

The authors would like to thank the scientists and research support staff at the National Museum of Marine Biology and Aquarium, especially Chih-Jui (Ray) Tan for field assistance and site environmental data. Additional thanks to Anderson Mayfield for sharing laboratory space at the NMMBA, and to Ross Cunning and Stephanie Rosales for bioinformatics assistance.

SUPPLEMENTARY MATERIAL

The Supplementary Material for this article can be found online at: https://www.frontiersin.org/articles/10.3389/fmars.2021.814124/full#supplementary-material

REFERENCES

Akram, M. (2014). Citric acid cycle and role of its intermediates in metabolism. *Cell Biochem. Biophys.* 68, 475–478. doi: 10.1007/s12013-013-9750-1

Amin, S. A., Green, D. H., Hart, M. C., Kupper, F. C., Sunda, W. G., and Carrano, C. J. (2017). Photolysis of ion – siderophore chelates promotes bacteria – algal mutualism Photolysis of iron – siderophore chelates promotes bacterial – algal mutualism. *Environ. Sci.* 106, 2–7.

Anderson, M. J. (2017). "Permutational multivariate analysis of variance (PERMANOVA)," in *Wiley StatsRef Stat. Ref. Online*, eds N. Balakrishnan, T. Colton, B. Everitt, W. Piegorsch, F. Ruggeri, and J. L. Teugels (Hoboken, NJ: John Wiley & Sons), 1–15. doi: 10.1002/9781118445112.stat07841

Apprill, A. (2020). The role of symbioses in the adaptation and stress responses of marine organisms. *Ann. Rev. Mar. Sci.* 12, 291–314. doi: 10.1146/annurev-marine-010419-010641

Apprill, A., McNally, S., Parsons, R., and Weber, L. (2015). Minor revision to V4 region SSU rRNA 806R gene primer greatly increases detection of SAR11 bacterioplankton. *Aquat. Microb. Ecol.* 75, 129–137. doi: 10.3354/ame01753

Assis, J. M., Villela, H., Abreu, F., Duarte, G., Roj, L., and Peixoto, R. (2020). Delivering beneficial microorganisms for corals (BMCs): rotifers as carriers of coral probiotics. *Front. Microbiol.* 11:608506. doi: 10.3389/fmicb.2020.608506

Avila-Magaña, V., Kamel, B., DeSalvo, M., Gómez-Campo, K., Enríquez, S., Kitano, H., et al. (2021). Elucidating gene expression adaptation of phylogenetically divergent coral holobionts under heat stress. *Nat. Commun.* 12:5731. doi: 10.1038/s41467-021-25950-4

Barfield, S. J., Aglyamova, G. V., Bay, L. K., and Matz, M. V. (2018). Contrasting effects of *Symbiodinium* identity on coral host transcriptional profiles across latitudes. *Mol. Ecol.* 27, 3103–3115. doi: 10.1111/mec.14774

Benavides, M., Bednarz, V. N., and Ferrier-Pagès, C. (2017). Diazotrophs: overlooked key players within the coral symbiosis and tropical reef ecosystems? *Front. Mar. Sci.* 4:10. doi: 10.3389/fmars.2017.00010

Blackall, L. L., Wilson, B., and Van Oppen, M. J. H. (2015). Coral-the world's most diverse symbiotic ecosystem. *Mol. Ecol.* 24, 5330–5347. doi: 10.1111/mec.13400

Bokulich, N. A., Kaehler, B. D., Rideout, J. R., Dillon, M., Bolyen, E., Knight, R., et al. (2018). Optimizing taxonomic classification of marker-gene amplicon sequences with QIIME 2's q2-feature-classifier plugin. *Microbiome* 6, 1–17. doi: 10.1186/s40168-018-0470-z

Bolger, A. M., Lohse, M., and Usadel, B. (2014). Trimmomatic: a flexible trimmer for Illumina sequence data. *Bioinformatics* 30, 2114–2120. doi: 10.1093/bioinformatics/btu170a

Bolyen, E., Dillon, M., Bokulich, N. A., Abnet, C., Al-Ghalith, G., Alexander, H., et al. (2018). QIIME 2: reproducible, interactive, scalable, and extensible microbiome data science. *PeerJ Preprints* 6:e27295v2. doi: 10.7287/peerj.preprints.27295

Boulotte, N. M., Dalton, S. J., Carroll, A. G., Harrison, P. L., Putnam, H. M., Peplow, L. M., et al. (2016). Exploring the *Symbiodinium* rare biosphere provides evidence for symbiont switching in reef-building corals. *ISME J.* 10, 2693–2701. doi: 10.1038/ismej.2016.54

Brener-Raffalli, K., Clerissi, C., Vidal-Dupiol, J., Adjeroud, M., Bonhomme, F., Pratlong, M., et al. (2018). Thermal regime and host clade, rather than geography, drive *Symbiodinium* and bacterial assemblages in the Scleractinian coral *Pocillopora damicornis* sensu lato. *Microbiome* 6:39. doi: 10.1186/s40168-018-0423-6

Callahan, B. J., McMurdie, P. J., Rosen, M. J., Han, A. W., Johnson, A. J. A., and Holmes, S. P. (2016). DADA2: high resolution sample inference from Illumina amplicon data. *Nat. Methods* 13, 581–583. doi: 10.1038/nmeth.3869

Camp, E. F., Kahlke, T., Nitschke, M. R., Varkey, D., Fisher, N. L., Fujise, L., et al. (2020). Revealing changes in the microbiome of Symbiodiniaceae under thermal stress. *Environ. Microbiol.* 22, 1294–1309. doi: 10.1111/1462-2920.14935

Chen, H., and Boutros, P. C. (2011). VennDiagram: a package for the generation of highly-customizable Venn and Euler diagrams in R. *BMC Bioinformatics* 12:35. doi: 10.2307/2689606

Chuang, P. (2020). Signaling pathways in the coral polyp bail-out response. *Coral Reefs* 39, 1535–1548. doi: 10.1007/s00338-020-01983-x

Cleves, P. A., Shumaker, A., Lee, J. M., Putnam, H. M., and Bhattacharya, D. (2020a). Unknown to known: advancing knowledge of coral gene function. *Trends Genet.* 36, 93–104. doi: 10.1016/j.tig.2019.11.001

Cleves, P. A., Tinoco, A., Bradford, J., Perrin, D., Bay, L. K., and Pringle, J. (2020b). Reduced heat tolerance in a coral carrying CRISPR-induced mutations in the gene for a heat-shock transcription factor. *Proc. Natl. Acad. Sci. U.S.A.* 117, 28899–28905. doi: 10.1073/pnas.1920779117

Connelly, M. T., McRae, C. J., Liu, P.-J., and Traylor-Knowles, N. (2020). Lipopolysaccharide treatment stimulates *Pocillopora* coral genotype-specific

immune responses but does not alter coral-associated bacteria communities. *Dev. Comp. Immunol.* 109:103717. doi: 10.1016/j.dci.2020.103717

Costa, R. M., Cárdenas, A., Loussert-fonta, C., Toullec, G., Meibom, A., Voolstra, C. R., et al. (2021). Surface topography, bacterial carrying capacity, and the prospect of microbiome manipulation in the sea anemone coral model Aiptasia. *Front. Microbiol.* 12:637834. doi: 10.3389/fmicb.2021.637834

Cunning, R., and Baker, A. C. (2020). Thermotolerant coral symbionts modulate heat stress-responsive genes in their hosts. *Mol. Ecol.* 29, 2940–2950. doi: 10.1111/mec.15526

Cunning, R., Bay, R. A., Gillette, P., Baker, A. C., and Traylor-Knowles, N. (2018). Comparative analysis of the *Pocillopora damicornis* genome highlights role of immune system in coral evolution. *Sci. Rep.* 8:16134. doi: 10.1038/s41598-018-34459-8

Damjanovic, K., van Oppen, M. J. H., Menéndez, P., and Blackall, L. L. (2019). Experimental inoculation of coral recruits with marine bacteria indicates scope for microbiome manipulation in *Acropora tenuis* and *Platygyra daedalea*. *Front. Microbiol.* 10:1702. doi: 10.3389/fmicb.2019.01702

Dobin, A., Davis, C. A., Schlesinger, F., Drenkow, J., Zaleski, C., Jha, S., et al. (2013). STAR: ultrafast universal RNA-seq aligner. *Bioinformatics* 29, 15–21. doi: 10.1093/bioinformatics/bts635

Domin, H., Zurita-Gutiérrez, Y. H., Scotti, M., Buttlar, J., Humeida, U. H., and Fraune, S. (2018). Predicted bacterial interactions affect in vivo microbial colonization dynamics in *Nematostella*. *Front. Microbiol.* 9:728. doi: 10.3389/fmicb.2018.00728

Dungan, A. M., van Oppen, M. J., and Blackall, L. L. (2021). Short-term exposure to sterile seawater reduces bacterial community diversity in the sea anemone, *Exaiptasia diaphana*. *Front. Mar. Sci.* 7:599314. doi: 10.3389/fmars.2020.599314

Engelberts, J. P., Robbins, S. J., Damjanovic, K., and Webster, N. S. (2021). Integrating novel tools to elucidate the metabolic basis of microbial symbiosis in reef holobionts. *Mar. Biol.* 168, 1–19. doi: 10.1007/s00227-021-03952-6

Epstein, H. E., Torda, G., Munday, P. L., and van Oppen, M. J. H. (2019). Parental and early life stage environments drive establishment of bacterial and dinoflagellate communities in a common coral. *ISME J.* 13, 1635–1638. doi: 10.1038/s41396-019-0358-3

Fernandes, A. D., Macklaim, J. M., Linn, T. G., Reid, G., and Gloor, G. B. (2013). ANOVA-Like differential expression (ALDEx) analysis for mixed population RNA-Seq. *PLoS One* 8:e67019. doi: 10.1371/journal.pone.0067019

Fernandes, A. D., Reid, J. N. S., Macklaim, J. M., McMurrough, T. A., Edgell, D. R., and Gloor, G. B. (2014). Unifying the analysis of high-throughput sequencing datasets: characterizing RNA-seq, 16S rRNA gene sequencing and selective growth experiments by compositional data analysis. *Microbiome* 2, 1–13. doi: 10.1186/2049-2618-2-15

Ferrier-Pagès, C., Martinez, S., Grover, R., Cybulski, J., Shemesh, E., and Tchernov, D. (2021). Tracing the trophic plasticity of the coral–dinoflagellate symbiosis using amino acid compound-specific stable isotope analysis. *Microorganisms* 9:182. doi: 10.3390/microorganisms9010182

Fox, M. D., Elliott Smith, E. A., Smith, J. E., and Newsome, S. D. (2019). Trophic plasticity in a common reef-building coral: insights from δ13C analysis of essential amino acids. *Funct. Ecol.* 33, 2203–2214. doi: 10.1111/1365-2435.13441

Geissler, L., Meunier, V., Rädecker, N., Perna, G., Rodolfo-Metalpa, R., Houlbrèque, F., et al. (2021). Highly variable and non-complex diazotroph communities in corals from ambient and high CO2 environments. *Front. Mar. Sci.* 8:754682. doi: 10.3389/fmars.2021.754682

Gélin, P., Postaire, B., Fauvelot, C., and Magalon, H. (2017). Reevaluating species number, distribution and endemism of the coral genus *Pocillopora* Lamarck, 1816 using species delimitation methods and microsatellites. *Mol. Phylogenet. Evol.* 109, 430–446. doi: 10.1016/j.ympev.2017.01.018

Gilbert, J. A., Hill, R., Doblin, M. A., and Ralph, P. J. (2012). Microbial consortia increase thermal tolerance of corals. *Mar. Biol.* 159, 1763–1771. doi: 10.1007/s00227-012-1967-9

Glasl, B., Herndl, G. J., and Frade, P. R. (2016). The microbiome of coral surface mucus has a key role in mediating holobiont health and survival upon disturbance. *ISME J.* 10, 2280–2292. doi: 10.1038/ismej.2016.9

Glaze, T. D., Erler, D. V., and Siljanen, H. M. P. (2021). Microbially facilitated nitrogen cycling in tropical corals. *ISME J.* 16, 68–77. doi: 10.1038/s41396-021-01038-1

Gloor, G. B., and Reid, G. (2016). Compositional analysis: a valid approach to analyze microbiome high-throughput sequencing data. *Can. J. Microbiol* 703, 692–703.

Gloor, G. B., Macklaim, J. M., Pawlowsky-Glahn, V., and Egozcue, J. J. (2017). Microbiome datasets are compositional: and this is not optional. *Front. Microbiol.* 8:2224. doi: 10.3389/fmicb.2017.02224

Gunderson, A. R., Armstrong, E. J., and Stillman, J. H. (2016). Multiple stressors in a changing world: the need for an improved perspective on physiological responses to the dynamic marine environment. *Ann. Rev. Mar. Sci.* 8, 357–378. doi: 10.1146/annurev-marine-122414-033953

Haydon, T. D., Seymour, J. R., Raina, J. B., Edmondson, J., Siboni, N., Matthews, J. L., et al. (2021). Rapid shifts in bacterial communities and homogeneity of symbiodiniaceae in colonies of *Pocillopora acuta* transplanted between reef and mangrove environments. *Front. Microbiol.* 12:756091. doi: 10.3389/fmicb.2021.756091

Hodgson, G. (1990). Tetracycline reduces sedimentation damage to corals. *Mar. Biol.* 104, 493–496.

Hopkinson, B. M., and Morel, F. M. M. (2009). The role of siderophores in iron acquisition by photosynthetic marine microorganisms. *BioMetals* 22, 659–669. doi: 10.1007/s10534-009-9235-2

Huerta-Cepas, J., Forslund, K., Coelho, L. P., Szklarczyk, D., Jensen, L. J., Von Mering, C., et al. (2017). Fast genome-wide functional annotation through orthology assignment by eggNOG-mapper. *Mol. Biol. Evol.* 34, 2115–2122. doi: 10.1093/molbev/msx148

Hume, B. C. C., Smith, E. G., Ziegler, M., Hugh, J., Burt, M. W. J. A., and Voolstra, C. R. (2019). SymPortal: a novel analytical framework and platform for coral algal symbiont next – generation sequencing ITS2 profiling. *Mol. Ecol. Resour.* 19, 1063–1080. doi: 10.1111/1755-0998.13004

Jiang, S., Zhou, Z., Sun, Y., Zhang, T., and Sun, L. (2020). Coral gasdermin triggers pyroptosis. *Sci. Immunol.* 5:eabd2591. doi: 10.1126/SCIIMMUNOL.ABD2591

Johnston, E. C., Forsman, Z. H., Flot, J.-F., Schmidt-Roach, S., Pinzón, J. H., Knapp, I. S. S., et al. (2017). A genomic glance through the fog of plasticity and diversification in Pocillopora. *Sci. Rep.* 7:5991. doi: 10.1038/s41598-017-06085-3

Katoh, K., and Standley, D. M. (2013). MAFFT multiple sequence alignment software version 7: improvements in performance and usability. *Mol. Biol. Evol.* 30, 772–780. doi: 10.1093/molbev/mst010

Keshavmurthy, S., Kuo, C., Huang, Y., and Carballo-Bolaños, R. (2019). Coral reef resilience in taiwan: lessons from long- term ecological research on the coral reefs of Kenting national park (Taiwan). *J. Mar. Sci. Eng.* 7:388. doi: 10.3390/jmse7110388

Keshavmurthy, S., Meng, P. J., Wang, J. T., Kuo, C. Y., Yang, S. Y., Hsu, C. M., et al. (2014). Can resistant coral-*Symbiodinium* associations enable coral communities to survive climate change? A study of a site exposed to long-termhot water input. *PeerJ* 2:e327. doi: 10.7717/peerj.327

Kirk, A. L., Clowez, S., Lin, F., Grossman, A. R., and Xiang, T. (2020). Transcriptome reprogramming of symbiodiniaceae *Breviolum minutum* in response to casein amino acids supplementation. *Front. Physiol.* 11:574654. doi: 10.3389/fphys.2020.574654

Ladner, J. T., Barshis, D. J., and Palumbi, S. R. (2012). Protein evolution in two co-occurring types of *Symbiodinium*: an exploration into the genetic basis of thermal tolerance in *Symbiodinium* clade D. *BMC Evol. Biol.* 12:217. doi: 10.1186/1471-2148-12-217

Langfelder, P., and Horvath, S. (2008). WGCNA: an R package for weighted correlation network analysis. *BMC Bioinformatics* 9:559. doi: 10.1186/1471-2105-9-559

Lesser, M. P., Morrow, K. M., Pankey, S. M., and Noonan, S. H. C. (2018). Diazotroph diversity and nitrogen fixation in the coral *Stylophora pistillata* from the Great Barrier Reef. *ISME J.* 12, 813–824. doi: 10.1038/s41396-017-0008-6

Li, H., and Durbin, R. (2009). Fast and accurate short read alignment with Burrows-Wheeler transform. *Bioinformatics* 25, 1754–1760. doi: 10.1093/bioinformatics/btp324

Li, J., Long, L., Zou, Y., and Zhang, S. (2020). Microbial community and transcriptional responses to increased temperatures in coral *Pocillopora damicornis* holobiont. *Soc. Appl. Microbiol.* 23, 826–843. doi: 10.1111/1462-2920.15168

Li, J., Long, L., Zou, Y., and Zhang, S. (2021). Microbial community and transcriptional responses to increased temperatures in coral *Pocillopora damicornis* holobiont. *Environ. Microbiol.* 23, 826–843.

Liao, Y., Smyth, G. K., and Shi, W. (2014). FeatureCounts: an efficient general purpose program for assigning sequence reads to genomic features. *Bioinformatics* 30, 923–930. doi: 10.1093/bioinformatics/btt656

Lin, M. F., Takahashi, S., Forêt, S., Davy, S. K., and Miller, D. J. (2019). Transcriptomic analyses highlight the likely metabolic consequences of colonization of a cnidarian host by native or non-native *Symbiodinium* species. *Biol. Open* 8, 1–11. doi: 10.1242/bio.038281

Liu, H., Stephens, T. G., González-Pech, R. A., Beltran, V. H., Lapeyre, B., Bongaerts, P., et al. (2018). *Symbiodinium* genomes reveal adaptive evolution of functions related to coral-dinoflagellate symbiosis. *Commun. Biol.* 1:95. doi: 10.1038/s42003-018-0098-3

Love, M. I., Huber, W., and Anders, S. (2014). Moderated estimation of fold change and dispersion for RNA-seq data with DESeq2. *Genome Biol.* 15:550. doi: 10.1186/s13059-014-0550-8

Maher, R. L., Rice, M. M., McMinds, R., and Burkepile, D. E. (2019). Multiple stressors interact primarily through antagonism to drive changes in the coral microbiome. *Sci. Rep.* 9:6834. doi: 10.1038/s41598-019-43274-8

Maire, J., Girvan, S. K., Barkla, S. E., David, A. P., Blackall, L. L., and Van Oppen, M. J. H. (2021). Intracellular bacteria are common and taxonomically diverse in cultured and in hospite algal endosymbionts of coral reefs. *ISME J.* 15, 2028–2042. doi: 10.1038/s41396-021-00902-4

Martinez Arbizu, P. (2020). *pairwiseAdonis: Pairwise Multilevel Comparison Using Adonis. R Package Version 0.4.*

Matthews, J. L., Raina, J. B., Kahlke, T., Seymour, J. R., van Oppen, M. J. H., and Suggett, D. J. (2020). Symbiodiniaceae-bacteria interactions: rethinking metabolite exchange in reef-building corals as multi-partner metabolic networks. *Environ. Microbiol.* 22, 1675–1687. doi: 10.1111/1462-2920.14918

Matz, M. V. (2019). *KOGMWU: Functional Summary and Meta-Analysis of Gene Expression Data. R Package Version 1.2.* Available online at: https://cran.r-project.org/web/packages/KOGMWU/index.html (accessed February 19, 2019).

Mayfield, A. B., Wang, Y. B., Chen, C.-S., Lin, C. Y., and Chen, S. H. (2014). Compartment-specific transcriptomics in a reef-building coral exposed to elevated temperatures. *Mol. Ecol.* 23, 5816–5830. doi: 10.1111/mec.12982

McDonald, D., Clemente, J. C., Kuczynski, J., Rideout, J. R., Stombaugh, J., Wendel, D., et al. (2012). The Biological Observation Matrix (BIOM) format or: how I learned to stop worrying and love the ome-ome. *Gigascience* 464, 1–6. doi: 10.1186/2047-217X-1-7

McMurdie, P. J., and Holmes, S. (2013). phyloseq: an R package for reproducible interactive analysis and graphics of microbiome census data. *PLoS One* 8:e61217. doi: 10.1371/journal.pone.0061217

Medrano, E., Merselis, D. G., Bellantuono, A. J., and Rodriguez-Lanetty, M. (2019). Proteomic Basis of symbiosis: a heterologous partner fails to duplicate homologous success in a novel cnidarian- Symbiodiniaceae mutualism. *Front. Microbiol.* 10:1153. doi: 10.3389/FMICB.2019.01153

Motone, K., Takagi, T., Aburaya, S., Miura, N., Aoki, W., and Ueda, M. (2020). A zeaxanthin-producing bacterium isolated from the algal phycosphere protects coral endosymbionts from environmental stress. *MBio* 11:e01019-19.

Murillo-Rincon, A. P., Klimovich, A., Pemöller, E., Taubenheim, J., Mortzfeld, B., Augustin, R., et al. (2017). Spontaneous body contractions are modulated by the microbiome of Hydra. *Sci. Rep.* 7:15937. doi: 10.1038/s41598-017-16191-x

Neave, M. J., Rachmawati, R., Xun, L., Michell, C. T., Bourne, D. G., Apprill, A., et al. (2017). Differential specificity between closely related corals and abundant *Endozoicomonas* endosymbionts across global scales. *ISME J.* 11, 186–200. doi: 10.1038/ismej.2016.95

Neely, K. L., Macaulay, K. A., Hower, E. K., and Dobler, M. A. (2020). Effectiveness of topical antibiotics in treating corals affected by Stony Coral Tissue Loss Disease. *PeerJ* 8:e9289. doi: 10.7717/peerj.9289

O'Brien, P. A., Webster, N. S., Miller, D. J., and Bourne, D. G. (2019). Host-Microbe coevolution: applying evidence from model systems to complex marine invertebrate holobionts. *MBio* 10:e02241-18. doi: 10.1128/mBio.02241-18

Oksanen, J., Blanchet, F. G., Friendly, M., Kindt, R., Legendre, P., McGlinn, D., et al. (2019). *vegan: Community Ecology Package*.

Olson, N. D., Ainsworth, T. D., Gates, R. D., and Takabayashi, M. (2009). Diazotrophic bacteria associated with Hawaiian *Montipora* corals: diversity and abundance in correlation with symbiotic dinoflagellates. *J. Exp. Mar. Biol. Ecol.* 371, 140–146. doi: 10.1016/j.jembe.2009.01.012

Palarea-Albaladejo, J., and Martín-Fernández, J. A. (2015). ZCompositions – R package for multivariate imputation of left-censored data under a compositional approach. *Chemom. Intell. Lab. Syst.* 143, 85–96. doi: 10.1016/j.chemolab.2015.02.019

Park, S., Choi, S. J., Park, J. M., and Yoon, J. H. (2017). *Alteromonas aestuariivivens* sp. nov., isolated from a tidal flat. *Int. J. Syst. Evol. Microbiol.* 67, 2791–2797. doi: 10.1099/ijsem.0.002023

Peixoto, R. S., Rosado, P. M., Leite, D. C., de, A., Rosado, A. S., and Bourne, D. G. (2017). Beneficial microorganisms for corals (BMC): proposed mechanisms for coral health and resilience. *Front. Microbiol.* 8:341. doi: 10.3389/fmicb.2017.00341

Peixoto, R. S., Sweet, M., Villela, H. D. M., Cardoso, P. M., Thomas, T., Voolstra, C. R., et al. (2021). Coral probiotics: premise, promise, prospects. *Annu. Rev. Anim. Biosci.* 9, 265–288. doi: 10.1146/annurev-animal-090120-115444

Pinzón, J. H., Sampayo, E., Cox, E., Chauka, L. J., Chen, C. A., Voolstra, C. R., et al. (2013). Blind to morphology: genetics identifies several widespread ecologically common species and few endemics among Indo-Pacific cauliflower corals (*Pocillopora*, Scleractinia). *J. Biogeogr.* 40, 1595–1608. doi: 10.1111/jbi.12110

Pogoreutz, C., Rädecker, N., Cárdenas, A., Gärdes, A., Wild, C., and Voolstra, C. R. (2018). Dominance of Endozoicomonas bacteria throughout coral bleaching and mortality suggests structural inflexibility of the *Pocillopora verrucosa* microbiome. *Ecol. Evol.* 8, 2240–2252. doi: 10.1002/ece3.3830

Pollock, F. J., McMinds, R., Smith, S., Bourne, D. G., Willis, B. L., Medina, M., et al. (2018). Coral-associated bacteria demonstrate phylosymbiosis and cophylogeny. *Nat. Commun.* 9:4921. doi: 10.1038/s41467-018-07275-x

Poquita-Du, R. C., Huang, D., Chou, L. M., Mrinalini, and Todd, P. A. (2019). Short term exposure to heat and sediment triggers changes in coral gene expression and photo-physiological performance. *Front. Mar. Sci.* 6:121. doi: 10.3389/fmars.2019.00121

Price, M. N., Dehal, P. S., and Arkin, A. P. (2010). FastTree 2 – approximately maximum-likelihood trees for large alignments. *PLoS One* 5:e9490. doi: 10.1371/journal.pone.0009490

Quast, C., Pruesse, E., Yilmaz, P., Gerken, J., Schweer, T., Yarza, P., et al. (2013). The SILVA ribosomal RNA gene database project: improved data processing and web-based tools. *Nucleic Acids Res.* 41, 590–596. doi: 10.1093/nar/gks1219

R Core Team (2020). *R: A Language and Environment for Statistical Computing*. Vienna: R Foundation for Statistical Computing.

Rädecker, N., Pogoreutz, C., Gegner, H. M., Cárdenas, A., Perna, G., Geißler, L., et al. (2021). Heat stress reduces the contribution of diazotrophs to coral holobiont nitrogen cycling. *ISME J.* doi: 10.1038/s41396-021-01158-8

Raina, J. B., Dinsdale, E. A., Willis, B. L., and Bourne, D. G. (2010). Do the organic sulfur compounds DMSP and DMS drive coral microbial associations? *Trends Microbiol.* 18, 101–108. doi: 10.1016/j.tim.2009.12.002

Reich, H. G., Rodriguez, I. B., LaJeunesse, T. C., and Ho, T. Y. (2020). Endosymbiotic dinoflagellates pump iron: differences in iron and other trace metal needs among the Symbiodiniaceae. *Coral Reefs* 39, 915–927. doi: 10.1007/s00338-020-01911-z

Robbins, S. J., Singleton, C. M., Chan, C. X., Messer, L. F., Geers, A. U., Ying, H., et al. (2019). A genomic view of the reef-building coral *Porites lutea* and its microbial symbionts. *Nat. Microbiol.* 4, 2090–2100. doi: 10.1038/s41564-019-0532-4

Rosado, P. M., Leite, D. C. A., Duarte, G. A. S., Chaloub, R. M., Jospin, G., Nunes da Rocha, U., et al. (2018). Marine probiotics: increasing coral resistance to bleaching through microbiome manipulation. *ISME J.* 13, 921–936. doi: 10.1038/s41396-018-0323-6

Santoro, E. P., Borges, R. M., Espinoza, J. L., Freire, M., Messias, C. S. M. A., Villela, H. D. M., et al. (2021). Coral microbiome manipulation elicits metabolic and genetic restructuring to mitigate heat stress and evade mortality. *Sci. Adv.* 7, 19–21. doi: 10.1126/sciadv.abg3088

Schalk, I. J., Hannauer, M., and Braud, A. (2011). New roles for bacterial siderophores in metal transport and tolerance. *Environ. Microbiol.* 13, 2844–2854. doi: 10.1111/j.1462-2920.2011.02556.x

Schmidt-Roach, S., Miller, K. J., Lundgren, P., and Andreakis, N. (2014). With eyes wide open: a revision of species within and closely related to the *Pocillopora damicornis* species complex (Scleractinia; Pocilloporidae) using morphology and genetics. *Zool. J. Linn. Soc.* 170, 1–33. doi: 10.1111/zoj.12092

Shilling, E. N. (2020). *Stony Coral Tissue Loss Disease Intervention Strategies for Montastrea cavernosa.* Master's thesis. Ann Arbor, MI: ProQuest.

Soffer, N., Gibbs, P. D. L., and Baker, A. C. (2008). "Practical applications of contaminant-free Symbiodinium cultures grown on solid media," in *Proceedings of the 11th International Coral Reef Symposium*, Ft. Lauderdale, FL, 159–163.

Sweet, M. J., Croquer, A., and Bythell, J. C. (2014). Experimental antibiotic treatment identifies potential pathogens of white band disease in the endangered Caribbean coral *Acropora cervicornis*. *Proc. R. Soc. B Biol. Sci.* 281, 20140094–20140094. doi: 10.1098/rspb.2014.0094

Sweet, M., and Bythell, J. C. (2015). White syndrome in *Acropora muricata*: nonspecific bacterial infection and ciliate histophagy. *Mol. Ecol.* 24, 1150–1159. doi: 10.1111/mec.13097

Tandon, K., Lu, C.-Y., Chiang, P.-W., Wada, N., Yang, S.-H., Chan, Y.-F., et al. (2020). Comparative genomics: dominant coral-bacterium *Endozoicomonas acroporae* metabolizes dimethylsulfoniopropionate (DMSP). *ISME J.* 14, 1290–1303. doi: 10.1038/s41396-020-0610-x

Thompson, J. R., Rivera, H. E., Closek, C. J., and Medina, M. (2015). Microbes in the coral holobiont: partners through evolution, development, and ecological interactions. *Front. Cell. Infect. Microbiol.* 4:176. doi: 10.3389/fcimb.2014.00176

Tout, J., Siboni, N., Messer, L. F., Garren, M., Stocker, R., Webster, N. S., et al. (2015). Increased seawater temperature increases the abundance and alters the structure of natural *Vibrio* populations associated with the coral *Pocillopora damicornis*. *Front. Microbiol.* 6:432. doi: 10.3389/fmicb.2015.00432

Traylor-Knowles, N., Granger, B. R., Lubinski, T. J., Parikh, J. R., Garamszegi, S., Xia, Y., et al. (2011). Production of a reference transcriptome and transcriptomic database (PocilloporaBase) for the cauliflower coral, *Pocillopora damicornis*. *BMC Genomics* 12:585. doi: 10.1186/1471-2164-12-585

Vavilin, D. V., and Vermaas, W. F. J. (2002). Regulation of the tetrapyrrole biosynthetic pathway leading to heme and chlorophyll in plants and cyanobacteria. *Physiol. Plant.* 115, 9–24. doi: 10.1034/j.1399-3054.2002.1150102.x

Vidal-Dupiol, J., Dheilly, N. M., Rondon, R., Grunau, C., Cosseau, C., Smith, K. M., et al. (2014). Thermal stress triggers broad *Pocillopora damicornis* transcriptomic remodeling, while *Vibrio coralliilyticus* infection induces a more targeted immuno-suppression response. *PLoS One* 9:e107672. doi: 10.1371/journal.pone.0107672

Voolstra, C. R., Suggett, D. J., Peixoto, R. S., Parkinson, J. E., Quigley, K. M., Silveira, C. B., et al. (2021). Extending the natural adaptive capacity of coral holobionts. *Nat. Rev. Earth Environ.* 2, 747–762. doi: 10.1038/s43017-021-00214-3

Voss, J. D., Shilling, E. N., and Combs, I. R. (2019). *Intervention and Fate Tracking for Corals Affected by Stony Coral Tissue Loss Disase in the Northern Florida Reef Tract*. Miami, FL: Florida DEP, 1–23.

Walker, B. K., Turner, N. R., Noren, H. K. G., Buckley, S. F., and Pitts, K. A. (2021). Optimizing Stony Coral Tissue Loss Disease (SCTLD) intervention treatments on *Montastraea cavernosa* in an endemic zone. *Front. Mar. Sci.* 8:666224. doi: 10.3389/fmars.2021.666224

Walker, B., and Pitts, K. (2019). *SE FL Reef-Building-Coral Response to Amoxicillin Intervention and Broader-Scale Coral Disease Intervention*. Miami, FL: Florida DEP, 12.

Wang, Y., Wang, H., Liu, J., Lai, Q., Shao, Z., Austin, B., et al. (2010). *Aestuariibacter aggregatus* sp. nov., a moderately halophilic bacterium isolated from seawater of the Yellow Sea. *FEMS Microbiol. Lett.* 309, 48–54. doi: 10.1111/j.1574-6968.2010.02011.x

Weber, L., DeForce, E., and Apprill, A. (2017). Optimization of DNA extraction for advancing coral microbiota investigations. *Microbiome* 5:18. doi: 10.1186/s40168-017-0229-y

Wecker, P., Lecellier, G., Guibert, I., Zhou, Y., Bonnard, I., and Berteaux-Lecellier, V. (2018). Exposure to the environmentally-persistent insecticide chlordecone induces detoxification genes and causes polyp bail-out in the coral P. *damicornis*. *Chemosphere* 195, 190–200. doi: 10.1016/j.chemosphere.2017.12.048

Weiland-Bräuer, N., Pinnow, N., Langfeldt, D., Roik, A., Güllert, S., Chibani, C. M., et al. (2020). The native microbiome is crucial for offspring generation and fitness of *Aurelia aurita*. *MBio* 11:e02336-20. doi: 10.1128/mBio.02336-20

Wickham, H. (2016). *ggplot2: Elegant Graphics for Data Analysis*. New York, NY: Springer-Verlag New York.

Wickham, H., Averick, M., Bryan, J., Chang, W., McGowan, L. D., François, R., et al. (2019). Welcome to the {tidyverse}. *J. Open Source Softw.* 4:1686. doi: 10.21105/joss.01686

Wilkins, L. G. E., Leray, M., Dea, A. O., Yuen, B., Peixoto, R., Pereira, T. J., et al. (2019). Host-associated microbiomes drive structure and function of marine ecosystems. *PLoS Biol.* 17:e3000533. doi: 10.1371/journal.pbio.3000533

Work, T. M., and Aeby, G. S. (2014). Microbial aggregates within tissues infect a diversity of corals throughout the Indo-Pacific. *Mar. Ecol. Prog. Ser.* 500, 1–9. doi: 10.3354/meps10698

Wright, R. M., Aglyamova, G. V., Meyer, E., and Matz, M. V. (2015). Gene expression associated with white syndromes in a reef building coral, *Acropora hyacinthus*. *BMC Genomics* 16:371. doi: 10.1186/s12864-015-1540-2

Xia, Y., and Sun, J. (2017). Hypothesis testing and statistical analysis of microbiome. *Genes Dis.* 4, 138–148. doi: 10.1016/j.gendis.2017.06.001

Zaneveld, J. R., Burkepile, D. E., Shantz, A. A., Pritchard, C. E., McMinds, R., Payet, J. P., et al. (2016). Overfishing and nutrient pollution interact with temperature to disrupt coral reefs down to microbial scales. *Nat. Commun.* 7:11833. doi: 10.1038/ncomms11833

Zaneveld, J. R., McMinds, R., and Thurber, R. V. (2017). Stress and stability: applying the Anna Karenina principle to animal microbiomes. *Nat. Microbiol.* 2:17121. doi: 10.1038/nmicrobiol.2017.121

Zhang, R., Yu, K., Li, A., Wang, Y., and Huang, X. (2019). Antibiotics in corals of the South China Sea: occurrence, distribution, bioaccumulation, and considerable role of coral mucus. *Environ. Pollut.* 250, 503–510. doi: 10.1016/j.envpol.2019.04.036

Zhang, R., Zhang, R., Yu, K., Wang, Y., Huang, X., Pei, J., et al. (2018). Occurrence, sources and transport of antibiotics in the surface water of coral reef regions in the South China Sea: potential risk to coral growth. *Environ. Pollut.* 232, 450–457. doi: 10.1016/j.envpol.2017.09.064

Zhang, Y., Yang, Q., Ling, J., Long, L., Huang, H., Yin, J., et al. (2021). Shifting the microbiome of a coral holobiont and improving host physiology by inoculation with a potentially beneficial bacterial consortium. *BMC Microbiol.* 21:130. doi: 10.1186/s12866-021-02167-5

Zhang, Y., Zhou, Z., Wang, L., and Huang, B. (2018). Transcriptome, expression, and activity analyses reveal a vital heat shock protein 70 in the stress response of stony coral *Pocillopora damicornis*. *Cell Stress Chaperones* 23, 711–721. doi: 10.1007/s12192-018-0883-4

Zhou, Z., Yu, X., Tang, J., Wu, Y., Wang, L., and Huang, B. (2018). Systemic response of the stony coral *Pocillopora damicornis* against acute cadmium stress. *Aquat. Toxicol.* 194, 132–139. doi: 10.1016/j.aquatox.2017.11.013

Zhou, Z., Zhang, G., Chen, G., Ni, X., Guo, L., Yu, X., et al. (2017). Elevated ammonium reduces the negative effect of heat stress on the stony coral *Pocillopora damicornis*. *Mar. Pollut. Bull.* 118, 319–327. doi: 10.1016/j.marpolbul.2017.03.018

Zhou, Z., Zhang, K., Wang, L., Su, Y., Wang, J., Song, T., et al. (2021). Nitrogen availability improves the physiological resilience of coral endosymbiont *Cladocopium goreaui* to high temperature. *J. Phycol.* 57, 1187–1198. doi: 10.1111/jpy.13156

Ziegler, M., Grupstra, C. G. B., Barreto, M. M., Eaton, M., BaOmar, J., Zubier, K., et al. (2019). Coral bacterial community structure responds to environmental change in a host-specific manner. *Nat. Commun.* 10:3092. doi: 10.1038/s41467-019-10969-5

Ziegler, M., Seneca, F. O., Yum, L. K., Palumbi, S. R., and Voolstra, C. R. (2017). Bacterial community dynamics are linked to patterns of coral heat tolerance. *Nat. Commun.* 8:14213. doi: 10.1038/ncomms14213

Conflict of Interest: The authors declare that the research was conducted in the absence of any commercial or financial relationships that could be construed as a potential conflict of interest.

Advantages of publishing in Frontiers

OPEN ACCESS
Articles are free to read for greatest visibility and readership

FAST PUBLICATION
Around 90 days from submission to decision

HIGH QUALITY PEER-REVIEW
Rigorous, collaborative, and constructive peer-review

TRANSPARENT PEER-REVIEW
Editors and reviewers acknowledged by name on published articles

Frontiers
Avenue du Tribunal-Fédéral 34
1005 Lausanne | Switzerland

Visit us: www.frontiersin.org
Contact us: frontiersin.org/about/contact

REPRODUCIBILITY OF RESEARCH
Support open data and methods to enhance research reproducibility

DIGITAL PUBLISHING
Articles designed for optimal readership across devices

FOLLOW US
@frontiersin

IMPACT METRICS
Advanced article metrics track visibility across digital media

EXTENSIVE PROMOTION
Marketing and promotion of impactful research

LOOP RESEARCH NETWORK
Our network increases your article's readership